Summary of a Thesis Entitled

AUTOMATIC CONTROL OF A CLASS OF NONLINEAR PROCESSES

Submitted to the University of Glasgow

for the Degree of Doctor of Philosophy

by

Charles Norman Kerr, B.Sc., M.S.

May 1964

SUMMARY

The class of nonlinear process presented in this study is characterised by a differential equation involving products bo of the output variable with derivatives of the input, and of derivatives of the output with the input. It is described as "output-dependent" since its dynamic behaviour at a mean, operating, output level changes with that level, and it is sho that the nuclear reactor on an accepted approximation is of th class.

The processes studied each incorporate a gain element of either of two types, the gains of which are functions of the process output. There is a progressive development from the gain elements to selected first-order, and thence to second-order, controlled processes. Extensive use is made of phase-plane techniques in the study, as well as other forms of analy transformations due to Poincaré are introduced and applied wit effect to the behaviour at infinity in the phase plane, and repeated applications of the Direct Method of Lyapunov produce successively improved definitions of the limits of operation f stable responses. Some of these applications display new approaches to the use of the Direct Method.

The stability behaviour of each system following large st changes in input is clearly indicated by diagrams, which it is

shown may not be obtained by a locally-linearised treatment involving the concept of a roots-surface. In particular, the controlled nuclear reactor on the above-mentioned approximatio is shown to be stable following step inputs of reactivity of any magnitude in either direction.

AUTOMATIC CONTROL OF A CLASS OF NONLINEAR PROCESSES

A Thesis Submitted

to the University of Glasgow

for the Degree of Doctor of Philosophy

by

Charles Norman Kerr, B.Sc., M.S.

May 1964

CONTENTS

SUMMARY

The class of nonlinear process presented in this study is characterised by a differential equation involving products both of the output variable with derivatives of the input, and of derivatives of the output with the input. It is described as "output-dependent" since its dynamic behaviour at a mean, operating, output level changes with that level, and it is shown that the nuclear reactor on an accepted approximation is of this class.

The processes studied each incorporate a gain element of either of two types, the gains of which are functions of the process output. There is a progressive development from the gain elements to selected first-order, and thence to second-order, controlled processes. Extensive use is made of phase-plane techniques in the study, as well as other forms of analysis; transformations due to Poincaré are introduced and applied with effect to the behaviour at infinity in the phase plane, and repeated applications of the Direct Method of Lyapunov produce successively improved definitions of the limits of operation for stable responses. Some of these applications display new approaches to the use of the Direct Method.

The stability behaviour of each system following large step changes in input is clearly indicated by diagrams, which it is

shown may not be obtained by a locally-linearised treatment involving the concept of a roots-surface. In particular, the controlled nuclear reactor on the above-mentioned approximation is shown to be stable following step inputs of reactivity of any magnitude in either direction.

ACKNOWLEDGEMENTS

The author wishes to acknowledge with thanks the help of his supervisor throughout the project, Professor G.D.S. MacLellan. He is also indebted to the U.K.A.E.A.(Winfrith) for its interest and support through its Research Agreement A/WIN/EMR 47 , and in particular that of Lt.- Cdr.P.K. M'Pherson , R.N.(Ret'd), Head of Dynamics Group.

NOTATION

The page numbers indicate where the symbol is first defined.

Symbol	Page no.	Description
$a_{11, 12}$ $a_{21, 22}$	112	Coefficients of linear terms in differential equations
a_0, a_n a_m, a_{m0}	Introd.	Coefficients of output and product terms in equation (I.1)
b, b_n	Introd.	Coefficients of input terms in equation (I.1)
D		Differential operator in time t
$_mD_{k-1}$	113	Coefficient of k'th term of v_m
$f_{1, 2}$	112	Functions of x and y in differential equations
$f_{11, 21}$	112	Linear function components of $f_{1, 2}$
j		$j^2 = -1$
K	2	Gain factor
k		Dummy index
L_n	88	Measure of a region of asymptotic stability
l		Dummy index
m		" "
N	100	Parameter defined as R/ζ^2
n		Dummy index
$P_{1, 2}$	112	Nonlinear function components of $f_{1, 2}$
p		Complex variable
p_n	12	Coefficients of operational polynomial

q_m	12	Coefficients of operational polynomial
R	89	Parameter defined as $\sqrt{(K\vartheta_{if}+K-1)^2+4K}$
R_m	113	Homogeneous function of m'th degree in x and y
r	88	Radial co-ordinate
S, S'	72	Directions of trajectories on isoclines
T, T_m		Time constants of processes
T'	33	Equivalent time constant
t		Time
u	78	Variable related to ϑ_o
V_n	91	Lyapunov functions
v	83	Variable related to ϑ_o
v(x,y)	113	Lyapunov function in the method of Zubov
v_m	113	m'th member of a series approximation to v(x,y)
$v^{(n)}$	114	Series approximation to n'th degree for v(x,y)
$w_{1,2}$	114	Sets of points for which $dv_2/dt = 0$
$w_{1,2}^{(n)}$	115	Sets of points for which $dv^{(n)}/dt = 0$
x		Replaces φ_1 in Section 3.4c
y		Replaces φ'_2 in Section 3.4c
Z	78	Variable related to ϑ_o
$\alpha_{11,12,21}$	109	Coefficients of ∇V
γ	88	Angular co-ordinate
ζ	64	Damping factor of second-order process
ζ'	140	Equivalent damping factor
η	139	Figure of merit

ϑ		Input to uncontrolled process
ϑ_i		Input to controlled process
ϑ_m	64	An intermediate variable
ϑ_o		Output of controlled or uncontrolled process
$\vartheta_{1,2}$	74	State variables related to ϑ_o and $d\vartheta_o/dt$
ϑ'_1	92	State variable related to ϑ_o
$\Lambda_{1,2}$	4	Roots of equation (1.1.3)
λ	2	Multiplicative nonlinearity parameter
π		Denotes multiplication
σ		Real frequency component
σ'	33	Equivalent real pole
τ	78	Variable related to t and ϑ_o
$\varphi_{1,2}$	92	State variables related to ϑ_o and $d\vartheta_o/dt$
φ'_2	115	A state variable related to $d\vartheta_o/dt$
$\varphi(x,y)$	113	Positive definite function of x and y
$\varphi_m(x,y)$	113	m'th degree component of $\varphi(x,y)$
Ω_n	86	Boundary of a region of asymptotic stability
ω		Imaginary frequency component
ω_n	64	Natural frequency of second-order process
ω'	140	Equivalent natural frequency

$(\ )_e$	Denotes the equilibrium value of bracketed variable
$(\ )_f$	" " final " " " "
$(\ )_o$	" " initial " " " "
$\delta(\ )$	Denotes a small increment or perturbation from equilibrium in the bracketed variable

INTRODUCTION

Representation of the behaviour of a real physical process by a linear model, although convenient, is often unjustifiable. In many instances a process, whose normal operation within a certain range conforms closely to the linear, requires some nonlinear description for operation beyond this range. Similar remarks apply to the control system incorporating a controlled process.

The region of normal operation may frequently be definable in terms of a unique set of limits on the variables in the system. A type of nonlinear control system exists, however, which operates in a limited region associated with an equilibrium condition that is variable. For limited operation about an equilibrium level, the behaviour may be considered as linear but its dynamic characteristics may depend on the equilibrium level; such an approach will be termed "local linearisation". Since the nature of the local responses varies with the equilibrium state, which can be defined by the input or output level, an adequate description for such a system is "input-, or "output-, dependent".

For some processes of this type, there may be only one equilibrium value of the process input, namely zero. In such cases, where a situation exists similar to a pole at the origin in the linear process, the output may have any value at

equilibrium while the input is zero, and the behaviour must be described as output dependent. It is for this reason that the general class of process is chosen to be considered as output, rather than input, dependent.

In practice, much information may be available relating to the locally linearised dynamic behaviour of a controlled process which is obviously output dependent. This is certainly the case in the field of nuclear reactor control, where normal operation involves relatively small variations about any one of many equilibrium states within a wide range. Introducing a three-dimensional extension of the conventional roots-locus concept, this information may be presented compactly as a series of roots-locus plots in the complex plane where the third dimension is the modifying parameter, i.e. system output. A "roots-surface" is therefore derived, from the shape of which the small-signal response of the closed-loop system can be deduced directly for all values of output and of loop gain.

An output dependent system may be subjected, however, to disturbances producing responses too large to be considered local. It is thus of general interest to discover what relations, if any, may exist between the characteristics of the roots-surface and the response of the closed-loop system for large variations

in its state. M'Pherson[1,2] has given a detailed appreciation of the value of such an extension of the linearised information to the full nonlinear behaviour; Williams[3] also has drawn attention to this general problem of the validity of dynamical models. On the basis of these relations, design procedures in the complex frequency domain might be developed for the control of output dependent processes; such procedures would possess advantages similar to those of the roots–locus method of synthesis for linear systems and for systems which contain single nonlinear elements, and would afford simultaneous information about the corresponding large–scale behaviour.

The variety of output dependent processes is, however, great. This study is restricted to the group of processes for which the input ϑ and the output ϑ_o are related by a differential equation of the general form

$$\sum_{1}^{m} \left(a_m + a_{mo}\vartheta \right) \frac{d^m \vartheta_o}{dt^m} + \left(a_o + a_{oo}\vartheta + \sum_{1}^{n} a_{on} \frac{d^n \vartheta}{dt^n} \right) \vartheta_o$$

$$= b + b_o \vartheta + \sum_{1}^{n} b_n \frac{d^n \vartheta}{dt^n} \qquad (I.1)$$

in which any a or b may be negative or zero, and which is characterised by the presence of products both of ϑ_o with derivatives of ϑ, and of derivatives of ϑ_o with ϑ. Particular

Superscripts refer to the Bibliography on pp. 201 – 204

examples of this type are:

$$\text{(i)}\quad \frac{d^2\vartheta_o}{dt^2} + \left(a_1 + a_{10}\vartheta \right) \frac{d\vartheta_o}{dt} + \left(a_{00}\vartheta + a_{01}\frac{d\vartheta}{dt} \right) \vartheta_o = 0$$

$$\text{(ii)}\quad \frac{d^2\vartheta_o}{dt^2} + \left(a_0 + a_{00}\vartheta \right) \vartheta_o = 0$$

$$\text{(iii)}\quad \frac{d^2\vartheta_o}{dt^2} + \left(a_1 + a_{10}\vartheta \right) \frac{d\vartheta_o}{dt} + a_{00}\vartheta\vartheta_o = b + b_0\vartheta$$

(i) represents the response of a nuclear reactor on a one-point, one delayed-neutron-group basis, where ϑ_o is the neutron population and ϑ the reactivity; (ii) represents[4] the relation between vagus inhibition changes, ϑ, and heart beat rate; and (iii) represents[5] the control of the carbon dioxide concentration in the bloodstream by respiration rate.

An interesting aspect of the general differential equation (I.1) of the process invites comment. In the strict mathematical sense, the equation is in fact linear in ϑ_o: since the input ϑ is some deterministic or stochastic function of t, the output is defined by an equation of the form

$$f_m(t)\frac{d^m\vartheta_o}{dt^m} + f_{m-1}(t)\frac{d^{m-1}\vartheta_o}{dt^{m-1}} + \ldots + f_0(t)\,\vartheta_o = F(t) \qquad (I.2)$$

which is a linear differential equation with time-varying coefficients. In the control engineering sense, however, the term linear implies that the principle of superposition holds and vice versa: in terms of the commonly encountered

nonhomogeneous linear differential equation, with constant coefficients,

$$a_m \frac{d^m \vartheta_o}{dt^m} + a_{m-1} \frac{d^{m-1} \vartheta_o}{dt^{m-1}} + \ldots + a_0 \vartheta_o = F(t) \qquad (I.3)$$

this principle states that if $\vartheta_o(t)$ and $\vartheta_o'(t)$ are the corresponding responses to the forcing functions $F(t)$ and $F'(t)$ respectively, then the response of ϑ_o to a linear combination $c_1 F(t) + c_2 F'(t)$ is given by the corresponding linear combination $c_1 \vartheta_o(t) + c_2 \vartheta_o'(t)$. In the case of equation (I.2), however, the principle of superposition clearly does not apply, since the time-varying coefficients of the left-hand side are functions of the forcing function $\vartheta(t)$. Thus, although the equation is strictly linear, it expresses a strongly nonlinear relationship between forcing function and response. This nonlinearity is even more clearly displayed in the closed-loop around the process, when ϑ is a function of the difference between the closed-loop input ϑ_i and output ϑ_o : in this event, the relevant equation is nonlinear in ϑ_o in the strict mathematical sense also.

This dissertation reports the investigations into the control of several particular output dependent processes described by equation (I.1). A principal objective has been to disclose any relations which may exist between the roots-surfaces and the responses of the closed-loop systems in these particular cases, and possibly to generalise by extension. Each

process has an output dependent gain only, of one of two types referred to as α and β; in other words, none of the dynamic parameters are output dependent.

CHAPTER 1

The Output Dependent Gain Elements

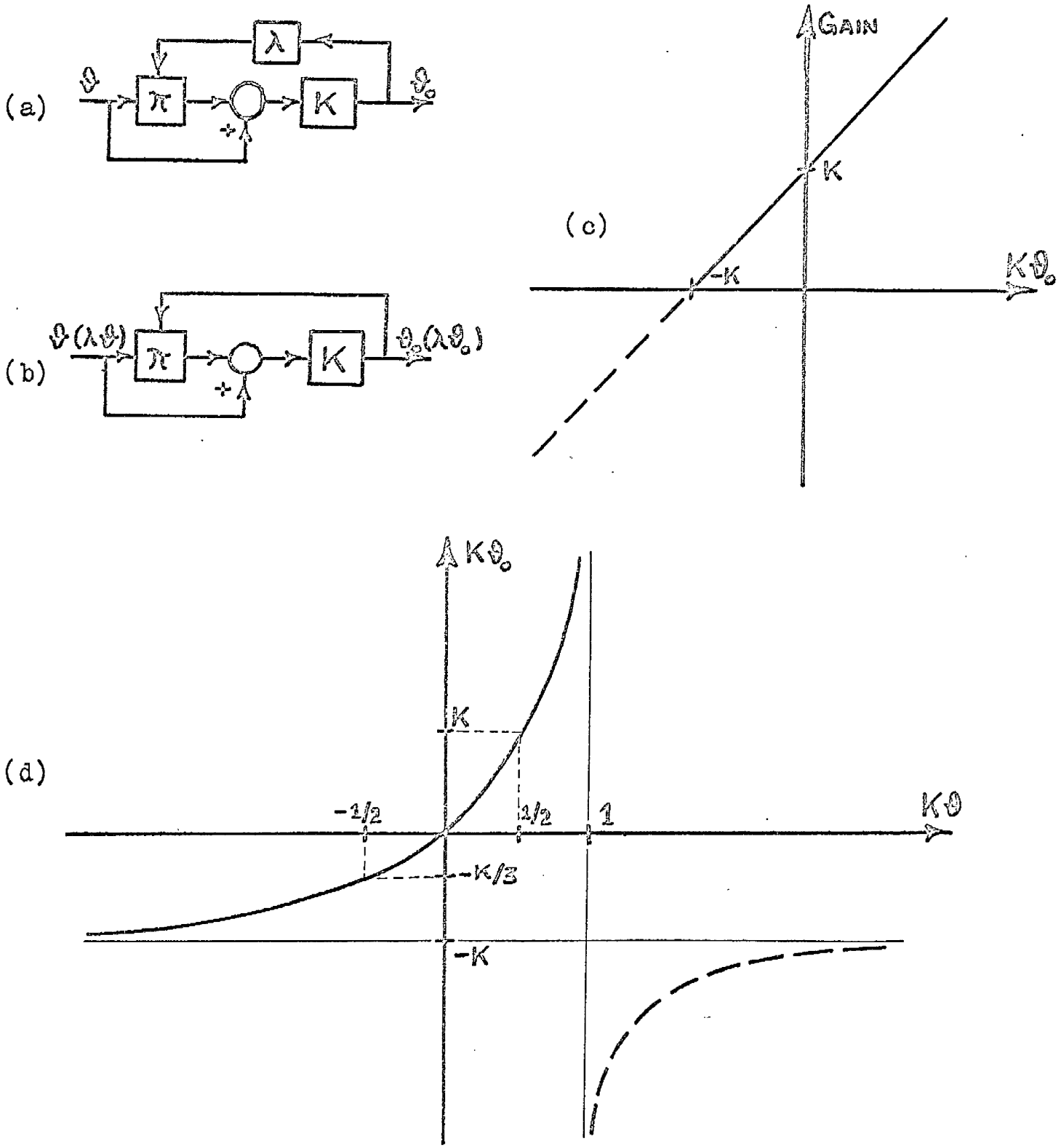

Figure 1.1 (a) Block diagram for α type of gain element
(b) Alternative block diagram to (a), involving groups ϑ and ϑ_0 (i.e. $\lambda\vartheta$ and $\lambda\vartheta_0$)
(c) α – type gain characteristic
(d) Input–output relationship

CHAPTER 1

The Output Dependent Gain Elements

1.1 α type of gain element

A gain element may be described as the simplest process, i.e. one with a non-dynamic character. In view of this, the terms ϑ and ϑ_o are used in this chapter for the input and output of the gain element, as for a process.

At the start it was thought advisable to study the most basic of output dependent gain elements, that which has a linear dependence of gain on output through a small parameter λ. In the adopted notation,

$$\text{gain} = K(1+\lambda\vartheta_o) \qquad (1.1.1)$$

Suitable block diagrams and the gain characteristic are shown in Figure 1.1. It is immediately apparent, since λ occurs only in association with ϑ_o, that the significant variable is the group $\lambda\vartheta_o$ rather than ϑ_o alone. For economy, this group is hereafter referred to simply by ϑ_o — as are $\lambda\vartheta$, etc. by ϑ, etc. — but it is understood that a value of any variable involves the magnitudes both of the relevant signal and the multiplicative parameter as defined.

The relationship between input and output is given by

$$K\vartheta_o = K\frac{K\vartheta}{1-K\vartheta} \qquad (1.1.2)$$

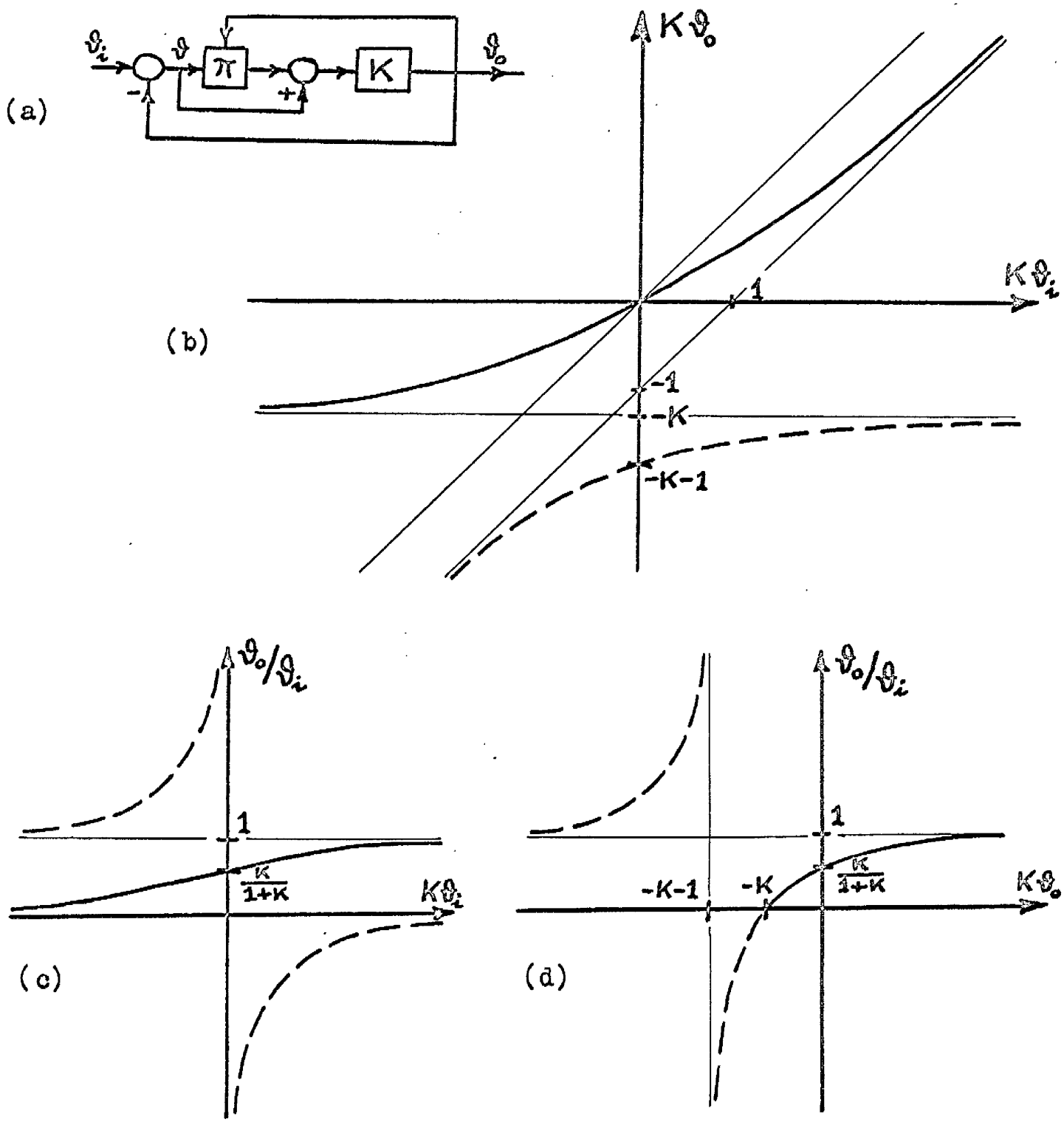

Figure 1.2 (a) Block diagram for the element in a closed loop
(b) Characteristic of a closed loop around the α type of gain element
(c) Overall gain of the closed loop as a function of $K\vartheta_i$
(d) Overall gain of the closed loop as a function of $K\vartheta_o$

and is seen (Figure 1.1) to be single-valued throughout. Parts of characteristics which correspond to negative gain, i.e. for $K\vartheta_o < -K$, appear generally in broken lines. The groups $K\vartheta$, etc. are used for a reason that emerges in Section 1.2.

If a loop is closed proportionally around the element, as in the block diagram of Figure 1.2, $\vartheta = \vartheta_i - \vartheta_o$ and the closed-loop characteristic is given by

$$(K\vartheta_o)^2 + (1 + K - K\vartheta_i) K\vartheta_o - K.K\vartheta_i = 0 \qquad (1.1.3)$$

the $K\vartheta_o$ roots of which are

$$\Lambda_1 = \tfrac{1}{2}\left[-1-K+K\vartheta_i + \sqrt{(1-K-K\vartheta_i)^2 + 4K}\right]$$

$$\Lambda_2 = \tfrac{1}{2}\left[-1-K+K\vartheta_i - \sqrt{(1-K-K\vartheta_i)^2 + 4K}\right]$$

$$\Lambda_1 > -K > \Lambda_2$$

$K\vartheta_o$ is now the double-valued function of the input $K\vartheta_i$ shown in Figure 1.2(b), whose values Λ_1 correspond to positive gain and Λ_2 to negative gain.

To depict completely the operation of the element, it is useful to show the overall gain of the closed-loop round it. In Figure 1.2(c) and (d), the ratio $\vartheta_o / \vartheta_i$ is plotted against both $K\vartheta_i$ and $K\vartheta_o$, according to the expressions

$$\frac{\vartheta_o}{\vartheta_i} = \frac{\Lambda_1}{K\vartheta_i} \text{ or } \frac{\Lambda_2}{K\vartheta_i} = \frac{K + K\vartheta_o}{1 + K + K\vartheta_o} \qquad (1.1.4)$$

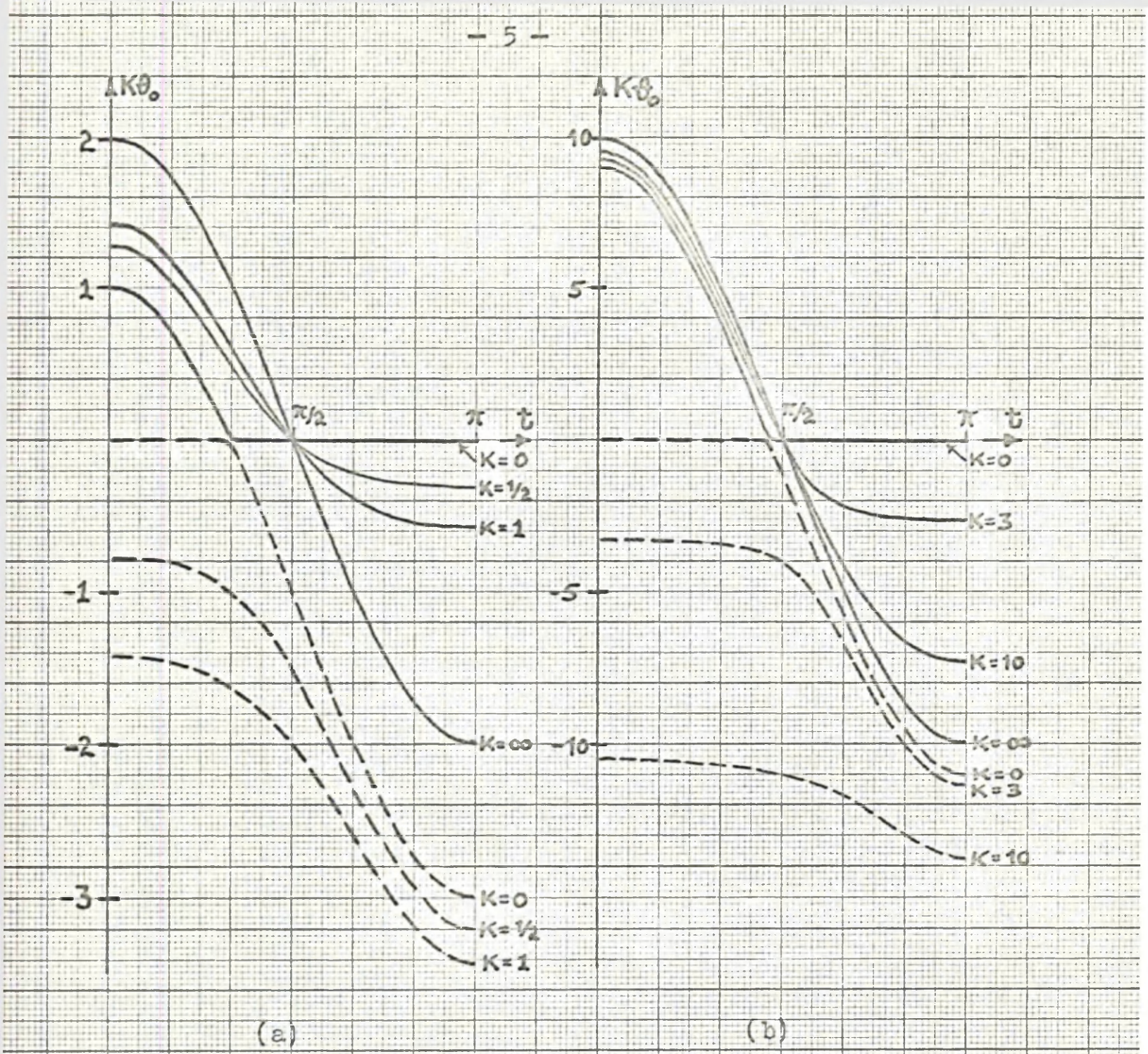

Figure 1.3: Response in $K\theta_0$, for variable K, to a sinusoidal input of (a) $K\theta_i = 2\cos t$, (b) $K\theta_i = 10\cos t$

The overall gain of the closed-loop may be positive for any value of $K\theta_i$, in which case the variable gain is itself positive, and may be positive for negative $K\theta_i$, in which case the variable gain is negative. It is also possible to have the overall gain negative for positive $K\theta_i$, in which case the variable gain is negative.

Emphasis of the operation in the closed-loop is given by the illustration of Figure 1.3. This sets out the responses of $K\theta_o$ to sinusoidal inputs $K\theta_i$ of two different amplitudes, for various values of K. Although the information presented is already contained in equation (1.1.3) and Figure 1.2(b), Figure 1.3 demonstrates the effect of K on the behaviour, which may be described in either of two ways:-

(i) as may be seen from either (a) or (b) of the figure, if K increases while $K\theta_i$ remains constant, the behaviour becomes more nearly linear: this might be expected intuitively, since the magnitude of the input is diminishing;

or (ii) as may be seen from comparative inspection of (a) and (b), if $K\theta_i$ increases while K remains constant, the behaviour becomes more nonlinear; the input magnitude increases.

1.2 β type of gain element

The β type of gain element represents a stronger dependence

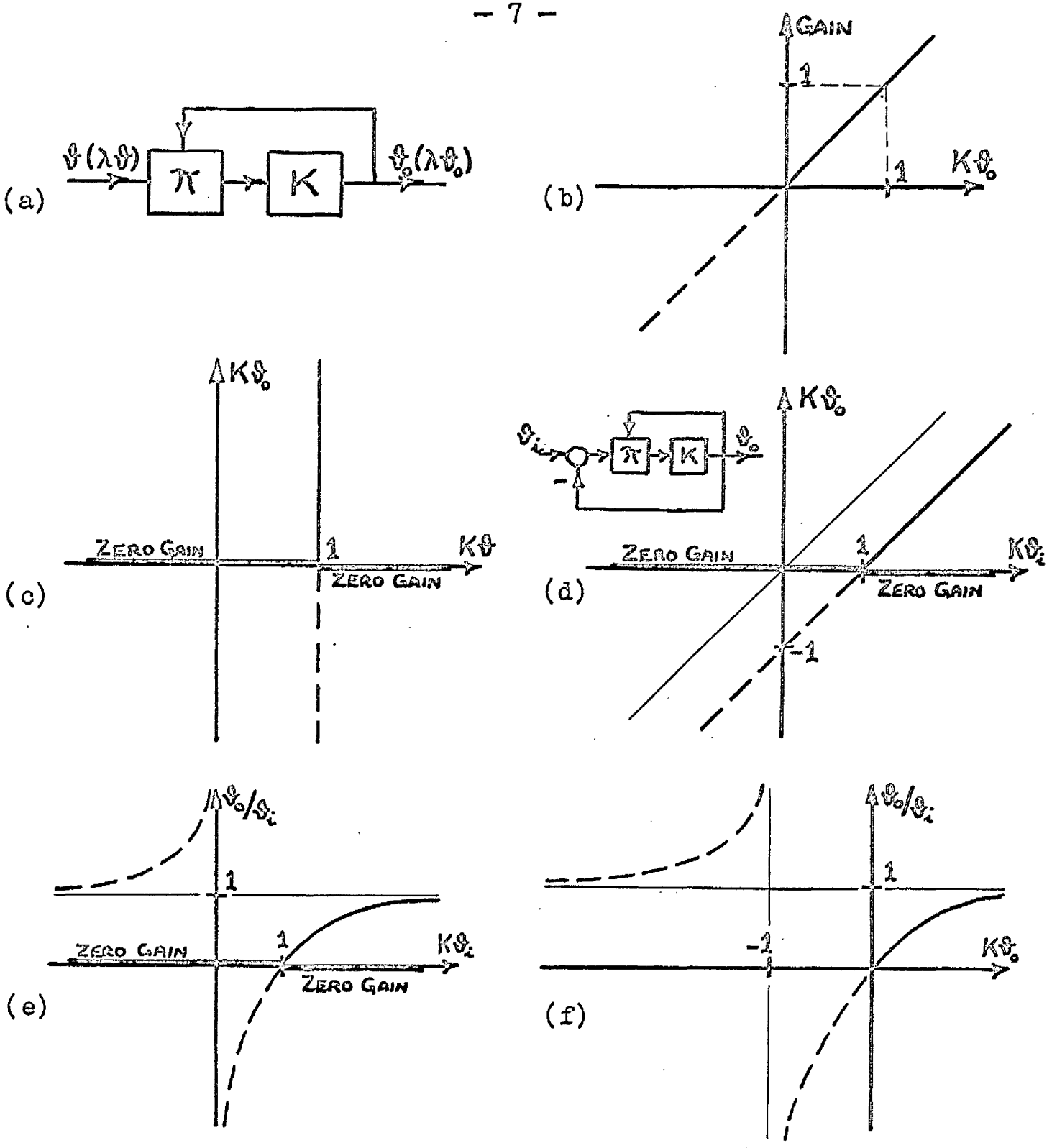

Figure 1.4

Characteristics of β–type gain element: (a) block diagram, (b) gain, (c) input–output

Characteristics of element in a closed loop: (d) input–output, (e) and (f) overall gain as functions of $K\vartheta_i$ and $K\vartheta_o$ respectively

of gain on output than does the α - type. Whilst the latter has a linear dependence, given by equation (1.1.1), resulting in zero gain at the critical value of $\vartheta_o = -1$, the β type has a gain which is directly proportional to output, i.e.

$$\text{gain} = K\vartheta_o \qquad (1.2.1)$$

for which the critical value of output is zero. This behaviour is of considerable interest since the gain of the nuclear reactor increases proportionally with the power output.

A suitable block diagram and the gain characteristic are shown in Figure 1.4(a) and (b). By comparison with Figure 1.1(c) or equation (1.1.1), this element may be considered as that special case of the α - type in which K has tended to zero while the group $K\vartheta_o$ has remained finite and non-zero. In other words, for ever-increasing signal magnitudes and ever-decreasing values of K, the α - type behaviour approaches that of the type β. The β characteristics may thus be deduced from the figures and equations of the previous Section, resulting in the relationships illustrated in Figure 1.4(c) to (f) and in the following equations:-

input - output relationship:	$K\vartheta_o = 0$, independent of $K\vartheta$ $K\vartheta_o$ independent of $K\vartheta$, for $K\vartheta = 1$	(1.2.2)
closed - loop characteristic:	$(K\vartheta_o)^2 + (1 - K\vartheta_i)\,K\vartheta_o = 0$ the roots Λ_1, Λ_2 of which are $K\vartheta_o = K\vartheta_i - 1$ or 0	(1.2.3)

closed-loop gain characteristic:

$$\vartheta_o/\vartheta_i = 1 - 1/K\vartheta_i \quad \text{or} \quad 0 = \frac{K\vartheta_o}{1 + K\vartheta_o} \qquad (1.2.4)$$

It is not necessary to display the β-type responses to sinusoidal inputs $K\vartheta_i$, corresponding to Figure 1.3. These are already available on that figure, being the responses for $K = 0$, and are given by the expressions for Λ_1 and Λ_2 following equation (1.2.3).

1.3 Processes incorporating α-type gain elements

In this Section, attention is given to some general aspects of processes which incorporate an α-type gain element. The next Section deals similarly with processes which incorporate a β-type gain element.

As a preliminary, the local linearisation of the process equation (I.1) of the Introduction is discussed. This general differential equation is repeated here for convenience:

$$\sum_1^m (a_m + a_{m0}\vartheta)\frac{d^m\vartheta_o}{dt^m} + (a_0 + a_{00}\vartheta + \sum_1^n a_{0n}\frac{d^n\vartheta}{dt^n})\vartheta_o = b + b_0\vartheta + \sum_1^n b_n\frac{d^n\vartheta}{dt^n}$$

The equation for an equilibrium state follows from setting all the derivatives in the above equation to zero: if the equilibrium values of ϑ and ϑ_o are denoted by ϑ_e and ϑ_{oe}, it is

$$\vartheta_{oe} = \frac{b + b_0\vartheta_e}{a_0 + a_{00}\vartheta_e} \quad \text{or} \quad \vartheta_e = \frac{b - a_0\vartheta_{oe}}{a_{00}\vartheta_{oe} - b_0} \qquad (1.3.1)$$

The input is now considered to have a small perturbation $\delta\vartheta(t)$ from its equilibrium value, producing a perturbation $\delta\vartheta_o(t)$ in the output: substitution of $\vartheta = \vartheta_e + \delta\vartheta$, $\vartheta_o = \vartheta_{oe} + \delta\vartheta_o$ into equation (I.1), with the use of equation (1.3.1), produces the following differential equation relating $\delta\vartheta_o$ to $\delta\vartheta$

$$\sum_{0}^{m} (a_m + a_{m0}\vartheta_e) \frac{d^m\delta\vartheta_o}{dt^m} + \sum_{0}^{m} a_{m0}\delta\vartheta \frac{d^m\delta\vartheta_o}{dt^m} + \sum_{1}^{n} a_{0n}\delta\vartheta_o \frac{d^n\delta\vartheta}{dt^n}$$

$$= \sum_{0}^{n} (b_n - a_{0n}\vartheta_{oe}) \frac{d^n\delta\vartheta}{dt^n} \qquad (1.3.2)$$

After making the following assumptions, which certainly hold for sufficiently small perturbations, that

$$\left| b_0 - a_{00}\vartheta_{oe} \right| \gg \left| \sum_{0}^{m} a_{m0} \frac{d^m\delta\vartheta_o}{dt^m} \right| , \quad -\infty < t < \infty$$

$$\text{and} \quad \left| b_n - a_{0n}\vartheta_{oe} \right| \gg \left| a_{0n}\delta\vartheta_o \right| , \quad n = 1, 2, \ldots n \qquad (1.3.3)$$

equation (1.3.2) reduces to

$$\sum_{0}^{m} (a_m + a_{m0}\vartheta_e) \frac{d^m\delta\vartheta_o}{dt^m} = \sum_{0}^{n} (b_n - a_{0n}\vartheta_{oe}) \frac{d^n\delta\vartheta}{dt^n} \qquad (1.3.4)$$

For zero values of $\delta\vartheta$, $\delta\vartheta_o$, and their derivatives at $t = 0$, the transformed version of equation (1.3.4) gives the small-signal transfer function to be

$$\frac{\delta\vartheta_o(p)}{\delta\vartheta(p)} = \frac{\sum_{0}^{n} (b_n - a_{0n}\vartheta_{oe}) p^n}{\sum_{0}^{m} (a_m + a_{m0}\vartheta_e) p^m} \qquad (1.3.5)$$

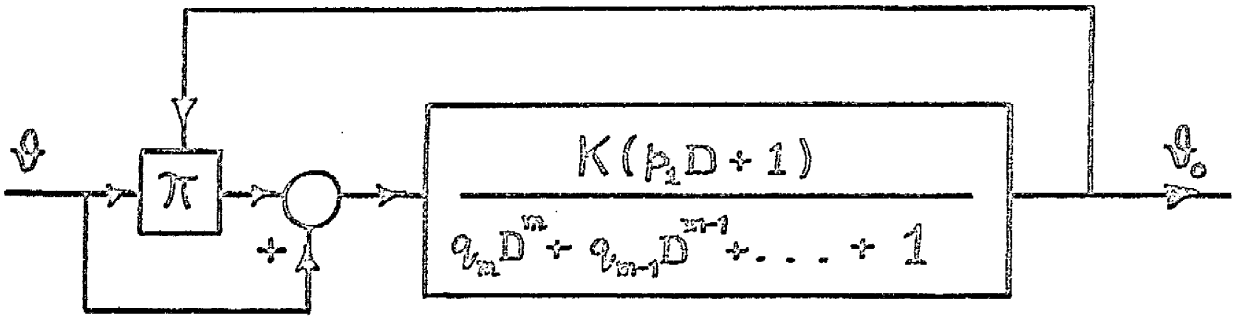

(a)

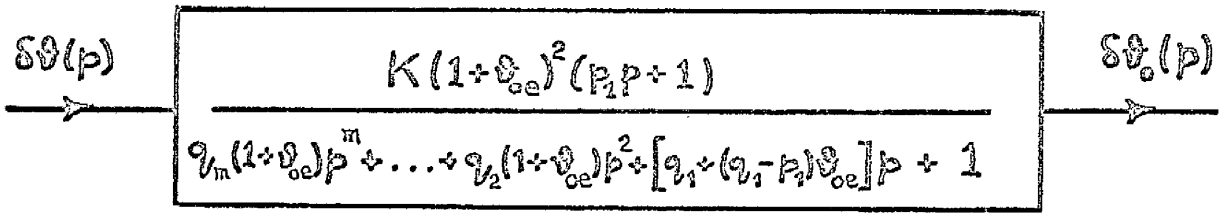

(b)

Figure 1.5 (a) Block diagram of a process incorporating an α — type gain element

(b) Small—signal transfer function for the above process

in terms of the complex variable p. Use of equation (1.3.1) to eliminate ϑ_e produces the desired final result:

$$\frac{\delta\vartheta_o(p)}{\delta\vartheta(p)} = \frac{(a_{00}\vartheta_{oe} - b_0)\sum_0^n (b_n - a_{0n}\vartheta_{oe})\,p^n}{\sum_0^m \left[(a_{m0}b - a_m b_0) + (a_m a_{00} - a_{m0}a_0)\vartheta_{oe}\right] p^m} \qquad (1.3.6)$$

The form of the small-signal transfer function, and thus the nature of local responses, are heavily dependent on the equilibrium value of output, as described in the Introduction.

A process incorporating an α type gain element is shown in general block diagram form in Figure 1.5(a). The gain parameter K of the bare element has been replaced by a transfer function, whose numerator is of first order and whose denominator is of m'th order; since D can be set to zero at equilibrium, the static behaviour is that of the bare α type gain element.

The operation of the process is described by the equation

$$\left[q_m D^m + q_{m-1} D^{m-1} + \ldots + 1\right]\vartheta_o = K\left[p_1 D + 1\right](1 + \vartheta_o)\vartheta \qquad (1.3.7)$$

which on expansion becomes

$$\sum_2^m q_m \frac{d^m\vartheta_o}{dt^m} + (q_1 - Kp_1\vartheta)\frac{d\vartheta_o}{dt} + \left(1 - K\vartheta - Kp_1\frac{d\vartheta}{dt}\right)\vartheta_o$$

$$= K\vartheta + Kp_1\frac{d\vartheta}{dt} \qquad (1.3.8)$$

Equation (1.3.8) is seen to be a particular form of the equation (I.1), where

$$a_{10} = a_{01} = -b_1 = -Kp_1,\ a_{00} = -b_0 = -K,\ a_0 = 1,\ a_m = q_m \quad \text{for } m \geqslant 1$$

$$\text{and} \quad b = a_{m0} = a_{0n} = b_n = 0 \quad \text{for all } m,n > 1 \qquad (1.3.9)$$

Substitution of these values in (1.3.6) produces the relevant small-signal transfer function:

$$\frac{\delta\vartheta_o(p)}{\delta\vartheta(p)} = \frac{K(1+\vartheta_{oe})^2(p_1p+1)}{q_m(1+\vartheta_{oe})p^m+\ldots+q_2(1+\vartheta_{oe})p^2+\left[q_1+(q_1-p_1)\vartheta_{oe}\right]p+1} \qquad (1.3.10)$$

for which a block diagram is Figure 1.5(b).

Thus, although the output dependency in the process is only in the gain factor, the values of the small-signal poles as well as the small-signal gain depend in general on the mean output level. Furthermore, the gain dependency for small-signal response is not a linear one similar to that in the process, but varies instead as $(1+\vartheta_{oe})^2$. This effect may also be noticed from considering the non-dynamic case of the process, i.e. where $p_1 = q_1 = q_2 = \ldots = q_m = 0$ and the process has degenerated into the bare α - type gain element: the static small-signal transfer function becomes

$$\delta\vartheta_o/\delta\vartheta = K(1+\vartheta_{oe})^2 \qquad (1.3.11)$$

which agrees with the expression, derived from (1.1.2),

$$\frac{d\vartheta_o}{dt} = K(1+\vartheta_o)^2 .$$

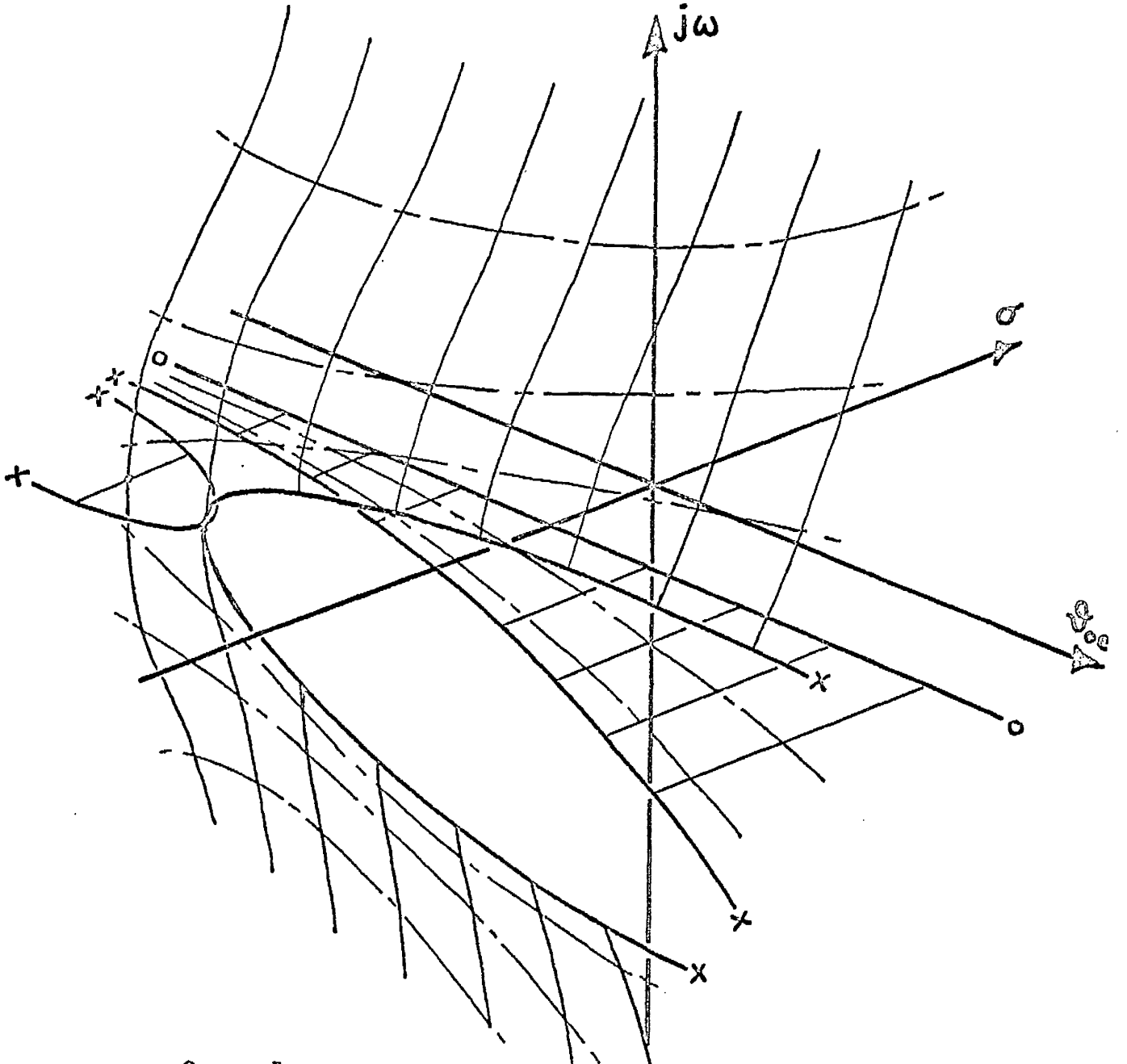

o ——— o Open-loop zero path

——— Roots-loci for const. values of ϑ_{oe}

x ——— x Open-loop pole path

- ——— - Closed-loop pole paths for various values of K

Figure 1.6 : An illustration of the roots-surface concept

If the process is considered to be controlled proportionally in a closed loop, the small-signal roots-loci are different for each different value of ϑ_{oe}, due to the changing open-loop pole-zero pattern and gain. This leads to the presentation of the complete set of roots-loci as a roots-surface in the three dimensions of real and imaginary frequency components and mean output level ϑ_{oe}; the roots-surface may be in several parts, just as the roots-locus may possess several branches, and an illustration is given in Figure 1.6. Corresponding to the transfer function (1.3.10), the open-loop zero at $-1/p_1$ is independent of ϑ_{oe}, but the open-loop poles may describe complex paths as ϑ_{oe} varies; the closed-loop poles may therefore describe equally complex paths, one set of paths for each value of K.

The complexity of the roots-surface is much reduced in a special case of the process of Figure 1.5(a). If all the coefficients q_m and the factor K are so large in relation to unity and p_1 that the characteristic equation (1.3.7) becomes

$$D\left[q_m D^{m-1} + q_{m-1} D^{m-2} + \ldots + q_1 \right] \vartheta_o = K\left[p_1 D + 1 \right](1 + \vartheta_o)\vartheta \quad (1.3.12)$$

the transfer function (1.3.10) assumes the form

$$\frac{\delta\vartheta_o(p)}{\delta\vartheta(p)} = \frac{K(1 + \vartheta_{oe})(p_1 p + 1)}{p(q_m p^{m-1} + q_{m-1} p^{m-2} + \ldots + q_1)} \quad (1.3.13)$$

In other words, if the process dynamics have a pole at the

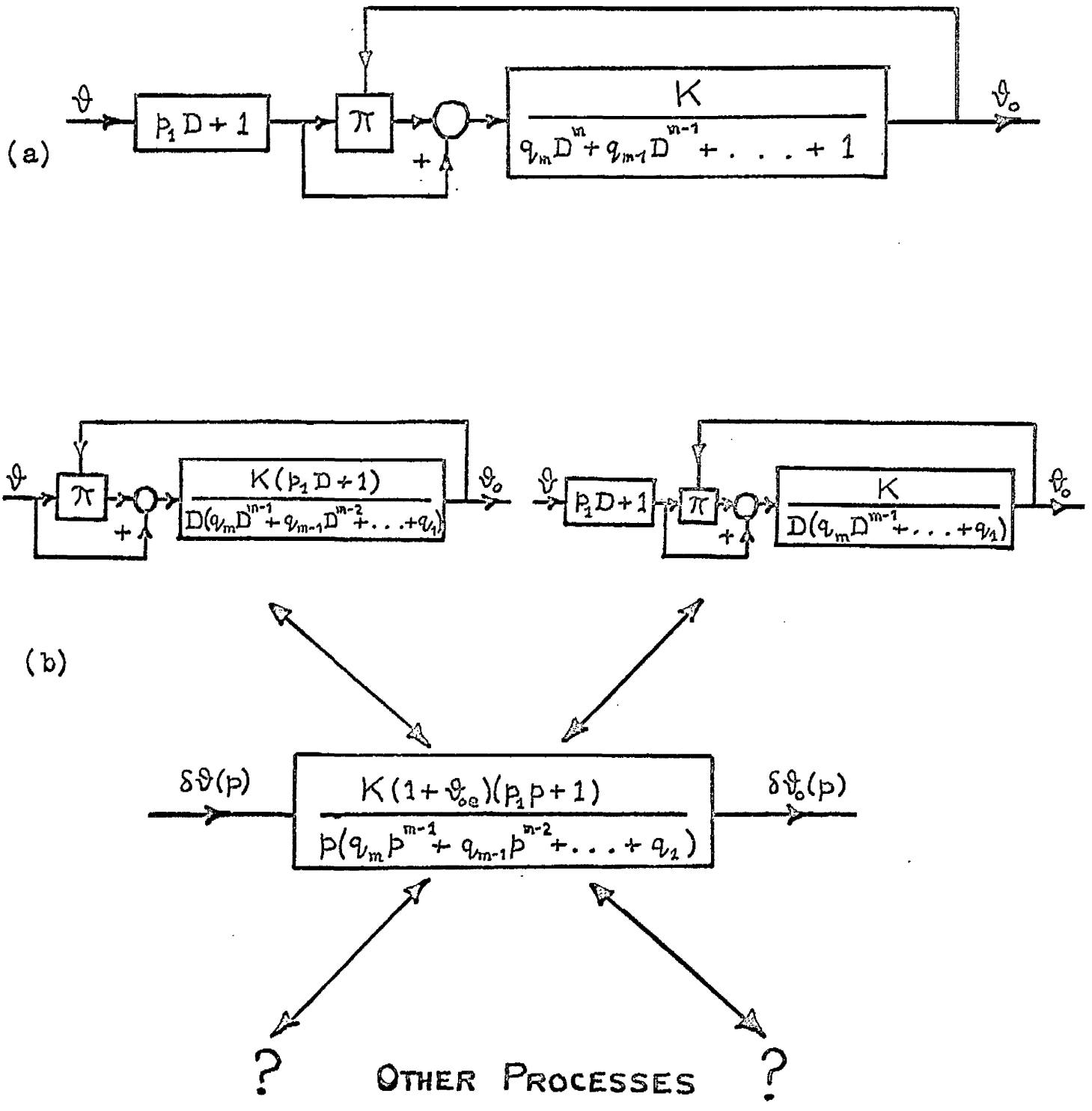

Figure 1.7(a) Block diagram of a process associated with that of Figure 1.5(a)

(b) An illustration of the non–uniqueness of the small–signal transfer function to a particular process

origin, the small-signal transfer function has a gain which varies linearly with ϑ_{oe} and dynamics which correspond to those of the process, being independent of ϑ_{oe}. In this event, the roots-surface reduces to a roots-locus, the form of which is independent of ϑ_{oe}, and on which the closed-loop poles lie at positions corresponding to the variable gain $K(1+\vartheta_{oe})$.

In conclusion of this Section, one other feature of this type of process is discussed. In place of the process of Figure 1.5(a), consider the associated process with an $\alpha-$ type gain element shown in Figure 1.7(a), in which the lead term $(p_1 D+1)$ precedes the gain element. The response of this process is described by the equation

$$\sum_{1}^{m} q_m \frac{d^m \vartheta_o}{dt^m} + \left(1 - K\vartheta - Kp_1 \frac{d\vartheta}{dt}\right)\vartheta_o = K\vartheta + Kp_1 \frac{d\vartheta}{dt} \qquad (1.3.14)$$

Comparison with equation (1.3.8) shows that, in the identification of this process as one described by equation (I.1), the relations (1.3.9) apply with the sole alteration that $a_{10} = 0$. The relevant small-signal transfer function is therefore obtained from (1.3.6) as

$$\frac{\delta\vartheta_o(p)}{\delta\vartheta(p)} = \frac{K(1+\vartheta_{oe})^2(p_1 p+1)}{q_m(1+\vartheta_{oe})p^m + \ldots + q_1(1+\vartheta_{oe})p+1} \qquad (1.3.15)$$

If the coefficient p_1 is zero the two associated processes are

identical, and the two transfer functions (1.3.10) and (1.3.15) have accordingly the same form. But in addition, if all the coefficients q_m and the factor K are so large in relation to unity that the characteristic equation becomes

$$D\left[q_m D^{m-1} + q_{m-1} D^{m-2} + \ldots + q_1\right]\vartheta_o = K(1 + \vartheta_o)\left[p_1 D + 1\right]\vartheta \qquad (1.3.16)$$

the small-signal transfer function (1.3.15) assumes the form

$$\frac{\delta\vartheta_o(p)}{\delta\vartheta(p)} = \frac{K(1 + \vartheta_{oe})(p_1 p + 1)}{p(q_m p^{m-1} + q_{m-1} p^{m-2} + \ldots + q_1)} \qquad (1.3.17)$$

Since this is identical with (1.3.13), the small-signal transfer function of the special case of the original process is not unique to it: it has been shown to be shared with at least the same case of the associated process, as illustrated in Figure 1.7(b).

The disclosure that a roots-surface of a process may not be unique to that process places a severe restriction at the outset on the capability of the roots-surface to give information about large-scale behaviour, as outlined in the Introduction. In the example above, the large-scale responses of the two associated processes will clearly differ, yet any deductions about these responses from their common roots-surface would apply to each.

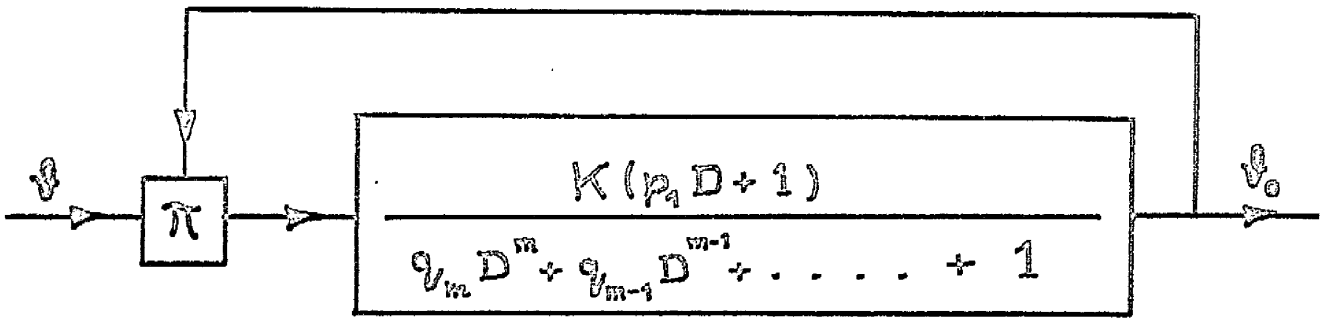

Figure 1.8 : Block diagram of a process incorporating a β – type gain element

1.4 Processes incorporating β — type gain elements

A process incorporating a β — type gain element is shown in general block diagram form in Figure 1.8; it corresponds to the process of the previous Section in which the α — type is replaced by the β — type of gain element. The static behaviour of the process is therefore that of the bare β — type gain element, which is shown in Section 1.2 to be deducible from the characteristics of the α — type.

The equation describing this process is

$$\sum_{2}^{m} q_m \frac{d^m \vartheta_o}{dt^m} + (q_1 - Kp_1 \vartheta) \frac{d\vartheta_o}{dt} + (1 - K\vartheta - Kp_1 \frac{d\vartheta}{dt}) \vartheta_o = 0 \qquad (1.4.1)$$

which is obtainable from equation (1.3.8) by letting K tend to zero while $K\vartheta_o$ and $K\vartheta$ remain finite and non-zero. Thus, the dynamic behaviour of this process may be similarly deduced from that of the corresponding process incorporating an α — type element. In particular, if the numerator and denominator of (1.3.10) are divided by $(1 + \vartheta_{oe})$, and K is set to zero, the small-signal transfer function of this process is given as

$$\frac{\delta\vartheta_o(p)}{\delta\vartheta(p)} = \frac{K\vartheta_{oe} (p_1 p + 1)}{p \left(q_m p^{m-1} + \ldots + q_2 p + (q_1 - p_1) \right)} \qquad (1.4.2)$$

Since the dynamics of the transfer function are not dependent on output, the roots-surface reduces to a roots-locus in every case of this process, not only in a special case as for the

α — type process.

In this special case, when the process dynamics have a pole at the origin, the dynamics of the transfer function correspond to those of the process itself, as before. In the general case, however, (1.4.2) indicates that the transfer function has a pole at the origin even if the process dynamics have not.

Finally, the aspect of non-uniqueness of the roots-surface can be demonstrated by this process also. By comparing the special case mentioned above with the corresponding one of the associated process, where the lead term ($p_1 D + 1$) precedes the gain element, a common transfer function results.

CHAPTER 2

The Control of some First-Order Output-Dependent Processes

(a)

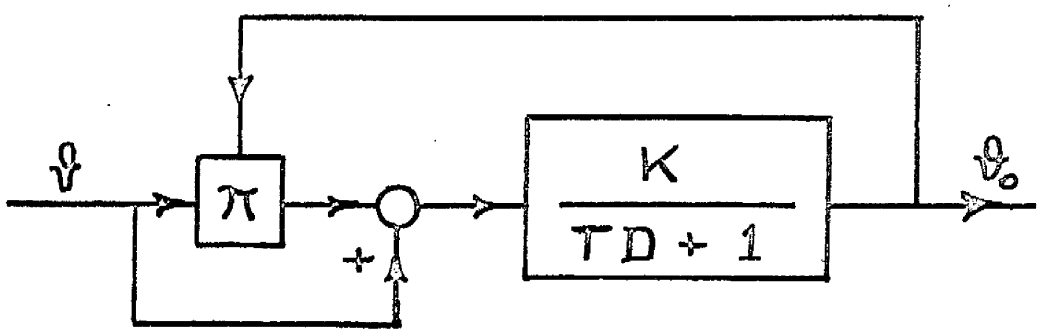

(b)

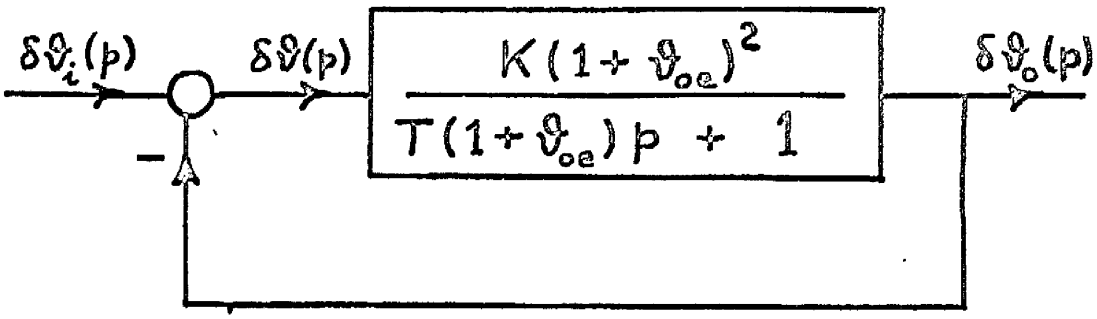

Figure 2.1 (a) Block diagram of a first-order process, incorporating an α – type gain element

(b) Block diagram for perturbations in a closed loop round the above process

CHAPTER 2

The Control of some First-Order Output-Dependent Processes

2.1 A process with an α-type gain element

Figure 2.1(a) is a block diagram of the process chosen for initial detailed investigation. The special case in which the first-order lag is replaced by integration is treated in the next section.

In terms of the general formulation of Section 1.3, the coefficients p_1 and q_m are zero for m greater than one and $q_1 = T$, for this process. Accordingly, the characteristic equation is obtained from equation (1.3.8) as

$$T\frac{d\vartheta_o}{dt} + (1 - K\vartheta)\vartheta_o = K\vartheta \qquad (2.1.1)$$

and the small-signal transfer function from equation (1.3.10) as

$$\frac{\delta\vartheta_o(p)}{\delta\vartheta(p)} = \frac{K(1+\vartheta_{oe})^2}{T(1+\vartheta_{oe})p + 1} \qquad (2.1.2)$$

The interrelations of small variations in the variables when the process is controlled proportionally in a closed loop are indicated by the block diagram of Figure 2.1(b).

Proceeding to the construction of the roots-surface in the $(\sigma, j\omega, \vartheta_{oe})$ space, Figure 2.2(a), the path of the open-loop pole at $-1/T(1+\vartheta_{oe})$ is drawn first. Since the roots-locus

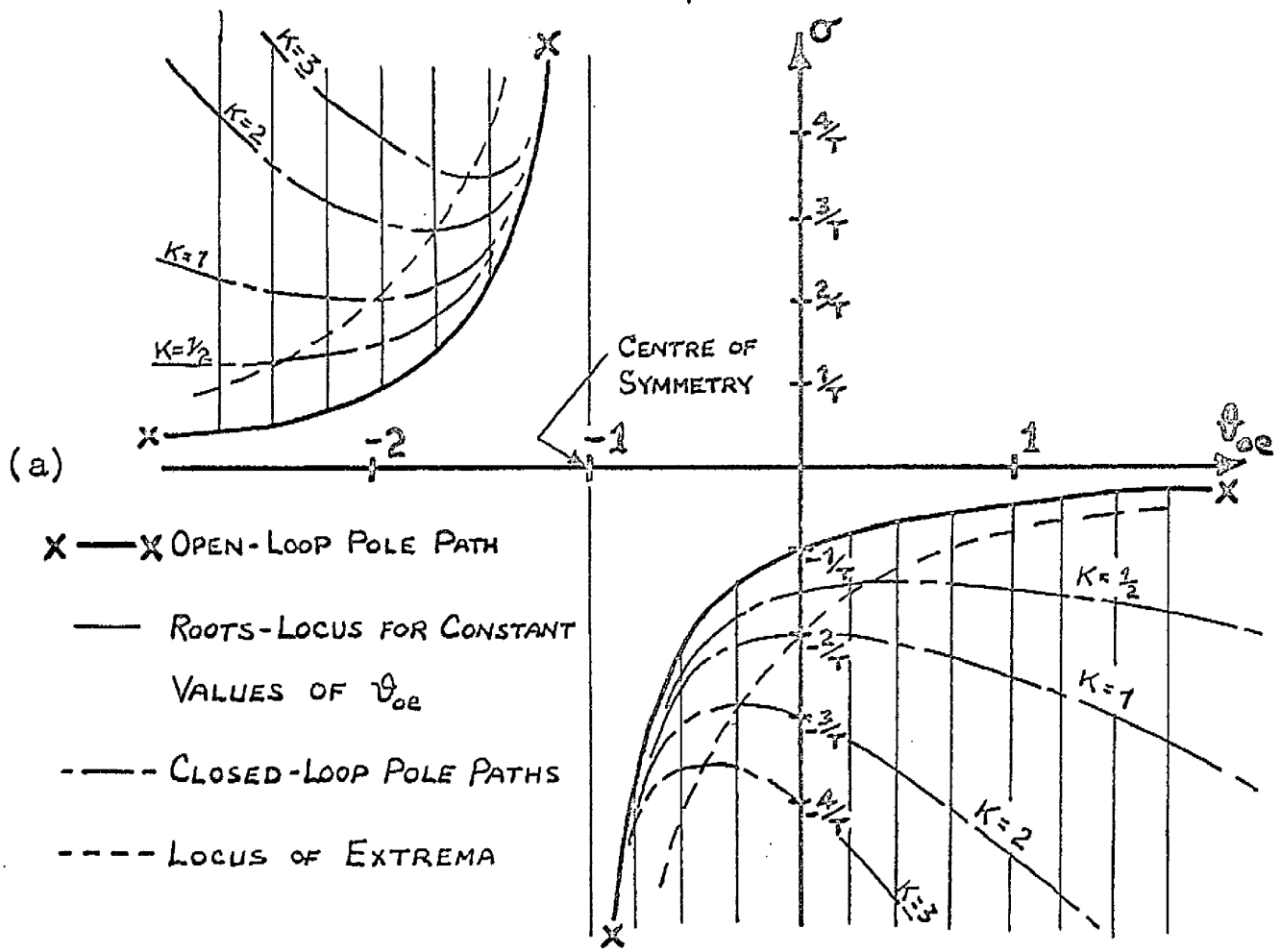

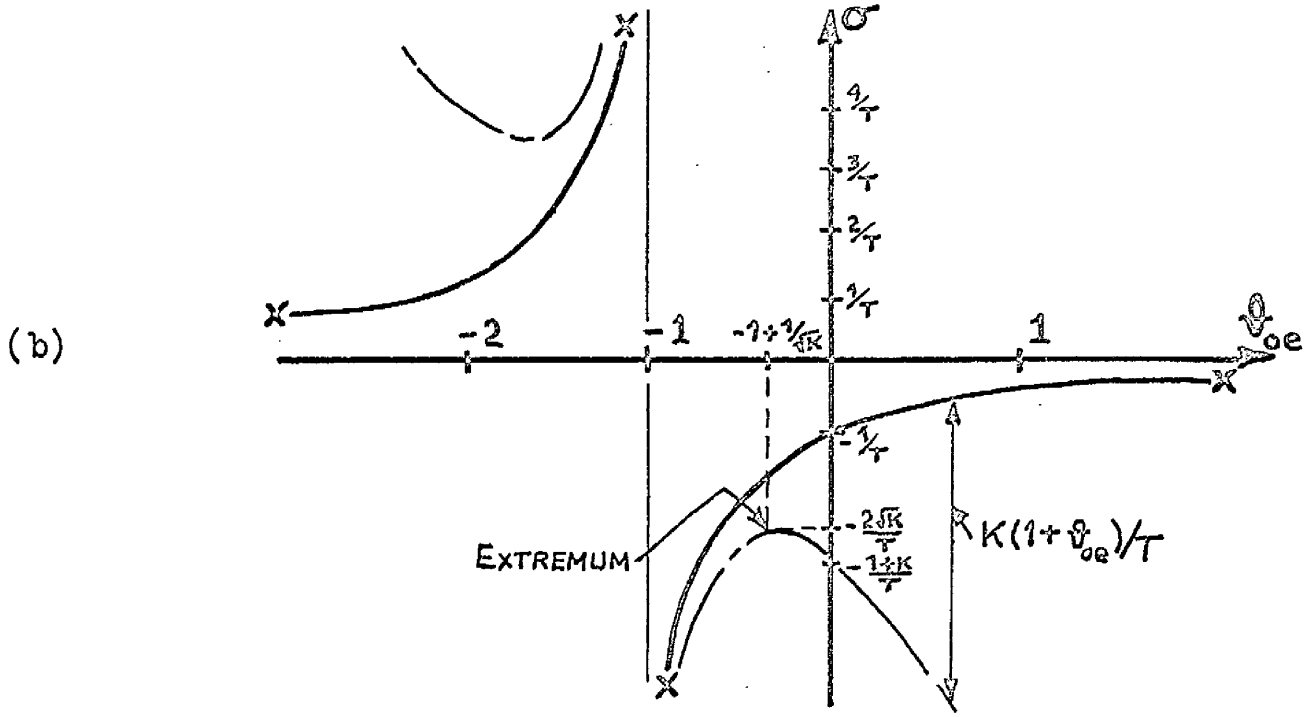

Figure 2.2 (a) Roots-surface for the system of Figure 2.1(b)

(b) An alternative to (a), in terms of the factor K

at any value ϑ_{oe} is a straight line extending from the open-loop pole position parallel to the σ axis, the whole roots-surface lies entirely in the (σ, ϑ_{oe}) plane, obviating the necessity of a three-dimensional presentation for this system. It should be noted that the point $\sigma = 0$, $\vartheta_{oe} = -1$ is a centre of symmetry for the open-loop pole path: for $\vartheta_{oe} > -1$, the pole has only negative values, which tend to zero for large ϑ_{oe} and become increasingly negative as ϑ_{oe} tends to -1, and its positive values for $\vartheta_{oe} < -1$ conform to the property of symmetry.

Due to the simplicity of this system, the location of the closed-loop pole on the roots-locus for any values of K and ϑ_{oe} is readily obtained from the magnitude relation

$$\left| \frac{K(1+\vartheta_{oe})^2}{T(1+\vartheta_{oe})p+1} \right| = 1 \qquad (2.1.3)$$

The closed-loop pole lies at a distance of $K(1+\vartheta_{oe})/T$ from the open-loop pole, the former having a more negative value than the latter if $\vartheta_{oe} > -1$ and a more positive value if $\vartheta_{oe} < -1$. The explicit expression for the closed-loop pole position is therefore

$$\sigma = -\frac{1+K(1+\vartheta_{oe})^2}{(1+\vartheta_{oe})T} \qquad (2.1.4)$$

and several paths are shown on the figure for various values of K. Each path has turning points at $\vartheta_{oe} = -1 \pm 1/\sqrt{K}$, for which

the maximum and minimum values of the closed-loop pole are $\pm 2\sqrt{K}/T$, and the locus of extrema is given by

$$\sigma = -2/T(1+\vartheta_{oe}) \qquad (2.1.5)$$

It is in fact not necessary to draw many closed-loop pole paths for various values of K. In a first-order system, there is only one closed-loop pole whose distance from the open-loop pole has a simple dependency on ϑ_{oe} and K, as follows from (2.1.3). The roots-surface may therefore be drawn as in Figure 2.2(b), in which the single closed-loop pole path lies at a distance of $K(1+\vartheta_{oe})/T$ from the open-loop pole path and replaces the one-parameter family of paths of Figure 2.2(a). The essential behaviour of the closed-loop pole and the corresponding local transient responses is now clear. For a given value of K, responses are stable if $\vartheta_{oe} > -1$ and the time constant of the response is a maximum at a certain value of ϑ_{oe}; for progressively greater values of ϑ_{oe}, and for progressively smaller values which still exceed -1, the speed of the responses increases.

Attention is now turned from the small-signal behaviour to the transient response to large steps of input. The system is assumed to be initially in equilibrium, so that the static relationship is that of the α-type gain element, equation (1.1.3). For given $K\vartheta_{io}$, the output $K\vartheta_{oo}$ may be either Λ_{1o} or Λ_{2o}, and

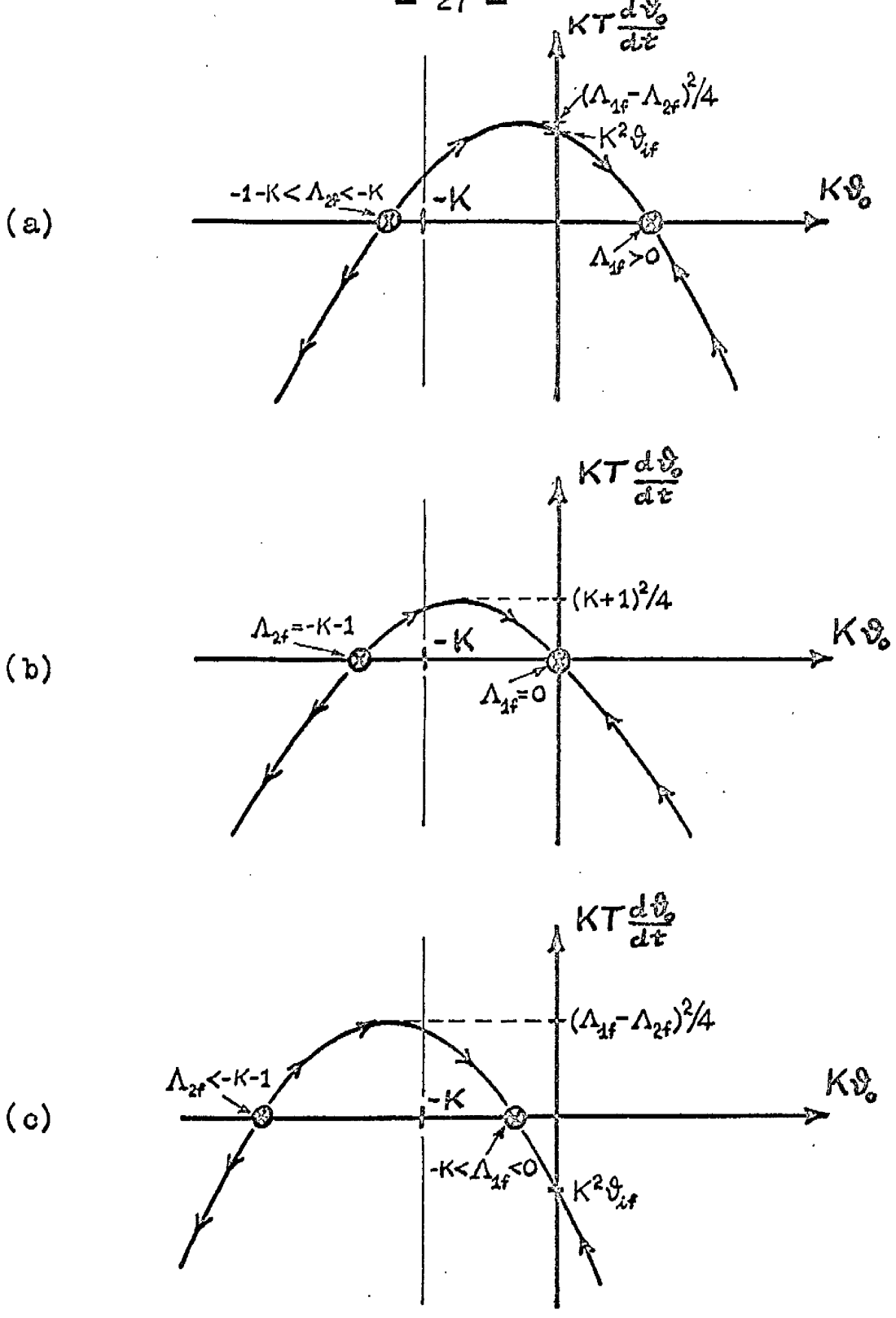

⊗ denotes a singularity in the phase plane

Figure 2.3: Phase plane diagrams of the transient response of the first-order system with an α-type gain element for (a) $\vartheta_{if} > 0$, (b) $\vartheta_{if} = 0$, (c) $\vartheta_{if} < 0$

the roots–surface indicates that Λ_{1o} (for which $\vartheta_{oo} > -1$) represents an initially stable equilibrium, Λ_{2o} ($\vartheta_{oo} < -1$) an initially unstable equilibrium. The input is subjected to a step at $t = 0$ to the value of ϑ_{if}, and the system responds according to equation (2.1.1) in which $\vartheta = \vartheta_{if} - \vartheta_o$, i.e. according to

$$T\frac{d\vartheta_o}{dt} + (1 - K\vartheta_{if} + K\vartheta_o)\,\vartheta_o = K\vartheta_{if} - K\vartheta_o \qquad (2.1.6)$$

with the initial condition $\vartheta_o = \vartheta_{oo}$ at $t = 0$. In view of equation (1.1.3), the above may be written as

$$KT\frac{d\vartheta_o}{dt} = -(K\vartheta_o - \Lambda_{1f})(K\vartheta_o - \Lambda_{2f}) \qquad (2.1.7)$$

The solution of equation (2.1.7) can be represented by the "phase line" of $K\vartheta_o$ (see Andronow and Chaikin[6]), but more information is conveyed by using the phase plane of $K\vartheta_o$ and $KT\, d\vartheta_o / dt$, Figure 2.3. There is only one trajectory for a first–order system and a single diagram is strictly sufficient, but three different diagrams are given to illustrate the cases when $\vartheta_{if} > 0$, $\vartheta_{if} = 0$, and $\vartheta_{if} < 0$. The trajectory is parabolic, with a maximum value for $KT\, d\vartheta_o / dt$ of $(\Lambda_{1f} - \Lambda_{2f})^2 / 4$ at $K\vartheta_o = (\Lambda_{1f} + \Lambda_{2f}) / 2$, and the singularities at $K\vartheta_o = \Lambda_{1f}$ and Λ_{2f} are always to the right and the left, respectively, of the critical value $K\vartheta_o = -K$. The response is seen to be unstable if $K\vartheta_{oo} \leqslant \Lambda_{2f}$, and otherwise stable to $K\vartheta_o = \Lambda_{1f}$.

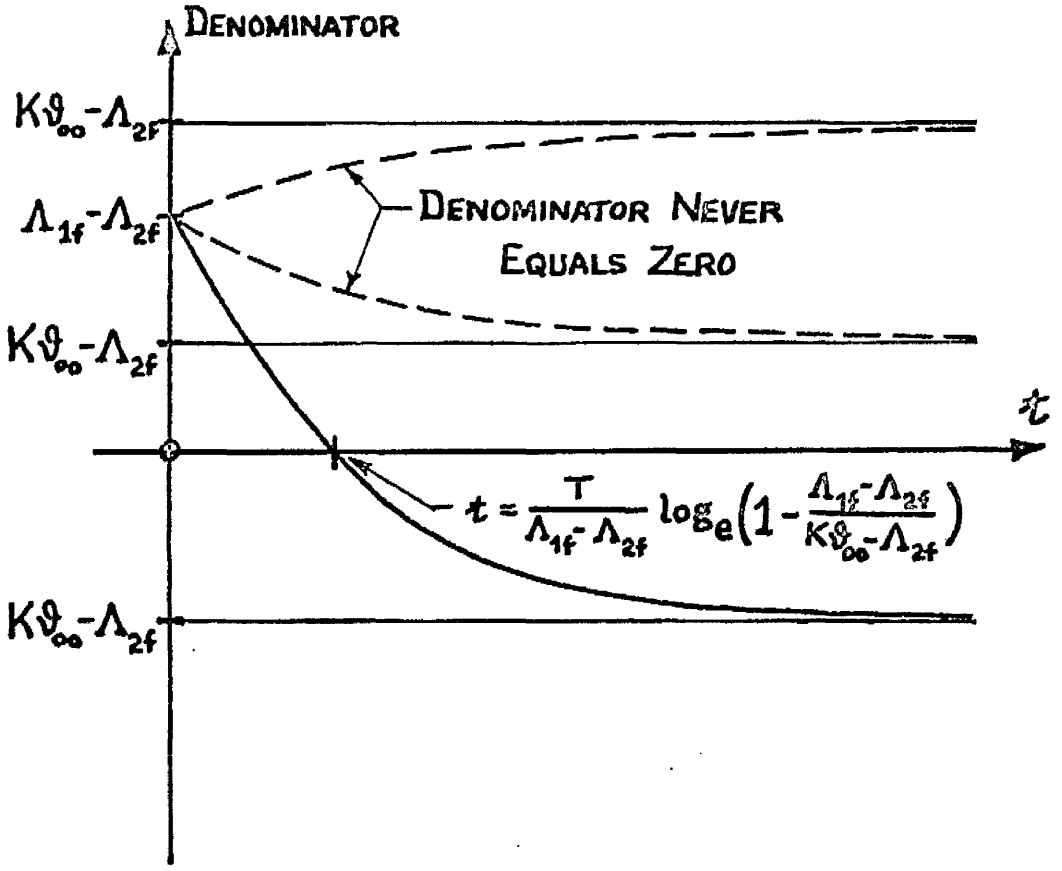

Figure 2.4 : Denominator of equation (2.1.9) as a function of time.

The solution is obtainable, however, in closed form: being a variables-separable equation, (2.1.7) may be written as

$$\int_{K\vartheta_{oo}}^{K\vartheta_o} \frac{d\,K\vartheta_o}{(K\vartheta_o - \Lambda_{1f})(K\vartheta_o - \Lambda_{2f})} = -\int_0^t \frac{dt}{T} \qquad (2.1.8)$$

leading to the solution

$$K\vartheta_o = \frac{\Lambda_{1f}(K\vartheta_{oo} - \Lambda_{2f}) - \Lambda_{2f}(K\vartheta_{oo} - \Lambda_{1f})\, e^{-(\Lambda_{1f} - \Lambda_{2f})t/T}}{(K\vartheta_{oo} - \Lambda_{2f}) - (K\vartheta_{oo} - \Lambda_{1f})\, e^{-(\Lambda_{1f} - \Lambda_{2f})t/T}} \qquad (2.1.9)$$

In the above expression, the exponent is always negative, since $\Lambda_{1f} - \Lambda_{2f} = +\sqrt{(1 - K - K\vartheta_{1f})^2 + 4K}$; hence the denominator equals zero at a time $t > 0$ given by

$$(\Lambda_{1f} - \Lambda_{2f})\,t/T = \log_e\left(1 - \frac{\Lambda_{1f} - \Lambda_{2f}}{K\vartheta_{oo} - \Lambda_{2f}}\right) \qquad (2.1.10)$$

which exists only if $K\vartheta_{oo} < \Lambda_{2f}$. This is illustrated by Figure 2.4 in which the denominator is sketched as a function of time. Thus, if $K\vartheta_{oo} < \Lambda_{2f}$ the response is violently unstable, the output tending to infinity at the finite value of time given by (2.1.10): this is to be compared with the possible behaviour of a linear system whose output, though unstable, has a finite value for all instants in time. But if $K\vartheta_{oo} > \Lambda_{2f}$, the output is asymptotically stable to the value $K\vartheta_o = \Lambda_{1f}$.

(a)

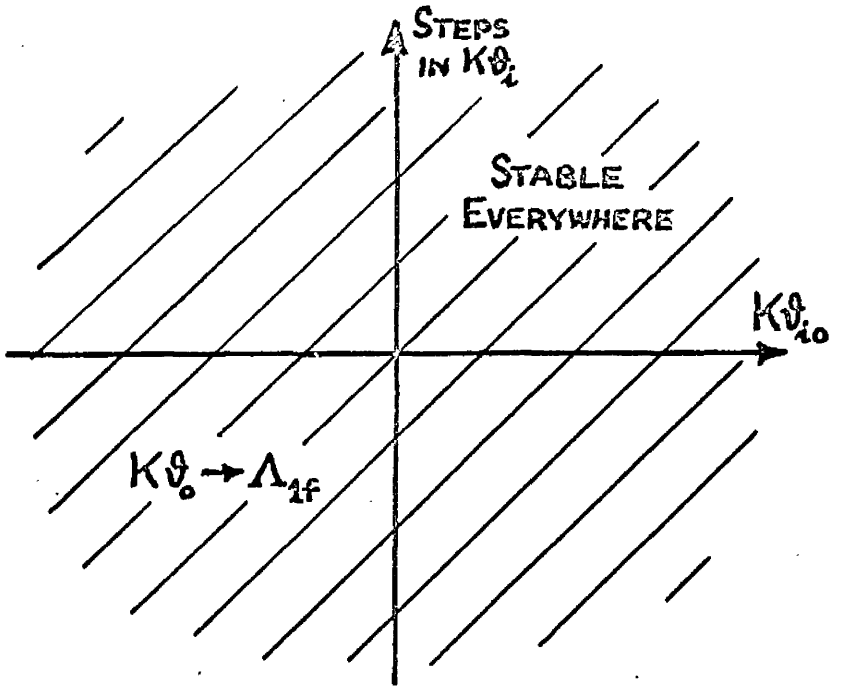

(b)

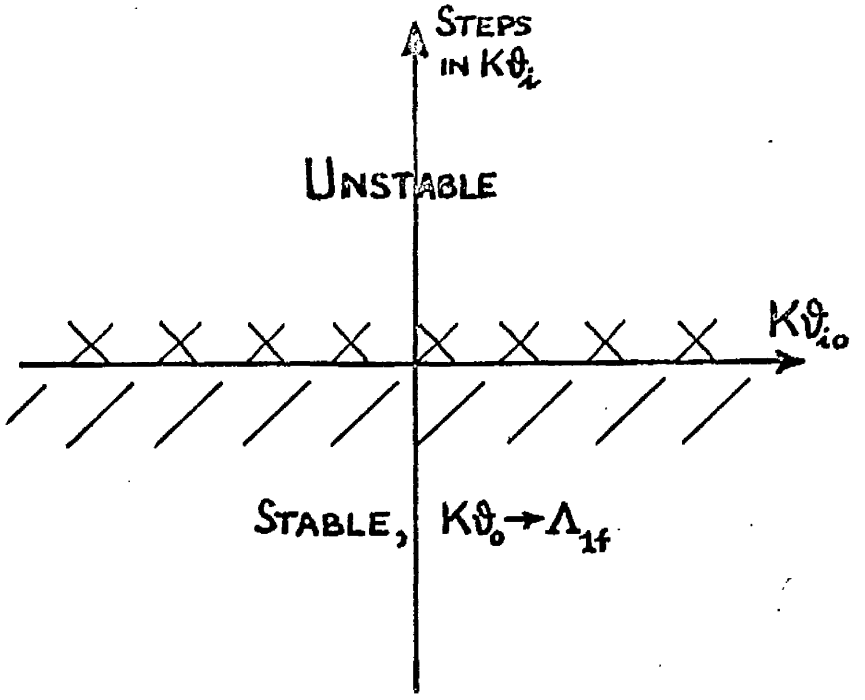

Figure 2.5: Stability diagrams for the step response of the first-order system with α-type gain element from
(a) initially stable states
(b) initially unstable states

To discover the criteria of stability in terms of the input values, use is made of the following extension of the inequality in (1.1.3):

$$\Lambda_{1o} > -K > \Lambda_{2f}$$

Because instability results only if $K\vartheta_{oo} \leqslant \Lambda_{2f}$, the response is stable for any value of ϑ_{if} if $K\vartheta_{oo} = \Lambda_{1o}$: this corresponds to a half–trajectory in the phase plane starting from a point for which $K\vartheta_o > -K$. But if $K\vartheta_{oo} = \Lambda_{2o}$, the response is stable only if $\Lambda_{2o} > \Lambda_{2f}$ which implies $\vartheta_{if} < \vartheta_{io}$: this corresponds to a half–trajectory in the phase–plane starting from a point for which $-K > K\vartheta_o > \Lambda_{2f}$. In other words, if the system is initially stable it remains stable following a step in input of any magnitude in either direction. But if the system is initially in unstable equilibrium, it may be brought into a stable state by applying a negative step of input of any magnitude. This behaviour may be appreciated by the consideration that, if the system is initially unstable, the gain is negative; to arrive at a stable state, the output must increase beyond the critical value, which calls for a decrease in the input in view of the initially negative gain.

A summary of the behaviour in regard to stability is given in Figure 2.5 in terms of the steps in $K\vartheta_i$ from an initial value of $K\vartheta_{io}$. A feature to note of such diagrams is that the $K\vartheta_{io}$ axis

must belong to a region of appropriate behaviour; that is, for the diagram relating to initially stable states, any point on the $K\vartheta_{io}$ axis corresponds to the system input not being subject to any change and must therefore belong to a region of stability, and correspondingly for the initially unstable case. In the particular case of Figure 2.5(b), the $K\vartheta_{io}$ axis is the included boundary of the region of unstable behaviour.

In an effort to correlate stable step responses of this system with the form of the roots-surface, the response (2.1.9) may be approximated by a single exponential relation

$$K\vartheta_o = \Lambda_{1f} - (\Lambda_{1f} - K\vartheta_{oo}) \, e^{-t/T'} \qquad (2.1.11)$$

where the equivalent time constant T' is chosen to give in some sense an optimum representation. A convenient measure of the quality of the response is provided by the time integral of the transient deviations of the output from its final value, i.e. by

$$\int_0^\infty (\Lambda_{1f} - K\vartheta_o) \, dt \qquad (2.1.12)$$

Through equating the value of this integral arising from the approximating response (2.1.11) to the value from the actual response (2.1.9), (cf. Nechleba[7]), the value of the equivalent pole σ' is given as

$$\sigma' = -\frac{1}{T'} = -\frac{K\vartheta_{oo} - \Lambda_{1f}}{T \log \left(1 + \frac{K\vartheta_{oo} - \Lambda_{1f}}{\Lambda_{1f} - \Lambda_{2f}} \right)} \doteq -\frac{K\vartheta_{oo} - \Lambda_{1f}}{T \log \left(1 - \frac{K\vartheta_{oo} - \Lambda_{1f}}{T\sigma_f} \right)} \qquad (2.1.13)$$

$$\text{since } \Lambda_{1f}-\Lambda_{2f}=\frac{K+(K+\Lambda_{1f})^2}{K+\Lambda_{1f}}=-T\sigma_f$$

This expresses the equivalent pole as a function of the initial and final values of $K\vartheta_o$ and of the value of the small-perturbation pole σ_f at the final value of output. Furthermore, if

$$\left|\Lambda_{1f}-K\vartheta_{oo}\right|<\left|\Lambda_{1f}-\Lambda_{2f}\right| \qquad (2.1.14)$$

so that the expansion $\log_e(1+x)=x-\frac{1}{2}x^2+\frac{1}{3}x^3-\ldots.$ converges, then

$$\sigma' = \sigma_f/(1-\tfrac{1}{2}\mu+\tfrac{1}{3}\mu^2-\ldots.) \qquad (2.1.15)$$

$$\text{where } \mu=\frac{K\vartheta_{oo}-\Lambda_{1f}}{T\sigma_f}$$

The inequality (2.1.14) reduces to $2\Lambda_{1f}-\Lambda_{2f} > K\vartheta_{oo} > \Lambda_{2f}$, since $\Lambda_{1f}>\Lambda_{2f}$: thus the expression (2.1.15), which may be preferable to (2.1.13), is valid for a stable response if $K\vartheta_{oo} < 2\Lambda_{1f}-\Lambda_{2f}$.

An alternative means of defining T' does not require the solution of the differential equation (2.1.7), as does (2.1.12) (cf. Morgan[8]). In this method,

$$T' = (\Lambda_{1f}-K\vartheta_{oo})\Big/2\left[\frac{d\,K\vartheta_o}{dt}\right]_{av} \qquad (2.1.16)$$

$$\text{where } \left[\frac{d\,K\vartheta_o}{dt}\right]_{av}=\frac{1}{\Lambda_{1f}-K\vartheta_{oo}}\int_{K\vartheta_{oo}}^{\Lambda_{1f}}\frac{d\,K\vartheta_o}{dt}.d\,K\vartheta_o$$

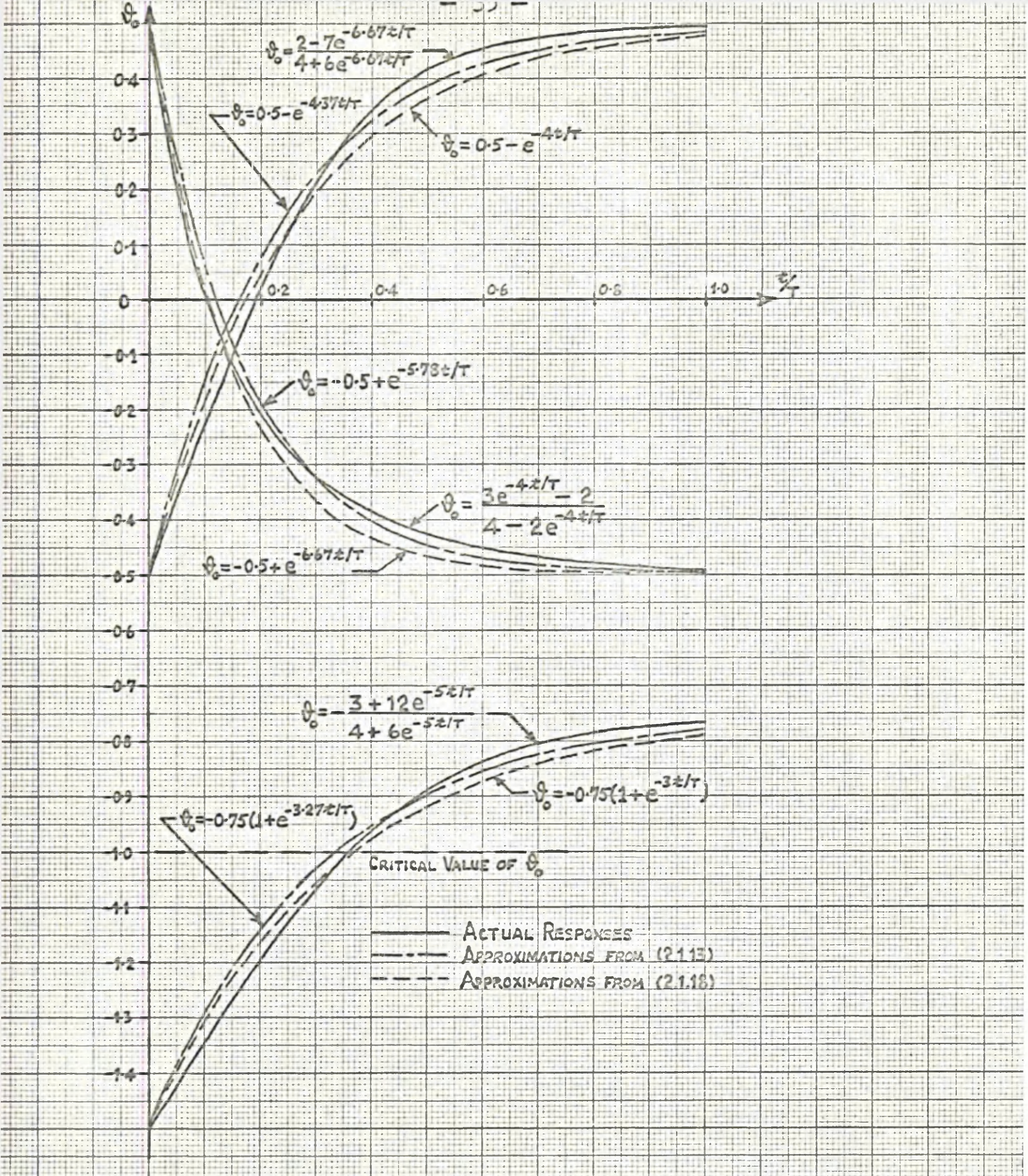

Figure 2.6: Typical stable responses of the first-order system with an a-type gain element, with corresponding approximations according to equations (2.1.13) and (2.1.18).

which yields a compatible definition of the time constant in the case of the linear first-order response. After obtaining the mean value of the first derivative of $K\vartheta_o$ over the range $K\vartheta_{oo} \leqslant K\vartheta_o \leqslant \Lambda_{1f}$, the value of the equivalent pole is given as

$$\sigma' = -\frac{\Lambda_{1f}^2 + (4K + 2K\vartheta_{oo})\Lambda_{1f} + K(3 + 3K + 2K\vartheta_{oo})}{3T(K + \Lambda_{1f})} \qquad (2.1.17)$$

Alternatively, if the appropriate substitutions are made from equation (2.1.4), there results more simply

$$\sigma' = \frac{1}{3}\sigma_f + \frac{2}{3}\sigma_o + \frac{2}{3}\frac{K(\Lambda_{1f} - K\vartheta_{oo})}{T(K + \Lambda_{1f})(K + K\vartheta_{oo})} \qquad (2.1.18)$$

The accuracy of representation by the equivalent time constants is illustrated in Figure 2.6 by the responses for $K = 4$, with $K\vartheta_{oo} = \pm 2$ and $\Lambda_{1f} = \mp 2$ respectively, and a response from an unstable equilibrium for $K = 4$, $K\vartheta_{oo} = -6$ and $\Lambda_{1f} = -3$: in each case, the movement of the small-perturbation pole is considerable. It appears that the use of either equivalent pole is of adequate accuracy for engineering purposes in estimating the nature of large transients.

The foregoing discussion relates to the response of this system from equilibrium following a single input step. Since the system theoretically requires an infinite time to reach equilibrium again, it is of interest to consider the overall

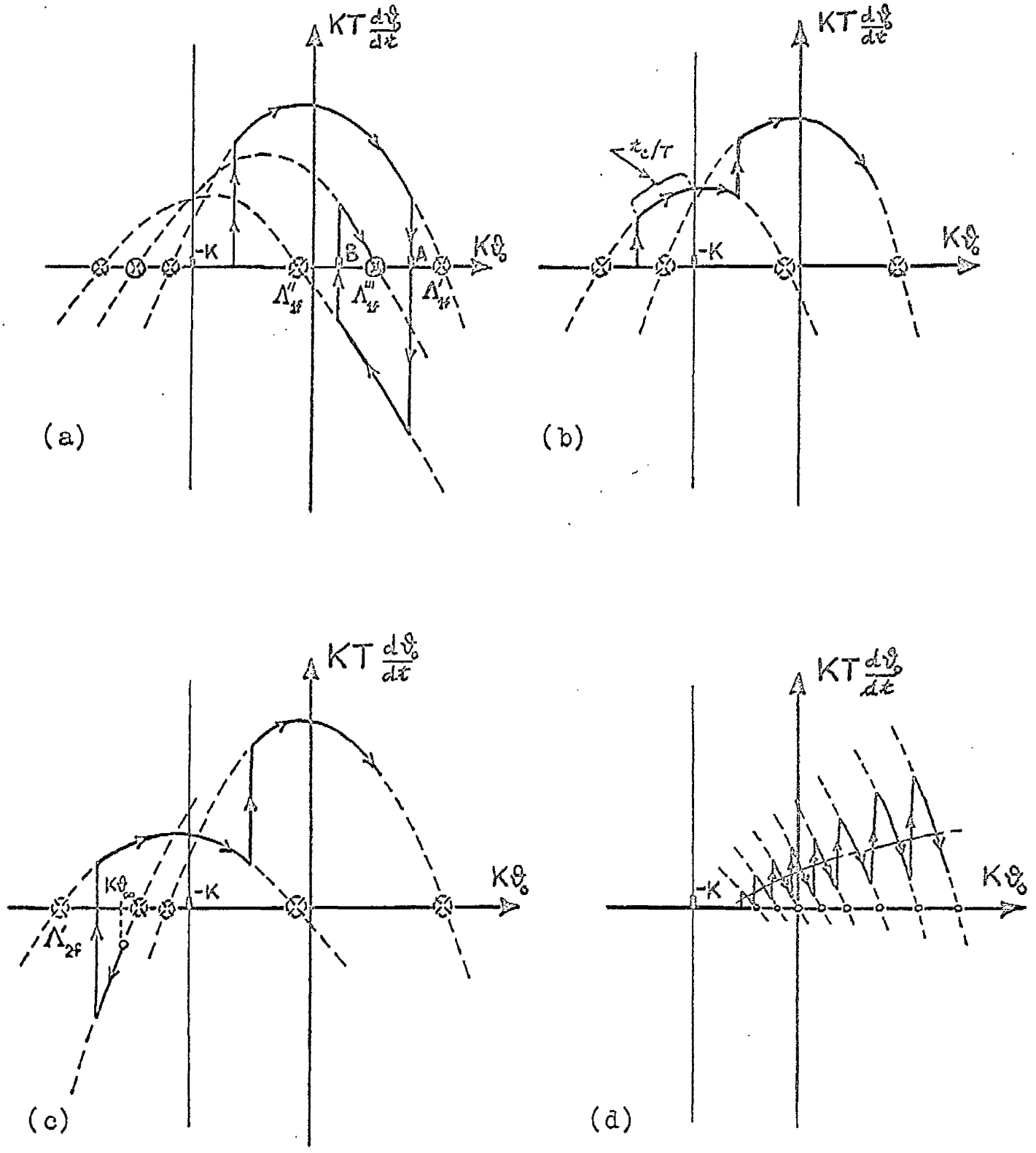

Figure 2.7 : Phase plane diagrams of the responses of the first-order system with an a-type gain element to various sequences of input steps.

response to a sequence of input steps, each step being applied before the response to the preceding one is over. In every time interval between pairs of steps the response is described by equation (2.1.9), in which Λ_{1f} and Λ_{2f} are associated with the current value of $K\vartheta_{if}$, and $K\vartheta_{oo}$ equals the value of $K\vartheta_o$ achieved at the end of the preceding interval. The following three situations are considered separately, and are depicted in Figure 2.7: (a) the normal situation where the system is in a stable state ($\vartheta_o > -1$) at the start of the period considered, which may be stable equilibrium or convergence to it; (b) the unlikely situation where the system is in unstable equilibrium initially; and (c) the more probable alternative to (a), where the system is initially unstable and diverging. The diagram (a) refers to a sequence of three steps: after the first step, the system output follows the asymptotically stable path towards Λ'_{1f}, which is shown by broken lines; but when $K\vartheta_o = A, < \Lambda'_{1f}$ the input is decreased such that Λ''_{1f} is less than A and the output begins to follow the appropriate path towards Λ''_{1f}; finally, when $K\vartheta_o = B, > \Lambda''_{1f}$ the input is increased such that $\Lambda''_{1f} < \Lambda'''_{1f} < \Lambda'_{1f}$ and the output tends asymptotically to Λ'''_{1f}. Similar diagrams may be drawn for any sequence of input steps of any magnitudes, since Figure 2.5(a) assures that step responses are always stable from initially stable states. The diagram (b) outlines the response from an initially unstable equilibrium:

so long as the input is decreased, the output tends towards a stable equilibrium and $\vartheta_o > -1$ after a time t_c given by

$$(\Lambda_{1f} - \Lambda_{2f}) t_c/T = \log_e \frac{(K\vartheta_{oo} - \Lambda_{1f})(K + \Lambda_{2f})}{(K\vartheta_{oo} - \Lambda_{2f})(K + \Lambda_{1f})} \qquad (2.1.19)$$

which for the response of Figure 2.6 from $\vartheta_{oo} = -1{\cdot}5$ is $t_c = 0{\cdot}358T$: as soon as the critical value of output is passed, input steps after any fashion may be applied and the system remains stable. In diagram (c), the output is shown diverging from the value $K\vartheta_{oo}$ at $t = 0$; if, at any instant before the time given by (2.1.10) has elapsed, the input is decreased so that Λ'_{2f} is less than the instantaneous value of $K\vartheta_o$, the system is rescued from divergence; after a further time given by (2.1.19), the system is stable and remains so following any input steps.

Information about the transient response to any input function may be obtained from a diagram similar to Figure 2.7(a), by considering the input function as the limiting case of a certain sequence of small input steps. For example, the response to a ramp input commencing at $t = 0$ can be depicted by the succession of responses of Figure 2.7(d) to progressively increasing values of Λ_{1f}, the representation improving as the size of the incremental steps decreases and the frequency increases. The important fact which is revealed without any further specific investigation is that the transient response to

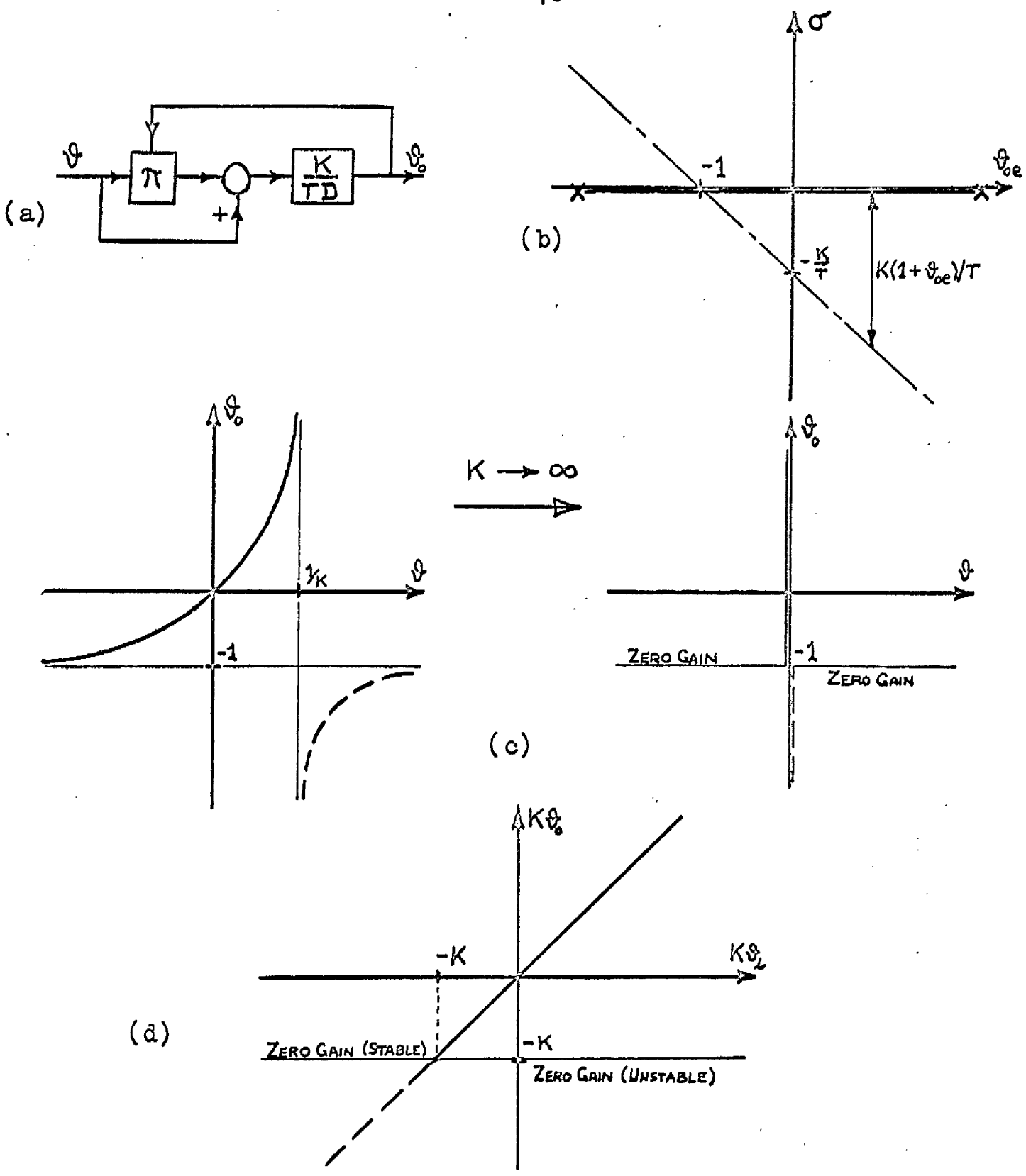

Figure 2.8 : A process comprising an α element followed by integration; (a) block diagram, (b) roots—surface, (c) derivation of static characteristic from Figure 1.1(d), (d) static characteristic of the closed-loop system.

any bounded input function is therefore stable, provided the system is initially stable.

The above discussion has referred in particular to responses to step inputs. It is clear, however, that the expressions (2.1.9) et al. are valid also for responses due to step changes in the value of K with the input constant.

2.2 A special case of the process of Section 2.1

Instead of the process of the previous section, consider that shown in Figure 2.8(a). In accordance with the general discussion in Section 1.3 of processes with a pole at the origin, this process may be regarded as that special case of the preceding one in which both K and T are very large in comparison to unity. Its direct characteristics and those of the closed-loop system round it may thus be inferred from the previous results, with one reservation to be discussed later.

If K and T in equation (2.1.2) are very large, the resulting small-signal transfer function is

$$\frac{\delta\vartheta_o(p)}{\delta\vartheta(p)} = \frac{K(1+\vartheta_{oe})}{Tp} \qquad (2.2.1)$$

for which the corresponding roots-surface is Figure 2.8(b). The static behaviour may be obtained from that of the α-type element in which $K \to \infty$; thus, the characteristic of the process alone is obtained from Figure 1.1(d) as in Figure 2.8(c) in accordance

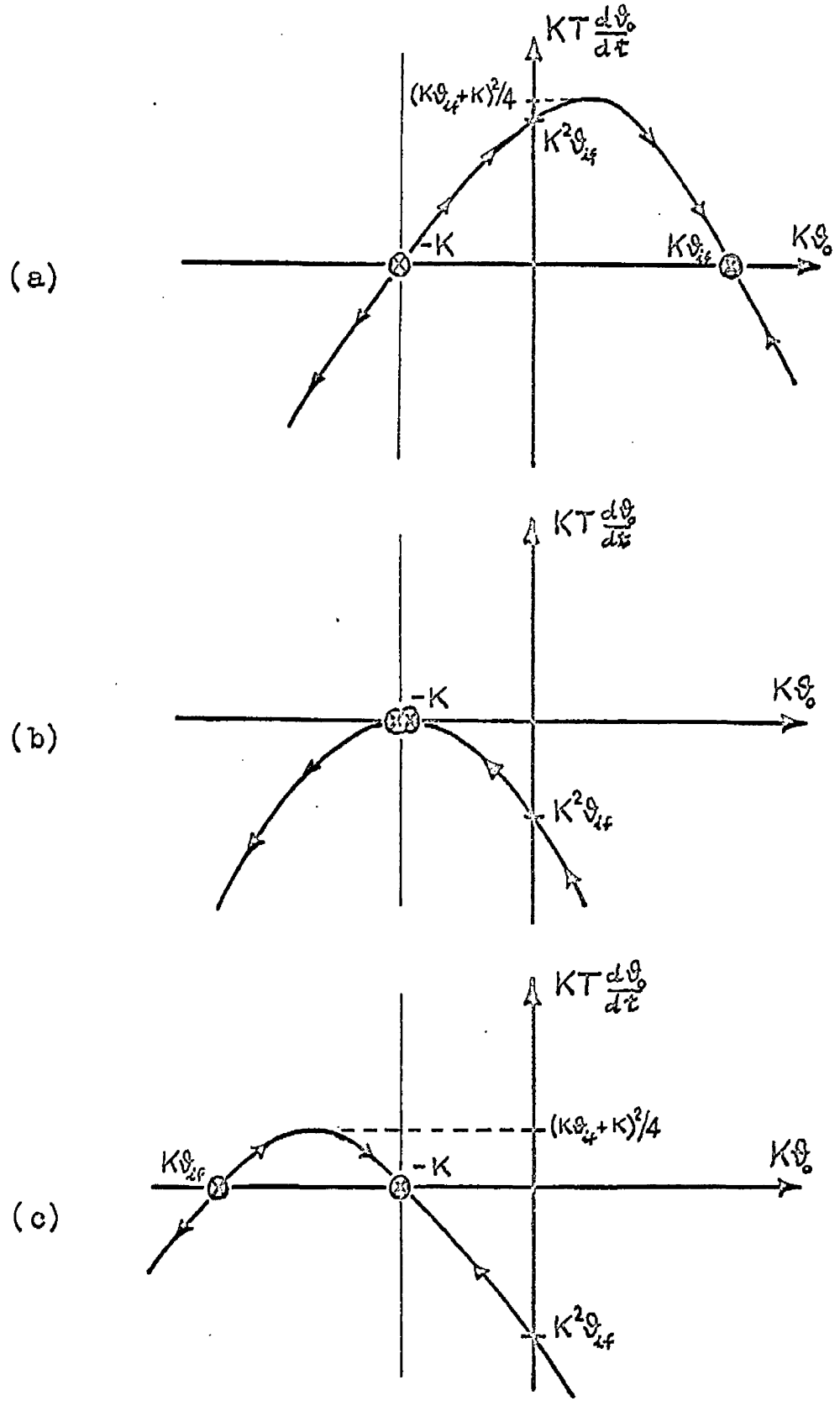

Figure 2.9 : Phase plane diagrams of the transient response of the system with an α element followed by integration for
(a) $\vartheta_{if} > -1$, (b) $\vartheta_{if} = -1$, (c) $\vartheta_{if} < -1$

with the equation

$$\vartheta_o = -1 \text{ independent of } \vartheta$$
$$\vartheta_o \text{ independent of } \vartheta, \text{ for } \vartheta = 0 \qquad (2.2.2)$$

while the resulting static characteristic of the closed-loop system is Figure 2.8(d). The two possible values of output for any value of input are now

$$\begin{matrix}\Lambda_1 = K\vartheta_i \\ \Lambda_2 = -K\end{matrix} \text{ for } K\vartheta_i > -K, \quad \begin{matrix}\Lambda_1 = -K \\ \Lambda_2 = K\vartheta_i\end{matrix} \text{ for } K\vartheta_i < -K \qquad (2.2.3)$$

and the roots-surface indicates that $\Lambda_{1o} = K\vartheta_{io}$ (positive gain) represents an initially stable equilibrium, $\Lambda_{2o} = K\vartheta_{io}$ (negative gain) an initially unstable equilibrium, but it gives no indication of the stability of the zero-gain equilibrium state; however, since the process is a limiting case of the previous one, it may be deduced that the zero-gain initial state ($\vartheta_{oo} = -1$) is stable if $\vartheta_{io} < -1$ and unstable if $\vartheta_{io} > -1$.

Following a change in input to ϑ_{if}, the transient response is described by

$$KT\frac{d\vartheta_o}{dt} = -(K\vartheta_o - K\vartheta_{if})(K\vartheta_o + K) \qquad (2.2.4)$$

with the initial condition $\vartheta_o = \vartheta_{oo}$ at $t = 0$. The relevant phase plane diagrams, which may be obtained from Figure 2.3, are given in Figure 2.9; one of the singularities always lies at the critical value $K\vartheta_o = -K$, and responses are seen to be unstable

(a)

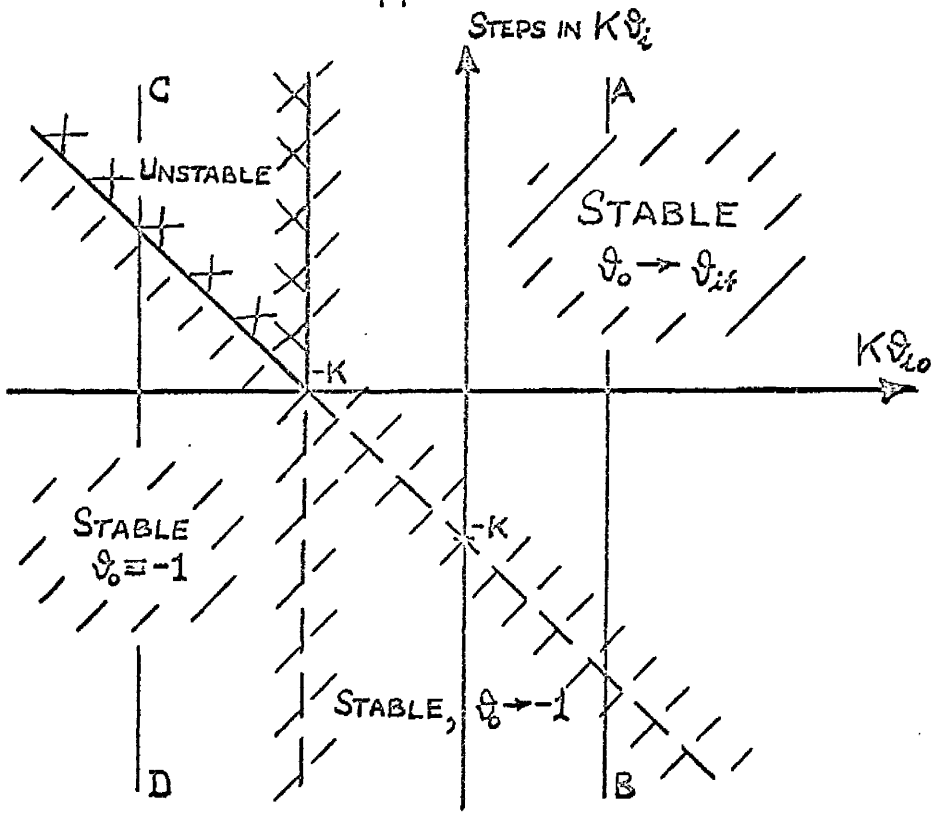

(b)

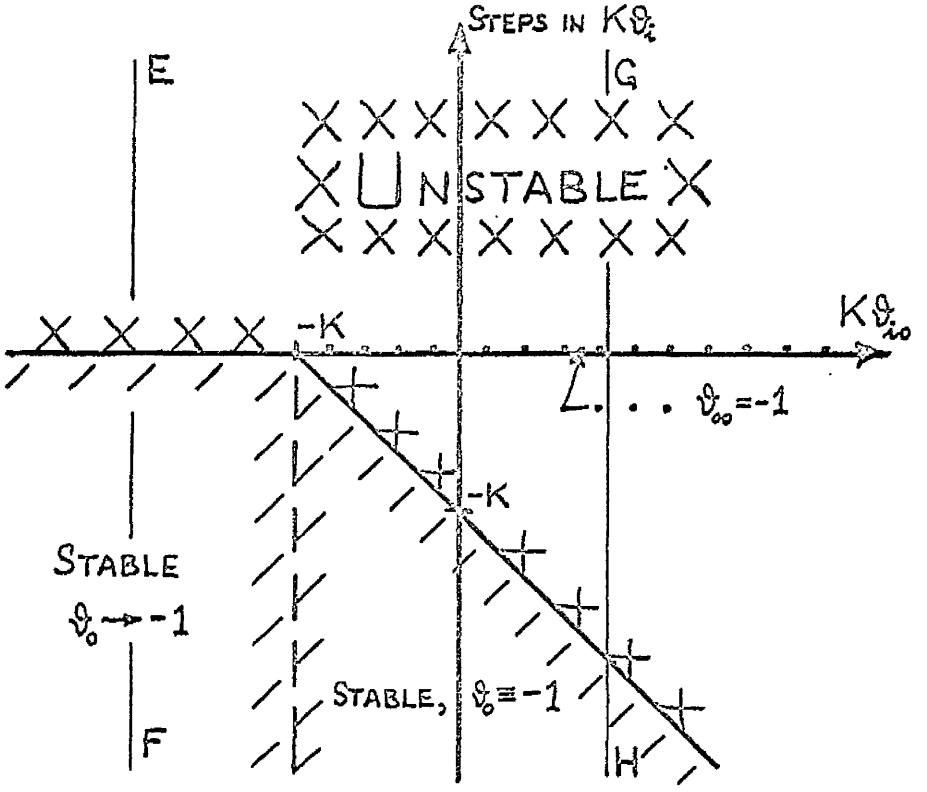

Figure 2.10 : Stability diagrams for the step response of the system with an α element followed by integration from

(a) initially stable states

(b) initially unstable states.

if $K\vartheta_{oo} \leqslant -K$ in cases (a) and (b) or if $K\vartheta_{oo} \leqslant K\vartheta_{if}$ in case (c), and otherwise stable to $\vartheta_o = \vartheta_{if}$ in case (c) or to $\vartheta_o = -1$ in cases (a) and (b). The closed form solution follows from equation (2.1.9), in which $\Lambda_{1f} = K\vartheta_{if}$ or $-K$, $\Lambda_{2f} = -K$ or $K\vartheta_{if}$ respectively, as

$$K\vartheta_o = \frac{K\vartheta_{if}(K\vartheta_{oo}+K)+K(K\vartheta_{oo}-K\vartheta_{if})\,e^{-(K+K\vartheta_{if})t/T}}{(K\vartheta_{oo}+K)-(K\vartheta_{oo}-K\vartheta_{if})\,e^{-(K+K\vartheta_{if})t/T}} \qquad (2.2.5)$$

The finite time taken for a diverging output to become infinite in this system is therefore

$$K(\vartheta_{if}+1)t/T = \log_e\left(1-\frac{\vartheta_{if}+1}{\vartheta_{oo}+1}\right) \qquad (2.2.6)$$

At this point, where stability diagrams similar to those of Figure 2.5 are to be obtained, it is important not to make false deductions on the basis of infinitely large K. The diagrams for this system are therefore derived from first principles, after which their relations to those of Figure 2.5 are discussed. To construct Figure 2.10(a), the diagram for the behaviour from initially stable states, consider firstly the situation for any input $K\vartheta_{io}$ greater than $-K$, which is indicated by the line AB: from equation (2.2.3), $K\vartheta_{oo} = K\vartheta_{io} > -K$ for initial stability and the phase plane trajectories indicate that a response from $K\vartheta_{oo} > -K$ is stable to $\vartheta_o = \vartheta_{if}$ if $\vartheta_{if} > -1$ and stable to $\vartheta_o = -1$

if $\vartheta_{if} \leqslant -1$. Now if $\vartheta_{if} \gtrless -1$, the step in $K\vartheta_i \gtrless -(K + K\vartheta_{io})$, so that consideration of all possible lines AB defines those regions indicated of stable responses in which $\vartheta_o \rightarrow \vartheta_{if}$ or -1. To complete Figure 2.10(a), consider the initially stable situation for any input $K\vartheta_{io} \leqslant -K$, line CD: since $K\vartheta_{oo} = -K$, the phase plane trajectories indicate that a response is stable if $\vartheta_{if} < -1$ — the output remains at the value -1 — and is unstable if $\vartheta_{if} \geqslant -1$. By interpreting this in terms of a step in $K\vartheta_i$, and considering the totality of lines CD, the regions of stability at $\vartheta_o \equiv -1$ and of instability are defined, which completes the diagram.

Figure 2.10(b) is constructed by similar arguments: for any $K\vartheta_{io} < -K$(line EF), $K\vartheta_{oo} = K\vartheta_{io} < -K$; responses are stable to $\vartheta_o = -1$ if $\vartheta_{if} < \vartheta_{io}$, i.e. for a negative step, and are otherwise unstable: for any $K\vartheta_{io} \geqslant -K$ (line GH), $K\vartheta_{oo} = -K$; responses are stable (ϑ_o remains at -1) if $K\vartheta_{if} < -K$, i.e. for a step in $K\vartheta_i < -(K + K\vartheta_{io})$, and are otherwise unstable.

The possibility is now evident of incorrect deductions in attempts to arrive at the complicated nature of these diagrams via those of Figure 2.5. With care, this may be acheived, as follows for Figure 2.10(a) from Figure 2.5(a): consider any value of $K\vartheta_{io} > -K$ on the earlier diagram, which indicates that the response is stable to $K\vartheta_o = \Lambda_{1f}$ for any step. Equation

(2.2.3) states that Λ_{1f} for this system becomes either $K\vartheta_{if}$ if $K\vartheta_{if} > -K$ or $-K$ if $K\vartheta_{if} < -K$, so that if the step in $K\vartheta_i$ is greater or less than $-K-K\vartheta_{if}$ the response is stable to $\vartheta_o = \vartheta_{if}$ or -1 respectively. For values of $K\vartheta_{io} < -K$, responses are still indicated as stable to $K\vartheta_o = \Lambda_{1f}$ for any step, but now $K\vartheta_{oo} = -K$: therefore, if the step in $K\vartheta_i < -K - K\vartheta_{io}$, $\Lambda_{1f} = -K$ and the output remains at the value $\vartheta_o = -1$: if the step in $K\vartheta_i > -K - K\vartheta_{io}$, $\Lambda_{1f} = K\vartheta_{if}$ but the output does <u>not</u> converge on ϑ_{if}, since the initial state $\vartheta_{oo} = -1$ has become an unstable one (Λ_{2o}) due to the increase in $K\vartheta_{if}$ beyond $-K$.

The stability characteristics of this special case of the first-order system therefore differ from those of the system itself. From an initially stable state, the system output does not always follow the input: excluding zero-gain initial states, if the magnitude of a negative step is too great the system ends up in what may be termed the 'shutdown' state of zero gain: and once in the stable shutdown state, it remains there unless caused to go unstable by too large a positive step. From an initially unstable state, this system may not be rescued and left in a finally useful (stable) state: the best that can be achieved is to leave it in the stable shutdown state. Thus, the only region of practical operation is that in Figure 2.10(a) in which $\vartheta_o \rightarrow \vartheta_{if}$ and $\vartheta_{oo} = \vartheta_{io} \neq -1$; responses of practical

interest are therefore described by the following simplification of equation (2.2.5) in terms of only input values :

$$\vartheta_o = \frac{\vartheta_{if}(\vartheta_{io}+1)+(\vartheta_{io}-\vartheta_{if})\,e^{-K(\vartheta_{if}+1)t/T}}{(\vartheta_{io}+1)-(\vartheta_{io}-\vartheta_{if})\,e^{-K(\vartheta_{if}+1)t/T}} \qquad (2.2.7)$$

The corresponding expressions to (2.1.13) et seq. for the equivalent poles of this system are as follows :— using the integral criterion,

$$\sigma' = -\frac{K(\vartheta_{if}-\vartheta_{io})}{T\log_e\left(1+\frac{\vartheta_{if}-\vartheta_{io}}{\vartheta_{io}+1}\right)} = -\frac{K(\vartheta_{io}-\vartheta_{if})}{T\log_e\left(1+\frac{\vartheta_{io}-\vartheta_{if}}{\vartheta_{if}+1}\right)} \qquad (2.2.8)$$

Since $\vartheta_{if} > 1$ and $\vartheta_{io} > 1$, the inequalities below hold :

$$\text{if } \vartheta_{if} < \vartheta_{io}, \quad \left|\frac{\vartheta_{if}-\vartheta_{io}}{\vartheta_{io}+1}\right| = \left|1-\frac{\vartheta_{if}+1}{\vartheta_{io}+1}\right| < 1$$

$$\text{if } \vartheta_{if} > \vartheta_{io}, \quad \left|\frac{\vartheta_{io}-\vartheta_{if}}{\vartheta_{if}+1}\right| = \left|1-\frac{\vartheta_{io}+1}{\vartheta_{if}+1}\right| < 1 \qquad (2.2.9)$$

which allow the use of the converging expansion for $\log_e(1+x)$ to give

$$\text{if } \vartheta_{if} > \vartheta_{io}, \ \sigma' = \sigma_f/(1-\tfrac{1}{2}\mu+\tfrac{1}{3}\mu^2-..), \ \text{where } \mu = \frac{\vartheta_{io}-\vartheta_{if}}{\vartheta_{if}+1}$$

$$\text{if } \vartheta_{if} < \vartheta_{io}, \ \sigma' = \sigma_o/(1-\tfrac{1}{2}\mu+\tfrac{1}{3}\mu^2-..), \ \text{where } \mu = \frac{\vartheta_{if}-\vartheta_{io}}{\vartheta_{io}+1} \qquad (2.2.10)$$

since $\sigma_e = -K(1+\vartheta_{ie})/T$.

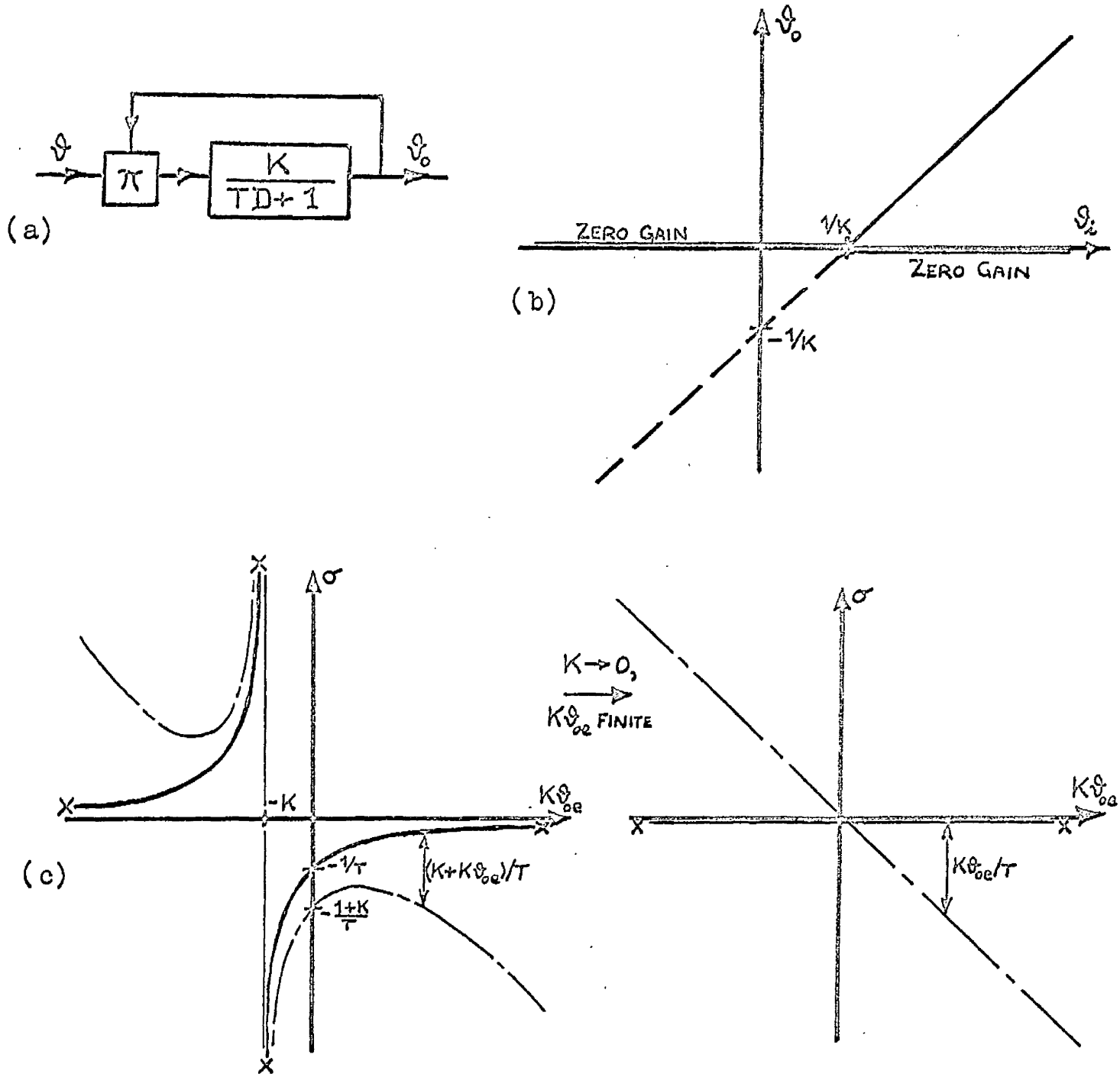

Figure 2.11 : A first-order process with a β-type gain element;
(a) block diagram
(b) static characteristic of the closed-loop system - a repeat of Figure 1.4(d)
(c) derivation of the roots-surface from Figure 2.2(b)

Using the average derivative criterion,

$$\sigma' = -\frac{K\vartheta_{if}^2 + (4 + 2\vartheta_{io})K\vartheta_{if} + (3 + 3K + 2K\vartheta_{io})}{3T(1 + \vartheta_{if})} \qquad (2.2.11)$$

$$= \frac{1}{3}\sigma_f + \frac{2}{3}\sigma_o + \frac{2}{3}\frac{\vartheta_{if} - \vartheta_{io}}{T(1 + \vartheta_{if})(1 + \vartheta_{io})} \qquad (2.2.12)$$

2.3 A process with a β–type gain element

Figure 2.11(a) is a block diagram of the first–order process with a β–type gain element chosen for investigation. It may represent approximately[9] the nuclear reactor in the fast accident condition, when the delayed neutrons are overrun by prompt neutrons, for which the differential equation is

$$\frac{dn}{dt} = \frac{\delta k - \beta}{l} n \qquad (2.3.1)$$

n = neutron population

δk = reactivity (input)

β = total fraction of delayed neutrons

l = generation time of neutrons

The special case in which the first–order lag is replaced by integration is treated in the next section.

Reference to Figure 2.1(a) shows that this process is the β–element equivalent of that of Section 2.1. On the basis of the general approach of Section 1.4, all the characteristics of

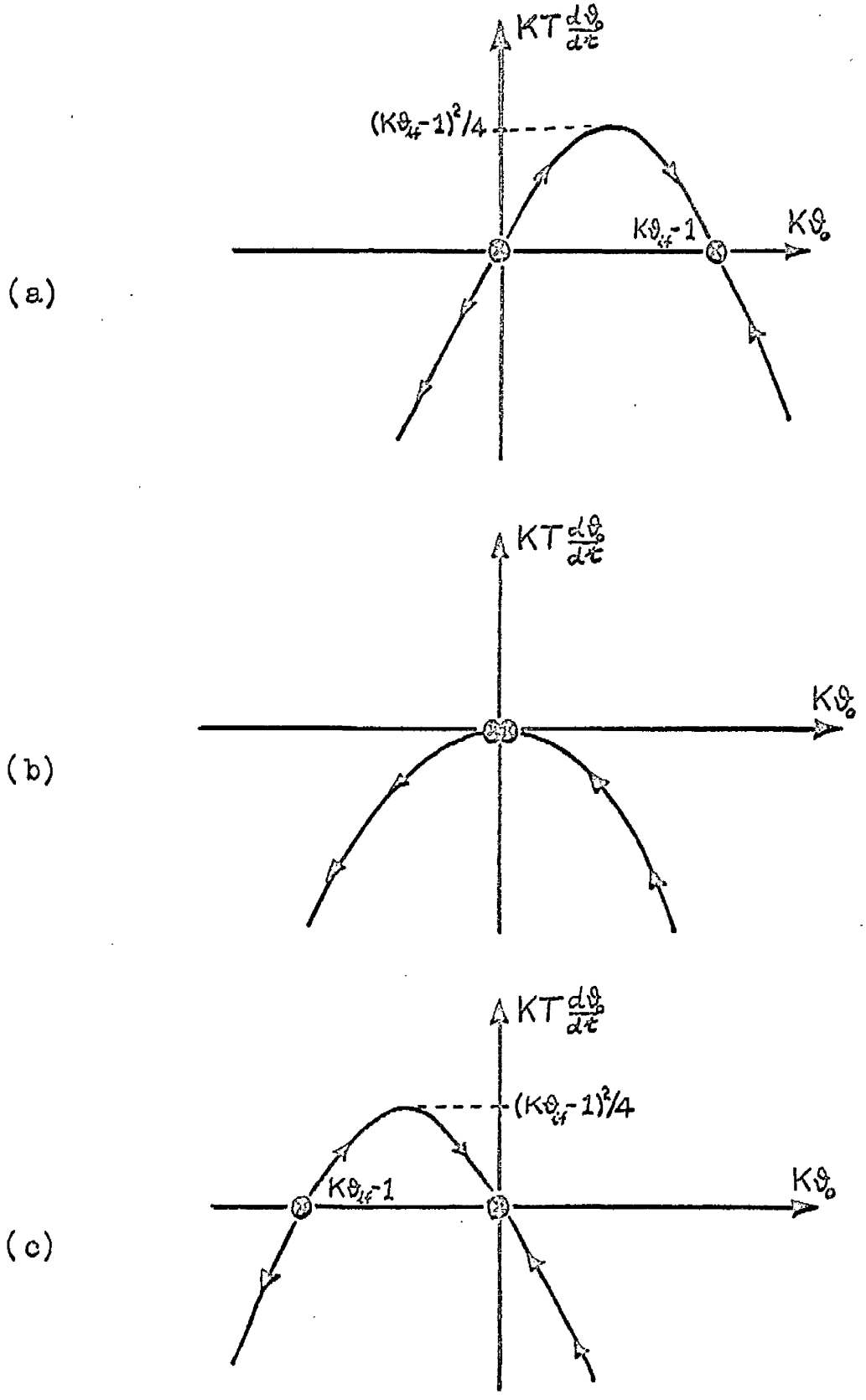

Figure 2.12 : Phase plane diagrams of the transient response of the first-order system with a β-type gain element for (a) $K\vartheta_{if} > 1$, (b) $K\vartheta_{if} = 1$, (c) $K\vartheta_{if} < 1$

this system are deducible from those of the α–element process of Section 2.1, by considering the gain factor K to be decreased to zero while $K\vartheta$, etc. remain finite and non–zero.

The static characteristics have already been presented in Figure 1.4, but the closed–loop relationship is displayed again for convenience in Figure 2.11(b); the two possible values of output for any value of input are

$$\left.\begin{aligned}\Lambda_1 &= K\vartheta_i - 1\\ \Lambda_2 &= 0\end{aligned}\right\} \text{ for } K\vartheta_i > 1\,, \qquad \left.\begin{aligned}\Lambda_1 &= 0\\ \Lambda_2 &= K\vartheta_i - 1\end{aligned}\right\} \text{ for } K\vartheta_i < 1 \qquad (2.3.2)$$

Figure 2.11(c) shows the derivation of the roots–surface from that of Figure 2.2(b); since $p_1 = 0$ for this process, the open–loop pole is always at the origin. The stability of equilibrium states follows both from the roots–surface and from the characteristics of the process of Section 2.1 by extension; i.e. Λ_{1o} is a stable initial state, Λ_{2o} is an unstable one, irrespective of the value of $K\vartheta_{io}$ and including zero–gain initial states.

Following a change in input to ϑ_{if}, the output responds according to

$$KT\frac{d\vartheta_o}{dt} = -K\vartheta_o\,(K\vartheta_o + 1 - K\vartheta_{if}) \qquad (2.3.3)$$

with $\vartheta_o = \vartheta_{oo}$ at $t = 0$. The phase plane trajectories (Figure 2.12) are again parabolic, being special instances of those of Figure 2.3; but since one of the singularities is at the origin,

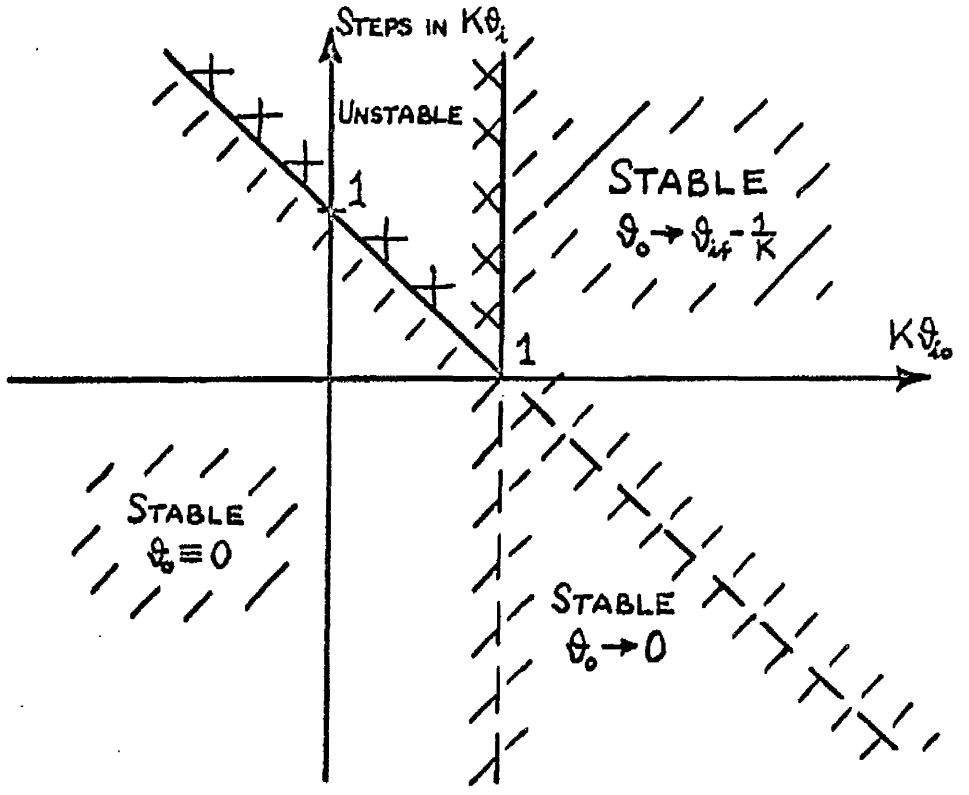

(a)

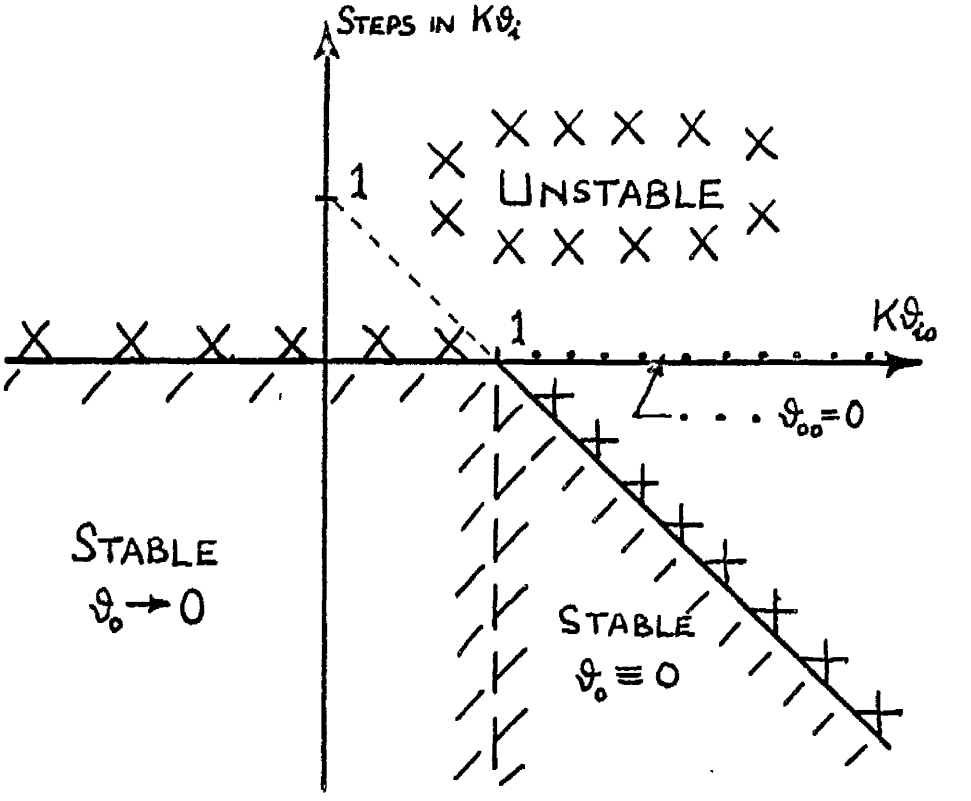

(b)

Figure 2.13: Stability diagrams for the step response of the first-order system with a β-type gain element from
(a) initially stable states
(b) initially unstable states.

responses are unstable if $K\theta_{oo} \leqslant 0$ in cases (a) and (b) or if $K\theta_{oo} \leqslant K\theta_{if}$ in case (c), and otherwise stable to $\theta_o = \theta_{if} - 1/K$ in case (c) or to $\theta_o = 0$ in cases (a) and (b). The closed-form solution follows from equation (2.1.9) in which $\Lambda_{1f} = K\theta_{if} - 1$ or 0, $\Lambda_{2f} = 0$ or $K\theta_{if} - 1$ respectively, as

$$K\theta_{oo} - (K\theta_{oo} - K\theta_{if} + 1) e^{K\theta_{oo}} (K\theta_{if} - 1) \qquad (2.3.4)$$

If especially $K\theta_{if} = 1$, case (b), the solution is

I: $$K\theta_o = K\theta_{oo} / (1 + K\theta_{oo} t/T)$$

$$K\theta_o = K\theta_{oo} / (1 + K\theta_{oo} t/T) \qquad (2.3.5)$$

The finite time taken for a diverging output to become infinite is therefore, in general,

$$t = \frac{T}{K\theta_{if} - 1} \log_e \frac{K\theta_{oo} - K\theta_{if} + 1}{K\theta_{oo}} \qquad (2.3.6)$$

and if $K\theta_{if} = 1$,

$$t = - T/K\theta_{oo}$$

Diagrams to indicate the stability behaviour following step inputs may be constructed on first principles; they may, however, be correctly obtained by extension from those of Figure 2.5, so long as care is exercised as mentioned at the similar development in the previous Section. The diagrams obtained for this system are shown in Figure 2.13, and in appearance are similar to those for the system with an α-type

element followed by integration: the common point of the various regions is different, being at $K\theta_{io} = 1$ rather than $-K$, and the values to which the output converges are altered. The only region of practical operation is that in Figure 2.13(a) in which $\theta_o \rightarrow \theta_{if} - 1/K$ and $\theta_{oo} = \theta_{io} - 1/K \neq 0$: responses of practical interest can therefore be described by the following version of equation (2.3.4) in terms of only input values:

$$K\theta_o = \frac{(K\theta_{io}-1)(K\theta_{if}-1)}{(K\theta_{io}-1)+(K\theta_{if}-K\theta_{io})\,e^{(1-K\theta_{if})t/T}} \qquad (2.3.7)$$

The analagous expressions to (2.1.13) et seq. for the equivalent poles of this system follow from equation (2.3.7):

using the integral criterion,

$$\sigma' = -\frac{K(\theta_{if}-\theta_{io})}{T\log\left(1+\frac{K(\theta_{if}-\theta_{io})}{K\theta_{io}-1}\right)} = -\frac{K(\theta_{io}-\theta_{if})}{T\log\left(1+\frac{K(\theta_{io}-\theta_{if})}{K\theta_{if}-1}\right)} \qquad (2.3.8)$$

Since $K\theta_{if} > 1$ and $K\theta_{io} > 1$, the following inequalities hold:

$$\text{if } \theta_{if} < \theta_{io}, \left|\frac{K(\theta_{if}-\theta_{io})}{K\theta_{io}-1}\right| = \left|1-\frac{K\theta_{if}-1}{K\theta_{io}-1}\right| < 1$$

$$\text{if } \theta_{if} > \theta_{io}, \left|\frac{K(\theta_{io}-\theta_{if})}{K\theta_{if}-1}\right| = \left|1-\frac{K\theta_{io}-1}{K\theta_{if}-1}\right| < 1 \qquad (2.3.9)$$

which allow the use of the converging expansion for $\log_e(1+x)$ to give

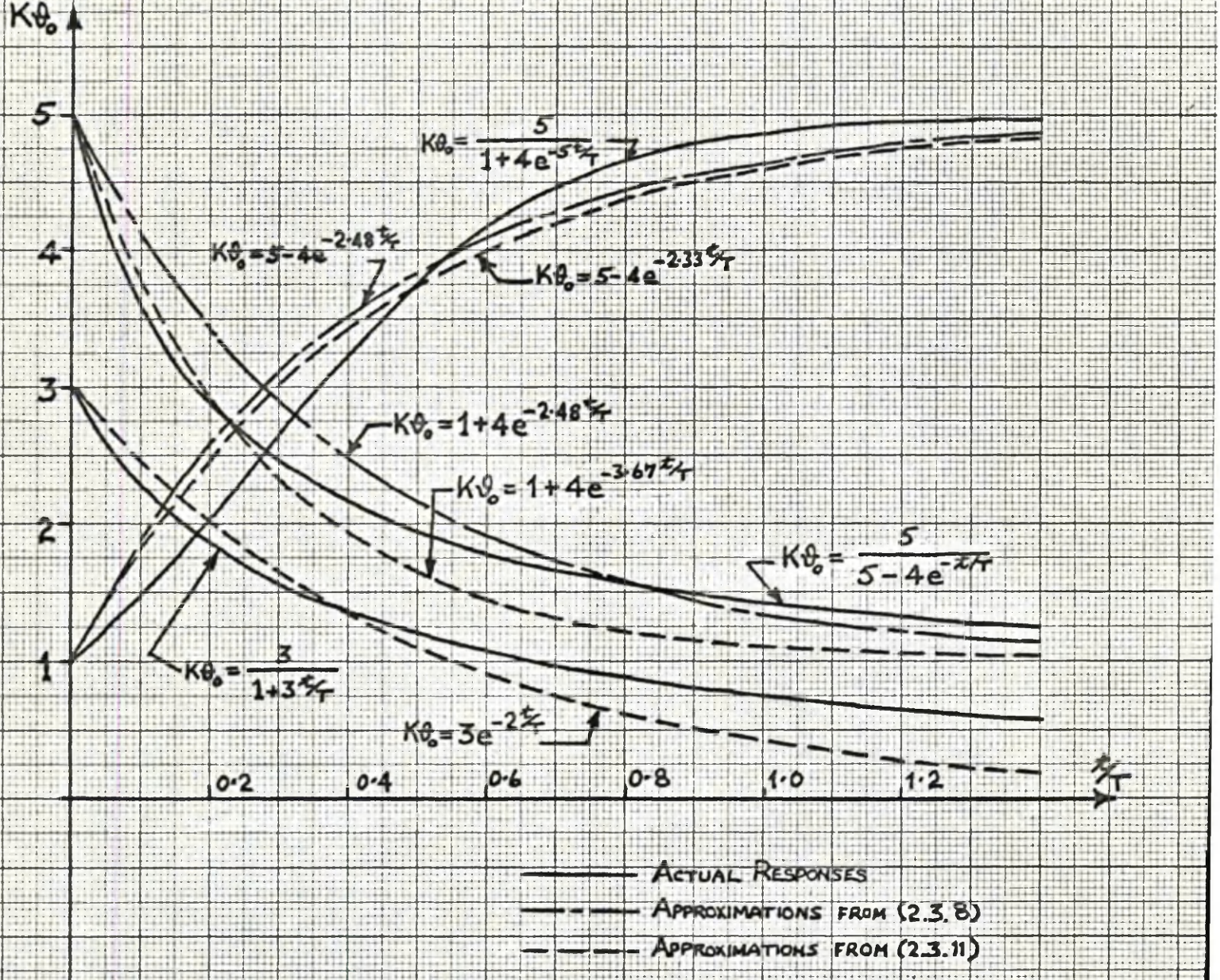

Figure 2.14: Typical stable responses of the first-order system with a β-type gain element, with corresponding approximations according to equations (2.3.8) and (2.3.11).

$$\text{if } \vartheta_{if} > \vartheta_{io},\ \sigma' = \sigma_f / \left(1 - \tfrac{1}{2}\mu + \tfrac{1}{3}\mu^2 - \ldots\right) \text{ where } \mu = \frac{K(\vartheta_{io} - \vartheta_{if})}{K\vartheta_{if} - 1}$$

(2.3.10)

$$\text{if } \vartheta_{if} < \vartheta_{io},\ \sigma' = \sigma_o / \left(1 - \tfrac{1}{2}\mu + \tfrac{1}{3}\mu^2 - \ldots\right) \text{ where } \mu = \frac{K(\vartheta_{if} - \vartheta_{io})}{K\vartheta_{io} - 1}$$

$$\text{since } \sigma_e = -(K\vartheta_{ie} - 1)/T \ .$$

Using the average derivative criterion, a simple result is obtained:

$$\sigma' = -(K\vartheta_{if} + 2K\vartheta_{io} - 3)/3T \qquad (2.3.11)$$

Finally, in the special case of $K\vartheta_{if} = 1$, the integral criterion produces an infinite value for T', i.e. an equivalent pole at the origin: this is because the time integral (2.1.12) of the transient deviations of the output does not have a finite value in this case. This result is worthless, but the value produced by the alternative criterion is simply $\sigma' = 2\sigma_o/3$.

The accuracy of representation by the equivalent time constants for this system is shown by the typical responses in Figure 2.14. A point to note about the expression (2.3.8) is that the same value of σ' results if $K\vartheta_{if}$ and $K\vartheta_{io}$ are interchanged, as demonstrated by the responses for $K\vartheta_{if} = 2$ or 6, $K\vartheta_{io} = 6$ or 2 respectively: in either case $\sigma' = -2{\cdot}48\ t/T$. This effect occurs also in the corresponding expression (2.2.8) of the preceding system, but not in the system of Section 2.1. In addition, the response from $K\vartheta_{oo} = 1$ is seen to have an inflexion

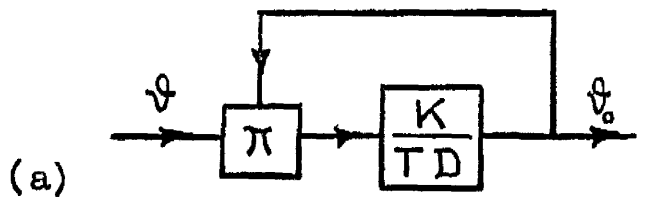

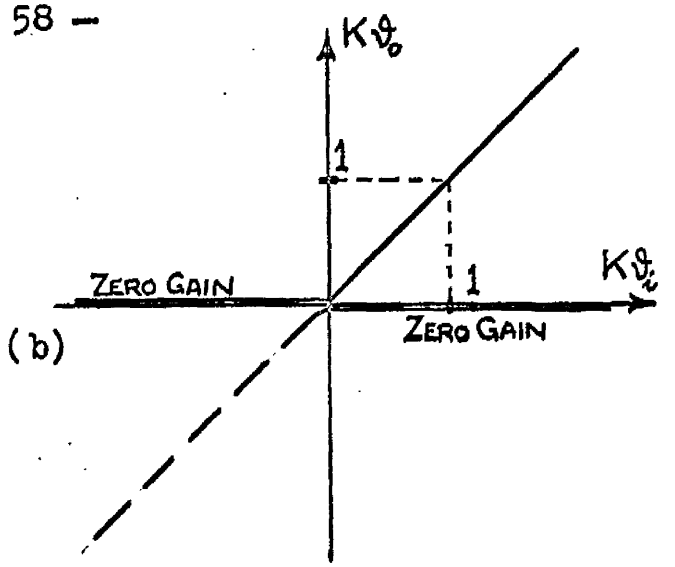

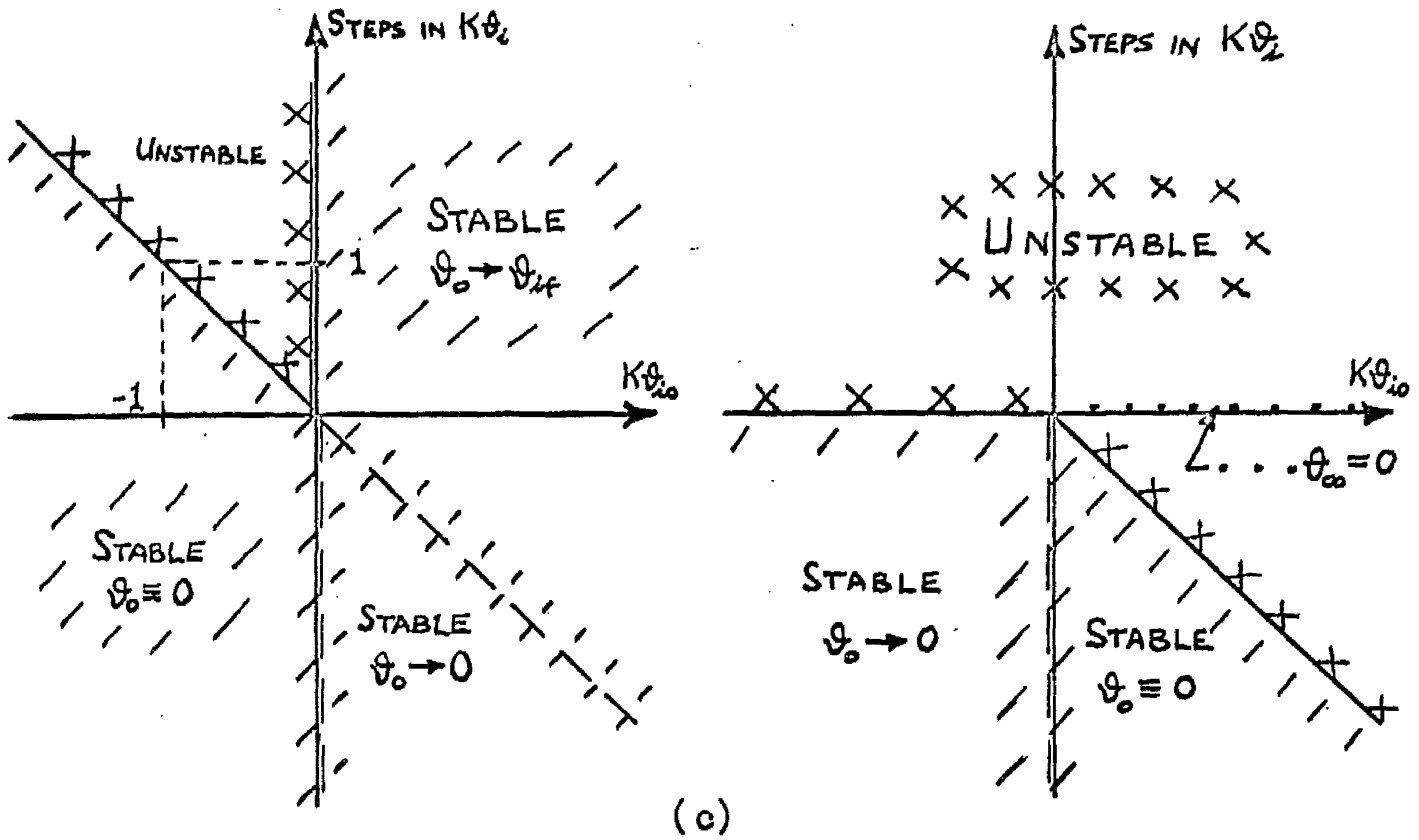

Figure 2.15 : A special case of the β–type process with a first–order lag;
(a) block diagram
(b) static closed–loop characteristic
(c) stability diagrams.

in it, at $K\vartheta_o = \frac{1}{2}(K\vartheta_{if} - 1) = 2{\cdot}5$; in fact, responses in any of the first-order systems have inflexions corresponding to the apex of the parabolic trajectory in the phase plane, if $K\vartheta_{oo}$ is sufficiently small. This suggests that a better approximation to the form of these responses might be effected with a second-order, overdamped linear expression, but the complexity of this approach prevented its use. Apart from the independent choice of the two equivalent time constants according to suitable criteria, a third factor requires determination: for a good approximation the value of the initial velocity of the output has to be non-zero and is therefore involved.

2.4 A special case of the process of Section 2.3

Just as the α-type process with a pole at the origin can be regarded as a special case of the α-type process with a first-order lag, so can all the characteristics of the process of Figure 2.15(a) be deduced from those of the process of the previous section. For this purpose, the factors K and T are considered to be very large in comparison to unity; the resulting characteristics are described quite briefly.

The static characteristic, Figure 2.15(b), of the closed-loop system follows from Figure 2.11(b); the two possible values of output for any value of input are

$$\begin{matrix}\Lambda_1 = K\theta_i \\ \Lambda_2 = 0\end{matrix} \quad \text{for } K\theta_i > 0\,, \qquad \begin{matrix}\Lambda_1 = 0 \\ \Lambda_2 = K\theta_i\end{matrix} \quad \text{for } K\theta_i < 0 \qquad (2.4.1)$$

The roots–surface is identical to the previous one, Figure 2.11(c), providing another example of its non–uniqueness to a certain process. Following a change in input to θ_{if}, the response is described by

$$KT\frac{d\theta_o}{dt} = -K\theta_o\,(K\theta_o - K\theta_{if}) \qquad (2.4.2)$$

so that phase plane diagrams are very similar to those of Figure 2.12 : there is always a singularity at the origin, while the second one is at $K\theta_o = K\theta_{if}$ rather than $K\theta_{if} - 1$, and the maximum value of $KT\,d\theta_o/dt$ is now $(K\theta_{if})^2/4$.

The explicit solutions of equation (2.4.2) give the response to be

$$K\theta_o = \frac{K\theta_{if}}{1 + \left(\dfrac{\theta_{if}}{\theta_{oo}} - 1\right) e^{-K\theta_{if}\,t/T}} \qquad (2.4.3)$$

$$= \frac{K\theta_{oo}}{1 + K\theta_{oo}\,t/T} \qquad \text{if } K\theta_{if} = 0$$

A diverging output becomes infinitely great at a time

$$t = \frac{T}{K\theta_{if}} \log\left(1 - \frac{\theta_{if}}{\theta_{io}}\right) \qquad (2.4.4)$$

$$= -T/K\theta_{oo} \qquad \text{if } K\theta_{if} = 0$$

The stability diagrams, Figure 2.15(c), may be obtained from Figure 2.13 by letting K tend to infinity; they indicate that the only region of practical interest is that in which $\theta_o \longrightarrow \theta_{if}$ and $\theta_{oo} = \theta_{io} \neq 0$. The corresponding expressions to (2.3.8) et seq. for the equivalent poles of this system are as follows:–

using the integral criterion,

$$\sigma' = -\frac{K(\theta_{if}-\theta_{io})}{T\log\left(1+\frac{\theta_{if}-\theta_{io}}{\theta_{io}}\right)} = -\frac{K(\theta_{io}-\theta_{if})}{T\log\left(1+\frac{\theta_{io}-\theta_{if}}{\theta_{if}}\right)} \qquad (2.4.5)$$

if $\theta_{if} > \theta_{io}$, $\sigma' = \sigma_f / (1-\frac{1}{2}\mu+\frac{1}{3}\mu^2-..)$ where $\mu = \dfrac{\theta_{io}-\theta_{if}}{\theta_{if}}$

if $\theta_{if} < \theta_{io}$, $\sigma' = \sigma_o / (1-\frac{1}{2}\mu+\frac{1}{3}\mu^2-..)$ where $\mu = \dfrac{\theta_{if}-\theta_{io}}{\theta_{io}}$

since $\sigma_e = -K\theta_{ie}/T$;

using the average derivative criterion,

$$\sigma' = -(K\theta_{if} + 2K\theta_{io})/3T$$
$$= 2\sigma_o/3 \quad \text{if} \quad K\theta_{if} = 0 \qquad (2.4.6)$$

2.5 Some general remarks

The foregoing investigations into selected first-order output-dependent processes do not strengthen the argument for obtaining information about large-scale behaviour from the roots-surface. The entire stability diagrams of any of the

preceding three sections could not be deduced from the appearance of the corresponding roots-surface: only the simpler diagrams of the first process considered might be constructed through intuitive reasoning from its roots-surface. Expressions for equivalent time constants have been arrived at which appear to be of reasonable use in estimating the form of transient responses; however, the time constants are not functions only of small-signal time constants at suitable output levels, but also depend on values of the input and/or output, initially or finally. No means has been discovered of predicting the form of the transient response directly from the roots-surface, in the simplest case of first-order systems.

CHAPTER 3

The Control of a Second-Order Process with an α-Type Gain Element

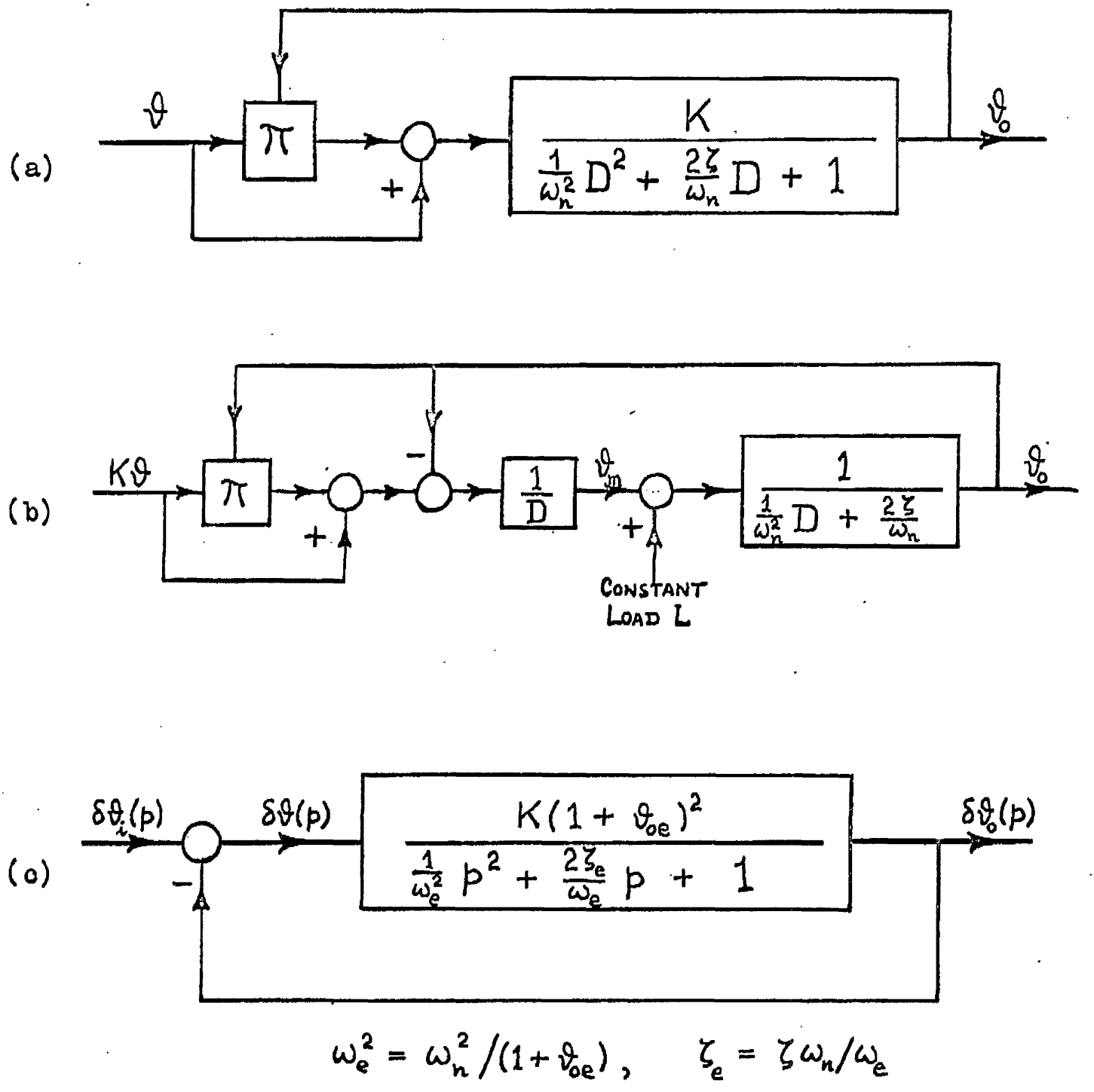

$$\omega_e^2 = \omega_n^2/(1+\vartheta_{oe}), \qquad \zeta_e = \zeta\omega_n/\omega_e$$

Figure 3.1: (a) Block diagram of a second–order process, incorporating an α – type gain element
(b) Block diagram of an equivalent process to (a)
(c) Block diagram for perturbations in a closed loop around the process.

CHAPTER 3

The Control of a Second-Order Process with An α-Type Gain Element

3.1 Introductory aspects

In a progressive development of this study, a natural choice for a second-order process with an α-type gain element to follow the first-order process of Section 2.1 is that for which Figure 3.1(a) is a block diagram. With the notation of the general process of Section 1.3, the coefficients p_1 and q_m are zero for m greater than two, q_1 equals $2\zeta/\omega_n$, and $q_2 = 1/\omega_n^2$ for this process. The differential equation is, in accordance with the general form (1.3.8), the following:

$$\frac{1}{\omega_n^2}\frac{d^2\vartheta_o}{dt^2} + \frac{2\zeta}{\omega_n}\frac{d\vartheta_o}{dt} + (1 - K\vartheta)\,\vartheta_o = K\vartheta \qquad (3.1.1)$$

The block diagram of Figure 3.1(a) is not, of course, a unique representation, and a suggested alternative is given in Figure 3.1(b): this process could be described by the pair of equations

$$\frac{1}{\omega_n^2}\frac{d\vartheta_o}{dt} + \frac{2\zeta}{\omega_n}\vartheta_o = \vartheta_m + L$$

$$\frac{d\vartheta_m}{dt} = K(1 + \vartheta_o)\vartheta - \vartheta_o \qquad (3.1.2)$$

which are equivalent to equation (3.1.1) if the intermediate variable ϑ_m is eliminated.

The static characteristic is that of the bare α – type gain element, Figure 1.1(d), and the small-signal transfer function follows from equation (1.3.10) as: –

$$\frac{\delta\vartheta_o(p)}{\delta\vartheta(p)} = \frac{K(1+\vartheta_{oe})^2}{(1+\vartheta_{oe})p^2/\omega_n^2 + 2\zeta(1+\vartheta_{oe})p/\omega_n + 1} \qquad (3.1.3)$$

Defining the small-signal natural frequency ω_e and damping factor ζ_e of the process to be

$$\omega_e^2 = \omega_n^2/(1+\vartheta_{oe}), \qquad \zeta_e = \zeta\omega_n/\omega_e \qquad (3.1.4)$$

the transmission from $\delta\vartheta_i$ to $\delta\vartheta_o$ when the process is controlled proportionally in a closed loop is indicated by the block diagram of Figure 3.1(c).

Since the open-loop singularities are output-dependent, the related roots-surface is three-dimensional in contrast to the planar surface of a first-order process. Construction of the roots-surface is carried out using the normalised frequency components σ/ω_n and $j\omega/\omega_n$, thus: the values of the two open-loop poles are given by

$$(\sigma + j\omega)/\omega_n = \left(-\zeta_e\omega_e \pm \omega_e\sqrt{\zeta_e^2 - 1}\right)/\omega_n = -\zeta \pm \sqrt{\zeta^2 - \frac{1}{1+\vartheta_{oe}}} \qquad (3.1.5)$$

so that, for $-1 < \vartheta_{oe} \leqslant 1/\zeta^2 - 1$, the real part $-\zeta$ is constant while the imaginary part tends to infinity as ϑ_{oe} tends to -1 and to zero as ϑ_{oe} tends to $(1/\zeta^2 - 1)$, giving a complex pole-pair:

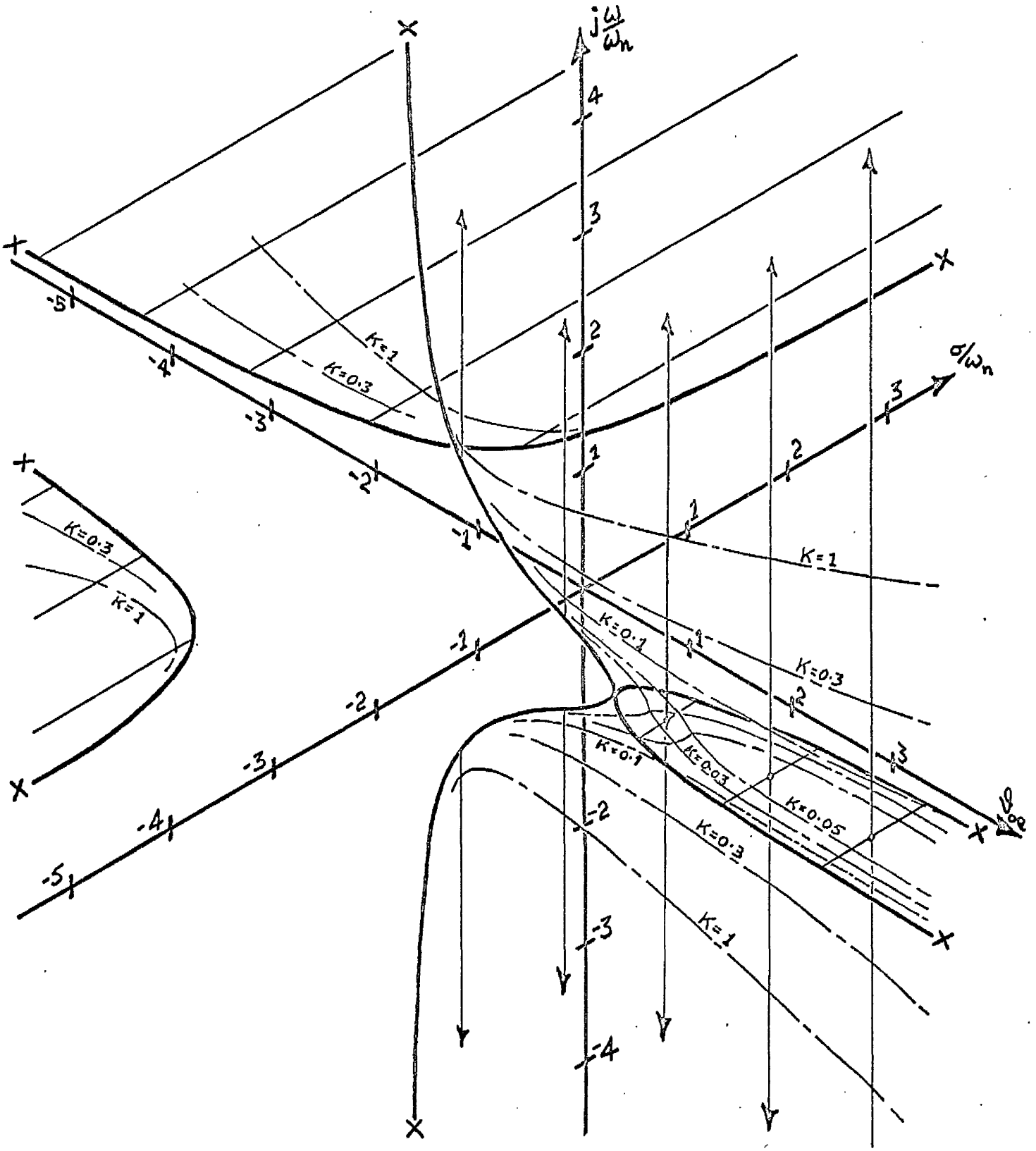

Figure 3.2: Roots-surface for a second-order process with an α — type gain element, in which $\zeta = 0{\cdot}707$

for $\vartheta_{oe} > 1/\zeta^2 - 1$ or $\vartheta_{oe} < -1$ the imaginary part is zero and the paths of the two distinct poles lie only in the real plane. To every value of ζ there corresponds a different roots-surface; for illustration, Figure 3.2 is drawn for $\zeta = 0{\cdot}707$, with the result that the roots-surface consists of:

(a) for $-1 < \vartheta_{oe} < 1$, the portions of the $\sigma/\omega_n = -\zeta$ plane "above and below" the open-loop pole paths;

(b) for $\vartheta_{oe} > 1$, the whole of the $\sigma/\omega_n = -\zeta$ plane together with the portion of the $j\omega/\omega_n = 0$ plane between the open-loop pole paths; and

(c) for $\vartheta_{oe} < -1$, the portions of the $j\omega/\omega_n = 0$ plane "to the left and to the right" of the open-loop pole paths.

Because in this case the roots-surface is composed of portions of two planes, rather than of a more general surface, the parts of the roots-surface may be presented as in Figure 3.3 in which a symmetric half of the portion of the plane $\sigma/\omega_n = -0{\cdot}707$ is rabatted into the $j\omega/\omega_n = 0$ plane. Also, the roots-surface is not really required as an aid to find the closed-loop poles: being only a second-order system, the values of the closed-loop poles are known explicitly to be

$$(\sigma + j\omega)/\omega_n = -\zeta \pm \sqrt{\zeta^2 - \frac{1 + K(1 + \vartheta_{oe})^2}{1 + \vartheta_{oe}}} \qquad (3.1.6)$$

The closed-loop pole paths, a few of which are drawn on Figures 3.2 and 3.3, lie in the real plane for $\vartheta_{oe} < -1$; and if $K \leq \zeta^4/4$,

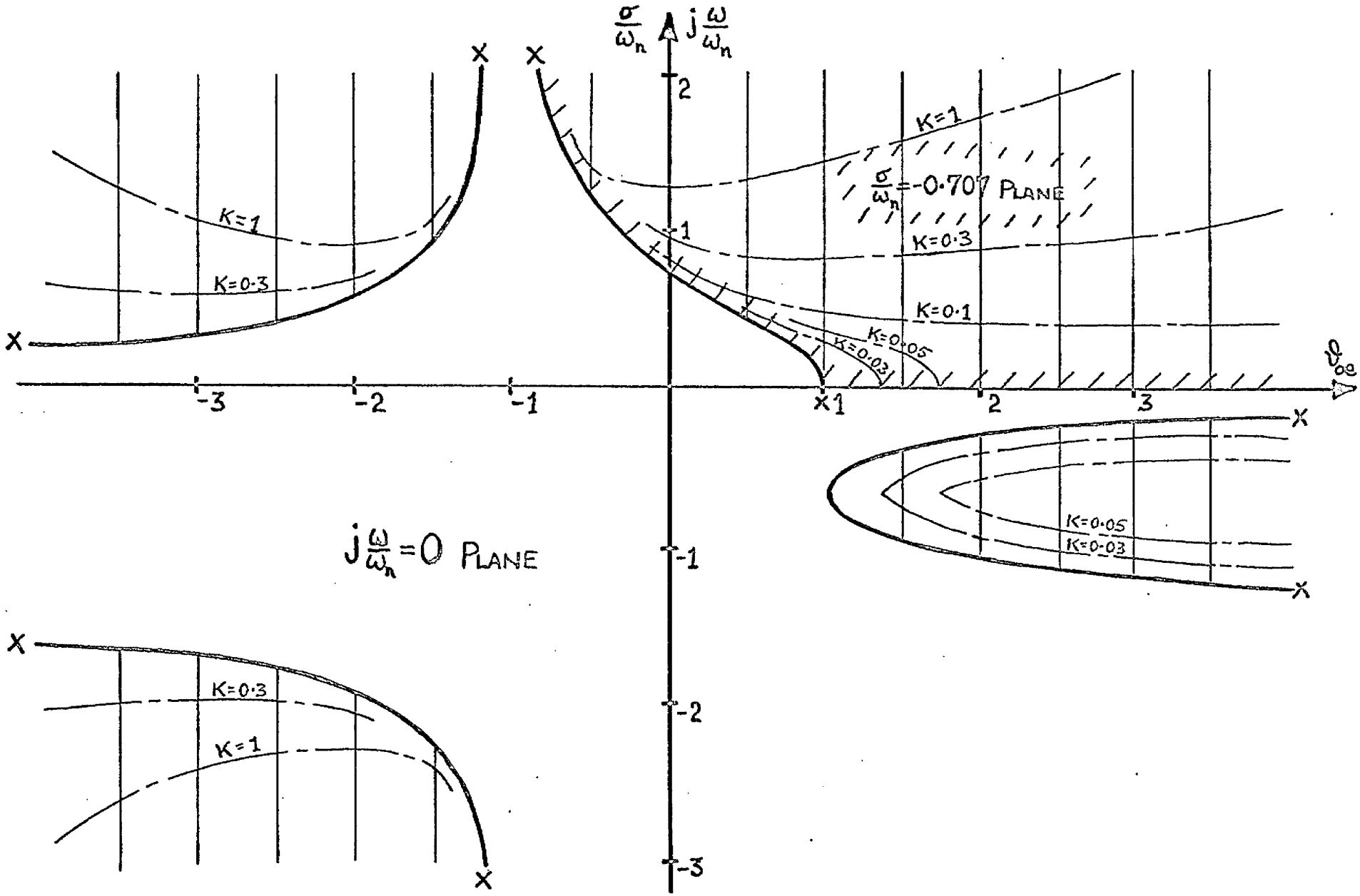

Figure 3.3 : Two-plane presentation of the roots-surface of Figure 3.2 .

the paths lie in the real plane for

$$-1+\frac{1}{2K}\left[\zeta^2-\sqrt{\zeta^4-4K}\right]<\vartheta_{oe}<-1+\frac{1}{2K}\left[\zeta^2+\sqrt{\zeta^4-4K}\right] \qquad (3.1.7)$$

but if $K>\zeta^4/4$ the paths do not enter the real plane for $\vartheta_{oe}>-1$.

Examination of the surd in (3.1.6) shows it to have extrema at $\vartheta_{oe}=-1\pm 1/K$, so that the least oscillatory small-signal response, or that with the greatest time constant, for a given value of K occurs around this mean value of output: reference to equation (2.1.4) et seq. shows this value to be identical with that for extrema in the closed-loop pole of the first-order system. As a last general remark, the roots-surface again indicates that for any given $K\vartheta_{io}$ and K the value Λ_{1o} represents an initially stable equilibrium, Λ_{2o} an initially unstable equilibrium.

3.2 The phase portraits for transient responses

This Section deals with both the familiar phase-plane portrait for transient responses and the less familiar, complementary, global representation of the behaviour throughout the entire phase space. The system input is assumed to have the value ϑ_{if} for $t>0$; at $t=0$, the output may be in either equilibrium state Λ_{1o} or Λ_{2o} corresponding to $K\vartheta_{io}$, or changing with time in a previous, uncompleted transient response. The output behaviour is therefore described by equation (3.1.1) in

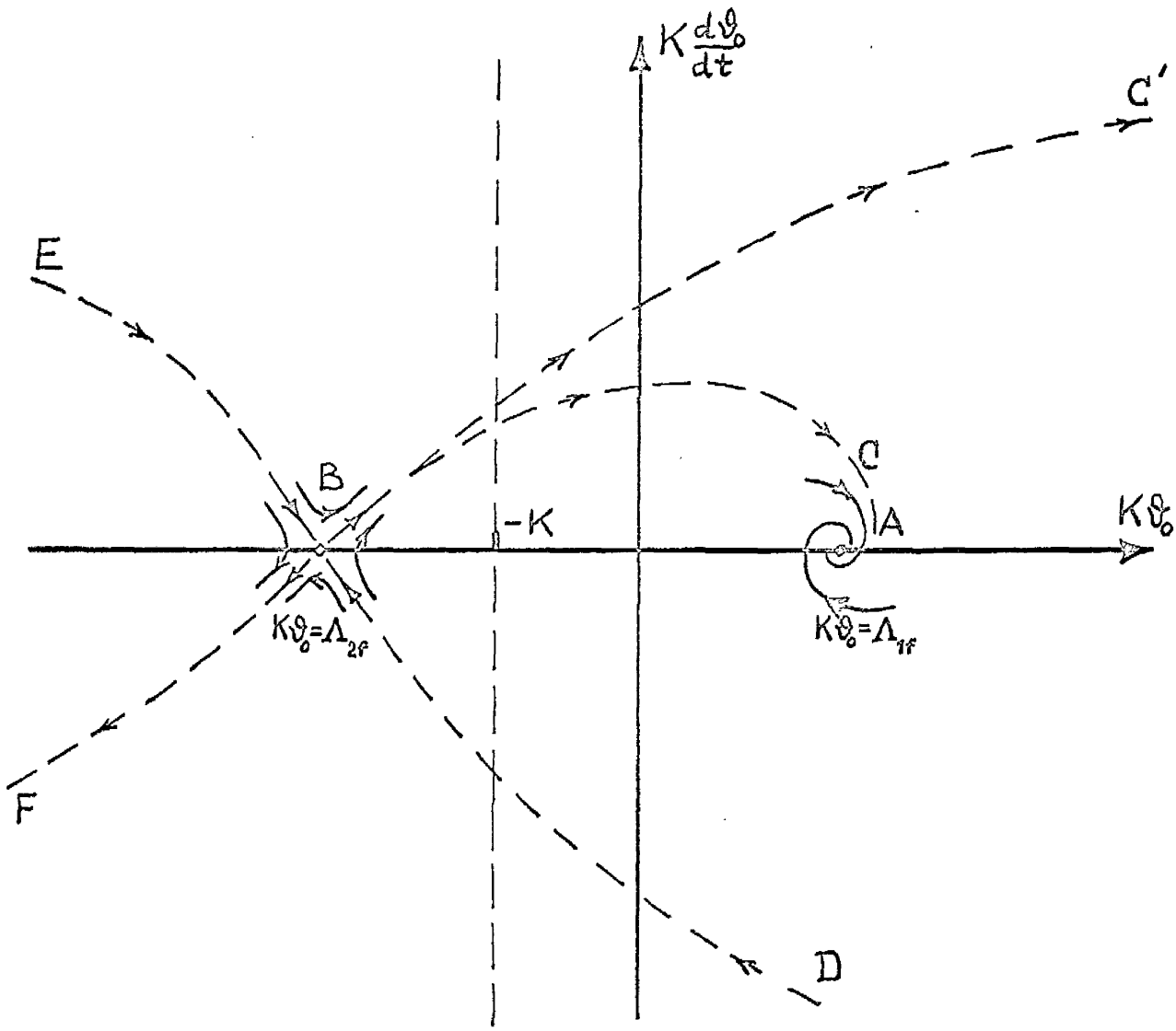

Figure 3.4 : Preliminary sketch of the phase plane portrait for the second-order system with an α - type gain element .

which $\vartheta = \vartheta_i - \vartheta_o$, i.e. by

$$\frac{K}{\omega_n^2}\frac{d^2\vartheta_o}{dt^2} + \frac{2\zeta K}{\omega_n}\frac{d\vartheta_o}{dt} + (1 + K - K\vartheta_{if})K\vartheta_o + (K\vartheta_o)^2 = K^2\vartheta_{if} \qquad (3.2.1)$$

The critical points in the phase plane of $K\vartheta_o$ and $K\,d\vartheta_o/dt$ correspond to equilibrium states of the system, of which there are two, so that their positions are:

(A) $K\vartheta_o = \Lambda_{1f}$, $K\,d\vartheta_o/dt = 0$, and (B) $K\vartheta_o = \Lambda_{2f}$, $K\,d\vartheta_o/dt = 0$

Now the roots–surface indicates that local behaviour around A is asymptotically stable to it, since both roots have negative real parts at A for any K and ζ: to be precise, if the roots at any Λ_{1f} are complex, the singularity at A is a stable focus, while if the roots are purely real – for $K \leqslant \zeta^4/4$, and Λ_{1f} within the range (3.1.7) – the singularity at A is a stable node. The roots–surface also indicates that local behaviour around B is unstable; since there is always one positive and one negative real root, the singularity at B is a saddle point (rather than an unstable node).

The information obtained thus far allows the sketch portrait of Figure 3.4 to be drawn; the singularity at A may be a stable node rather than a focus. The essential features of the full portrait could be discovered if the locations of the four separatrices of the saddle point were known throughout the phase plane; it is evident that the departing separatrix for $K\,d\vartheta_o/dt > 0$

may either wind on to the focus (BC) or avoid it (BC'), that neither of the converging separatrices (BD, BE) can come from the focus, and that the fourth separatrix (BF) cannot terminate at A, as this requires that it crosses either BD or BE and trajectories are only concurrent at singularities. But no further conclusions for the general case of equation (3.2.1) can be drawn without consideration of the behaviour at infinity.

To arrive at the portrait in a particular case of equation (3.2.1), however, the method of isoclines may be used. Since

$$K\frac{d^2\vartheta_o}{dt^2} = \left(K\frac{d\vartheta_o}{dt}\right)\frac{d}{d\vartheta_o}\frac{d\vartheta_o}{dt} = \left(K\frac{d\vartheta_o}{dt}\right)\frac{d}{dK\vartheta_o}\left(K\frac{d\vartheta_o}{dt}\right)$$

equation (3.2.1) may be written as

$$\left(K\frac{d\vartheta_o}{dt}\right)\frac{d}{dK\vartheta_o}\left(K\frac{d\vartheta_o}{dt}\right) + 2\zeta\omega_n\left(K\frac{d\vartheta_o}{dt}\right) = -\omega_n^2(K\vartheta_o - \Lambda_{1f})(K\vartheta_o - \Lambda_{2f})$$

or

$$K\frac{d\vartheta_o}{dt} = -\frac{\omega_n^2(K\vartheta_o - \Lambda_{1f})(K\vartheta_o - \Lambda_{2f})}{2\zeta\omega_n + \frac{d}{dK\vartheta_o}\left(K\frac{d\vartheta_o}{dt}\right)} \qquad (3.2.2)$$

Thus, the equation in the phase plane of an isocline on which all trajectories have the constant direction S is

$$K\frac{d\vartheta_o}{dt} = -\frac{\omega_n^2(K\vartheta_o - \Lambda_{1f})(K\vartheta_o - \Lambda_{2f})}{2\zeta\omega_n + S} \qquad (3.2.3)$$

so that by plotting many isoclines, with superimposed lineal

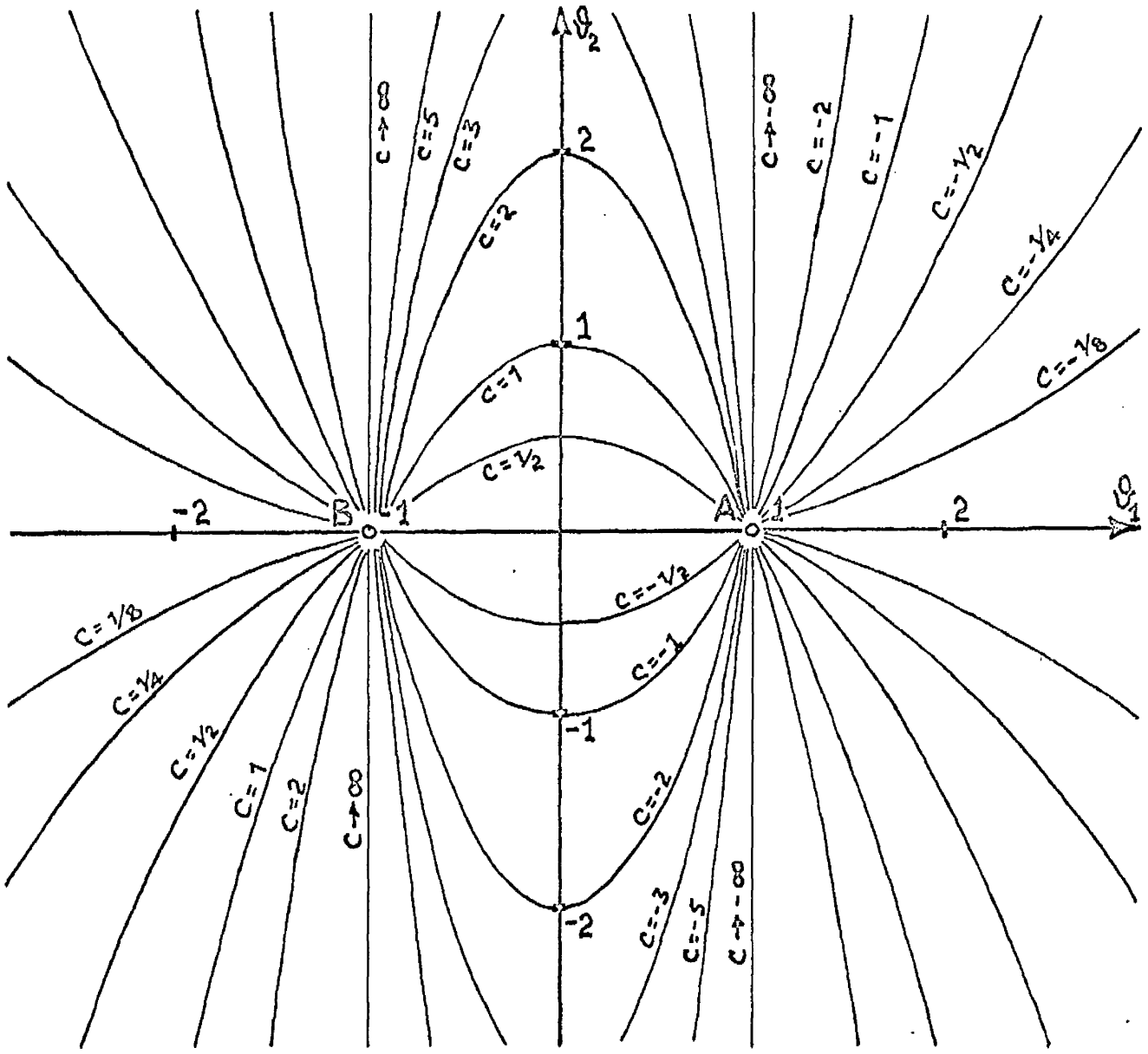

(a)

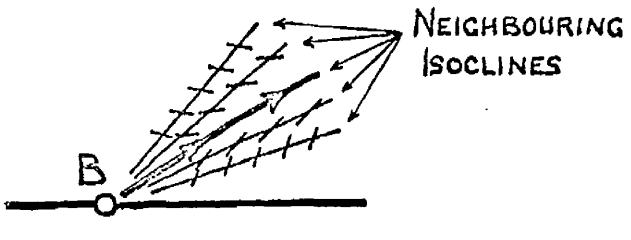

(b)

Figure 3.5: (a) Isoclines in the plane of ϑ_1 and ϑ_2

(b) Determination of the directions of the separatrices at the saddle point B .

elements in appropriate orientations, the trajectories are built up to produce the portrait. However, to each different set of values of ζ, ω_n, Λ_{1f} and Λ_{2f} corresponds a different pattern of isoclines in the phase plane; to reduce the work involved in drawing several portraits, the following linear transformation is useful:

$$\text{let } \vartheta_1 = \frac{2K\vartheta_o - (\Lambda_{1f} + \Lambda_{2f})}{\Lambda_{1f} - \Lambda_{2f}}, \quad \vartheta_2 = \frac{2}{\Lambda_{1f} - \Lambda_{2f}} K \frac{d\vartheta_o}{dt} \qquad (3.2.4)$$

Since $S = \frac{d}{dK\vartheta_o}\left(K\frac{d\vartheta_o}{dt}\right) = \frac{d\vartheta_2}{d\vartheta_1}$, the equation (3.2.3) is transformed to

$$\vartheta_2 = C(1 - \vartheta_1^2) \qquad (3.2.5)$$

$$\text{where} \quad C = \frac{\omega_n^2(\Lambda_{1f} - \Lambda_{2f})}{4\zeta\omega_n + 2S}$$

By drawing portraits in the phase plane of ϑ_1 and ϑ_2, the singularities at A and B appear always at the points (1,0) and (-1,0) and the isoclines need only be drawn once, Figure 3.5(a): for a particular isocline, with the value C, substitution of the appropriate values of ζ, ω_n, Λ_{1f} and Λ_{2f} yields the direction S which it represents.

A useful guide in an accurate construction of the portrait is the actual directions of the separatrices at the critical point. These may be determined in this way: by differentiating (3.2.5) with respect to ϑ_1, the direction of the isocline

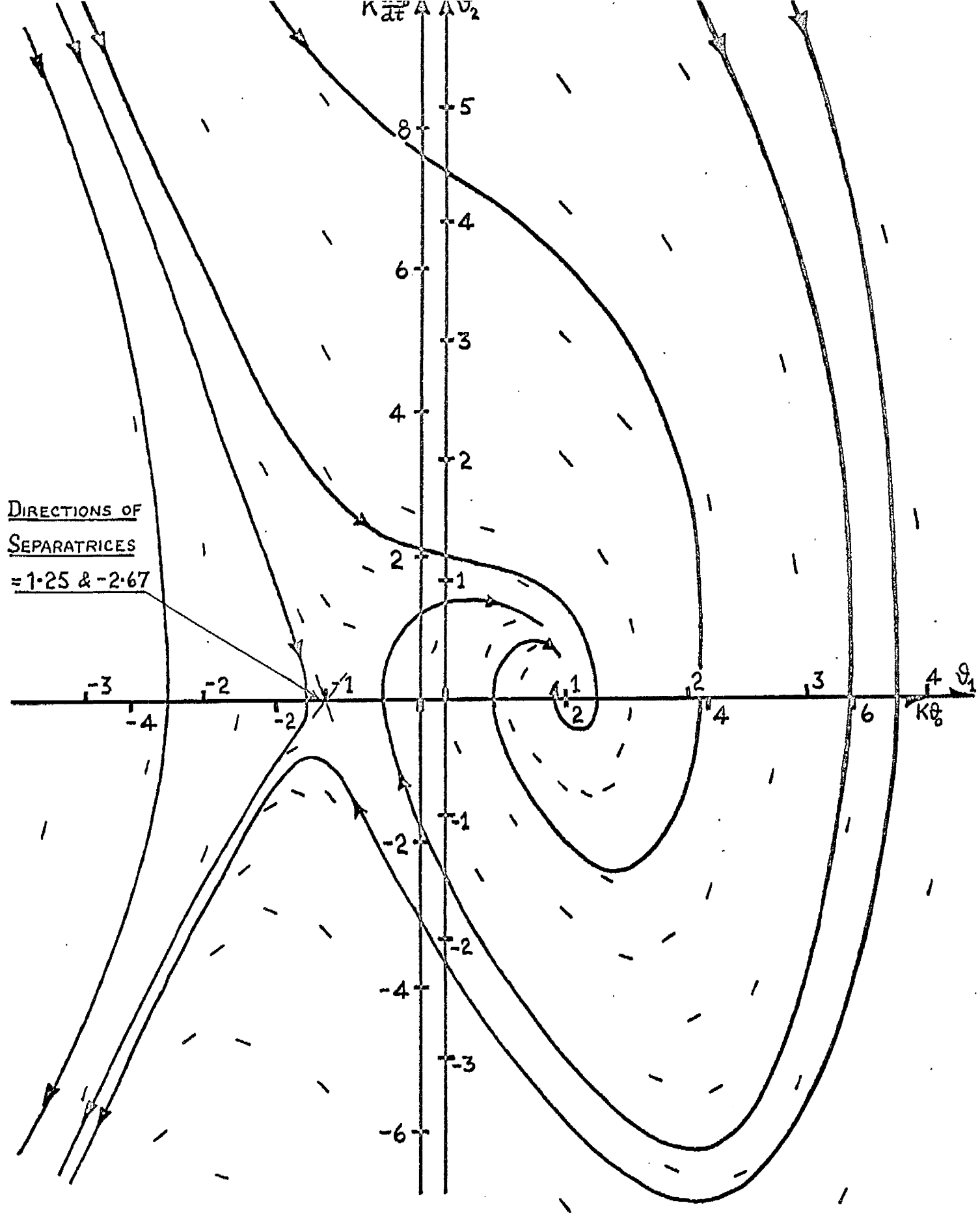

Figure 3.6 : Phase plane portrait for second-order system with α – type element, for $\zeta = 0.707$, $\omega_n = 1$, $K\theta_{if} = 8/3$ and $K = 1$.

associated with S at any point ϑ_1 is

$$\frac{d\vartheta_2}{d\vartheta_1} = \frac{\omega_n^2(\Lambda_{2f} - \Lambda_{1f})}{2\zeta\omega_n + S}\,\vartheta_1 \qquad (3.2.6)$$

Since all isoclines pass through a singularity, the direction of each isocline at B is given by (3.2.6) in which $\vartheta_1 = -1$, and the situation at B is indicated by Figure 3.5(b); a separatrix emerges from B along an isocline whose direction there equals the direction S of the trajectories on it, so that the directions of the separatrices are given by the two roots of

$$S = \frac{\omega_n^2(\Lambda_{1f} - \Lambda_{2f})}{2\zeta\omega_n + S}$$

$$\text{i.e. by} \quad S_{1,2} = -\zeta\omega_n \pm \omega_n\sqrt{\zeta^2 + \Lambda_{1f} - \Lambda_{2f}} \qquad (3.2.7)$$

As illustration, the completed phase plane portrait for $\zeta = 0{\cdot}707$, $\omega_n = 1$, $\Lambda_{1f} = 2$ and $\Lambda_{2f} = -4/3$, $K = 1$, for which $K\vartheta_{1f} = 8/3$, is shown in Figure 3.6. In this particular case, the separatrix BC of Figure 3.4 ends up at A, and BD enters the portrait in the upper half–plane, turning around A to arrive at B. To see whether this behaviour is representative of the general case or not, the behaviour far out in the plane – "at infinity" – must be investigated.

Poincaré[10] has presented suitable transformations for the determination of the behaviour in the entire phase space. The

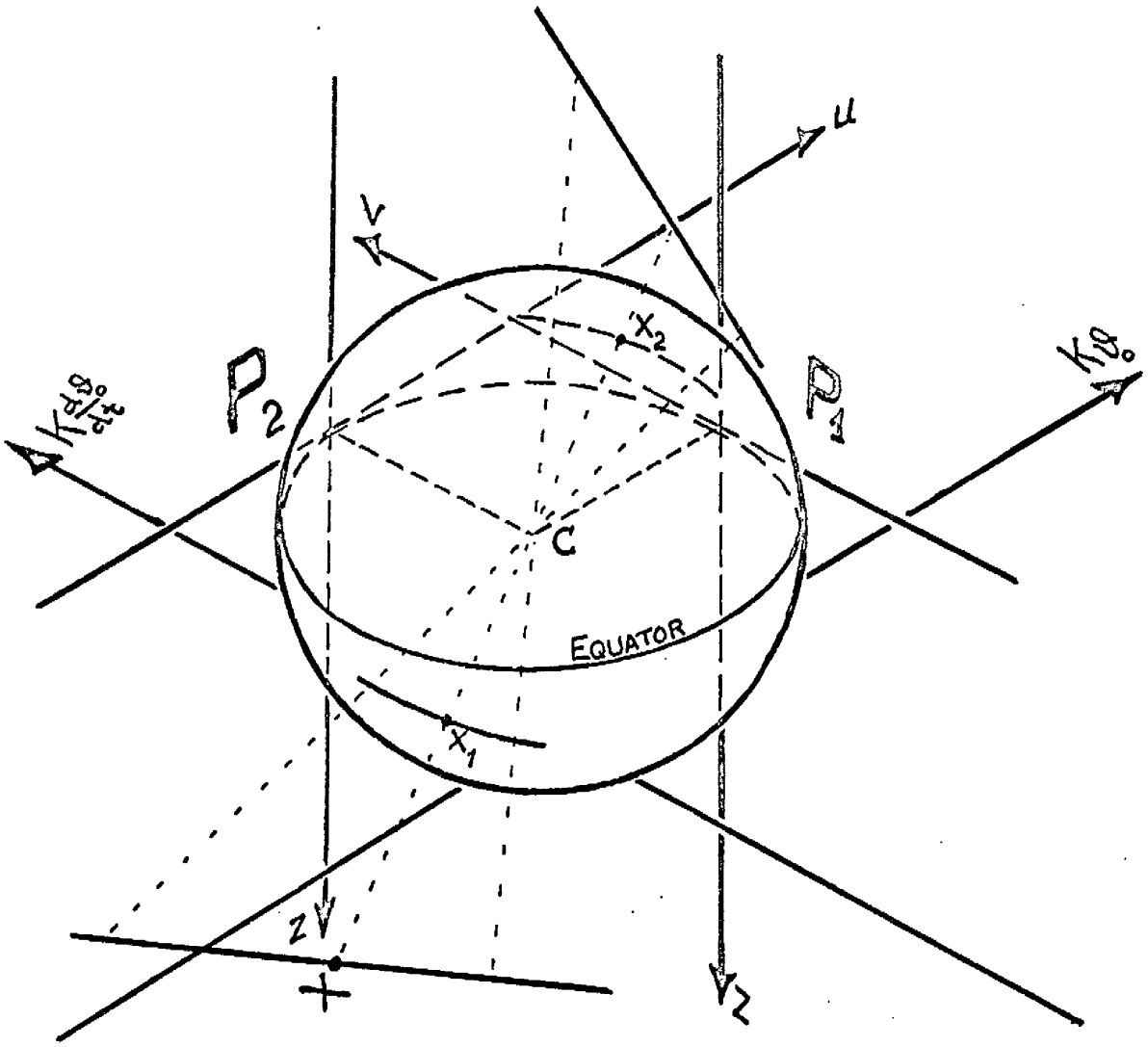

Figure 3.7 : The transformation for points at infinity.

treatment is extensive analytically with little indication of their application. Minorsky[11] outlines the procedure but quotes only one application (by Andronov) in nonlinear differential equations, which gives rise to singularities that are elementary. In contrast, the system in hand possesses complex singularities at infinity.

The transformations represent projections, which Poincaré terms gnomonical, from the phase plane on to the surface of a sphere, and thence back on to two mutually perpendicular planes normal to the phase plane. In terms of Figure 3.7, a point X in the phase plane is projected by a ray through the centre C of the unit radius sphere, which touches the phase plane at the origin, to give the corresponding points X_1 and X_2 on the surface. There is a one—to—one correspondence between a point on the sphere and a point in the phase plane (one—to—two in the reverse direction), and the topology of trajectories and singularities is conserved. Points on the equator correspond to points at infinity, and an arc of a great circle to a straight line, in the phase plane. From the sphere, a transfer may be made on to the planes P_1 and P_2 for clarity.

The first transformation to equation (3.2.1) consists in defining

$$K\vartheta_o = \frac{u}{Z}, \quad K\frac{d\vartheta_o}{dt} = \frac{1}{Z}, \quad dt = Z\,d\tau$$

$$\text{or} \quad Z = dt/K\,d\vartheta_o, \quad u = \vartheta_o\,dt/d\vartheta_o, \quad d\tau = dt/Z \qquad (3.2.8)$$

where u and Z are the coordinates of plane P_2

from which $$Z^2 K\, d\left(\frac{d\vartheta_o}{dt}\right) = -\,dZ$$

$$Z^2\, d(K\vartheta_o) = Z\,du - u\,dZ\,. \qquad (3.2.9)$$

It is to be noted that

$$\text{for } Z \gtrless 0,\ \tau \left\{ \begin{matrix} \text{increases} \\ \text{decreases} \end{matrix} \right\} \text{ as } t \text{ increases} \qquad (3.2.10)$$

On writing (3.2.1) in the form

$$K\frac{d}{dt}\left(\frac{d\vartheta_o}{dt}\right) + 2\zeta\omega_n K\frac{d\vartheta_o}{dt} = -\omega_n^2(K\vartheta_o - \Lambda_{1f})(K\vartheta_o - \Lambda_{2f})$$

and recognising the requirement of the equation

$$\frac{d(K\vartheta_o)}{dt} = K\frac{d\vartheta_o}{dt}$$

the transformation produces

$$-\frac{dZ}{Z^2}\frac{1}{Zd\tau} + 2\zeta\omega_n\frac{1}{Z} = -\omega_n^2\left(\frac{u}{Z} - \Lambda_{1f}\right)\left(\frac{u}{Z} - \Lambda_{2f}\right)$$

and $$\frac{Z\,du - u\,dZ}{Z^3\,d\tau} = \frac{1}{Z}$$

i.e. $$\left.\begin{aligned} \frac{dZ}{d\tau} &= 2\zeta\omega_n Z^2 + \omega_n^2 Z\,(u - Z\Lambda_{1f})(u - Z\Lambda_{2f}) \\ \text{and}\quad \frac{du}{d\tau} &= Z + \frac{u}{Z}\frac{dZ}{d\tau} \\ &= Z\,(1 + 2\zeta\omega_n u) + \omega_n^2 u\,(u - Z\Lambda_{1f})(u - Z\Lambda_{2f}) \end{aligned}\right\} \qquad (3.2.11)$$

All points in the phase plane except those on the $K\vartheta_o$ axis are represented on P_2: the points on the $K\vartheta_o$ axis are represented in the plane P_1, which in turn does not include the projection

of the $K\,d\vartheta_0/dt$ axis. As the set of points at infinity corresponds to the u axis ($Z=0$), the only singular point ($dZ/d\tau = du/d\tau = 0$) at infinity revealed by the system (3.2.11) is at $Z=u=0$. Furthermore, this is the only singular point of this system; for, if $Z \neq 0$, then the second of equations (3.2.11) gives

$$0 = Z + \frac{u}{Z}\cdot 0$$

which is incompatible with $Z \neq 0$.

To discover the form of the singularity consider the variational equations of (3.2.11) about $Z=u=0$:

$$\frac{d\,\delta Z}{d\tau} = \left(\frac{\partial}{\partial Z}\frac{dZ}{d\tau}\right)_{Z=u=0}\cdot \delta Z + \left(\frac{\partial}{\partial u}\frac{dZ}{d\tau}\right)_{Z=u=0}\cdot \delta u$$

$$\frac{d\,\delta u}{d\tau} = \left(\frac{\partial}{\partial Z}\frac{du}{d\tau}\right)_{Z=u=0}\cdot \delta Z + \left(\frac{\partial}{\partial u}\frac{du}{d\tau}\right)_{Z=u=0}\cdot \delta u$$

which are

$$\frac{d\,\delta Z}{d\tau} = 0\cdot\delta Z + 0\cdot\delta u$$

$$\frac{d\,\delta u}{d\tau} = 1\cdot\delta Z + 0\cdot\delta u$$

Because the coefficient determinant of these equations vanishes, the singularity is not elementary, i.e. it is neither a saddle point nor a node, since foci and centres are not found on the equator (trajectories cannot cross it). The form of the singularity must therefore be determined by the behaviour of trajectories near it, as follows.

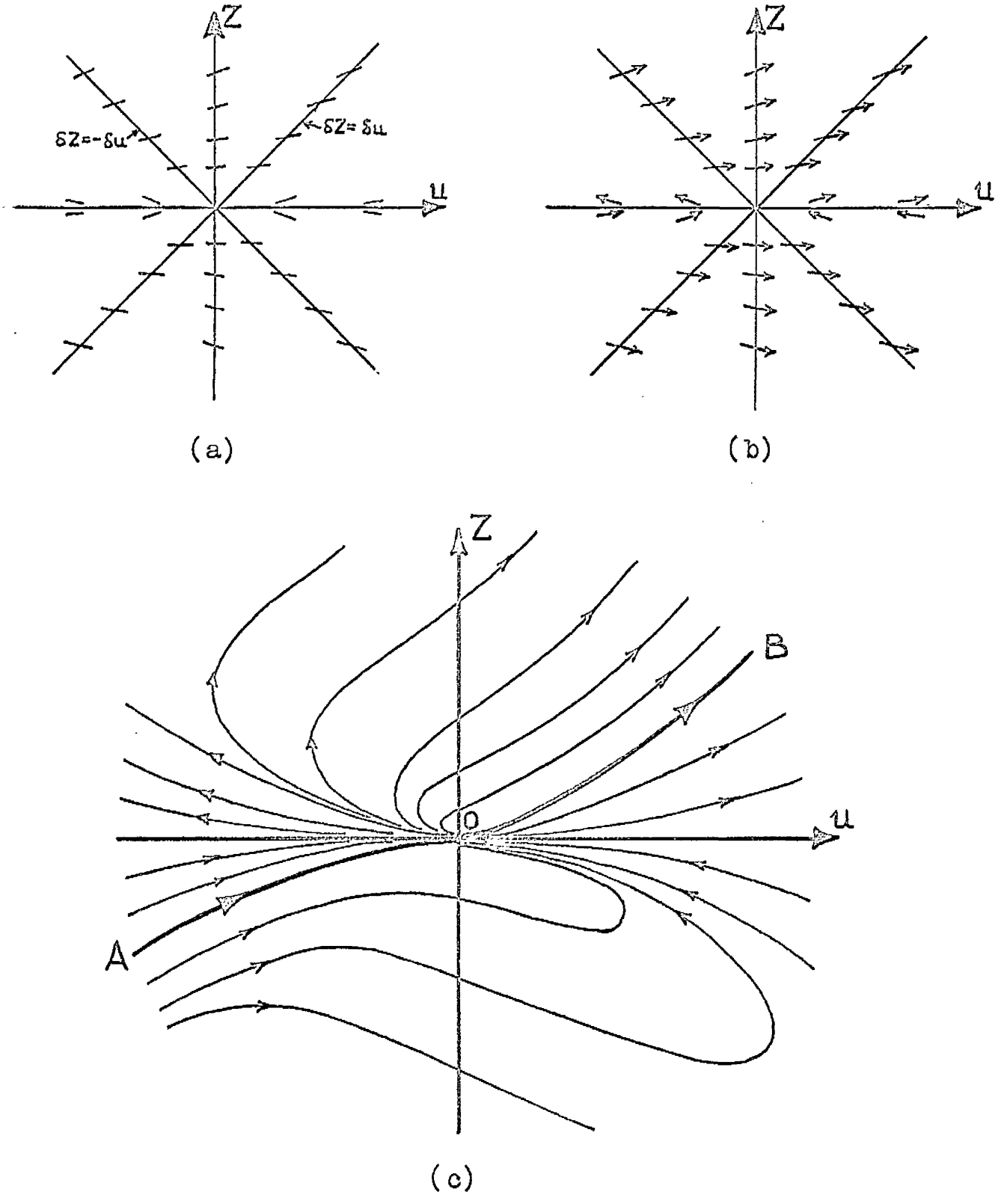

Figure 3.8 : (a) Gradients of trajectories near the singular point at infinity
(b) Directions of trajectories
(c) Nature of the singularity .

Consider the gradient of a trajectory in the u, Z plane:

$$\frac{dZ}{du} = \frac{2\zeta\omega_n Z^2 + \omega_n^2 Z(u - Z\Lambda_{1f})(u - Z\Lambda_{2f})}{Z(1 + 2\zeta\omega_n u) + \omega_n^2 u(u - Z\Lambda_{1f})(u - Z\Lambda_{2f})} \qquad (3.2.12)$$

(i) In the neighbourhood of the origin, Figure 3.8(a), on both lines for which $\delta Z = \pm \delta u$,

$$\frac{dZ}{du} \approx \frac{2\zeta\omega_n (\delta Z)^2}{\delta Z} \approx 2\zeta\omega_n (\delta Z),$$

omitting terms of higher order than first and second in the denominator and numerator of (3.2.12) respectively. Thus $dZ/du > 0$ for $\delta Z > 0$ and $dZ/du < 0$ for $\delta Z < 0$, irrespective of whether $\delta u \gtrless 0$. To add the sense of direction to the lineal elements, Figure 3.8(b), either of equations (3.2.11) may be used:

$$\frac{dZ}{d\tau} \approx 2\zeta\omega_n (\delta Z)^2 \quad \text{and} \quad \frac{du}{d\tau} \approx \delta Z$$

As $dZ/d\tau > 0$ for any δZ, $dZ/dt \gtrless 0$ for $\delta Z \gtrless 0$ in view of condition (3.2.10).

(ii) On the Z axis, $$\frac{dZ}{du} = 2\zeta\omega_n Z + \omega_n^2 \Lambda_{1f}\Lambda_{2f} Z^2$$

$$\approx 2\zeta\omega_n(\delta Z) \quad \text{near the origin.}$$

Thus, $dZ/du \gtrless 0$ for $\delta Z \gtrless 0$ as in (i), and as $dZ/d\tau \approx 2\zeta\omega_n(\delta Z)^2$ therefore $dZ/dt \gtrless 0$ for $\delta Z \gtrless 0$, again as in (i).

(iii) Close to the u axis, i.e. for $Z = \delta Z$ and $|u| \gg |\delta Z|$, equation (3.2.12) reduces to

$$\frac{dZ}{du} \approx \frac{\omega_n^2 u^2 \delta Z}{\omega_n^2 u^3} \approx \frac{\delta Z}{u}$$

so for $\delta Z > 0$, $\frac{dZ}{du}$ is small and $\left\{ \begin{matrix} \text{positive} \\ \text{negative} \end{matrix} \right\}$ as $u \gtrless 0$, and

for $\delta Z < 0$, $\frac{dZ}{du}$ is small and $\left\{ \begin{matrix} \text{negative} \\ \text{positive} \end{matrix} \right\}$ as $u \gtrless 0$.

The sense of direction is seen from $du/d\tau \approx \omega_n^2 u^3$ and condition (3.2.10), to be

condition (3.2.10), to be

$$\frac{du}{dt} \gtrless 0 \quad \text{as} \quad \delta Z \gtrless 0 \quad \text{if} \quad u > 0$$

$$\frac{du}{dt} \lessgtr 0 \quad \text{as} \quad \delta Z \gtrless 0 \quad \text{if} \quad u < 0 .$$

There is now sufficient information to define the behaviour of the trajectories to be as shown in Figure 3.8(c). The equator is not a trajectory as du/dt is not defined on it. Two trajectories, OA and OB, have special significance: all trajectories on one side of either of them approach or leave the origin in the positive u direction, while all those on the other side approach or leave the origin in the opposite direction. The behaviour suggests a possible coincidence of a stable and an unstable node, but a result given by Poincaré (ref.10, Ch.3, p.29) settles the issue after the transformation to plane P_1 has been considered.

The second transformation is described by

$$K\vartheta_o = \frac{1}{Z} , \quad K\frac{d\vartheta_o}{dt} = \frac{v}{Z} , \quad dt = Z d\tau \qquad (3.2.13)$$

from which $$Z^2\, d(K\vartheta_o) = -\,dZ$$

$$Z^2 K\, d\left(\frac{d\vartheta_o}{d\tau}\right) = Z\,dv - v\,dZ$$

The relation (3.2.10) between τ and t applies again. The transformed version of equation (3.2.1) is obtained as

$$-\frac{dZ}{Z^3 d\tau} = \frac{v}{Z}$$

$$\text{and } \frac{Z\,dv - v\,dZ}{Z^2}\frac{1}{Z d\tau} + 2\zeta\omega_n \frac{v}{Z} = -\omega_n^2\left(\frac{1}{Z} - \Lambda_{1f}\right)\left(\frac{1}{Z} - \Lambda_{2f}\right)$$

$$\left.\begin{aligned} \text{i.e. as } \frac{dZ}{d\tau} &= -vZ^2 \\ \text{and } \frac{dv}{d\tau} &= -2\zeta\omega_n vZ - \omega_n^2(1 - Z\Lambda_{1f})(1 - Z\Lambda_{2f}) + \frac{v}{Z}\frac{dZ}{d\tau} \\ &= -vZ(v + 2\zeta\omega_n) - \omega_n^2(1 - Z\Lambda_{1f})(1 - Z\Lambda_{2f}) \end{aligned}\right\} \quad (3.2.14)$$

Since for $Z = 0$, $dv/d\tau = -\omega_n^2 \neq 0$, there are no singular points at infinity on the $K\vartheta_o$ axis, and the singularity at infinity revealed by the first transformation is not represented in the plane P_1. The only singular points of system (3.2.14) occur for $v = 0$ at $Z = 1/\Lambda_{1f}$ or $Z = 1/\Lambda_{2f}$, which are the critical points already noted in the finite region of the phase plane.

The theorem of Poincaré referred to above states that, if the total number of nodes, foci, and saddle points on the sphere, not on the equator, are denoted by 2N, 2F, and 2S, and the numbers of nodes and saddle points on the equator are denoted

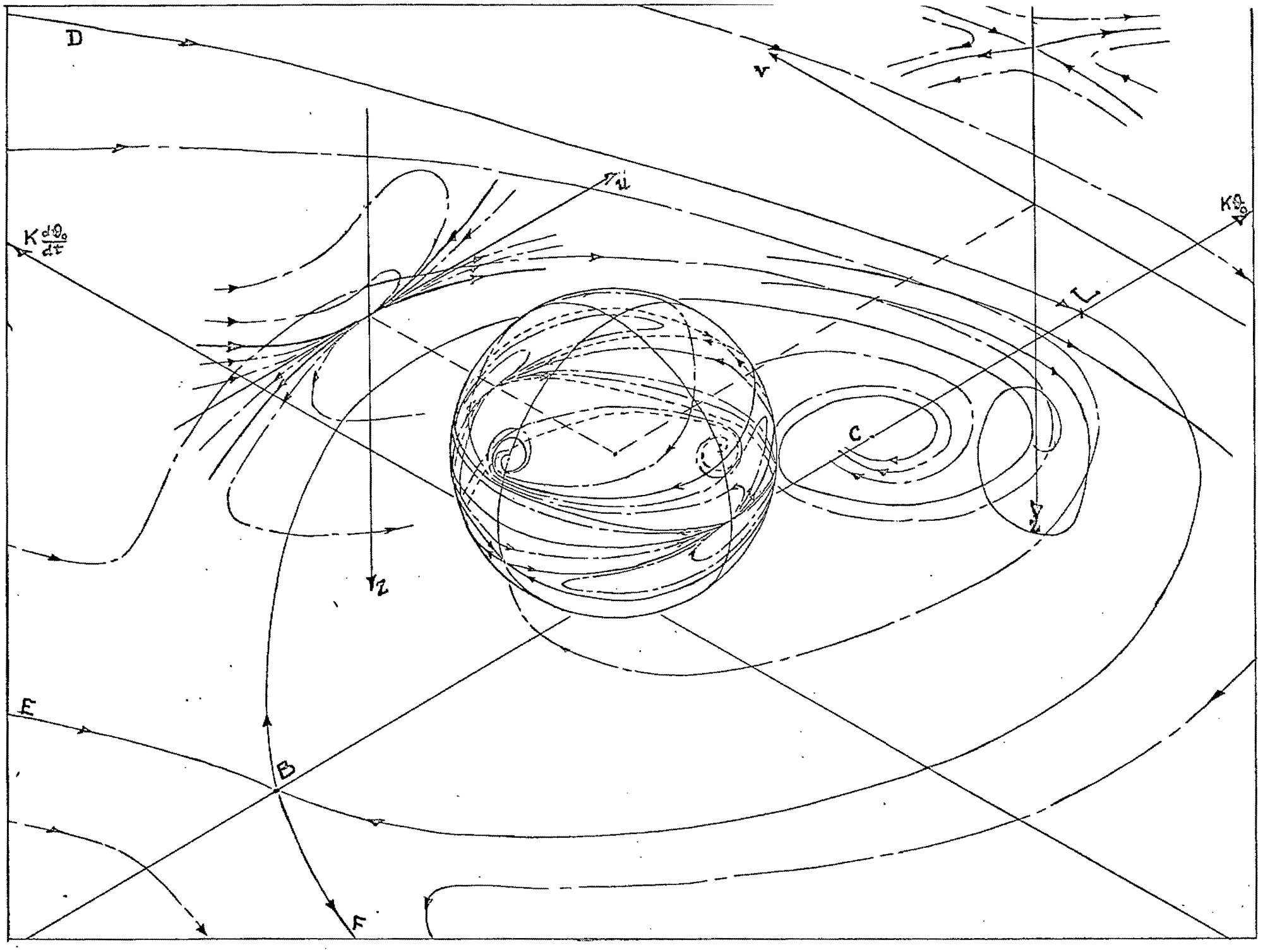

Figure 3.9: Global representation of the entire phase plane portrait.

by $2N_{oo}$ and $2S_{oo}$, then

$$N_{oo} + N + F = S_{oo} + S + 1 \qquad (3.2.15)$$

In the case of this system, $S = 1$, $N = 1$ or 0, $F = 0$ or 1 respectively, so that the number of nodes at $Z = u = 0$ exceeds the number of saddle points there by one. Therefore, the singularity consists of at least two nodes and one saddle point coalesced.

With the knowledge of the behaviour at infinity, the question of whether the phase plane portrait of Figure 3.6 is representative of the general case or not may be answered. By drawing the salient features on the sphere, Figure 3.9, it is seen that the separatrices BD, BE and BF must all terminate at the singularity at $Z = u = 0$, and that the fourth separatrix BC must terminate at A, in any case of equation (3.2.1). The nature of the phase plane portrait is therefore essentially similar to that of Figure 3.6 for all sets of values of ζ, ω_n, K and ϑ_{if}.

3.3 The stability of large transient responses

The phase portraits of the preceding Section indicate the existence in every case of a region of asymptotic stability to A. The boundary Ω of this region consists of the whole of the two separatrices EB and BD, so that the region extends to infinity in the positive $K\,d\vartheta_o/dt$ direction. The aim of this and further sections is to define the finite extent of the

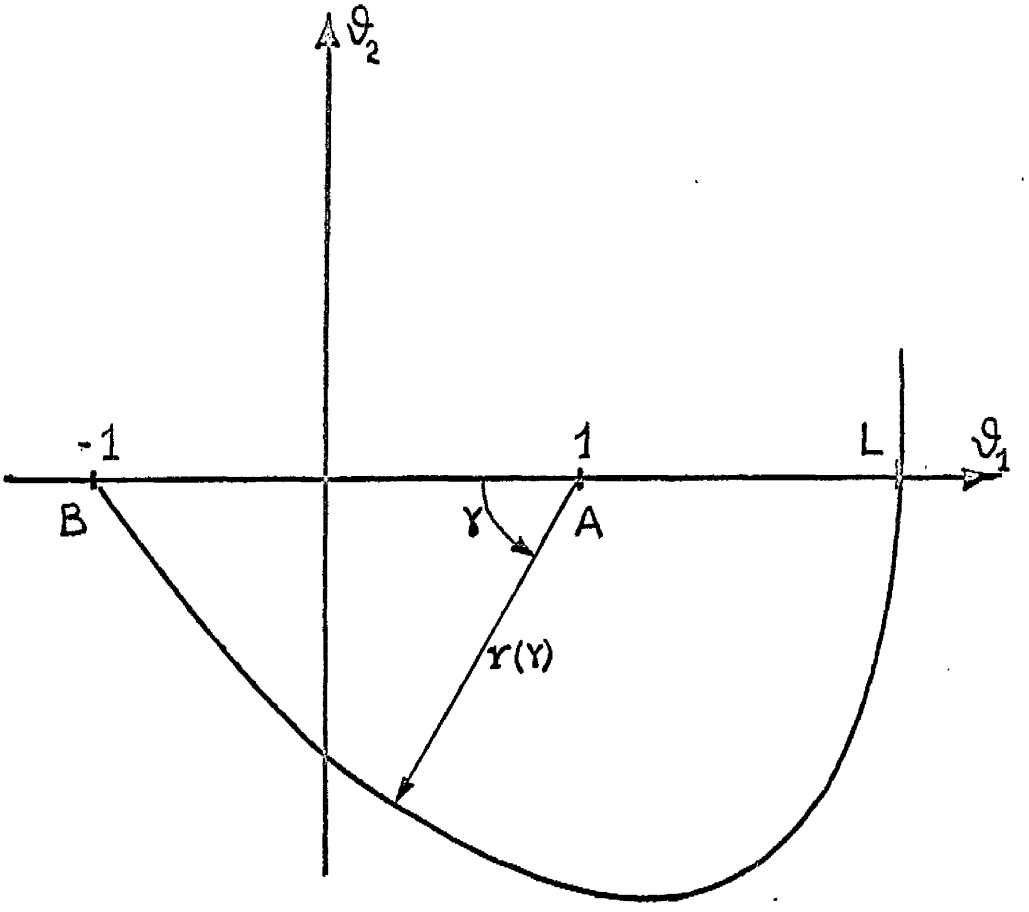

Figure 3.10 : The transformation (3.3.1) to polar coordinates .

region in other directions, for the general case of the system as described by equation (3.2.1).

The importance of this lies in the possibility of step responses from initially stable states being unstable, whereas for the companion first-order system of Section 2.1 such responses are always stable. The response is unstable if the representative point in the phase plane lies beyond Ω immediately after the step in input. Although bearing in mind that it is of interest to know the complete form of Ω, special attention is given to defining the point L at which the separatrix BD crosses the $K\vartheta_0$ axis for $K\vartheta_0 > \Lambda_{1f}$: this is a useful measure of the extent of the region, since it indicates the limits for stable responses from an initial equilibrium state.

A first approach may be an attempt to derive the equation of the separatrix, at least from B to L. Since it is, very approximately, of circular form around point A (Figure 3.10), it may be valuable to transform equation (3.2.5) from the rectangular coordinates ϑ_1 and ϑ_2 to the polar coordinates γ and $r(\gamma)$, where

$$\vartheta_1 = 1 - r\cos\gamma, \quad \vartheta_2 = -r\sin\gamma \qquad (3.3.1)$$

and to attempt a series solution for r in terms of γ. Thus, it is found that

$$\frac{d\vartheta_2}{d\vartheta_1} = \frac{\sin\gamma\frac{dr}{d\gamma} + r\cos\gamma}{\cos\gamma\frac{dr}{d\gamma} - r\sin\gamma}$$

and the equation describing trajectories appears now from (3.2.5) as

$$\frac{dr}{d\gamma} = r \sin\gamma \, \frac{\omega_n^2(\Lambda_{1f}-\Lambda_{2f})(2-r\cos\gamma)\cos\gamma + (4\zeta\omega_n \sin\gamma - 2\cos\gamma)}{\omega_n^2(\Lambda_{1f}-\Lambda_{2f})(2-r\cos\gamma)\cos^2\gamma + 2\sin\gamma(2\zeta\omega_n\cos\gamma + \sin\gamma)} \qquad (3.3.2)$$

The particular solution sought of this differential equation is that for which $r = 2$ at $\gamma = 0$ and $d\vartheta_2/d\vartheta_1$ at B has the negative value given by (3.2.7). For convenience, define

$$\Lambda_{1f}-\Lambda_{2f} = +\sqrt{(1-K-K\vartheta_{1f})^2+4K} = R \qquad (3.3.3)$$

so that $\left(\frac{dr}{d\gamma}\right)_B = 2\Big/\left(\frac{d\vartheta_2}{d\vartheta_1}\right)_B = 2\left(\zeta-\sqrt{R+\zeta^2}\right)/\omega_n R \qquad (3.3.4)$

If the solution is to be found in the form

$$r = A_0 + A_1\gamma + A_2\gamma^2 + A_3\gamma^3 + \ldots, \qquad (3.3.5)$$

it is clear from the foregoing that A_0 must equal 2, and A_1 must equal expression (3.3.4). If (3.3.5) and the convergent series for $\sin\gamma$ and $\cos\gamma$ are substituted in (3.3.2), and coefficients of like powers of γ are equated, the equation for the constant term gives

$$A_1\omega_n^2 R(2-A_0) = 0$$

which is satisfied by $A_0 = 2$: the equation for coefficients of γ then gives

$$A_1 (4\zeta\omega_n - A_1\omega_n^2 R) = -4$$

so that $A_1 = 2 \left(\zeta \pm \sqrt{R + \zeta^2} \right) / \omega_n R$

Choosing A_1 in accordance with (3.3.4), the equation for coefficients of γ^2 produces

$$A_2 = \frac{\zeta (\omega_n^2 R - 4) + (4 + 3\omega_n^2 R) \sqrt{R + \zeta^2}}{\zeta\omega_n^2 R + 3\omega_n^2 R \sqrt{R + \zeta^2}} \qquad (3.3.6)$$

The increasing complexity of the expressions for the coefficients A_n is apparent; in fact, the expression for A_3 is much too lengthy to be set out here. It appears that the series (3.3.5) is limited by practical considerations to the first three terms, and therefore the value for L given by r at $\gamma = \pi$ is liable to be most approximate. In addition, it is not known whether the approximation is greater or less than L, so it is concluded that this approach is of little value.

A more satisfactory approach lies in the use of the "Direct Method" of Lyapunov, as it has come to be called. After receiving little attention in Western countries since the original paper[12] in 1892, there has been in recent years a great increase in the literature available in English on the method. No attempt is made here to list all the appropriate references – a suitable bibliography is to be found in the papers by Kalman and Bertram[13]; only specific references are made to the

treatments by a few authors[14-19].

Since, in the type of system under consideration, there is always at least one other singularity in phase space besides that to which solutions may be stable (placed at the origin), it is impossible to find a Lyapunov function V with the ideal properties, i.e. (i) V to be positive definite, (ii) dV/dt , by virtue of the system equations, to be negative definite. In such systems, dV/dt is zero at one point (at least) outside the origin – the other singularity – so that at best dV/dt may be found to be negative semidefinite; there is generally a continuous set of points on which $dV/dt = 0$. Furthermore, it is unlikely that V is found to be positive definite, and a useful alternative is the existence of a finite region around the origin within which V is positive definite. A region of stability is guaranteed by a Theorem quoted by LaSalle and Lefschetz[14], and included here for convenience:

> let V be a scalar function, with continuous first partial derivatives, of the state variables of the system, and let Ω designate a bounded region within which $V < k$ (constant). If, within Ω, V is positive definite, dV/dt is negative semidefinite, and dV/dt is not identically zero along any trajectory of the system, then every solution starting inside Ω is asymptotically stable to the origin.

As mentioned above, a prerequisite of the method is to

describe the system by state variables such that the stable singularity is at their origin. If in equation (3.2.1) the variable ϑ_1' is introduced such that

$$\vartheta_1' = K\vartheta_o - \Lambda_{1f} \qquad (3.3.7)$$

in which $\Lambda_{1f} = \frac{1}{2}\left[-1-K+K\vartheta_{if}+R\right]$ by definition (3.3.3)

the system is described by the equation

$$\frac{d^2\vartheta_1'}{dt^2} + 2\zeta\omega_n\frac{d\vartheta_1'}{dt} + \omega_n^2\vartheta_1'(\vartheta_1'+R) = 0 \qquad (3.3.8)$$

which places A at $\vartheta_1' = 0$. The most convenient variable to use, however, is

$$\varphi_1 = \vartheta_1'/R = (K\vartheta_o - \Lambda_{1f})/R \qquad (3.3.9)$$

because equation (3.2.1) becomes

$$\frac{d^2\varphi_1}{dt^2} + 2\zeta\omega_n\frac{d\varphi_1}{dt} + \omega_n^2 R\varphi_1(\varphi_1+1) = 0 \qquad (3.3.10)$$

which places B at $\varphi_1 = -1$ with A at $\varphi_1 = 0$.

Finally, it is required to decompose (3.3.10) into a pair of first-order differential equations in the chosen state variables: one means of doing so is to choose

$$\begin{aligned}\frac{d\varphi_1}{dt} &= \omega_n\sqrt{R}\,\varphi_2 \\ \frac{d\varphi_2}{dt} &= -\omega_n(\sqrt{R}\,\varphi_1 + 2\zeta\varphi_2 + \sqrt{R}\,\varphi_1^2)\end{aligned} \qquad (3.3.11)$$

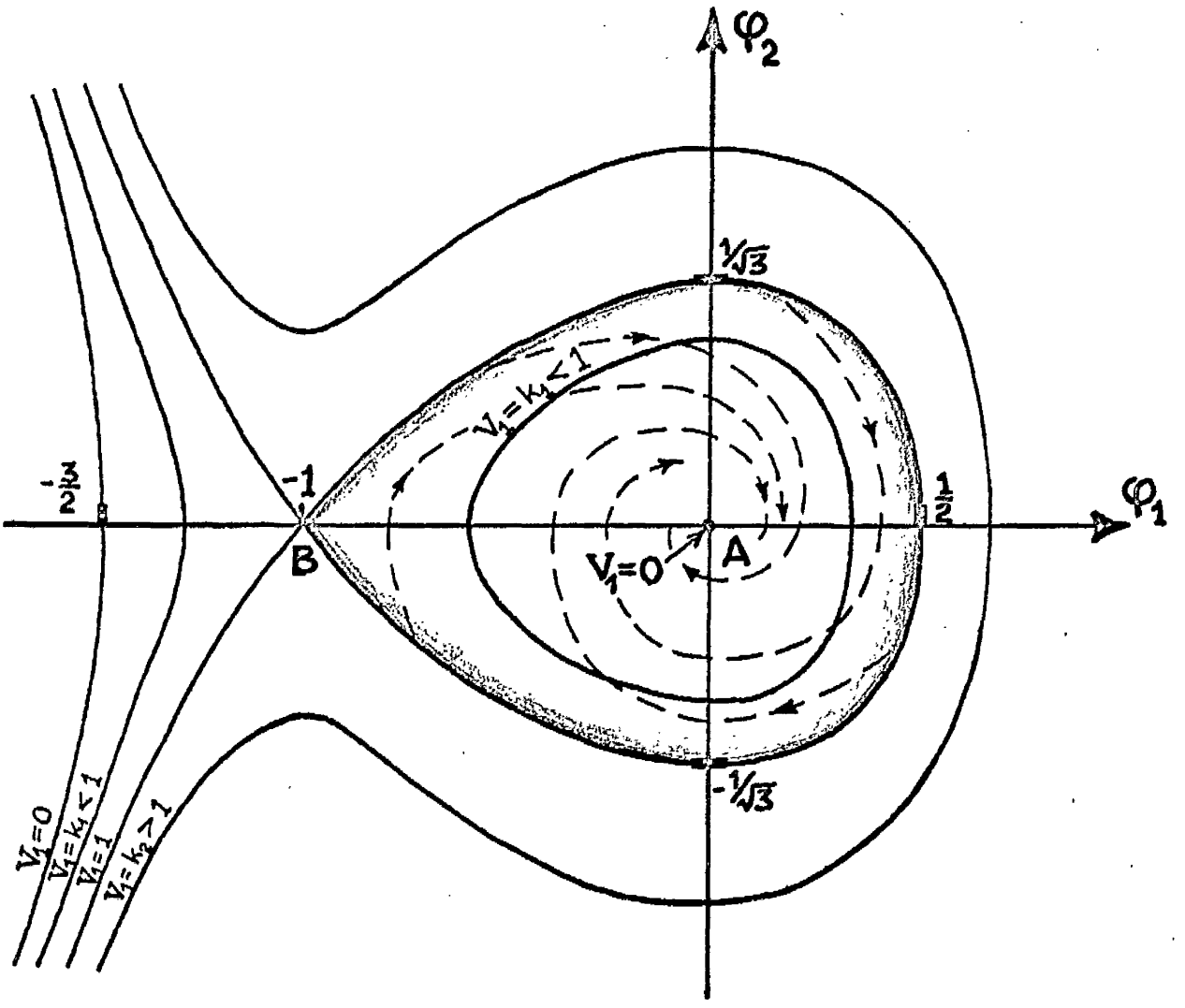

Figure 3.11 : Contours of the function V_1 , with the region of asymptotic stability Ω_1 shaded.

A first Lyapunov function $V(\varphi_1, \varphi_2)$ for system (3.3.11) has been found quite readily. Consider the function (cf. p. 63 of reference 14)

$$V_1 = 3\varphi_1^2 + 3\varphi_2^2 + 2\varphi_1^3 \qquad (3.3.12)$$

for which $\frac{dV_1}{dt} = \frac{\partial V_1}{\partial \varphi_1} \cdot \frac{d\varphi_1}{dt} + \frac{\partial V_1}{\partial \varphi_2} \cdot \frac{d\varphi_2}{dt}$

$$= 6\varphi_1 (1 + \varphi_1) \omega_n \sqrt{R} \varphi_2 - 6\varphi_2 \omega_n (\sqrt{R}\varphi_1 + 2\zeta\varphi_2 + \sqrt{R}\varphi_1^2)$$

$$= -12\zeta\omega_n \varphi_2^2$$

dV_1/dt is therefore negative semidefinite and is zero on the φ_1 axis, which includes the two singular points. V_1 is symmetric about the φ_1 axis, Figure 3.11, but is clearly not positive definite; it is zero at the origin and on the curve

$$\varphi_2 = \pm \frac{\varphi_1}{\sqrt{3}} \sqrt{-3 - 2\varphi_1}$$

which crosses the φ_1 axis at $-3/2$ and lies completely in the region $\varphi_1 < -3/2$. V_1 is therefore positive definite in the infinite half-space "to the right" of this curve. Contours of constant positive V_1 either form closed curves around the origin with an additional branch to the left of B, in the case of $V_1 = k_1 < 1$, or form open curves for $V_1 = k_2 > 1$: the greatest bounded region of positive V_1 is given by the curve $V_1 = 1$, which has two intersections with the φ_1 axis at B and a third at $\varphi_1 = \frac{1}{2}$, and intersections with the φ_2 axis at $\pm 1/\sqrt{3}$. This region (Ω_1)

is therefore one of asymptotic stability to the origin, since all the conditions in the above Theorem are met.

In order to define the form of Ω_1 more exactly, consider the gradient of V_1 contours: from (3.3.12),

$$\frac{d\varphi_2}{d\varphi_1} = -\frac{\varphi_1}{\varphi_2}(1+\varphi_1) \qquad (3.3.13)$$

for any contour $V_1 = k$. The gradient is zero for all k where $\varphi_1 = 0$, and is zero at $\varphi_1 = -1$ and infinite at $\varphi_2 = 0$ for all k except $k = 1$, when the gradient is indeterminate from (3.3.13): application of L'Hôpital 's rule, however, produces

$$\left(\frac{d\varphi_2}{d\varphi_1}\right)_B = -\left((1+2\varphi_1)/\frac{d\varphi_2}{d\varphi_1}\right)_B$$

$$\text{i.e. } \left(\frac{d\varphi_2}{d\varphi_1}\right)_B = \pm 1$$

Confining attention to the stability of responses from initial equilibrium states only, it is now possible to obtain stability diagrams similar to those of Figure 2.5 in terms of input steps from a given value of ϑ_{io}. From the relevant extent of Ω_1, i.e. on the φ_1 axis, from -1 (B) to 0·5 (L_1), it is evident that the restrictions on the magnitude of the input step for stable responses are

$$-R < K\vartheta_{oo} - \Lambda_{1f} < R/2$$

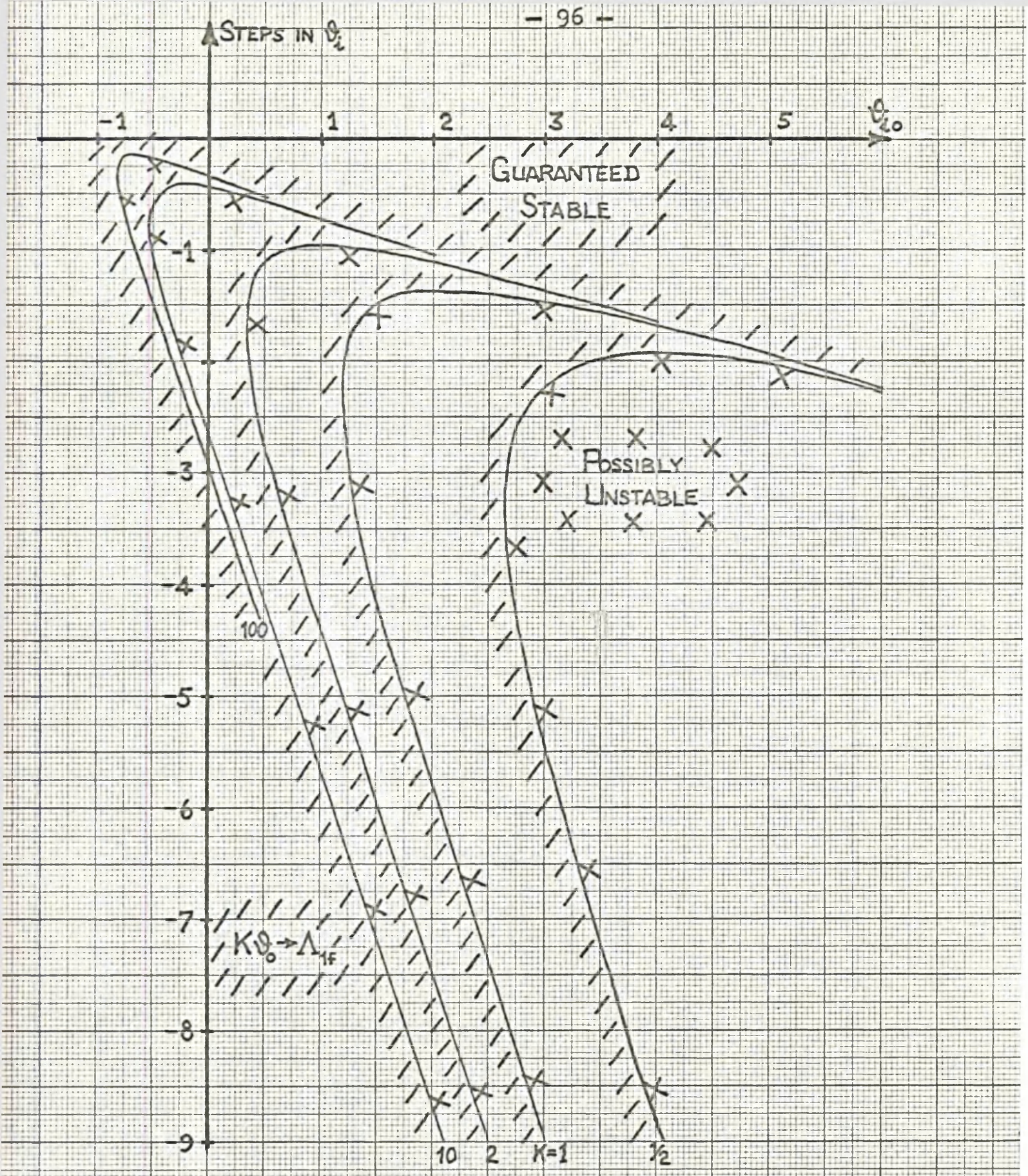

Figure 3.12: Stability diagram for the step response of the second-order system with a-type gain element from initially stable states.

Since the critical value of φ_1 (namely $[1-K-K\vartheta_{if}-R]/2R$), corresponding to $\vartheta_o = -1$, lies within the above range, the two separate ranges

$$\text{(a) } (1-K-K\vartheta_{if}-R)/2 < K\vartheta_{oo}-\Lambda_{1f} < R/2 \quad \text{and}$$
$$\text{(b) } -R < K\vartheta_{oo}-\Lambda_{1f} < (1-K-K\vartheta_{if}-R)/2 \qquad (3.3.14)$$

relate to stable and unstable initial equilibrium states respectively.

(a) The lower limit simply specifies that the initial equilibrium state is stable, but the upper limit gives

$$K\vartheta_{if} + 2\sqrt{(1-K-K\vartheta_{if})^2+4K} > K\vartheta_{io} + \sqrt{(1-K-K\vartheta_{io})^2+4K} \qquad (3.3.15)$$

as the condition for a stable response. Values of ϑ_{if} in terms of ϑ_{io} have been calculated for selected values of K from this expression, and after converting these to steps in ϑ_i in terms of ϑ_{io} the resulting diagram for the stability of responses from an initially stable equilibrium state appears as in Figure 3.12 .

This is quite different from Figure 2.5(a), in that a negative step within a certain range may lead to instability if $\vartheta_{io} > -1$. The qualification in this statement is intentional : because a Lyapunov function is a sufficient but not a necessary condition for stability, the proven existence of Ω_1 is a guarantee that responses are stable outwith the indicated region of instability, but it need not follow that responses are

unstable within it: the phase plane diagrams, however, reveal that there must be a region of instability of similar proportions, and the question of whether the greater part of the region of Figure 3.12 is indeed one of instability or not is pursued in subsequent Sections.

(b) The upper limit simply specifies that the initial equilibrium state is unstable, and the lower limit gives

$$K\vartheta_{if}-\sqrt{(1-K-K\vartheta_{if})^2+4K} < K\vartheta_{io}-\sqrt{(1-K-K\vartheta_{io})^2+4K} \qquad (3.3.16)$$

as the condition for a stable response. This reduces to the simple inequality $\vartheta_{if} < \vartheta_{io}$ for all values of ϑ_{io} and (positive) K, so that the application of a negative input step results in a final stable equilibrium state: the diagram in this case is the same as that of Figure 2.5(b). Since the boundary of Ω_1 passes through B, the region of asymptotic stability does not admit of any improvement for case (b), and it is not a case of a region of "possible" instability.

To conclude this Section, a particular feature of this system is noted. Whilst a stable response may result from an initially unstable state in which there is negative gain, as for the companion first-order system, it is also possible for this system to have a stable step response during which the gain of the element goes transiently negative. This is due to part of the region Ω_1 lying on the negative side of the critical value of φ_1 mentioned above.

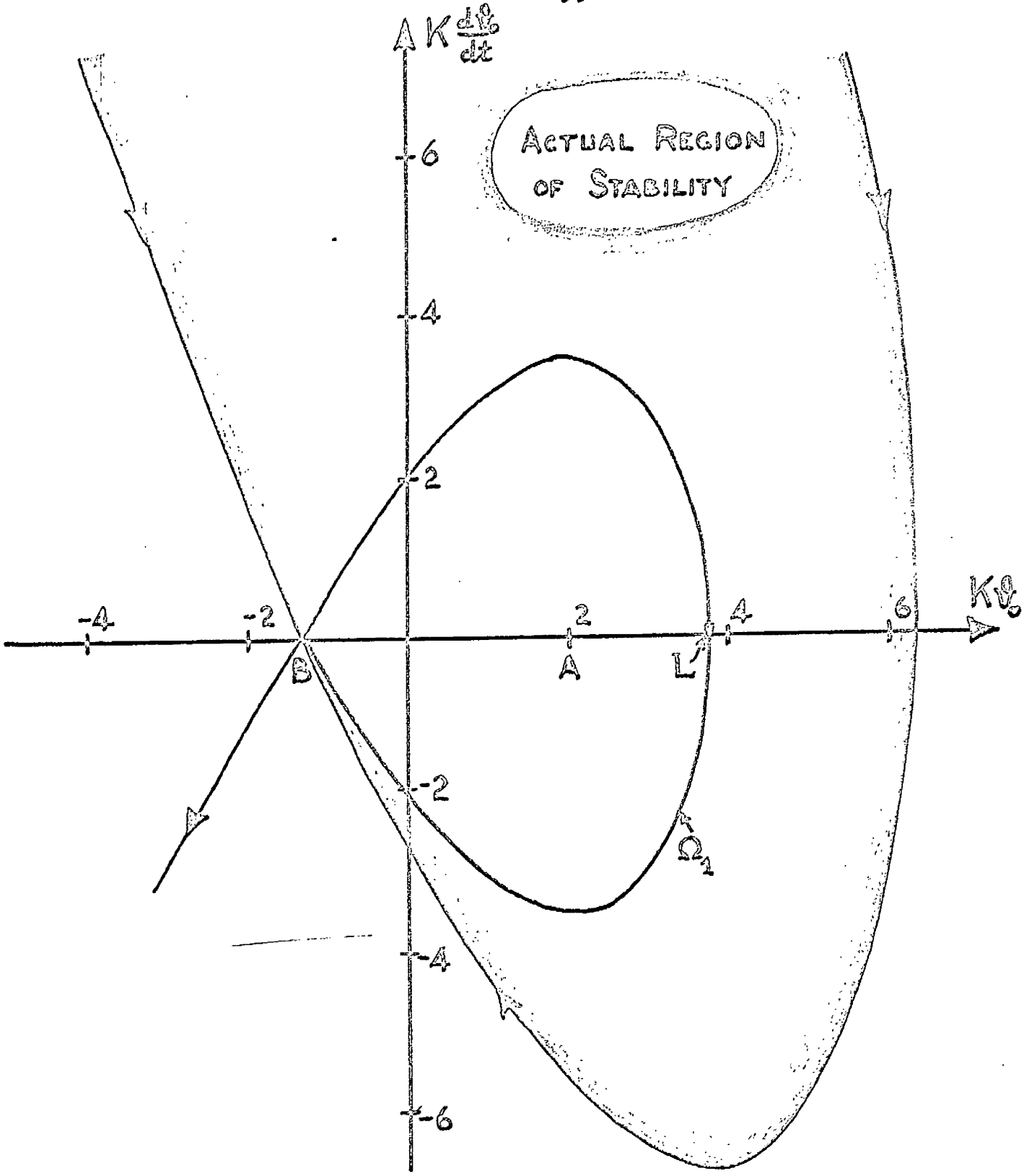

Figure 3.13 : An actual region of stability, with guaranteed region Ω_1.

3.4 Less restrictive regions of stability

3.4a A second Lyapunov function

If the boundary of Ω_1 is superimposed on any phase plane portrait, it is found that Ω_1 provides a rather conservative estimate of the actual region of stability, particularly in regard to the value for the intersection at L. This is indicated in Figure 3.13, which compares the actual region of stability in Figure 3.6 with Ω_1.

As a possible second Lyapunov function consider

$$V_2 = A\varphi_1^2 + B\varphi_2^2 + C\varphi_1\varphi_2 + D\varphi_1^2\varphi_2 + E\varphi_1\varphi_2^2 + F\varphi_2^3 + G\varphi_1^4 \qquad (3.4a.1)$$

in which the values of the coefficients A, B, . . are still to be appointed. In view of equations (3.3.11), the time derivative of V_2 is given by

$$\begin{aligned}\frac{dV_2}{dt} = {} & \zeta\omega_n\left[(\sqrt{N}C - 4B)\varphi_2^2 - \sqrt{N}C\varphi_1^2 - \sqrt{N}D\varphi_1^4 - 3\sqrt{N}F\varphi_1^2\varphi_2^2\right] + \\ & \zeta\omega_n\left[2(\sqrt{N}A - \sqrt{N}B - C)\varphi_1\varphi_2 - 2(\sqrt{N}B + D + \sqrt{N}E)\varphi_1^2\varphi_2 - \right. \\ & \sqrt{N}(C + D)\varphi_1^3 + (2\sqrt{N}D - 4E - 3\sqrt{N}F)\varphi_1\varphi_2^2 + \\ & \left.(\sqrt{N}E - 6F)\varphi_2^3 + 2\sqrt{N}(2G - E)\varphi_1^3\varphi_2\right]\end{aligned} \qquad (3.4a.2)$$

where $N = R/\zeta^2 > 0$.

From the infinite variety of sets of coefficients A, B, . . . , the following one has proved useful: to produce a form for dV_2/dt

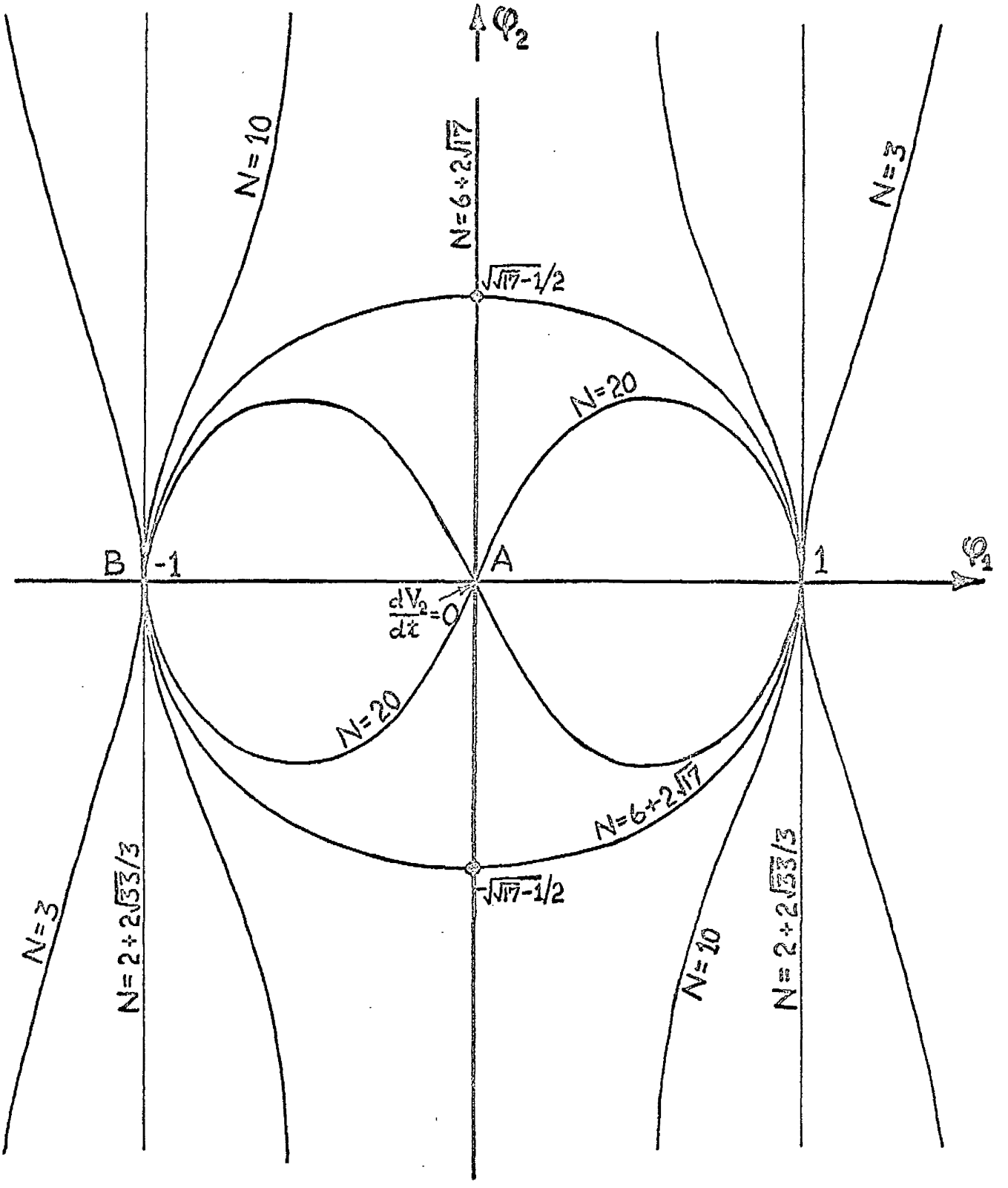

Figure 3.14 : Curves of zero dV_2/dt for various values of N .

which is symmetric about both axes, the coefficients of the six terms in the second group of (3.4a.2) are set to zero by the choice

$$A = 2(3N+8),\ B = 5N+8,\ C = \sqrt{N}(N+8),$$
$$D = -\sqrt{N}(N+8),\ E = -4N,\ F = -2N^{3/2}/3,\ \text{and}\ G = -2N \qquad (3.4a.3)$$

This gives

$$\frac{dV_2}{dt} = \zeta\omega_n\left[(N^2-12N-32)\varphi_2^2 + N(N+8)(\varphi_1^2-1)\varphi_1^2 + 2N^2\varphi_1^2\varphi_2^2\right] \qquad (3.4a.4)$$

so that both V_2 and dV_2/dt depend on the parameter N, whereas V_1 has none such dependence.

Considering firstly dV_2/dt after (3.4a.4), it is not even negative semidefinite everywhere as is dV_1/dt. The form of the curve $dV_2/dt = 0$, which separates regions of positive and negative dV_2/dt, may be seen by its representation as

$$\varphi_2^2 = \frac{N(N+8)\varphi_1^2(1-\varphi_1^2)}{(N^2-12N-32)+2N^2\varphi_1^2} \qquad (3.4a.5)$$

The curve intersects the φ_1 axis at ± 1 for all N. Examination of the sign variations of the numerator and denominator shows that, for $0 \leqslant N < 2+2\sqrt{33}/3$, two branches of the curve exist only in the regions $1 \leqslant \varphi_1^2 < (32+12N-N^2)/2N^2$ with the lines $\varphi_1 = \pm\sqrt{(32+12N-N^2)/2N^2}$ as asymptotes (see Figure 3.14); for $2+2\sqrt{33}/3 < N < 6+2\sqrt{17}$, two branches of the curve exist only in the regions $(32+12N-N^2)/2N^2 < \varphi_1^2 \leqslant 1$ with the lines

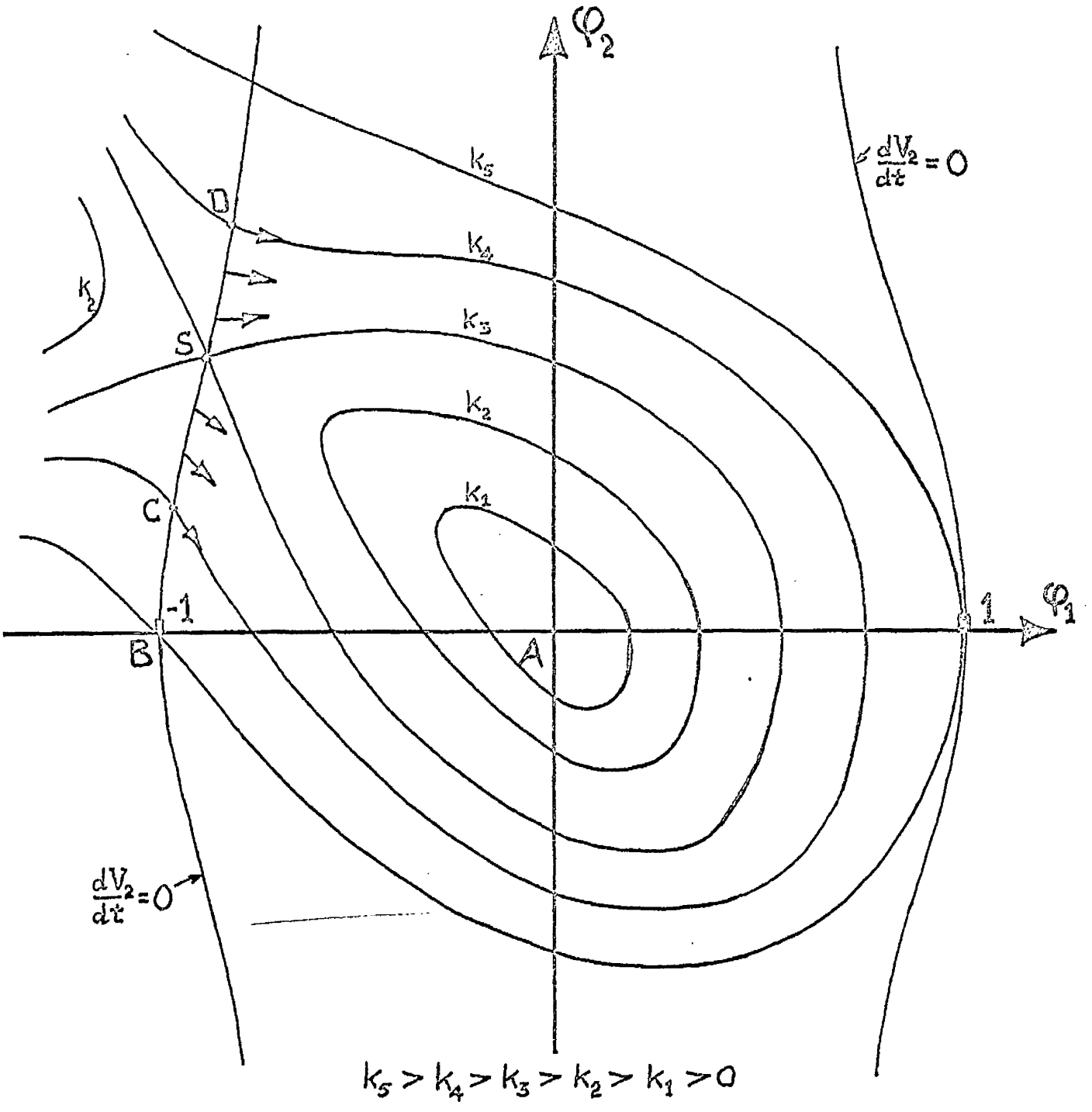

Figure 3.15 : Sketch of the contours of V_2 and the curves $dV_2/dt = 0$ for a value of N less than 8·0 approx.

$\varphi_1 = \pm\sqrt{(32 + 12N - N^2)/2N^2}$ as asymptotes; for $N = 2 + 2\sqrt{33}/3$, the two branches degenerate into the straight lines $\varphi_1 = \pm 1$; for $N = 6 + 2\sqrt{17}$, the curve is an ellipse, along with the φ_2 axis, with intersections at $\varphi_2 = \pm\sqrt{\sqrt{17} - 1}/2$; and for $N > 6 + 2\sqrt{17}$, the curve is a figure of eight with four intersections at the origin. In the regions between the branches dV_2/dt is non-positive, so that for values of N less than $6 + 2\sqrt{17}$ there is an infinitely long region of negative definite dV_2/dt straddling the φ_2 axis, which may be useful. The character of V_2 must now be examined to discover if any contour forms a closed region of positive definite V_2 within this region of negative definite dV_2/dt: if this exists, a larger region of asymptotic stability than Ω_1 may exist.

For any value of N, there is a curve $V_2 = 0$ which intersects the φ_1 axis at $\pm\sqrt{(3N + 8)/N}$ and the φ_2 axis at $3(5N + 8)/2N^{3/2}$, and below which V_2 is positive definite. As with the saddle point of the $V_1 = 1$ contour at B, there is a saddle point S on one of the V_2 contours, but in this case S always lies in the upper half-plane. Figure 3.15 shows the character of V_2 for a value of N less than 8·0 approximately: up to the limiting value of k_3, contours of constant positive V_2 form closed regions within the region of negative definite dV_2/dt, so that the region within $V_2 = k_3$ is, by the theorem quoted, one of asymptotic stability; but this region represents little, if any, improvement

over Ω_1. However, by a reductio ad absurdum consideration of the trajectories in the neighbourhood of S, it can be proved that S must lie on the upper left-hand branch of the curve $dV_2/dt = 0$, as indicated: it is therefore possible, by supplementing the theorem with a deduction from equations (3.3.11), to prove as below the existence of a larger region of stability.

Consider the region Ω_2 formed by $V_2 = k_4$ and closed by the portion CD of the curve $dV_2/dt = 0$. Throughout this region, dV_2/dt is negative definite, and no trajectory can leave the region across $V_2 = k_4$. At any point on CD, dV_2/dt is zero and a trajectory must run tangent to the V_2 contour through the point. Because CD lies where $\varphi_2 > 0$, the first of equations (3.3.11) states that $d\varphi_1/dt > 0$; hence, every trajectory from CD has a component of velocity in the positive φ_1 direction. From inspection of the directions of the V_2 contours relative to CD, it is evident that all trajectories crossing CD do so into the region Ω_2. Thus, the same purpose is fulfilled by CD as by the closing portion of the $V_2 = k_4$ contour required by the theorem, and Ω_2 must be a region of asymptotic stability.

For $N < 8{\cdot}0$ approximately, the contour $V_2 = k_5 = 4(N + 4)$ through B provides the limiting contour. The condition for a stable response from an initially stable equilibrium state is therefore

$$K\vartheta_{1f} + 3\sqrt{(1 - K - K\vartheta_{1f})^2 + 4K} > K\vartheta_{1o} + \sqrt{(1 - K - K\vartheta_{1o})^2 + 4K} \qquad (3.4a.6)$$

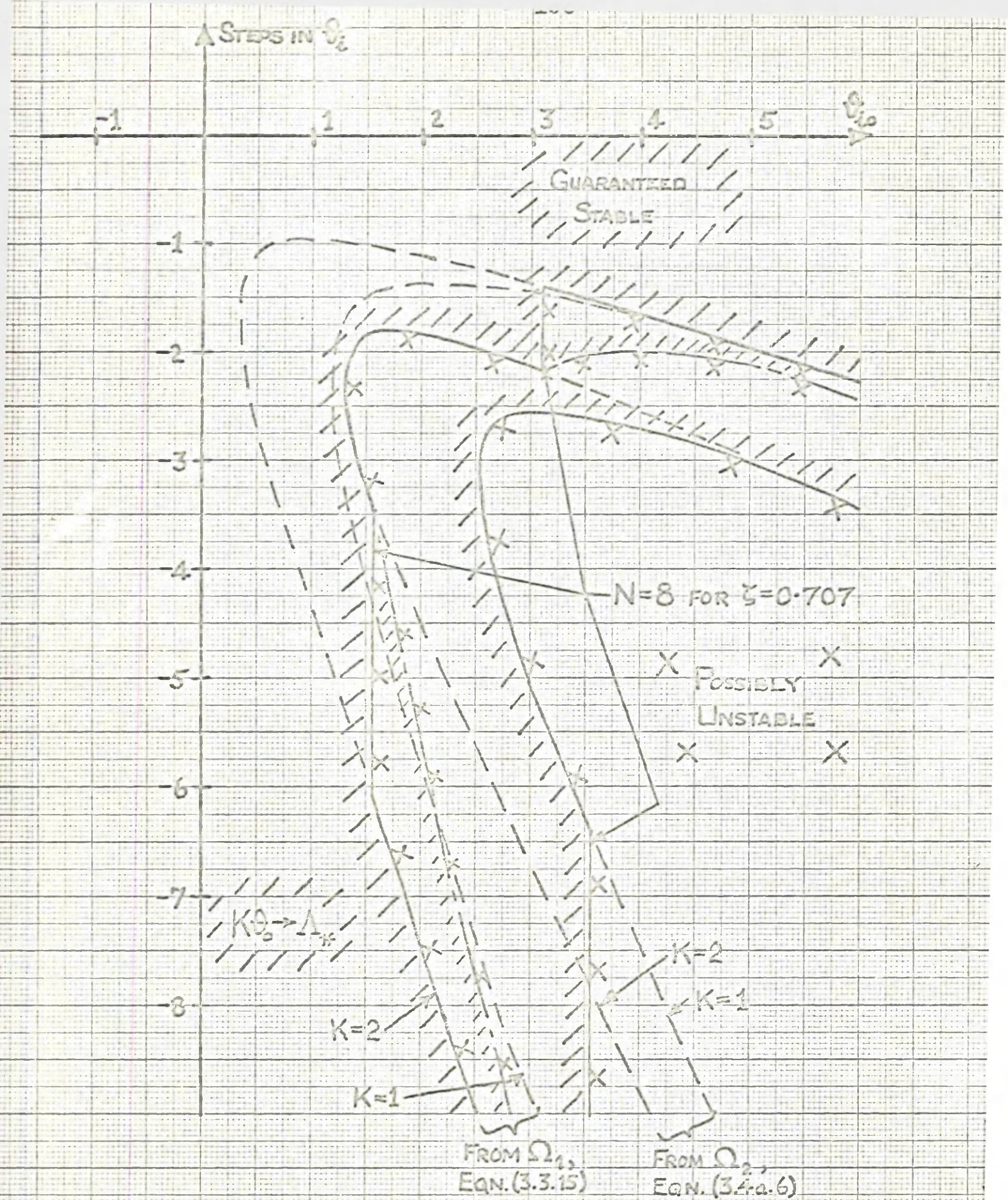

Figure 3.16 : Enlargement from Ω_2 of the regions of guaranteed stability of Figure 3.12.

in place of condition (3.3.15) from Ω_1. For $6 + 2\sqrt{17} \geqslant N \geqslant 8{\cdot}0$, however, the contour through B is unsuitable because it crosses the right-hand branch of the curve $dV_2/dt = 0$ for a negative value of φ_2 and/or because it does not form a closed region with CD. In this range of N, the contour with the greatest value between k_3 and k_5, which does not fail in this way, may be used to give improved bounds: a condition similar to (3.3.15) and (3.4a.6) is obtained, in which the coefficient of the left-hand radical lies between 2 and 3. For the limiting value of $N = 6 + 2\sqrt{17}$, this coefficient is 2·62 approximately from the contour $V_2 = 52$.

Figure 3.16 shows the enlargement, due to condition (3.4a.6), of the regions of guaranteed stability in Figure 3.12, and the corresponding reductions of the regions within which the step response may be unstable. The restriction of $N < 8{\cdot}0$ for the validity of (3.4a.6) implies that, for particular values of K and ζ, these enlargements are only valid for

$$\left[K\left(\xi_{1f} + 1\right) - 1\right]^2 < 4{\cdot}0\left(16\zeta^4 - K\right) \qquad (3.4a.7)$$

approximately; the Figure shows the extensions for $\zeta = 0{\cdot}707$ only. For values of N such that $8{\cdot}0 < N < 6 + 2\sqrt{17}$, boundaries are found lying between those from conditions (3.3.15) and (3.4a.6), certain sections only of which are likewise valid for given K and ζ: the form of the greatest extension from V_2 to the region of guaranteed stability is also indicated.

3.4b The method of Krasovskii and the Variable Gradient method of Schultz and Gibson

A few techniques do exist for the systematic production of Lyapunov functions, and brief attention is given here to two such procedures.

In that due to Krasovskii[15] in which the differential equations are described by

$$\frac{dx_i}{dt} = f_i(x_1, \ldots, x_n), \quad i = 1, \ldots, n$$

$$f_i(0) \equiv 0$$

one constructs the Jacobian matrix F for the system:

$$F = \begin{bmatrix} \partial f_1/\partial x_1 & \cdot & \cdot & \partial f_1/\partial x_n \\ \cdot & \cdot & \cdot & \cdot \\ \partial f_n/\partial x_1 & \cdot & \cdot & \partial f_n/\partial x_n \end{bmatrix}$$

Thereafter the symmetric matrix $\hat{F} = F + F'$, where F' is F transpose, is obtained, and if $\hat{F}$ can be shown (by Sylvester's criteria) to be positive definite, the system is guaranteed to be globally asymptotically stable. However, since the system in hand has been shown to be asymptotically stable only within a portion of state space, the method of Krasovskii is clearly inapplicable.

The second procedure is not restricted to the establishment of global stability, and is therefore applicable. As the name

implies, the Variable Gradient method of Schultz and Gibson[16] starts with an assumed variable gradient function ∇V from which V and dV/dt may be derived; the unknown elements of ∇V are determined by constraints on dV/dt and by the generalised curl equations which arise from the requirement that $\nabla \times \nabla V = 0$. In terms of equation (3.3.11), the gradient function is assumed to have the form

$$\nabla V = \begin{bmatrix} \nabla V_1 \\ \nabla V_2 \end{bmatrix} = \begin{bmatrix} a_{11}\varphi_1 + a_{12}\varphi_2 \\ a_{21}\varphi_1 + {}^{2}\varphi_2 \end{bmatrix}$$

where the coefficients a may be functions of φ_1 and φ_2, from which

$$V = \int_0^{\varphi} \nabla V' . d\varphi \quad \text{and} \quad \frac{dV}{dt} = \nabla V' . \frac{d\varphi}{dt} , \quad \varphi = \begin{bmatrix} \varphi_1 \\ \varphi_2 \end{bmatrix}$$

The curl equation on ∇V in this case is simply

$$\frac{\partial \nabla V_1}{\partial \varphi_2} = \frac{\partial \nabla V_2}{\partial \varphi_1}$$

Using equations (3.3.11), the general form for the time derivative of V appears as

$$\frac{dV}{dt} = \omega_n(\sqrt{R}a_{12} - 4\zeta)\varphi_2^2 - \omega_n\sqrt{R}a_{21}\varphi_1^2 + \omega_n(\sqrt{R}a_{11} - 2\zeta a_{21} - 2\sqrt{R})\varphi_1\varphi_2 - \omega_n\sqrt{R}(2\varphi_2 + a_{21}\varphi_1)\varphi_1^2 \qquad (3.4b.1)$$

The next step in the procedure is to constrain dV/dt to be at least negative semidefinite by selection of suitable expressions for the coefficients a; various ways of so doing have been tried,

the results of three of which follow: –

(i) Impose $\alpha_{12} = 0$, and $\alpha_{21} = C\varphi_2/\varphi_1$ (C a constant) to eliminate the term in φ_1^3 in (3.4b.1): then

$$\frac{dV}{dt} = -4\zeta\omega_n\varphi_2^2 - \omega_n\sqrt{R}C\varphi_1\varphi_2 + \omega_n(\sqrt{R}\alpha_{11} - 2\sqrt{R})\varphi_1\varphi_2 -$$

$$2\zeta\omega_n C\varphi_2^2 - \omega_n\sqrt{R}(2 + C)\varphi_1^2\varphi_2$$

$$= -2\zeta\omega_n(2 + C)\varphi_2^2 + \omega_n\sqrt{R}(\alpha_{11} - 2 - C)\varphi_1\varphi_2 - \omega_n\sqrt{R}(2 + C)\varphi_1^2\varphi_2$$

To make this negative semidefinite, let

$$\alpha_{11} = (2 + C)(1 + \varphi_1)$$

so that $\frac{dV}{dt} = -2\zeta\omega_n(2 + C)\varphi_2^2$ and $\nabla V = \begin{bmatrix} (2 + C)(1 + \varphi_1)\varphi_1 \\ (2 + C)\varphi_2 \end{bmatrix}$

It is seen that the curl equation is satisfied by this form of ∇V. Having constrained its time derivative in this way, the function V itself appears as

$$V = (2 + C)\int_{0,0}^{\varphi_1,\varphi_2} [(1 + \varphi_1)\varphi_1\, d\varphi_1 + \varphi_2\, d\varphi_2]$$

$$= (2 + C)(3\varphi_1^2 + 3\varphi_2^2 + 2\varphi_1^3)/6$$

which is seen (for $C = 4$) to be nothing but the function V_1 already found.

(ii) To obtain a different function, one may try setting $\alpha_{11} = 2 + 2\zeta\alpha_{21}/\sqrt{R}$ in (3.4b.1) to eliminate the term in $\varphi_1\varphi_2$ and $\alpha_{12} = 2\zeta/\sqrt{R}$ to produce a term in φ_2^2. This gives

$$\frac{dV}{dt} = -2\zeta\omega_n\varphi_2^2 - \omega_n\sqrt{R}\alpha_{21}\varphi_1^2 - \omega_n\sqrt{R}(2\varphi_2 + \alpha_{21}\varphi_1)\varphi_1^2$$

which may be made negative definite if $a_{21} = -2\varphi_2/\varphi_1$: but then

$$\nabla V = \begin{bmatrix} 2\varphi_1 - 2\zeta\varphi_2/\sqrt{R} \\ 0 \end{bmatrix}$$

and the curl equation cannot be satisfied, since $-2\zeta/\sqrt{R} \neq 0$.

(iii) In a further attempt, one may set $a_{21} = (C_2 + C_3\varphi_2)/\varphi_1$, to eliminate again the term in φ_1^3 in (3.4b.1), and $a_{12} = C_1$ to produce a term in φ_2^2, leading to

produce a term in φ_2^2, leading to

$$\frac{dV}{dt} = \omega_n(\sqrt{R}C_1 - 4\zeta - 2\zeta C_3)\varphi_2^2 - \omega_n\sqrt{R}C_2\varphi_1^2 + \omega_n\sqrt{R}(a_{11} - 2 - C_3)\varphi_1\varphi_2$$

The choice of $a_{11} = (2 + C_3)(1 + \varphi_1)$ eliminates the terms in $\varphi_1\varphi_2$ and $\varphi_1^2\varphi_2$, and to obtain at least a negative semidefinite form requires $C_2 = 0$. With these appointments the curl equation now gives that C_1 must be zero, and one has returned to the result of (i).

As demonstrated by the above, the Variable Gradient method has not produced any Lyapunov functions with negative semidefinite time derivative which are different from V_1.

3.4c The method of Zubov

The procedure of Zubov[17] for the construction of Lyapunov functions holds more promise, in the experience of this author, than does that of Schultz and Gibson. It is less dependent on the sort of intuitive trial and error required in the

determination of the coefficients α and guarantees the production of a V function to establish a region of asymptotic stability, whether global or not. Margolis and Vogt[18] have recently published a valuable account in English of the method, to which this author[19] has suggested some modifications; the main points are described below in terms of only a two-dimensional system, after which its application to the system in hand is discussed.

The notation adopted for the method describes the system as

$$\frac{dx}{dt} = f_1(x,y) = f_{11}(x,y) + \sum_{m_1+m_2 \geqslant 2}^{\infty} P_1(m_1,m_2) x^{m_1} y^{m_2}$$

$$\frac{dy}{dt} = f_2(x,y) = f_{21}(x,y) + \sum_{m_1+m_2 \geqslant 2}^{\infty} P_2(m_1,m_2) x^{m_1} y^{m_2} \qquad (3.4c.1)$$

in which $f_{11}(x,y) = a_{11}x + a_{12}y$

$f_{21}(x,y) = a_{21}x + a_{22}y$

are the linear function components of f_1 and f_2: the method presupposes that the origin $x = y = 0$ is asymptotically stable, and that the roots of the characteristic equation of the linear approximation all have negative, nonzero real parts.

Attention is focussed on the following partial differential equation in the function $v(x,y)$:

$$\frac{\partial v}{\partial x} f_1(x,y) + \frac{\partial v}{\partial y} f_2(x,y) = -\varphi(x,y)\left[1 - v(x,y)\right] \qquad (3.4c.2)$$

in which $\varphi(x,y) = \varphi_2(x,y) + \varphi_3(x,y) + \ldots + \varphi_m(x,y) + \ldots$ is some positive definite function of x and y, and φ_m is a homogeneous form of m'th degree in x and y. According to a theorem of Lyapunov, the function $v(x,y)$ can be uniquely determined in the form of a convergent power series going to zero for $x = y = 0$:

$$v(x,y) = v_2(x,y) + v_3(x,y) + \ldots + v_m(x,y) + \ldots \qquad (3.4c.3)$$

where $v_m(x,y) = {}_mD_0x^m + {}_mD_1x^{m-1}y + \ldots + {}_mD_{m-1}xy^{m-1} + {}_mD_my^m$

If equation (3.4c.2) is incapable of solution in closed form to give the exact function $v(x,y)$ for a particular $\varphi(x,y)$, it may be solved by the following set of recurrence equations

$$\begin{aligned} \frac{\partial v_2}{\partial x} f_{11} + \frac{\partial v_2}{\partial y} f_{21} &= -\varphi_2(x,y) \\ \frac{\partial v_m}{\partial x} f_{11} + \frac{\partial v_m}{\partial y} f_{21} &= R_m(x,y) \end{aligned} \qquad (3.4c.4)$$

in which

$$R_m = -\varphi_m + \sum_{j+k=m} \varphi_j v_k - \sum_{j+k=m+1} \left[\sum_{m_1+m_2=j} P_1(m_1, m_2) x^{m_1} y^{m_2} \frac{\partial}{\partial x} + \sum_{m_1+m_2=j} P_2(m_1, m_2) x^{m_1} y^{m_2} \frac{\partial}{\partial y} \right] v_k$$

$$j, k, m = 2, 3, 4, \ldots .$$

is a function of m'th degree in x and y which is known if each of the $v_2(x,y)$, $v_3(x,y)$, . . . $v_{m-1}(x,y)$ have already been

determined. Thus the sequence v_m is obtainable, giving the n'th degree series approximation $v^{(n)} = \sum_{2}^{n} v_m$ for the exact solution $v(x,y)$. The function $v_2(x,y)$ is guaranteed by a theorem of Lyapunov[12] to be a positive definite quadratic form.

Zubov shows that the boundary of the region Ω of asymptotic stability is given by the curves $v(x,y) = 1$, and that the stability is global if $v(x,y) < 1$ for all x and y. For the approximation $v^{(n)}$, it is important to discover what curves $v^{(n)} = c_1^{(n)}$ describe regions which are guaranteed to be contained within Ω and so provide approximations to it. Margolis and Vogt present theorems which establish regions of stability based on the first approximation $v^{(2)}$ and then on higher approximations $v^{(n)}$, but it has been considered necessary by this author to present the following modified versions of these theorems to allow the use of positive semidefinite functions φ: the proofs are to be found in ref.19.

Definition: define as w_2 the set of all points (x,y) for which $dv_2/dt = 0$, other than points for which

$$dv_2(x+\delta x, y+\delta y)/dt \leqslant 0 \text{ or } dv_2(x+\delta x, y+\delta y)/dt \geqslant 0$$

for all δx and all δy infinitesimally small. In other words, w_2 consists of all points of zero dv_2/dt which define boundaries between regions of positive and negative dv_2/dt, while excluded from w_2 are points of zero dv_2/dt which lie in surrounding regions of dv_2/dt with constant sign. Denote these excluded

points by w_1. Designate by c_1 the smallest value of v_2 on w_2.

(3.4c.5)

Theorem: the curve $v_2(x,y) = c_1$ is wholly contained in Ω, provided that the set of points w_1 for $v_2 < c_1$ is not a half-trajectory of the system. (3.4c.6)

Definition: $w_2^{(n)}(x,y)$ = all points (x,y) on which $dv^{(n)}/dt = 0$, other than those ($w_1^{(n)}$) for which

$$dv^{(n)}(x+\delta x,\ y+\delta y)/dt \leqslant 0 \quad \text{or} \quad dv^{(n)}(x+\delta x,\ y+\delta y)/dt \geqslant 0$$

for all δx and all δy infinitesimally small.

$$c_1^{(n)} = \min \left[v^{(n)}(x,y) \text{ on } w_2^{(n)}(x,y) \right] \qquad (3.4c.7)$$

Theorem: the curve $v^{(n)}(x,y) = c_1^{(n)}$ is wholly contained in Ω, provided that the set of points $w_1^{(n)}$ for $v^{(n)} < c_1^{(n)}$ is not a half-trajectory of the system. (3.4c.8)

Turning now to the application of this theory to the stability of the solutions of equation (3.3.10), it has been found preferable to decompose this equation into the following pair of first-order differential equations, rather than to continue with the equivalent pair (3.3.11):

$$\frac{d\varphi_1}{dt} = \omega_n(\sqrt{R}\,\varphi'_2 - 2\zeta\varphi_1) \quad \text{i.e.} \quad \frac{dx}{dt} = \omega_n(\sqrt{R}y - 2\zeta x)$$

$$\frac{d\varphi'_2}{dt} = -\omega_n\sqrt{R}\,\varphi_1(1+\varphi_1) \qquad \frac{dy}{dt} = -\omega_n\sqrt{R}\,x(1+x) \qquad (3.4c.9)$$

The new state variables φ_1 and φ'_2 are replaced for the time being

by x and y for clarity, and the singularities A and B of system (3.4c.9) are at $x = y = 0$ and $x = -1$, $y = -2/\sqrt{N}$ respectively.

The partial differential equation (3.4c.2) in this case appears as

$$\omega_n \frac{\partial v}{\partial x}(\sqrt{R}\,y - 2\zeta x) - \omega_n \sqrt{R} \frac{\partial v}{\partial y} x(1+x) = -(x^2+y^2)(1-v) \qquad (3.4c.10)$$

having chosen $\varphi(x,y)$ as the simplest of positive definite forms, namely (x^2+y^2). To solve this in closed form, one attempts the simultaneous solution of the associated ordinary differential equations

$$\frac{dx}{\sqrt{R}\,y - 2\zeta x} = -\frac{dy}{\sqrt{R}\,x(1+x)} = -\frac{\omega_n dv}{(x^2+y^2)(1-v)} \qquad (3.4c.11)$$

No such solution has been found for these equations, however, so that the exact description of the region of stability is unobtainable. Reverting to the approximate solution after (3.4c.4), and taking $\varphi = 2(x^2+y^2)$, i.e. $\varphi_2 = 2(x^2+y^2)$, $\varphi_m \equiv 0$ for $m > 2$, the first of equations (3.4c.4) gives

$$\omega_n({}_2D_0 x + {}_2D_1 y)(\sqrt{R}y - 2\zeta x) - \omega_n\sqrt{R}({}_2D_1 x + 2\,{}_2D_2 y)x = -2(x^2+y^2) \qquad (3.4c.12)$$

for the determination of the coefficients ${}_2D_k$. From this, it is readily found that

$$v_2 = \left[Nx^2 - 2\sqrt{N}xy + (N+2)y^2\right]/\zeta\omega_n N \quad \text{(positive definite)} \qquad (3.4c.13)$$

for which

$$\frac{dv_2}{dt} = -2(x^2+y^2) - (2N+4)x^2y/\sqrt{N} + 2x^3$$

The curve $2x^3 - [2 + (2N + 4)y/\sqrt{N}]x^2 = 2y^2$, which passes through the two singularities, is w_2; since this is a cubic, the determination of c_1 is clearly difficult and one is forced to abandon this attempt at the first level of approximation.

Using the positive semidefinite function $\varphi = 2y^2$, the coefficients ${}_2D_k$ follow from an equation similar to (3.4c.12) in which the right-hand side is just $-2y^2$. Hence,

$$v_2 = [Nx^2 - 4\sqrt{N}xy + (N + 4)y^2]/2\zeta\omega_n N \quad \text{(positive definite)}$$

for which (3.4c.14)

$$\frac{dv_2}{dt} = -2y^2 - (N + 4)x^2y/\sqrt{N} + 2x^3$$

The curve $2x^3 - (N + 4)yx^2/\sqrt{N} = 2y^2$ passes through the two singularities and is w_2; although one stage simpler than the previous expression for w_2, one is again faced at the outset with the simultaneous solution of a cubic and a quadratic equation.

However, if φ is taken as $2x^2$ the resulting form for v_2 is

$$v_2 = (x^2 + y^2)/2\zeta\omega_n \quad \text{(positive definite)}$$

for which (3.4c.15)

$$\frac{dv_2}{dt} = -2x^2(1 + \sqrt{N}y/2)$$

In this case, since the expression for dv_2/dt is factored, the straight line $y = -2/\sqrt{N}$ is w_2 while the y axis ($x = 0$) is w_1, and the singularities lie one on w_1 and the other on w_2.

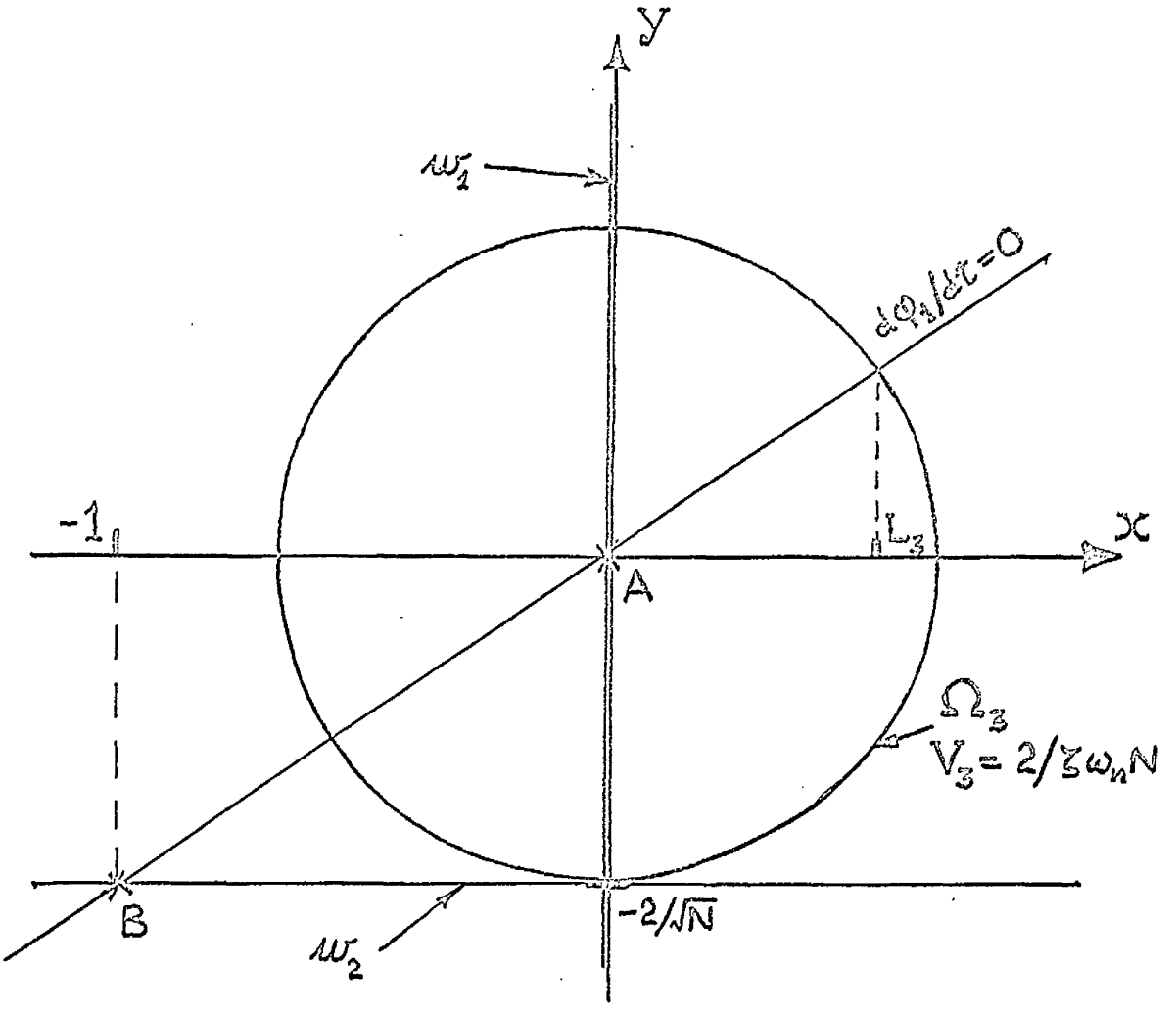

Figure 3.17 : Sketch of the Lyapunov function V_3, produced by the method of Zubov, and Ω_3.

Figure 3.17 shows the useful half-plane of negative semidefinite dv_2/dt. It is apparent that the minimum value (c_1) of v_2 on w_2 is $2/\zeta\omega_n N$, so that since the y axis for $|y| < 2/\sqrt{N}$ is not a solution the circular region $x^2 + y^2 = 4/N$ is one of asymptotic stability: v_2 in (3.4c.15) is therefore referred to as Lyapunov function V_3, and the circle as Ω_3. As stated early on in Section 3.3, the intersection L_3 of Ω_3 with the positive φ_1 axis in the phase plane is of particular interest: on this axis, $d\varphi_1/dt = 0$, so that the corresponding line in the system (3.4c.9) is $y = 2x/\sqrt{N}$. L_3 is therefore given by the value of $x > 0$ at which this line crosses Ω_3, namely

$$L_3 = 2/\sqrt{N+4} \qquad (3.4c.16)$$

If the approximation is continued to include the third-order terms of v_3, the second of equations (3.4c.4) gives

$$\omega_n({}_3D_0x^2 + {}_3D_1xy + {}_3D_2y^2)(\sqrt{R}y - 2\zeta x) - \omega_n\sqrt{R}({}_3D_1x^2 + {}_3D_2xy + {}_3D_3y^2)x$$

$$= R_3 = (y/\zeta\omega_n)(\omega_n\sqrt{R}x^2) \qquad (3.4c.17)$$

for the determination of the coefficients ${}_3D_k$. After equating the coefficients of similar terms, the form of v_3 is found to be

$$v_3 = (Nx^3 - 6\sqrt{N}x^2y - 4\sqrt{N}y^3)/3\zeta\omega_n(N+8)$$

for which

$$\frac{dv_3}{dt} = 2x^2\left[Nx^2 + 2Ny^2 + \sqrt{N}(N+8)y/2\right]/(N+8)$$

so that $v^{(3)} = V_3 + v_3$

$$= \left[3(N+8)(x^2+y^2) + 2Nx^3 - 12\sqrt{N}x^2y - 8\sqrt{N}y^3\right]/6\zeta\omega_n(N+8) \qquad (3.4c.18)$$

and $$\frac{dv^{(3)}}{dt} = \frac{dV_3}{dt} + \frac{dv_3}{dt} = -2x^2\left[(N+8) - Nx^2 - 2Ny^2\right]/(N+8) \qquad (3.4c.19)$$

Thus the y axis forms $w_1^{(3)}$ while $w_2^{(3)}$ is the ellipse $2Ny^2 + Nx^2 = N+8$ passing through B. To find $c_1^{(3)}$, one is again faced with the problem of finding the minimum of a cubic function such as (3.4c.18) on a quadratic curve, the ellipse: if the method of Lagrangian multipliers is invoked, the following equation

$$6(N+8)xy - 24\sqrt{N}xy^2 + 12Nx^2y + 12\sqrt{N}x^3 = 0$$

is obtained for simultaneous solution with the constraint equation of the ellipse, but this hardly reduces the difficulty. No means has been discovered to obtain the expression for $c_1^{(3)}$, which in any case must be a complicated function of N, and it is concluded that the best approximation to Ω for this system, obtainable from the method of Zubov, is Ω_3.

3.4d A method of undetermined coefficients

To summarise the experience so far of the methods of application of Lyapunov's Direct Method, the function V_1 was easily discovered and gives the region Ω_1 for all values of the parameter N. An improvement in the estimate of the actual region

of stability resulted from the establishment of the region Ω_2, but the effort involved was much greater and the region is only valid for a range of values of N. The method of Schultz and Gibson does not appear to be useful in the particular context of the system being studied: it requires the construction of a derivative function dV/dt which is at least negative semidefinite, and has not produced any function other than V_1. The method of Zubov was more successful in producing V_3, but V_3 is only a quadratic form. It appears that Zubov's elegant procedure holds much promise in application to a particular numerical case of a system, when the successive determination of higher-order approximations may be handled by a digital computer; but when working literally with the general case of a system, as in the present study, the fact that explicit solutions are only available to algebraic equations of low degree (possibly three or four) severely limits the level of approximation attainable for general analytical results.

While recognising this restriction to low-degree algebraic forms, it was thought possible to find further Lyapunov functions which would still improve the guaranteed region of stability in the general case of this system. A method of undetermined coefficients has been evolved which has had apparent success in this way, and which enjoys the advantages of greater simplicity and flexibility than the methods of Schultz and Gibson and of

Terms Produced in dV/dt	Terms in V											
	φ_1^2	$\varphi_1\varphi_2'$	$(\varphi_2')^2$	φ_1^3	$\varphi_1^2\varphi_2'$	$\varphi_1(\varphi_2')^2$	$(\varphi_2')^3$	φ_1^4	$\varphi_1^3\varphi_2'$	$\varphi_1^2(\varphi_2')^2$	$\varphi_1(\varphi_2')^3$	$(\varphi_2')^4$
φ_1^2	X	X										
$\varphi_1\varphi_2'$	X	X	X									
$(\varphi_2')^2$		X										
φ_1^3		X		X	X							
$\varphi_1^2\varphi_2'$			X	X	X	X						
$\varphi_1(\varphi_2')^2$					X	X	X					
$(\varphi_2')^3$						X						
φ_1^4					X			X	X			
$\varphi_1^3\varphi_2'$						X		X	X	X		
$\varphi_1^2(\varphi_2')^2$							X		X	X	X	
$\varphi_1(\varphi_2')^3$										X	X	X
$(\varphi_2')^4$											X	
φ_1^5									X			
$\varphi_1^4\varphi_2'$										X		
$\varphi_1^3(\varphi_2')^2$											X	
$\varphi_1^2(\varphi_2')^3$												X

Figure 3.18: Table of terms in V and dV/dt for equations (3.4c.9).

Zubov. It is a rationalisation of the procedure which produced V_2, and so starts with an assumed form for V in which the coefficients of the various terms are to be determined to render both V and dV/dt suitable.

The initial selection of terms to be included in the V function is aided by a table such as that shown in Figure 3.18, which applies to the system under discussion. In each column of this table is a statement of the terms produced in the function dV/dt by the presence of a particular term in the function V, having regard to the system equations (3.4c.9); there is a distinguishable pattern in this array. Since the form of V includes a general constant factor, only (n − 1) coefficients of its n terms may be considered undetermined; the values of these coefficients may be determined, wholly or in part, by any number up to (n − 1) of conditions on the terms in dV/dt. These conditions are generally such as eliminate terms of odd degree in dV/dt, which do not lead to sign definiteness.

The procedure as outlined so far is not of course sufficient to guarantee the production of a Lyapunov function; all it does is to facilitate the construction by trial and error of a possible function. There is no stipulation that dV/dt must be negative semidefinite everywhere, which means that for the type of system with a limited region of stability one is free to

search for a suitably limited region of negative semidefinite dV/dt around the origin. For dV_2/dt, this region is a strip on both sides of the φ_2 axis, valid only for $N < 6 + 2\sqrt{17}$. The use of this method is now demonstrated in its further application to the system of equations (3.4c.9).

For V to be positive definite near the origin, the terms of lowest degree in V must be a pair of equal, even degree in φ_1 and φ'_2 : thus the terms φ_1 and φ'_2 do not appear in the table, and it is natural to include firstly φ_1^2 and $B(\varphi'_2)^2$, B a constant, rather than φ_1^4 and $B(\varphi'_2)^4$ or others. The coefficient of φ_1^2, being unity, is the selected general constant factor of V, and the coefficients of all other terms are undetermined constants. The table indicates that this introduces in dV/dt one term in φ_1^2, one in $\varphi_1^2\varphi'_2$ and two in $\varphi_1\varphi'_2$: the whole coefficient of $\varphi_1\varphi'_2$ may then be made zero by the appropriate choice for B. To eliminate the term $\varphi_1^2\varphi'_2$ of odd degree, the coefficient C may be used if a term $C\varphi_1^3$ is included in V, but this introduces a term in φ_1^3 in dV/dt: to eliminate this in turn, the coefficient A may be used of a term $A\varphi_1\varphi'_2$ in V. The further terms introduced through $A\varphi_1\varphi'_2$ are only in φ_1^2, $(\varphi'_2)^2$ and $\varphi_1\varphi'_2$, the last of which is removed by the choice of B.

To proceed in this way,

$$V = \varphi_1^2 + A\varphi_1\varphi_2 + B(\varphi'_2)^2 + C\varphi_1^3 \qquad (3.4d.1)$$

so that generally

$$\frac{dV}{dt} = -\zeta\omega_n\Big[(4 + A\sqrt{N})\,\varphi_1^2 - A\sqrt{N}\,(\varphi'_2)^2 - 2(\sqrt{N} - A - B\sqrt{N})\varphi_1\varphi'_2 + (A\sqrt{N} + 6C)\varphi_1^3 + \sqrt{N}(2B - 3C)\varphi_1^2\varphi'_2\Big] \qquad (3.4d.2)$$

The coefficients of the last three terms in (3.4d.2) are made zero by the choice

$$A = \frac{4\sqrt{N}}{4-N}, \quad B = \frac{N}{N-4}, \quad \text{and} \quad C = \frac{2N}{3N-12}$$

which leaves the time derivative as

$$\frac{dV}{dt} = -4\zeta\omega_n\Big[\frac{4}{4-N}\varphi_1^2 + \frac{N}{N-4}(\varphi'_2)^2\Big] \qquad (3.4d.3)$$

It can be seen, without even considering the resulting form of V, that this procedure is useless; expression (3.4d.3) is not negative semidefinite even in the neighbourhood of the origin, since the two coefficients are of opposite sign. This failure could have been predicted, since the above elimination of three terms in (3.4d.2) leaves only the sum of two quadratic terms, which together may produce a sign definite function but not one that is sign semidefinite; a sign definite function is of no use, because as is mentioned in Section 3.3 the function dV/dt is at best negative semidefinite everywhere for this system.

In a further attempt with form (3.4d.1), the three constants can be so chosen as to eliminate again the terms in $\varphi_1\varphi'_2$ and $\varphi_1^2\varphi'_2$ and the term in $(\varphi'_2)^2$ rather than in φ_1^3. Thus, with $A = 0$, $B = 1$, $C = 2/3$,

$$V_4 = \varphi_1^2 + (\varphi'_2)^2 + \frac{2}{3}\varphi_1^3$$

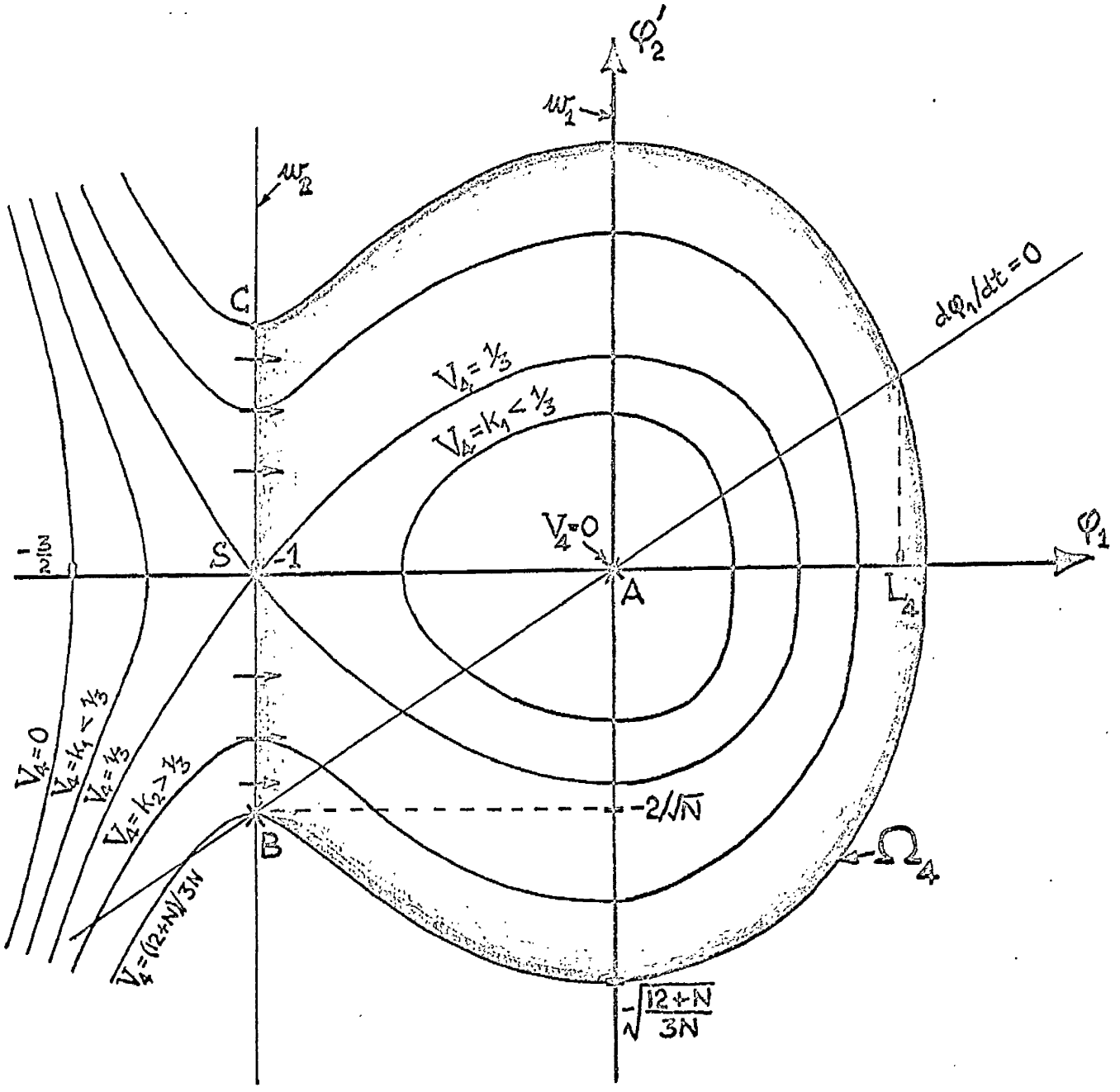

Figure 3.19 : Sketch of the function V_4 and the region Ω_4 of stability.

and $$\frac{dV_4}{dt} = -4\zeta\omega_n \varphi_1^2(1+\varphi_1) \qquad (3.4d.4)$$

and dV_4/dt is apparently negative semidefinite in the half–plane $\varphi_1 > -1$, for $\varphi_1 = 0$ is the set w_1 and $\varphi_1 = -1$ is w_2: see Figure 3.19. The function V_4 is seen to be the form in φ_1 and φ'_2 analogous to V_1 in φ_1 and φ_2, so that its nature need not be further described than it is in Figure 3.19. Accordingly, the closed region formed by the contour $V_4 = 1/3$, like Ω_1, is again one of asymptotic stability, because within it dV_4/dt is negative semidefinite and not identically zero on a trajectory; however, because B now lies at $\varphi_1 = -1$, $\varphi'_2 = -2/\sqrt{N}$, a larger region of stability may be proved to exist using a similar deduction to that used in arriving at Ω_2.

Consider the contour through B, for which $V_4 = (12+N)/3N$: this has intersections with the φ'_2 axis at $\pm\sqrt{(12+N)/3N}$, which points are further from the origin than $2/\sqrt{N}$. The region partly contained by this contour for $\varphi_1 > -1$ and closed by the portion BC of the line $\varphi_1 = -1$ is region Ω_4 of asymptotic stability, for the following reason: on BC, for which $\varphi_1 = -1$, $\varphi'_2 > -2/\sqrt{N}$, the first of equations (3.4c.9) gives

$$\frac{d\varphi_1}{dt} \geqslant 2\zeta\omega_n\left(\frac{\sqrt{N}}{2} - \frac{2}{\sqrt{N}} + 1\right), \quad \text{i.e.} \quad \frac{d\varphi_1}{dt} \geqslant 0$$

so that all trajectories which cross BC do so into the region Ω_4. It may be noted that the saddle point S of the contour $V_4 = 1/3$ again lies on the curve w_2.

It is once more of particular interest to determine L_4, the value of φ_1 at which the boundary Ω_4 intersects the line $d\varphi_1/dt = 0$ for $\varphi_1 > 0$. This requires the solution of the following cubic equation, which arises from the simultaneous solution of $V_4 = (12 + N)/3N$ with $\varphi'_2 = 2\varphi_1/\sqrt{N}$:

$$2N\varphi_1^3 + (3N + 12)\varphi_1^2 - (N + 12) = 0 \qquad (3.4d.5)$$

In general, the explicit (Cardan) solution of a cubic is rather unworkable; but in this case one root is already known, namely $\varphi_1 = -1$, since the boundary Ω_4 has been arranged to intersect the line $d\varphi_1/dt = 0$ at B for all N. By factoring out $(\varphi_1 + 1)$ from (3.4d.5), the quadratic equation

$$2N\varphi_1^2 + (N + 12)\varphi_1 - (N + 12) = 0$$

is left, whose roots give the other two intersections. Thus the required expression is

$$L_4 = \left[\sqrt{3(N + 12)(3N + 4)} - N - 12\right]/4N \qquad (3.4d.6)$$

The successful production of V_4 by this method of undetermined coefficients, in comparison with the result of (say) the method of Zubov, is due to the way in which a cubic function has been found usable by arranging that one root of the derived cubic equation is previously known. V_4 is, however, still not the best function achieved: while continuing to work with this form of function, but in more general terms, one further improvement has been made in the following way. Returning to (3.4d.1), again

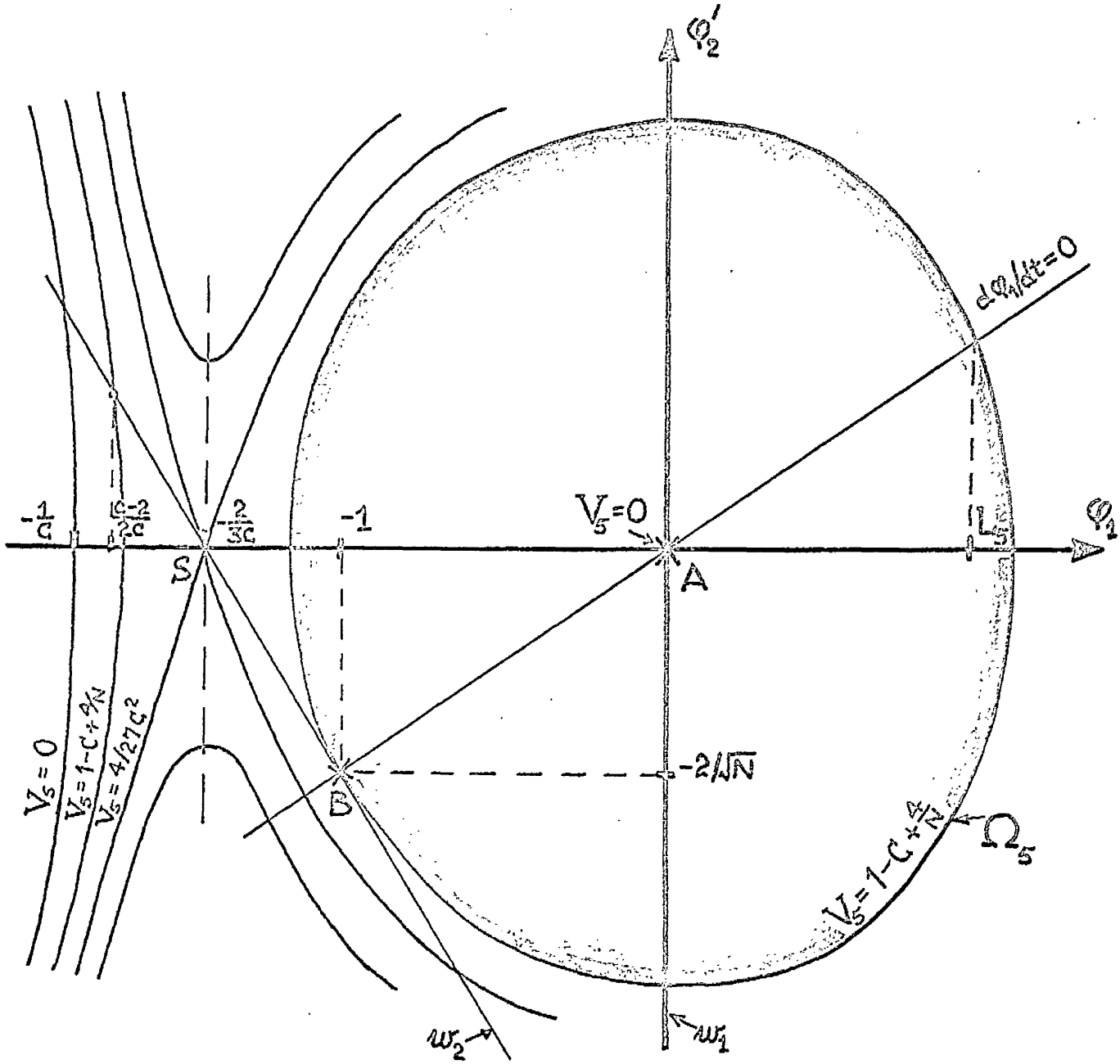

Figure 3.20 : Sketch of the function V_5 and the region Ω_5 of stability, when $N = 24\,c/(2-3c)^2$.

set $A = 0$ and $B = 1$ to eliminate the terms in $(\varphi'_2)^2$ and $\varphi_1\varphi'_2$ in dV/dt, but let C remain undetermined as yet within the range $0 \leqslant C \leqslant 2/3$. Then, rather than (3.4d.4), one has

$$V_5 = \varphi_1^2 + (\varphi'_2)^2 + C\varphi_1^3$$

$$\frac{dV_5}{dt} = -\zeta\omega_n\varphi_1^2\left[4 + 6C\varphi_1 + \sqrt{N}(2-3C)\varphi'_2\right] \qquad (3.4d.7)$$

so that there is a half-plane of negative semidefinite dV_5/dt "above and to the right of" the straight line through B with the equation

$$\varphi'_2 = -\frac{4}{\sqrt{N}(2-3C)} - \frac{6C}{\sqrt{N}(2-3C)}\varphi_1 \qquad (3.4d.8)$$

since $\varphi_1 = 0$ is the set w_1 and the line (3.4d.8) is w_2. It is seen that V_3 and V_4 are respectively the particular limiting cases of V_5 in which $C = 0$ and $C = 2/3$, and that one is now considering a half-plane of negative semidefinite dV_5/dt whose straight-line boundary through B may be inclined with any negative gradient between the horizontal and the vertical.

The form of V_5 is clearly similar to that of V_4; specifically, the contour $V_5 = 0$ lies in the half-plane $\varphi_1 < -1/C$, and point B lies on the contour $V_5 = 1 - C + 4/N$ (see Figure 3.20). By considering the discriminant of the cubic $V_5 = \varphi_1^2 + C\varphi_1^3$ it is found that the contour with the saddle point is $V_5 = 4/27\ C^2$, that S is at $\varphi_1 = -2/3C$, $\varphi'_2 = 0$, and that S again lies on w_2: thus, the contour through B forms a closed path around the origin so

long as $1 - C + 4/N < 4/27\ C^2$

$$\text{i.e. if } N > 108\ C^2/(2-3C)^2\,(1+3C) \qquad (3.4d.9)$$

The gradient at a point on any contour is given by

$$2\varphi'_2 \frac{d\varphi'_2}{d\varphi_1} = -2\varphi_1 - 3C\varphi_1^2 \qquad (3.4d.10)$$

so that the loci of extrema are the lines $\varphi_1 = 0$ and $\varphi_1 = -2/3C$; by considering the next higher derivative, it is found that no inflexions occur on the closed-path portions of contours for which $V_5 < 4/27\ C^2$. Now, from (3.4d.10), the gradient at B of the contour through it is $-\sqrt{N}(2-3C)/4$, while the gradient of the line w_2, equation (3.4d.8), is $-6C/\sqrt{N}(2-3C)$. Therefore the contour lies, locally, "above and to the right of" the line at B if they are tangent there; equating the gradients gives the condition for tangency as

$$N = 24\ C/(2-3C)^2 \qquad (3.4d.11)$$

If the two conditions (3.4d.9) and (3.4d.11) are taken together, since $24\ C\,(1+3C) > 108\ C^2$ reduces to the prescribed restriction $C < 2/3$, the conditions may both be satisfied: i.e. if $N = 24\ C/(2-3C)^2$, the contour at B is tangent to w_2 and forms a closed region around A. Finally, since this contour is closed and therefore has no inflexions on it, the closed region must lie entirely "above and to the right of" w_2, i.e. in the region of negative semidefinite dV_5/dt. To complete the description of this situation, the intersections of contour $V_5 = 1 - C + 4/N$

with w_2 when $N = 24\,C/(2-3C)^2$ are given by the roots of

$$2C\varphi_1^3 + (2+3C)\varphi_1^2 + 4\varphi_1 + (2-C) = 0$$

i.e. $$(\varphi_1+1)^2(2C\varphi_1+2-C) = 0$$

so that there is double contact at B, $\varphi_1 = -1$, and the third intersection is at $(C-2)/2C$: the last mentioned lies on the branch of the contour to the left of that with the saddle point, since $(C-2)/2C < -2/3C$ for $C < 2/3$.

Because all the conditions in the Theorem of Section 3.3 are met, the foregoing has established that a further region of asymptotic stability exists, whose boundary Ω_5 is described by

$$3N\varphi_1^2 + 3N(\varphi_2')^2 + \left[2(N+2) - 4\sqrt{N+1}\right]\varphi_1^3 = N + 8 + 4\sqrt{N+1} \qquad (3.4d.12)$$

The intercept of Ω_5 with the line $d\varphi_1/dt = 0$, for $\varphi_1 > 0$, is therefore given explicitly by

$$L_5 = \frac{\sqrt{3(N+8+4\sqrt{N+1})(3N+8-4\sqrt{N+1})} - N - 8 - 4\sqrt{N+1}}{4(N+2) - 8\sqrt{N+1}} \qquad (3.4d.13)$$

The derivation of L_5 from (3.4d.12) and the equation of $d\varphi_1/dt = 0$ is only possible since one root of the resulting cubic equation, namely $\varphi_1 = -1$, is previously known, just as explained in connection with L_4.

In summary, a comparison of the regions Ω_3, Ω_4 and Ω_5 is provided by Figure 3.21(a), which indicates the successive

(a)

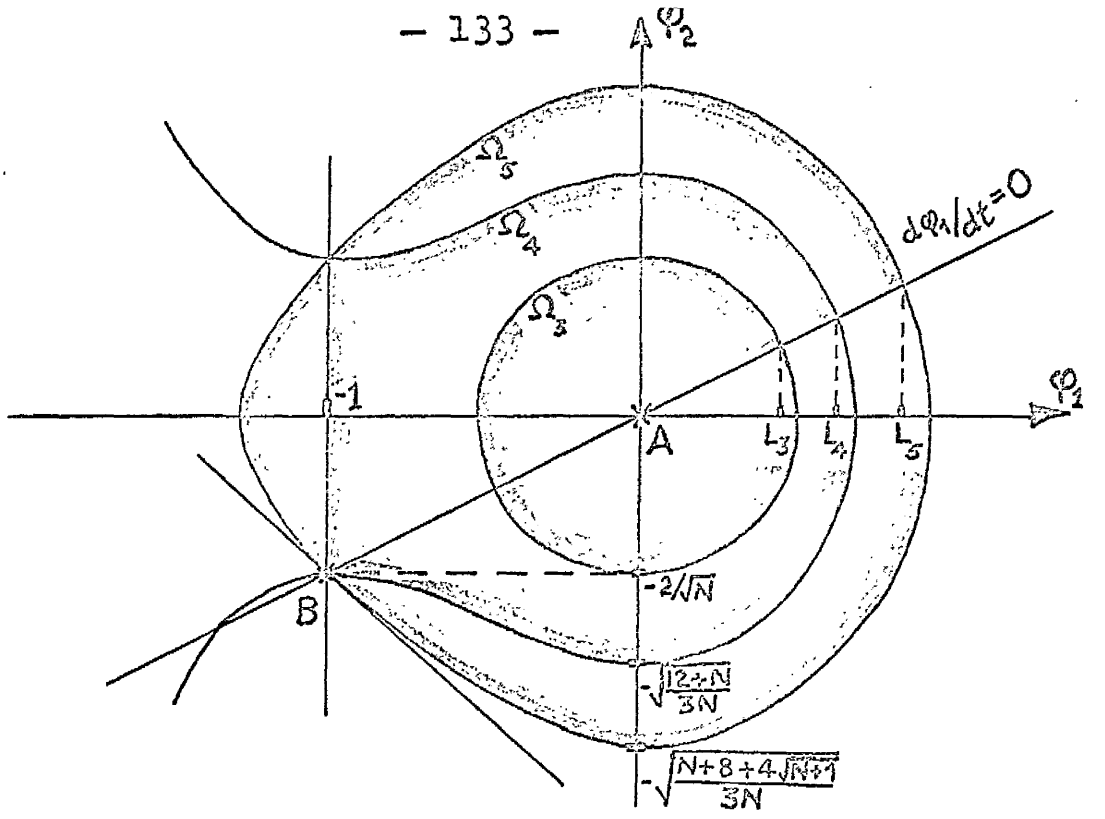

(b)

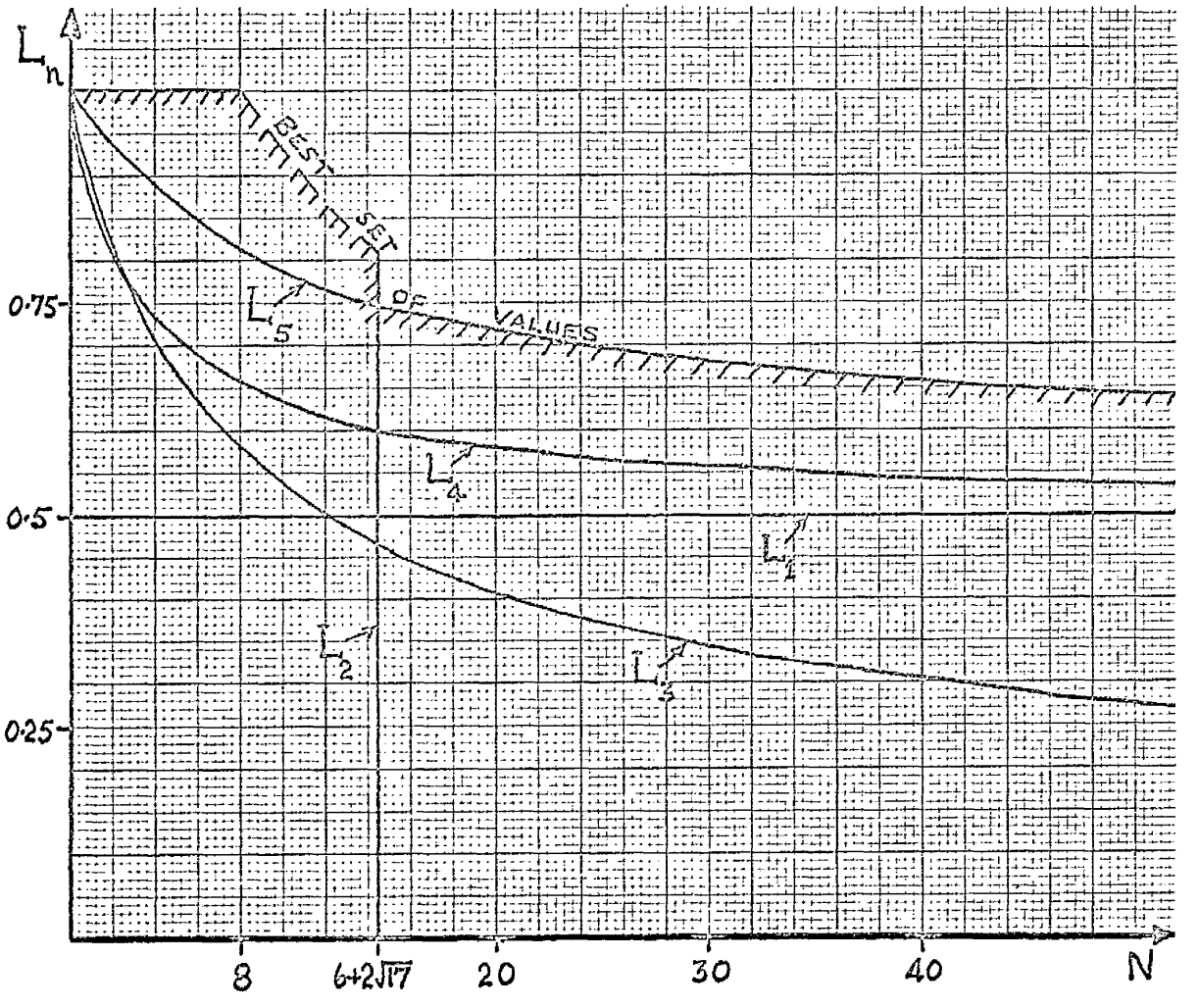

Figure 3.21 (a) A comparison of the regions Ω_3, Ω_4 and Ω_5

(b) The various measures L_n of Ω_n as functions of N.

enlargements of the guaranteed regions of stability in the general case of the system. A quantitative measure of Ω_n is provided by the functions $L_n(N)$, which are plotted in Figure 3.21(b). L_1, being equal to 0·5, is independent of N, and L_2 gives the greatest set of values of all, up to its limit of validity $N = 6 + 2\sqrt{17}$; L_3 represents no improvement over the combination of L_1 and L_2, since (3.4c.16) tends to zero with increasing N, but L_4 and L_5 in turn have values progressively greater than 0·5, for $N > 6 + 2\sqrt{17}$; applications of L'Hôpital's rule to (3.4d.6) and (3.4d.13) show that both L_4 and L_5 tend to 0·5 with increasing N. Thus, the best set of values for L obtained from the various V functions is

$$L = 1 \text{ for } 0 \leqslant N \leqslant 8{\cdot}0 \text{ (approx.)}$$

$$1 > L > 0{\cdot}81 \text{ (approx.) for } 8{\cdot}0 \text{ (approx.)} < N \leqslant 6 + 2\sqrt{17}$$

$$\text{and } L = L_5 \quad \text{for} \quad 6 + 2\sqrt{17} < N .$$

Before leaving the form (3.4d.7), it is worthwhile investigating if V_5 is the particular function of this class which produces the greatest values for L, in view of the improvement of L_5 over L_4. The range of the coefficient C for consideration is

$$\left[2 (N + 2) - 4\sqrt{N + 1} \right] / 3N \leqslant C \leqslant 2/3$$

since the above expressions for the gradients of the contour through B and of w_2 show that, within this range, the contour only intersects w_2 for $\varphi_1 \leqslant -1$; a region of stability may then

be formed by the part of this contour for $\varphi_1 > -1$ and closed by the line $\varphi_1 = -1$, using the previous argument, for all $C \neq [2(N+2) - 4\sqrt{N+1}]/3N$. It is readily found that the intersections of the boundary of such a region with the line $d\varphi_1/dt = 0$ are given by

$$(\varphi_1 + 1)\left[CN\varphi_1^2 + (4 + N - CN)\varphi_1 - (4 + N - CN)\right] = 0$$

so that the expression for L as a function of C and N is

$$L = \left[\sqrt{(4 + N - CN)(4 + N + 3CN)} + CN - 4 - N\right]/2CN \qquad (3.4d.14)$$

Partial differentiation of (3.4d.14) with respect to C gives

$$\frac{\partial L}{\partial C} = \frac{[4 + N]\left[\sqrt{(4 + N - CN)(4 + N + 3CN)} - CN - 4 - N\right]}{2C^2N\sqrt{(4 + N - CN)(4 + N + 3CN)}} \qquad (3.4d.15)$$

which is not zero for any value of C within the range; there is thus no (true) extremum of L with respect to C for these values of C. However, if $C = 2/3$, $\partial L/\partial C < 0$ for all N since

$$\sqrt{9N^2 + 120N + 144} < 12 + 5N \quad \text{for all N}$$

and if $C = [2(N+2) - 4\sqrt{N+1}]/3N$, $\partial L/\partial C$ is again negative for all N since

$$5N + 16 - 4\sqrt{N+1} > \sqrt{3(N + 8 + 4\sqrt{N+1})(3N + 8 - 4\sqrt{N+1})}$$

for all N. (This reduces to $N^4 > 0$). Thus, because L is a continuous function of C, the maximum value of L for any N occurs when $C = [2(N+2) - 4\sqrt{N+1}]/3N$; in other words, the best set L

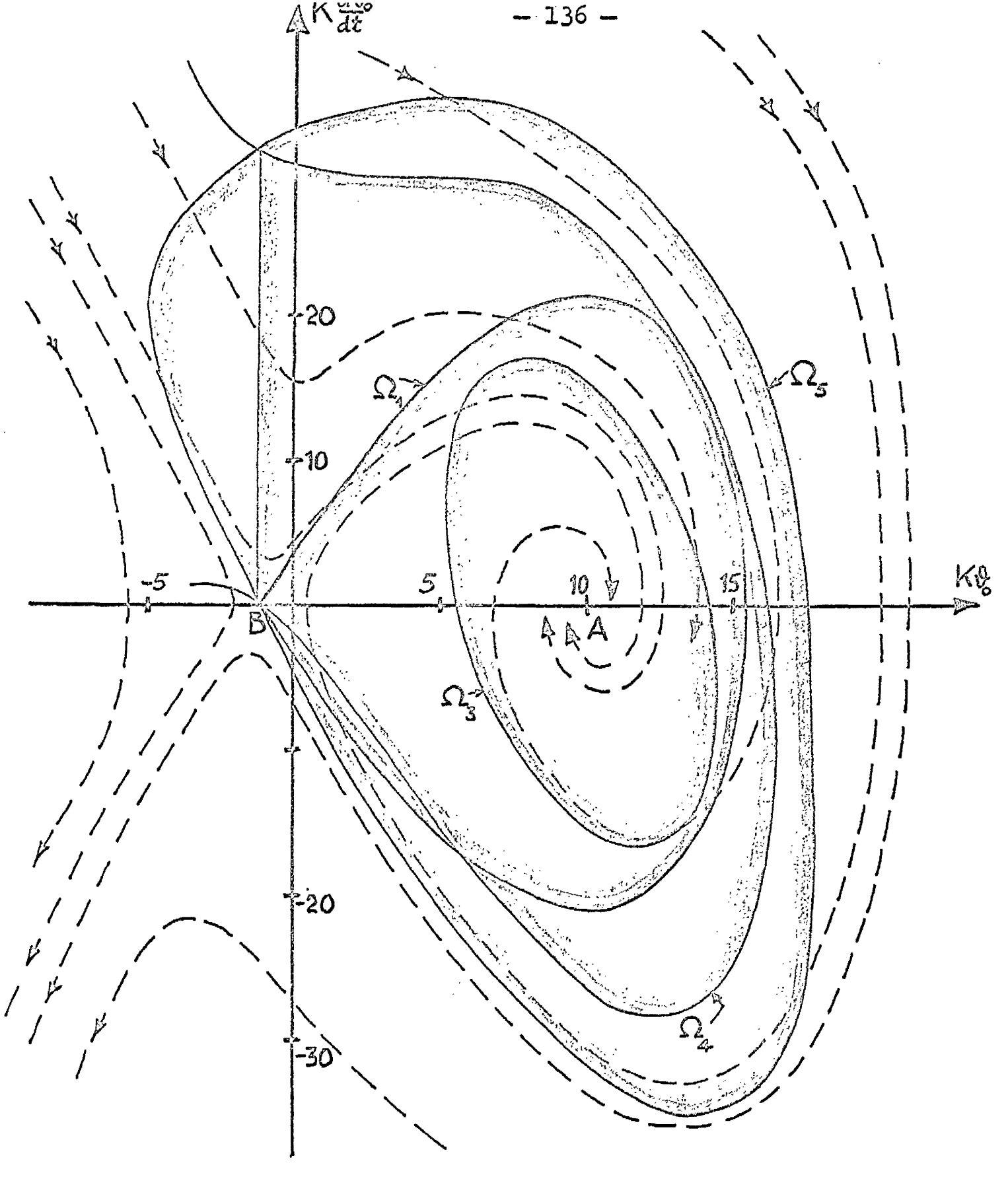

Figure 3.22 : Phase plane portrait for the second-order system with α - type element, for $\zeta = 0{\cdot}707$, $\omega_n = 1$, $K\theta_{if} = 10{\cdot}92$, $K = 1$, and $N = 22{\cdot}16$, showing the four applicable regions of stability.

obtainable from the form (3.4d.7) is in fact L_5 .

The improvement of the best composite function L(N), as defined above, over the uniform value 0·5 from L_1 may again be recorded diagrammatically as in Figure 3.16. Such a diagram shows the greatest enlargements obtained of the regions of guaranteed stability of Figure 3.12, the diagram of stability behaviour following steps in ϑ_i from initial stable values ϑ_{io} . However, since the boundary curves form a two-parameter family in K and ζ, as indicated by Figure 3.16, a complete set of such figures would be required for clarity, each one valid for one value of ζ and including the curves for a set of values of K. No attempt is made here to present such sets of curves, which may be constructed from the definition of N ($= R/\zeta^2$) and from the following condition

$$K\vartheta_{if} + \left[2\,L(N) + 1\right]\sqrt{(1-K-K\vartheta_{if})^2 + 4K} > K\vartheta_{io} + \sqrt{(1-K-K\vartheta_{io})^2 + 4K} \qquad (3.4d.16)$$

of which (3.3.15) and (3.4a.6) are particular instances.

In conclusion of this section, another representative phase-plane portrait for this system is shown in Figure 3.22, which has been drawn by the same method of isoclines as has Figure 3.6 . The four regions of stability (there is no Ω_2 for N = 22·16) are superimposed, demonstrating the distortion of their shapes which

accompanies the transformation from the $\varphi_1 - \varphi'_2$ system of variables back to the phase-plane: see the previous figure. It is evident that the boundary Ω_5 runs very close to considerable portions of the separatrices BD and BE which form the actual region of stability, but there is still an underestimate (17·81) of the point at which BD crosses the positive $K\vartheta_o$ axis, which appears to be 21 approximately.

3.5 Correlation with the roots-surface

To correlate the time behaviour of solutions with the roots-surface, an attempt has firstly been made to obtain a closed-form solution to equation (3.2.1), which describes the large-step response and which is repeated below for convenience:

$$\frac{d^2\vartheta_o}{dt^2} + 2\zeta\omega_n\frac{d\vartheta_o}{dt} + \omega_n^2(1 + K - K\vartheta_{if})\vartheta_o + \omega_n^2 K(\vartheta_o)^2 = \omega_n^2 K\vartheta_{if} \qquad (3.5.1)$$

A possible solution to an equation of the above type may be achieved by the following transformation, listed in the comprehensive catalogue of differential equations and their solutions by Murphy[20]:

$$\begin{aligned} &\text{let} \quad \vartheta_o(t) = u(z)\,v(t) + w(t) \;, \quad z = \varphi(t) \\ &\text{where} \quad 2(v'/v) + (\varphi''/\varphi') = -2\zeta\omega_n \\ &\qquad\quad \omega_n^2 K v = C(\varphi')^2 \\ &\text{and} \quad -2\omega_n^2 K w = (v''/v) + 2\zeta\omega_n(v'/v) + \omega_n^2(1 + K - K\vartheta_{if}) \end{aligned} \qquad (3.5.2)$$

By this, equation (3.5.1) is transformed to

$$u''(Z) = Cu^2 + G(Z) \qquad (3.5.3)$$

but as G(Z) is not linear, $- G = A + B/Z^4 -$, equation (3.5.3) has movable singular points in its solution, and no closed form solution of (3.5.1) is possible. The effort expended in the applications of Lyapunov's Direct Method follows, of course, from the impossibility of achieving a closed form solution which would likewise yield information about the stability of the system.

In some situations, it is known that an established Lyapunov function can be made to yield limited information about the time behaviour of solutions within the guaranteed region of stability. A figure of merit η is defined as

$$\eta = \left(- \frac{dV}{dt} / V \right)_{min}$$

being the minimum value of this expression within Ω ; an estimate of the largest time constant of responses is then given by $1/\eta$. However, a finite value for this time constant is only achieved if dV/dt is negative definite throughout Ω, and since the time derivative of any Lyapunov function in the system considered is at best negative semidefinite, no useful estimate of the time behaviour is possible in this way. In any case, if a result were obtained for η, it would only give a maximum decay time applicable to all responses within Ω, which would be of no value in

correlating the different time behaviours of solutions from different initial conditions with the characteristics of the roots — surface.

An attempt to obtain equivalent natural frequency and damping factor for responses has followed a method of "time-varying amplitude and phase" due to Grensted[21]. Thus, the actual response from (3.5.1) is represented by the form

$$\vartheta_o = \vartheta_{of} + a(t)\sin\psi(t) \qquad (3.5.4)$$

in which $a(t)$ and $\psi(t)$, the time-varying amplitude and phase respectively, are determined by (3.5.4) satisfying (3.5.1) at all instants of time. But rather than continuing with a and ψ, make the following definitions of time-varying frequency and damping factor:

$$\begin{aligned} &\text{define} \quad \zeta' = -\frac{da}{dt}\Big/ a\omega_n \quad \text{or} \quad a(t) = e^{-\int_0^t \zeta'\omega_n\, dt} \\ &\text{and} \quad \omega' = d\psi/dt \quad \text{or} \quad \psi(t) = \int_0^t \omega'\, dt \end{aligned} \qquad (3.5.5)$$

so that (3.5.4) becomes

$$\vartheta_o = \vartheta_{of} + A\, e^{-\int_0^t \zeta'\omega_n\, dt} \sin\left(\int_0^t \omega' dt + \varphi\right) \qquad (3.5.6)$$

in terms of the equivalent natural frequency, ω', and the equivalent damping factor, ζ', where A and φ are arbitrary constants.

Substitution of this form for ϑ_o in (3.5.1) gives

$$\left[(\zeta'\omega_n)^2-(\omega')^2-\omega_n\frac{d\zeta'}{dt}-2\zeta\zeta'\omega_n^2+\omega_n^2\frac{1+K(1+\vartheta_{of})^2}{1+\vartheta_{of}}\right]\sin\left(\int_0^t\omega'dt+\varphi\right)$$

$$+\left[\frac{d\omega'}{dt}-2\zeta'\omega'\omega_n+2\zeta\omega'\omega_n\right]\cos\left(\int_0^t\omega'dt+\varphi\right) \qquad (3.5.7)$$

$$+\frac{1}{2}\omega_n^2KA\,e^{-\int_0^t\zeta'\omega_n dt}\left[1-\cos 2\left(\int_0^t\omega'dt+\varphi\right)\right]=0$$

The satisfaction of (3.5.7) at all instants of time requires that all its three terms are separately zero by virtue of the forms of $\omega'(t)$ and $\zeta'(t)$: this is clearly impossible, and a first approximation ignores the third term whose coefficient, involving a negative exponential, decreases with time. The vanishing of the coefficients of the first two terms therefore requires that

$$(\omega')^2=\omega_n^2\frac{1+K(1+\vartheta_{of})^2}{1+\vartheta_{of}}+(\zeta'\omega_n)^2-\omega_n\frac{d\zeta'}{dt}-2\zeta\zeta'\omega_n^2 \qquad (3.5.8)$$

and $$\zeta'=\zeta+\frac{1}{2}\frac{d\omega'}{dt}/\omega'\omega_n=\zeta+\frac{d(\omega')^2}{dt}/4(\omega')^2\omega_n$$

which may be solved for by a converging iteration process:

$$(\omega_0')^2=\zeta_0'=0$$

$$(\omega_1')^2=\omega_n^2\frac{1+K(1+\vartheta_{of})^2}{1+\vartheta_{of}};\quad \zeta_1'=\zeta \qquad (3.5.9)$$

$$(\omega_2')^2=\omega_n^2\left[\frac{1+K(1+\vartheta_{of})^2}{1+\vartheta_{of}}-\zeta^2\right];\quad \zeta_2'=\zeta$$

$$(\omega_3')^2=(\omega_2')^2\quad;\qquad \zeta_3'=\zeta_2'$$

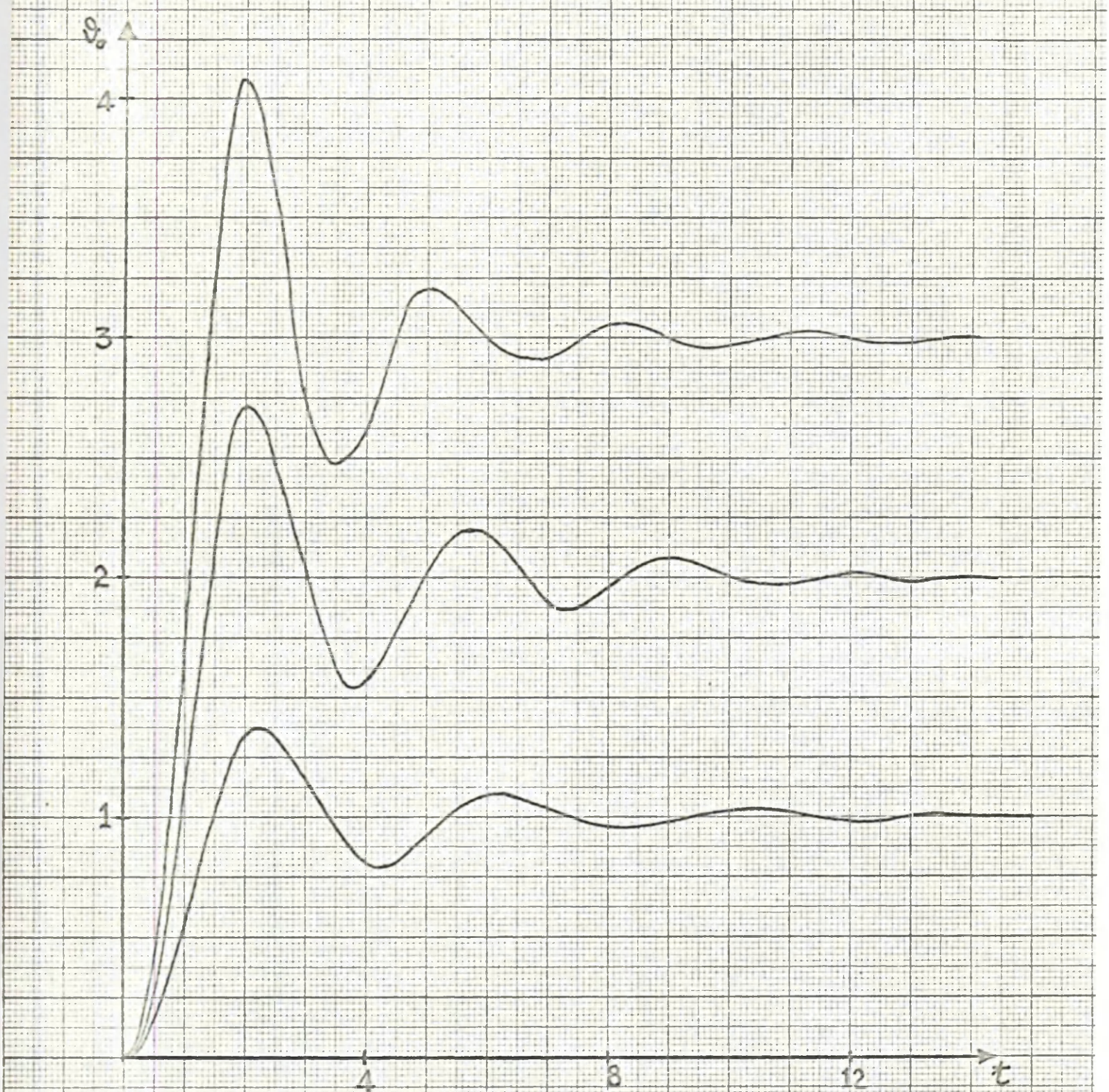

Figure 3.23: Three typical responses of the second-order system with an a gain element, for $K = 1$, $\omega_n = 1$, and $\zeta = 0.707$

The resulting expressions for $\omega'(t)$ and $\zeta'(t)$ are not in fact functions of time as allowed for by the method, and are simply the values for the small-signal natural frequency and damping factor as given by (3.1.6), evaluated at the final value of output. This is because the ignored third term of (3.5.7) represents the whole nonlinear effect of the system. Figure 3.23 shows the accuracy of this approximation by means of three step responses simulated on an analogue computer, for the process with $K = 1$, $\omega_n = 1$ and $\zeta = 0{\cdot}707$; the result (3.5.9) gives values for ω'/ω_n of 1·41, 1·68, and 1·93 for $\vartheta_{of} = 1$, 2 and 3 respectively, while the actual values from the figure each appear to be almost constant throughout a response at the values 1·59, 1·85, and 2·06 respectively; (3.5.9) also gives a constant value for ζ' of 0·707 compared with the computed values of 0·48, 0·56, and 0·62 initially (as determined on the basis of initial overshoot), all of which tend to 0·707 as the oscillations are damped out.

A better approximation has been sought by extending the method of Grensted to include a "correction coefficient" $\varepsilon(t)$ in the equivalent form (3.5.6): it was hoped that a suitable choice of $\varepsilon(t)$ would produce functions $\omega'(t)$ and $\zeta'(t)$ which, being time-varying, would give a better representation of actual responses. Proceeding thus, in place of (3.5.6) appears

$$\vartheta_o = \vartheta_{of} + A\,\varepsilon(t)\, e^{-\int_0^t \zeta'\omega_n dt} \sin\left(\int_0^t \omega' dt + \varphi\right) \qquad (3.5.10)$$

and the vanishing of the coefficients of the first two terms of the corresponding equation to (3.5.7) produces the equations

$$(\omega')^2 = \omega_n^2 \frac{1 + K(1 + \vartheta_{of})^2}{1 + \vartheta_{of}} + (\zeta'\omega_n)^2 - \omega_n \frac{d\zeta'}{dt} - 2(\zeta\omega_n + \frac{d\varepsilon}{dt}/\varepsilon)\zeta'\omega_n$$

$$+ \frac{d^2\varepsilon}{dt^2}/\varepsilon + 2\zeta\omega_n \frac{d\varepsilon}{dt}/\varepsilon \qquad (3.5.11)$$

and $\zeta' = \zeta + \frac{1}{2}\frac{d\omega'}{dt}/\omega'\omega_n + \frac{1}{2}\frac{d\varepsilon}{dt}/\omega_n\varepsilon = \zeta + \frac{d(\omega')^2}{dt}/4(\omega')^2\omega_n + \frac{1}{2}\frac{d\varepsilon}{dt}/\omega_n\varepsilon$

rather than (3.5.8). In obtaining (3.5.11), the term

$$\omega_n^2 KA\, \varepsilon^2(t)\, e^{-\int_0^t \zeta'\omega_n dt} \sin^2\left(\int_0^t \omega' dt + \varphi\right)$$

has been ignored; to minimise the misrepresentation due to this, assume the simplest form $\varepsilon(t) = 1 + ct$ and minimise the time integral I of the neglected term with respect to c, where

$$I = \int_0^\infty (1 + ct)^2\, e^{-\int_0^t \zeta'\omega_n dt} \sin^2\left(\int_0^t \omega' dt + \varphi\right) dt$$

The resulting equation for the vanishing of dI/dc is unworkable, unless to a first approximation ω' and ζ' are assumed to be constants (only in connection with this equation); in this event, the third equation along with the pair (3.5.11) to define $\omega'(t)$ and $\zeta'(t)$ appears as:

$$\zeta'\omega_n\left[(\zeta'\omega_n)^2+4(\omega')^2\right]^3+2\omega'(\zeta'\omega_n)^3\left[(\zeta'\omega_n)^2+4(\omega')^2\right](2\omega'\cos 2\varphi+\zeta'\omega_n\sin 2\varphi)+(\zeta'\omega_n)^4\left[(\zeta'\omega_n)^2+4(\omega')^2\right](2\omega'\sin 2\varphi-\zeta'\omega_n\cos 2\varphi)+c\left\{2\left[(\zeta'\omega_n)^2+4(\omega')^2\right]^3+8\omega'(\zeta'\omega_n)^4(2\omega'\cos 2\varphi+\zeta'\omega_n\sin 2\varphi)+2(\zeta'\omega_n)^3\left[(\zeta'\omega_n)^2-4(\omega')^2\right](2\omega'\sin 2\varphi-\zeta'\omega_n\cos 2\varphi)\right\}=0$$

where $$\sin 2\varphi=\frac{2\omega'(\zeta'\omega_n-c)}{(\zeta'\omega_n-c)^2+(\omega')^2}$$

$$\cos 2\varphi=\frac{(\zeta'\omega_n-c)^2-(\omega')^2}{(\zeta'\omega_n-c)^2+(\omega')^2}$$

The complexity of these equations is obvious: no solution has been found, nor has a better approximation to the form of responses by extension of the method of Grensted using any other form of function $\varepsilon(t)$.

The possibility has also been investigated of an extension to the methods, in Section 2.1, producing equivalent time constants for first-order systems. However, it is apparent that any approach based on the exact solution of the response equation — as the integral criterion of Section 2.1 — is futile, since this is unobtainable; attempts to extend the average derivative criterion, using either

$$\zeta'=\zeta\omega_n^2(\vartheta_{of}-\vartheta_{oo})\Big/2\left(\frac{d^2\vartheta_o}{dt^2}+2\zeta\omega_n\frac{d\vartheta_o}{dt}\right)_{av.},\qquad \omega'=\zeta\omega_n/\zeta'$$

$$\text{where } \left(\frac{d^2\vartheta_o}{dt^2} + 2\zeta\omega_n\frac{d\vartheta_o}{dt}\right)_{av.} = \frac{1}{\vartheta_{of}-\vartheta_{oo}}\int_{\vartheta_{oo}}^{\vartheta_{of}}\left(\frac{d^2\vartheta_o}{dt^2} + 2\zeta\omega_n\frac{d\vartheta_o}{dt}\right)d\vartheta_o$$

$$\text{or } \zeta' = \zeta\omega_n^2(\vartheta_{of}-\vartheta_{oo})/\sqrt{3}\left(\frac{d^2\vartheta_o}{dt^2} + 2\zeta\omega_n\frac{d\vartheta_o}{dt}\right)_{r.m.s.}, \quad \omega' = \zeta\omega_n/\zeta'$$

$$\text{where } \left[\left(\frac{d^2\vartheta_o}{dt^2} + 2\zeta\omega_n\frac{d\vartheta_o}{dt}\right)_{r.m.s.}\right]^2 = \frac{1}{\vartheta_{of}-\vartheta_{oo}}\int_{\vartheta_{oo}}^{\vartheta_{of}}\left(\frac{d^2\vartheta_o}{dt^2} + 2\zeta\omega_n\frac{d\vartheta_o}{dt}\right)^2 d\vartheta_o$$

have resulted in poor representation of typical responses by an equivalent second-order form. This sort of criterion appears to be incapable of extension to a second-order equation, since two independent parameters are to be determined by some averaging process on a single differential equation.

The conclusions to be drawn are

(i) that scant information is obtainable on the time behaviour of solutions which would allow of correlation with the movements of the small-signal roots in the roots-surface. The only result in this connection is that the actual response may be approximated by an equivalent second-order linear form, whose constant values of natural frequency and damping factor correspond to the small-signal roots at the final value of output; such a representation is obviously of limited value in large-scale responses:

(ii) that, although for the companion first-order system with

an α - element of Section 2.1 its roots-surface may predict the stability behaviour, the roots-surface of the second-order system fails in this way. It does still indicate that responses are stable from initially unstable states following negative steps of input, but fails to indicate the presence, and to define the limits, of the region of instability of Figure 3.12: in other words, the small-signal roots always have negative real parts for $\vartheta_{oe} > -1$, yet it has been shown that responses may be unstable from initially stable states if the input step is negative and lies within prescribed limits.

CHAPTER 4

The Control of a Second-Order Process with a β-Type Gain Element

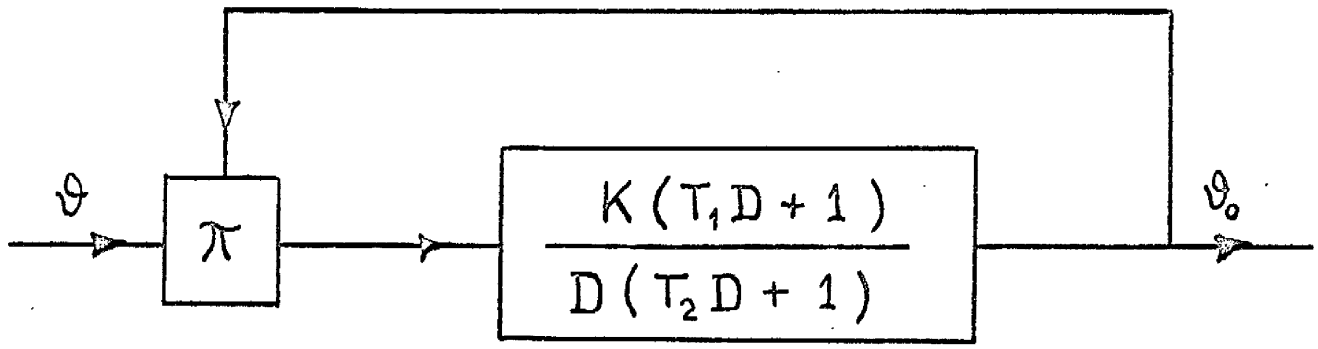

Figure 4.1 : Block diagram of a second – order process which incorporates a β – type gain element and may represent the nuclear reactor .

CHAPTER 4

The Control of a Second-Order Process with A β-Type Gain Element

4.1 Introductory aspects

Rather than study the corresponding process with a β-type gain element whose behaviour is obtainable by extension from that of the process with an α-type element of Chapter 3, the β-type second-order process chosen for investigation has one zero and one pole at the origin in its dynamics, as shown in Figure 4.1. The characteristic differential equation is apparently

$$T_2\frac{d^2\vartheta_o}{dt^2} + (1-KT_1\vartheta)\frac{d\vartheta_o}{dt} - K(\vartheta + T_1\frac{d\vartheta}{dt})\vartheta_o = 0 \qquad (4.1.1)$$

and two different cases must be distinguished, where

$$\text{I}: \ T_1 > T_2 \ , \quad \text{II}: \ T_1 < T_2 \ .$$

As mentioned in the Introduction, this process (in case I) represents the nuclear reactor on a one-point, one delayed-neutron-group basis, for which the differential equations are

$$\frac{dn}{dt} = \frac{\delta k-\beta}{l}n + \lambda C \ , \quad \frac{dC}{dt} = \frac{\beta}{l}n - \lambda C \qquad (4.1.2)$$

$$\text{or} \quad l\frac{d^2n}{dt^2} + (\beta + \lambda l - \delta k)\frac{dn}{dt} - (\lambda\,\delta k + \frac{d\,\delta k}{dt})n = 0$$

where n = neutron population

δk = reactivity (input)

C = delayed-neutron population

β = total fraction of delayed neutrons

l = generation time of neutrons

and λ = decay time of delayed neutrons

As follows from the relevant general form (1.4.2), the small-signal transfer function for either case I or II of this process is

$$\frac{\delta\vartheta_o(p)}{\delta\vartheta(p)} = \frac{K\vartheta_{oe}(T_1p+1)}{p(T_2p+1)} \qquad (4.1.3)$$

which is identical dynamically to the process itself, and in which the gain varies proportionally to the mean output level. The roots-surface therefore reduces to the conventional roots-locus, as mentioned in Section 1.4, on which the small-signal roots lie at positions corresponding to the variable gain; being only a second-order system, the roots are known explicitly as

$$\sigma + j\omega = -\left[K\vartheta_{oe}T_1 + 1 \pm \sqrt{(K\vartheta_{oe}T_1+1)^2 - 4K\vartheta_{oe}T_2}\right]/2T_2 \qquad (4.1.4)$$

In case I, the root paths lie only in the real plane, but in case II the roots become complex conjugates for a range of values of $K\vartheta_{oe}$. To define the forms of the root paths, the derivative of (4.1.4) with respect to $K\vartheta_{oe}$ is

$$-\left[T_1 \pm \frac{T_1(K\vartheta_{oe}T_1+1) - 2T_2}{\sqrt{(K\vartheta_{oe}T_1+1)^2 - 4K\vartheta_{oe}T_2}}\right]/2T_2$$

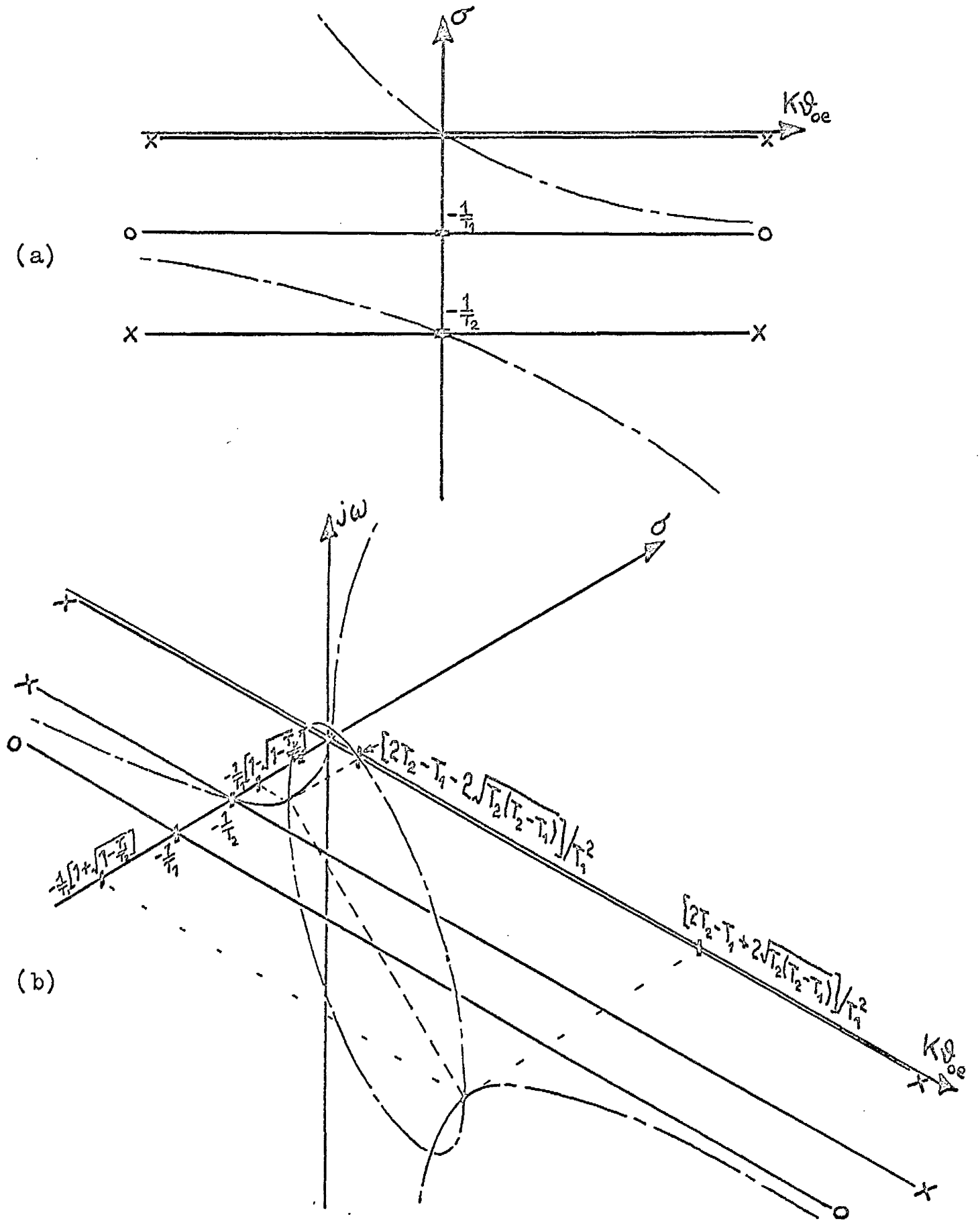

Figure 4.2: Roots–surfaces for a second–order process with a β–type gain element in
(a) case I, $T_1 > T_2$ (b) case II, $T_2 > T_1$

so that the gradients $d\sigma/d K\vartheta_{oe}$ at $K\vartheta_{oe} = 0$ are -1 and $(T_2 - T_1)/T_2$, and the gradient as $K\vartheta_{oe}$ tends to $\pm\infty$ is $-T_1/T_2$. The roots-surface for case I therefore appears (in two dimensions) as in Figure 4.2(a), and that for case II (in three dimensions) as in Figure 4.2(b). In the latter figure, the shape formed by the complex portion of the roots paths is an ellipse, since its projection on the σ, $j\omega$ plane is a circle and its projection on the σ, $K\vartheta_{oe}$ plane is a straight line: identification from (4.1.4) of the real and imaginary parts of the roots in this region, followed by elimination of the parameter $K\vartheta_{oe}$, gives the equation of this projection to be

$$\omega^2 + (\sigma + 1/T_1)^2 = (T_2 - T_1)/T_1^2 T_2$$

while the projection on the real plane is part of the line

$$\sigma = -(K\vartheta_{oe} T_1 + 1)/2T_2 .$$

The static characteristic of the closed-loop system is the same as that of the special case of the first-order system with a β-type element, Figure 2.15(b). For any value of $K\vartheta_i$, the output may have the same value or be zero. The roots-surface indicates for either case that, if $K\vartheta_i > 0$, equilibrium at $\vartheta_o = \vartheta_i$ is stable, and that, if $K\vartheta_i < 0$, equilibrium at $\vartheta_o = \vartheta_i$ is unstable due to the root in the "right half space", but it does not indicate whether the equilibrium at $\vartheta_o = 0$ (zero gain) is stable or unstable, since this is the critical case of a small-signal

pole at the origin: this point is decided below.

4.2 The phase portraits for transient responses

This Section demonstrates again the value of considering the complete phase portrait of a system, just as in Section 3.2 the behaviour in the general case of the previous system was defined by such consideration. The input to the closed-loop system in hand is assumed to have the value ϑ_{if} for $t > 0$; at $t = 0$, the output may be in any state, and its response is according to equation (4.1.1) in which $\vartheta = \vartheta_i - \vartheta_o$, $\vartheta_i = \vartheta_{if}$ and $d\vartheta_i/dt = 0$, i.e. to

$$T_2 \frac{d^2\vartheta_o}{dt^2} + (1 - KT_1\vartheta_{if} + 2KT_1\vartheta_o) \frac{d\vartheta_o}{dt} + K(\vartheta_o - \vartheta_{if})\vartheta_o = 0 \qquad (4.2.1)$$

The critical points in the phase plane of ϑ_o and $d\vartheta_o/dt$, corresponding to equilibrium states of the system, are at

$$(A)\ \vartheta_o = \vartheta_{if},\ d\vartheta_o/dt = 0 \ \text{ and } \ (B)\ \vartheta_o = 0,\ d\vartheta_o/dt = 0 .$$

As mentioned above, the nature of A is given by the roots-surface for all values of ϑ_{if} except zero, when A and B are coincident, but the nature of B is as yet undetermined. To be precise, the roots-surface shows that A is a saddle point in either case I or II if $K\vartheta_{if} < 0$, that A is a stable node in case I if $K\vartheta_{if} > 0$, and that A is either a stable node or a stable focus in case II if $K\vartheta_{if} > 0$: it is a stable focus if

		Singularity A at $\vartheta_o = \vartheta_{if}$	Singularity B at $\vartheta_o = 0$
Case I	$K\vartheta_{if} > 0$	Stable Node	Saddle Point
	$K\vartheta_{if} < 0$	Saddle Point	Stable Node
Case II	$K\vartheta_{if} \geqslant b$ and $a \geqslant K\vartheta_{if} > 0$	Stable Node	Saddle Point
	$b > K\vartheta_{if} > a$	Stable Focus	Saddle point
	$K\vartheta_{if} \leqslant -b$ and $-a \leqslant K\vartheta_{if} < 0$	Saddle Point	Stable Node
	$-b < K\vartheta_{if} < -a$	Saddle Point	Stable Focus

$$a = \left[2T_2 - T_1 - 2\sqrt{T_2(T_2 - T_1)}\right] / T_1^2$$

$$b = \left[2T_2 - T_1 + 2\sqrt{T_2(T_2 - T_1)}\right] / T_1^2$$

Figure 4.3: Natures of the singularities A and B of the second-order system with a β-type gain element.

$$\left[2T_2 - T_1 - 2\sqrt{T_2(T_2-T_1)}\right]/T_1^2 < K\vartheta_{if} < \left[2T_2 - T_1 + 2\sqrt{T_2(T_2-T_1)}\right]/T_1^2 .$$

The nature of B may be discovered by forming the relevant variational equations from (4.2.1), but it may also be found by applying to (4.2.1) the following linear transformation

$$\vartheta_o' = \vartheta_o - \vartheta_{if} \qquad (4.2.2)$$

so that the system is now described by the equation

$$T_2 \frac{d^2\vartheta_o'}{dt^2} + (1 + KT_1\vartheta_{if} + 2KT_1\vartheta_o') \frac{d\vartheta_o'}{dt} + K(\vartheta_o' + \vartheta_{if})\vartheta_o' = 0 \qquad (4.2.3)$$

with singularities A' ≡ A at $\vartheta_o' = 0$, B' ≡ B at $\vartheta_o' = -\vartheta_{if}$. Since (4.2.2) is identical to (4.2.3) if ϑ_{if} in the former is replaced by $-\vartheta_{if}$, the nature of the singularity B at $\vartheta_o = 0$ for positive $K\vartheta_{if}$ is identical to the nature of B' at $\vartheta_o' = -\vartheta_{if}$, i.e. of A at $\vartheta_o = \vartheta_{if}$ for negative $K\vartheta_{if}$, and vice versa; which is to say that B is a saddle point in either case I or II if $K\vartheta_{if} > 0$, that B is a stable node in case I if $K\vartheta_{if} < 0$, and that B is either a stable node or a stable focus in case II if $K\vartheta_{if} < 0$ as for A. The table which is Figure 4.3 sums up the natures of the singularities as derived.

At this stage, similar remarks may be made about the appearance of the phase portrait for the general case of this system as are made in Section 3.2, and supplemented by Figure 3.4, for the previous system. It is not yet possible to name the "source and sink" of the two separatrices of B to its right, and

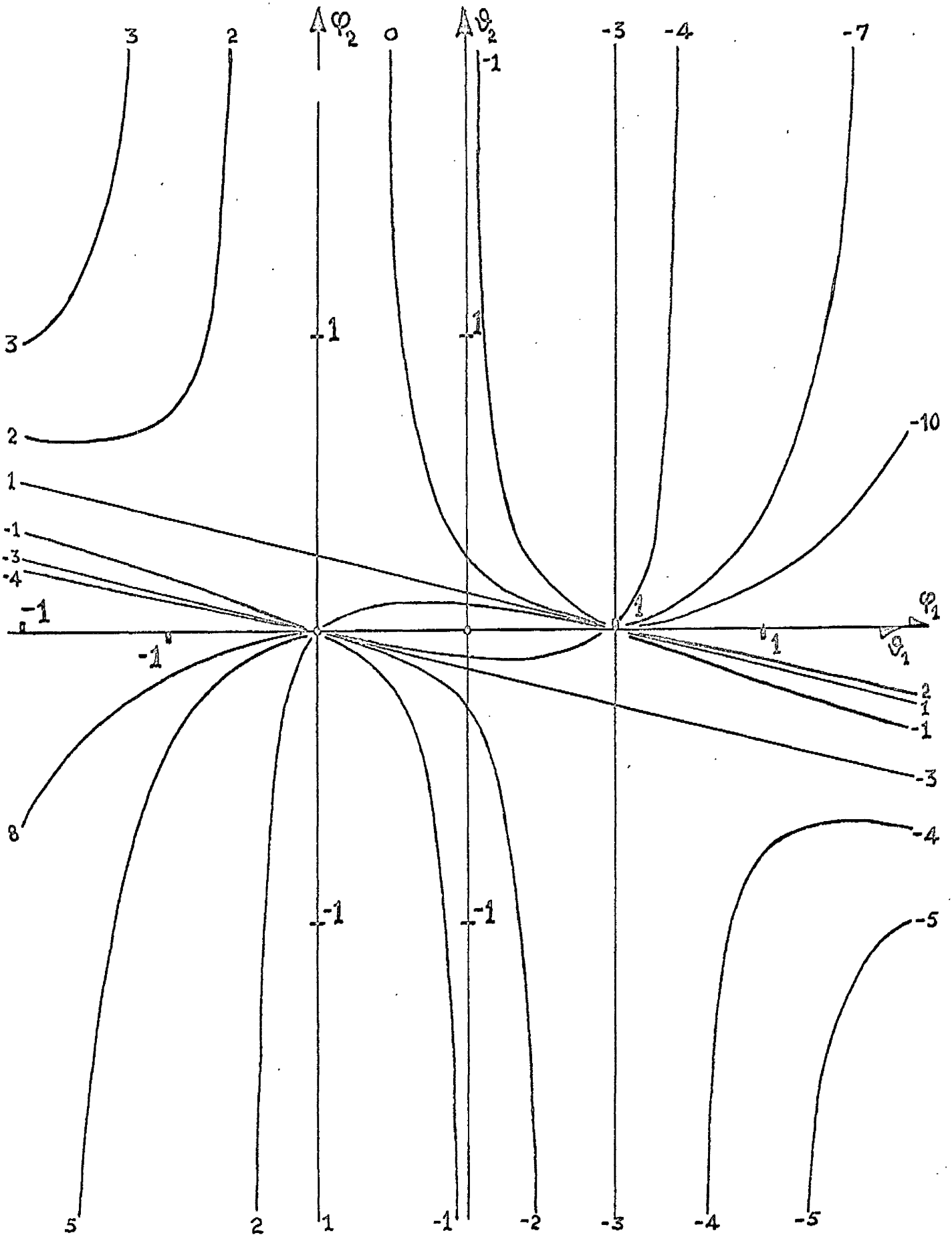

Figure 4.4: Isocline pattern for the particular case of the second-order system with β-element, for $T_1 = 2$, $T_2 = 1$, $K\vartheta_{if} = 1$.

this point of central importance has to be determined by consideration of the behaviour at infinity. However, in a particular case of equation (4.2.1), the finite phase portrait may be obtained from the isoclines whose equations are found to be

$$\frac{d\vartheta_o}{dt} = \frac{K(\vartheta_{if} - \vartheta_o)\vartheta_o}{KT_1(2\vartheta_o - \vartheta_{if}) + (1 + T_2 S)} \qquad (4.2.4)$$

where $S = d(d\vartheta_o/dt)/d\vartheta_o$ is the constant slope of trajectories on a particular isocline.

Introducing the normalised phase variables $\varphi_1 = \vartheta_o/\vartheta_{if}$ and $\varphi_2 = (d\vartheta_o/dt)/\vartheta_{if}$, equation (4.2.4) appears as

$$\varphi_2 = \frac{K(1 - \varphi_1)\varphi_1}{KT_1(2\varphi_1 - 1) + (1 + T_2 S)/\vartheta_{if}} \qquad (4.2.5)$$

with A at $\varphi_1 = 1$, $\varphi_2 = 0$ and B at $\varphi_1 = \varphi_2 = 0$. Since this form is more complicated than the corresponding equation (3.2.5), it is not possible to have a single pattern of isoclines valid for all sets of values of T_1, T_2 and $K\vartheta_{if}$: however, when drawing the isoclines for a particular set, as in Figure 4.4, it is useful to note that

$$\vartheta_2 = \frac{1 - 4\vartheta_1^2}{8T_1\vartheta_1 + 4(1 + T_2 S)/K\vartheta_{if}} \qquad (4.2.6)$$

after the linear transformation $\vartheta_1 = \varphi_1 - 1/2$, $\vartheta_2 = \varphi_2$, in which $S = d\vartheta_2/d\vartheta_1 = d(d\vartheta_o/dt)/d\vartheta_o$. This allows the use of symmetry, for the two branches of the isocline $S = -1/T_2$ have the origin

$\vartheta_1 = \vartheta_2 = 0$ as a centre of symmetry; furthermore, for the two branches of any other isocline S, the origin is a centre of symmetry for the two branches of the isocline S', where

$$S' = -(S + 2/T_2) \qquad (4.2.7)$$

A principal feature of the isocline pattern is the existence of a pair of isoclines whose branches are straight lines. The isocline with $S = -(K\vartheta_{if}T_1 + 1)/T_2$ consists of the lines

$$\varphi_2 = -\varphi_1/2T_1 \quad \text{and} \quad \varphi_1 = 1 \qquad (4.2.8)$$

while that for which $S = (K\vartheta_{if}T_1 - 1)/T_2$ consists of the lines

$$\varphi_2 = (1 - \varphi_1)/2T_1 \quad \text{and} \quad \varphi_1 = 0 \qquad (4.2.9)$$

In the pattern of Figure 4.4, these isoclines represent the slopes of -3 and 1 respectively.

The actual directions of the separatrices at the saddle point B follow from a procedure described in Section 3.2. Thus, differentiation of (4.2.5) with respect to φ_1 gives the direction of the isocline S at any point φ_1 as

$$\frac{d\varphi_2}{d\varphi_1} = \frac{K^2T_1(2\varphi_1 - 2\varphi_1^2 - 1) + K(1 - 2\varphi_1)(1 + T_2S)/\vartheta_{if}}{\left[KT_1(2\varphi_1 - 1) + (1 + T_2S)/\vartheta_{if}\right]^2} \qquad (4.2.10)$$

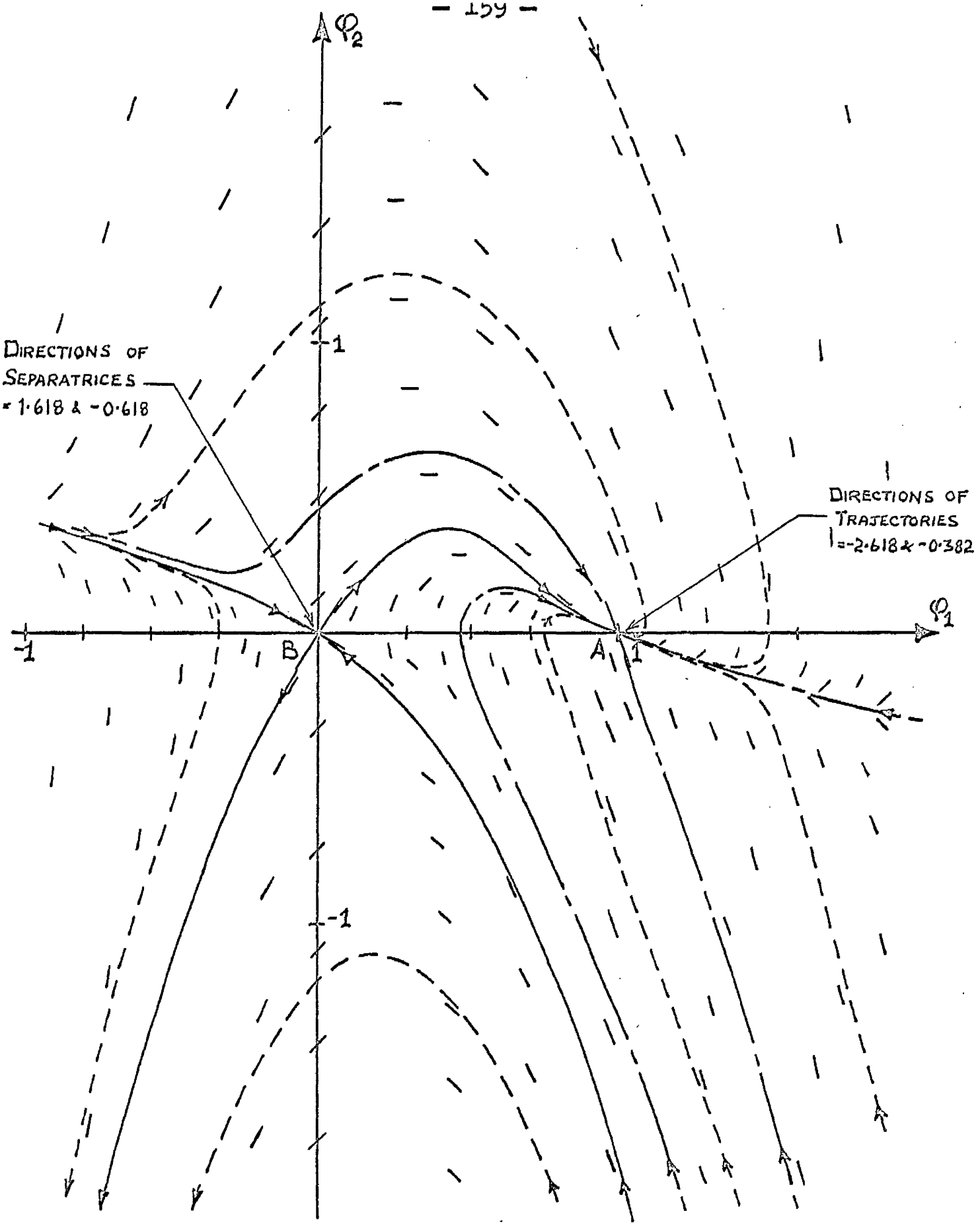

Figure 4.5: A specimen phase plane portrait for the second-order system with β-element, for $T_1 = 2$, $T_2 = 1$ and $K\theta_{if} = 1$: case I.

The actual directions of the separatrices at B are therefore the roots of the equation

$$S = \frac{K\vartheta_{if}}{T_2 S + 1 - K\vartheta_{if} T_1} \qquad (4.2.11)$$

namely $S_{1,2} = \left[K\vartheta_{if}T_1 - 1 \pm \sqrt{(K\vartheta_{if}T_1 - 1)^2 + 4K\vartheta_{if}T_2}\right]/2T_2$

which are seen to be real for all $K\vartheta_{if}$ except

$$-\left[2T_2 - T_1 + 2\sqrt{T_2(T_2 - T_1)}\right]/T_1^2 < K\vartheta_{if} < -\left[2T_2 - T_1 - 2\sqrt{T_2(T_2 - T_1)}\right]/T_1^2.$$

The values $S_{1,2}$ therefore correspond not only to the directions of the separatrices of the saddle point at B for $K\vartheta_{if} > 0$ but also to the directions of trajectories at the stable node at B when such exists. A similar procedure gives the following expressions for the directions of the separatrices at the saddle point at A for $K\vartheta_{if} < 0$ and the directions of trajectories at the stable node at A when such exists:

$$S_{1,2} = \left[-K\vartheta_{if}T_1 - 1 \pm \sqrt{(K\vartheta_{if}T_1 + 1)^2 - 4K\vartheta_{if}T_2}\right]/2T_2 \qquad (4.2.12)$$

For illustration in a typical case, the completed phase plane portrait for $T_1 = 2$, $T_2 = 1$, $K\vartheta_{if} = 1$ (case I) is shown in Figure 4.5 . In this particular instance, the separatrix approaching B from $\varphi_1 > 0$ does not appear to have previously crossed the φ_1 axis, in contrast to the behaviour of the corresponding separatrix of the previous system. To see whether this is representative of both cases I and II in general, the behaviour at infinity must be investigated.

The first transformation to equation (4.2.1) of the two introduced in Section 3.2 for the behaviour at infinity consists in defining

$$\vartheta_o = \frac{u}{Z} \ , \quad \frac{d\vartheta_o}{dt} = \frac{1}{Z} \ , \quad dt = Z\,d\tau$$

$$\text{or} \quad Z = dt/d\vartheta_o \ , \quad u = \vartheta_o\, dt/d\vartheta_o \ , \quad d\tau = dt/Z \qquad (4.2.13)$$

$$\text{from which} \quad Z^2\, d\left(\frac{d\vartheta_o}{dt}\right) = -\,dZ$$

$$Z^2\, d\vartheta_o = Z\,du - u\,dZ$$

$$\text{Thus, for} \quad Z \gtrless 0, \ \tau \left\{ \begin{matrix} \text{increases} \\ \text{decreases} \end{matrix} \right\} \ \text{as t increases} \qquad (4.2.14)$$

Equation (4.2.1) is then transformed to

$$\left.\begin{aligned} \frac{dZ}{d\tau} &= \left[K(u - \vartheta_{if} Z)\, uZ + (Z - K\vartheta_{if} T_1 Z + 2KT_1 u)\, Z\right]/T_2 \\ \text{and} \quad \frac{du}{d\tau} &= Z + \frac{u}{Z}\frac{dZ}{d\tau} \\ &= Z + \left[K(u - \vartheta_{if} Z)\, u^2 + (Z - K\vartheta_{if} T_1 Z + 2KT_1 u)\, u\right]/T_2 \end{aligned}\right\} \qquad (4.2.15)$$

By inspection, this system has two singular points at infinity, $Z = 0$, where $u = 0$ and $-2T_1$. Moreover, these are the only singular points, for if $Z \neq 0$ the second of equations (4.2.15) gives

$$0 = Z + \frac{u}{Z} \cdot 0$$

which is incompatible with $Z \neq 0$.

Considering the form firstly of the singularity at $Z = u = 0$, the variational equations of (4.2.15) at this point give

$$\frac{d\,\delta Z}{d\tau} = 0 \cdot \delta Z + 0 \cdot \delta u \qquad \frac{d\,\delta u}{d\tau} = 1 \cdot \delta Z + 0 \cdot \delta u$$

so that the nature of this complex singularity must also be determined by the behaviour of trajectories near it as follows: the gradient of a trajectory in the u, Z plane is

$$\frac{dZ}{du} = \frac{K(u - \vartheta_{if} Z)\, u + (Z - K\vartheta_{if} T_1 Z + 2KT_1 u)}{T_2 Z + K(u - \vartheta_{if} Z)\, u^2 + (Z - K\vartheta_{if} T_1 Z + 2KT_1 u)\, u} \, Z \qquad (4.2.16)$$

(i) In the neighbourhood of the singularity, on the line $\delta Z = \delta u$,

$$\frac{dZ}{du} \approx (1 + 2KT_1 - K\vartheta_{if} T_1)\, \delta Z / T_2 \approx C_1 \delta Z$$

and $$\frac{du}{d\tau} \approx \delta Z$$

(ii) In the neighbourhood of the singularity, on the line $\delta Z = -\delta u$,

$$\frac{dZ}{du} \approx (1 - 2KT_1 - K\vartheta_{if} T_1)\, \delta Z / T_2 \approx C_2 \delta Z$$

and $$\frac{du}{d\tau} \approx \delta Z$$

(iii) On the Z axis, $u = 0$ and

$$\frac{dZ}{du} = (1 - K\vartheta_{if} T_1)\, Z / T_2 = C_3 Z = C_3 \delta Z \quad \text{near the origin}$$

$$\frac{du}{d\tau} = Z = \delta Z \quad \text{near the origin}$$

(iv) Close to the u axis, i.e. for $Z = \delta Z$ and $|u| \gg |\delta Z|$, equation (4.2.16) reduces to

$$\frac{dZ}{du} \approx \frac{\delta Z}{u}$$

so for $\delta Z > 0$, $\frac{dZ}{du}$ is small and $\left\{ \begin{matrix} \text{positive} \\ \text{negative} \end{matrix} \right\}$ as $u \gtrless 0$, and

for $\delta Z < 0$, $\frac{dZ}{du}$ is small and $\left\{ \begin{matrix} \text{negative} \\ \text{positive} \end{matrix} \right\}$ as $u \gtrless 0$.

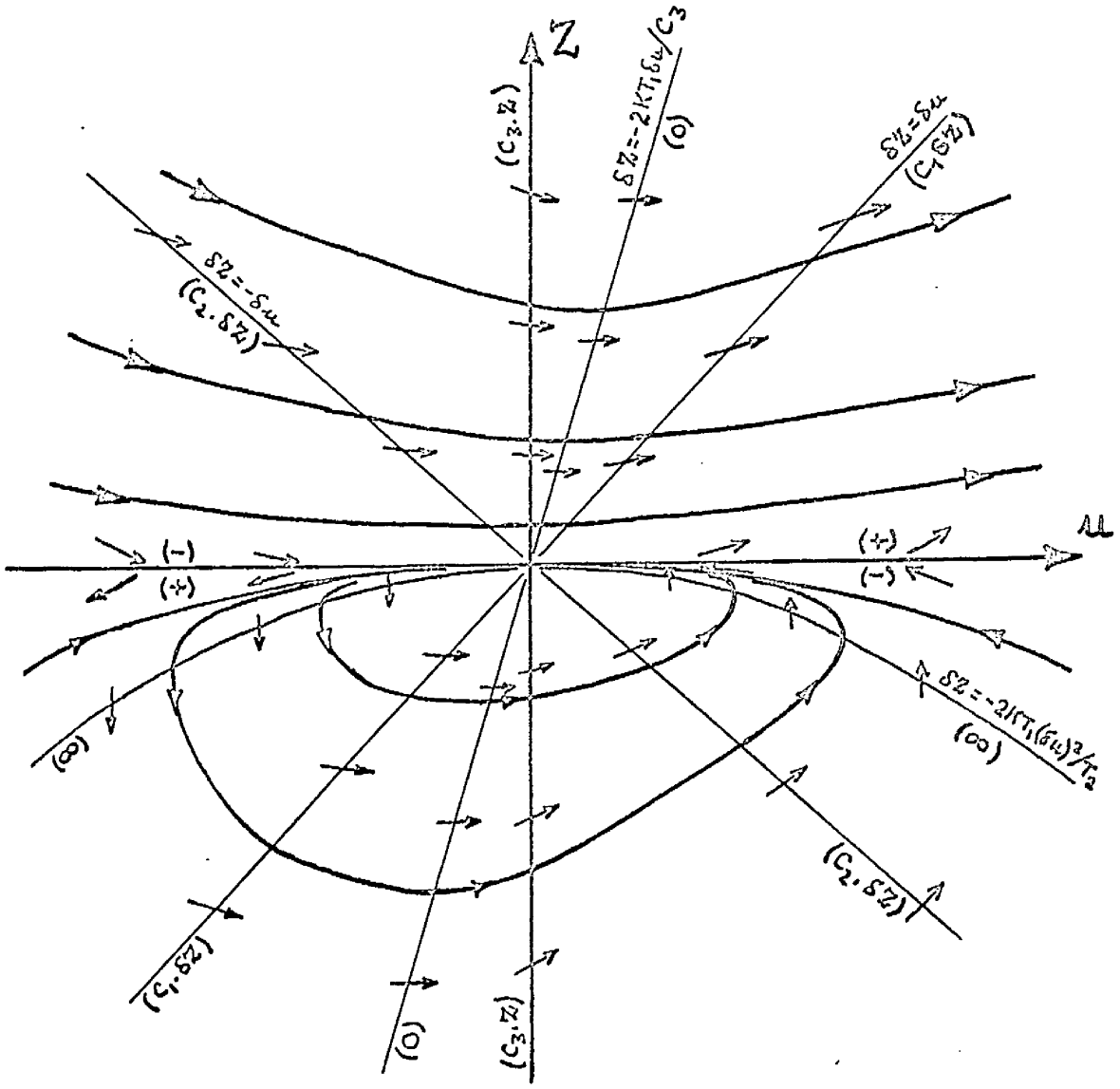

Figure 4.6 : Nature of the singularity at infinity, $Z = u = 0$, for $C_1 > 0$, $C_2 < 0$, $C_3 < 0$. (Directions of trajectories on various lines are in brackets).

The sense of direction is given to the trajectories from

$$\frac{du}{d\tau} \approx K\,(u + 2T_1)\,u^2/T_2$$

so that $\frac{du}{dt} \gtrless 0$ as $\delta Z \lessgtr 0$ if $u > 0$

and $\frac{du}{dt} \gtrless 0$ as $\delta Z \lessgtr 0$ if $0 > u > -2T_1$.

(v) dZ/du becomes infinite on the line

$$Z = \frac{Ku^2\,(u + 2T_1)}{K\vartheta_{if}u\,(u + T_1) - T_2 - u}$$

$$\approx -2KT_1(\delta u)^2/T_2 \quad \text{if } u = \delta u$$

which is a parabola, concave downwards, on which

$$\frac{dZ}{d\tau} = -\frac{K^2u^3\,(u + 2T_1)^2}{\left[K\vartheta_{if}u\,(u + T_1) - T_2 - u\right]^2} \approx -4T_1^2K^2(\delta u)^3/T_2^2$$

Thus, for $\delta u \gtrless 0$, $dZ/dt \gtrless 0$ since $\delta Z < 0$ in either case.

(vi) dZ/du is zero on $Z = 0$ and on the line

$$Z = \frac{Ku\,(u + 2T_1)}{K\vartheta_{if}u + K\vartheta_{if}T_1 - 1}$$

$$\approx \frac{2KT_1}{K\vartheta_{if}T_1 - 1}\,\delta u \approx -2KT_1\delta u/C_3 \quad \text{near the origin.}$$

On this line, $du/d\tau = Z \approx -2KT_1\delta u/C_3$.

There is now sufficient information to construct a sketch, as in Figure 4.6, of the singularity, but it is to be noted that

the slopes of the trajectories on the lines $\delta Z = \pm \delta u$ and $u = 0$, as well as the slope of the line on which $dZ/du = 0$, depend on the constants C_1 to C_3. The given Figure shows how the trajectories must behave in the vicinity of the origin for a set of parameters for which

$$C_1 > 0, \quad C_2 < 0, \quad C_3 < 0 .$$

Recognising that $C_1 > C_3 > C_2$, it is readily seen that the behaviour is not radically different for any other set of parameters K, T_1 and ϕ_{if}, and that all trajectories for $Z > 0$ pass by the singularity while those for $Z < 0$ form closed paths, starting and terminating at the singularity.

Turning now to the form of the singularity at $Z = 0$, $u = -2T_1$, the variational equations of (4.2.15) at this point give

$$\frac{d\,\delta Z}{d\tau} = 0.\delta Z + 0.\delta u$$

$$\frac{d\,\delta u}{d\tau} = \frac{T_2 - 2T_1 - 2K\phi_{if}T_1^2}{T_2}.\delta Z + \frac{4KT_1^2}{T_2}.\delta u$$

so that once more the singularity is complex in nature. The expression (4.2.16) for the gradient of trajectories is, of course, still appropriate and is used again to give the directions of trajectories on selected lines, since the equations of isoclines are too complicated.

(i) On the line $Z = u + 2T_1$, in the neighbourhood of the singularity where $Z = \delta Z \approx 0$,

$$\frac{dZ}{du} \approx \frac{1 + K\theta_{if}T_1 - 2KT_1}{T_2 - 2T_1 + 4KT_1^2 - 2K\theta_{if}T_1^2}\,\delta Z = C_4\,\delta Z$$

and $$\frac{du}{d\tau} \approx \left(T_2 - 2T_1 + 4KT_1^2 - 2K\theta_{if}T_1^2 \right) \delta Z/T_2 = C_5\,\delta Z$$

(ii) On the line $Z = -u - 2T_1$, in the neighbourhood of the singularity where $Z = \delta Z \approx 0$,

$$\frac{dZ}{du} \approx \frac{1 + K\theta_{if}T_1 + 2KT_1}{T_2 - 2T_1 - 4KT_1^2 - 2K\theta_{if}T_1^2}\,\delta Z = C_6\,\delta Z$$

and $$\frac{du}{d\tau} \approx \left(T_2 - 2T_1 - 4KT_1^2 - 2K\theta_{if}T_1^2 \right) \delta Z/T_2 = C_7\,\delta Z$$

(iii) On the line $u = -2T_1$,

$$\frac{dZ}{du} = \frac{1 + K\theta_{if}T_1}{T_2 - 2T_1 - 2K\theta_{if}T_1^2}\,Z = C_8\,Z$$

and $$\frac{du}{d\tau} = \left(T_2 - 2T_1 - 2K\theta_{if}T_1^2 \right) Z/T_2 = C_9\,Z$$

(iv) Close to the u axis, i.e. for $Z = \delta Z$ and $|u + 2T_1| \gg |\delta Z|$, equation (4.2.16) again reduces to

$$\frac{dZ}{du} \approx \frac{\delta Z}{u}$$

as in the case of the singularity at the origin, with the result that

for $\delta Z \gtrless 0$, $\frac{dZ}{du}$ is small and $\left\{ \begin{matrix} \text{negative} \\ \text{positive} \end{matrix} \right\}$ for either $u \gtrless -2T_1$.

Likewise, the sense of direction is again given by

$$\frac{du}{d\tau} \approx K\left(u + 2T_1 \right) u^2/T_2$$

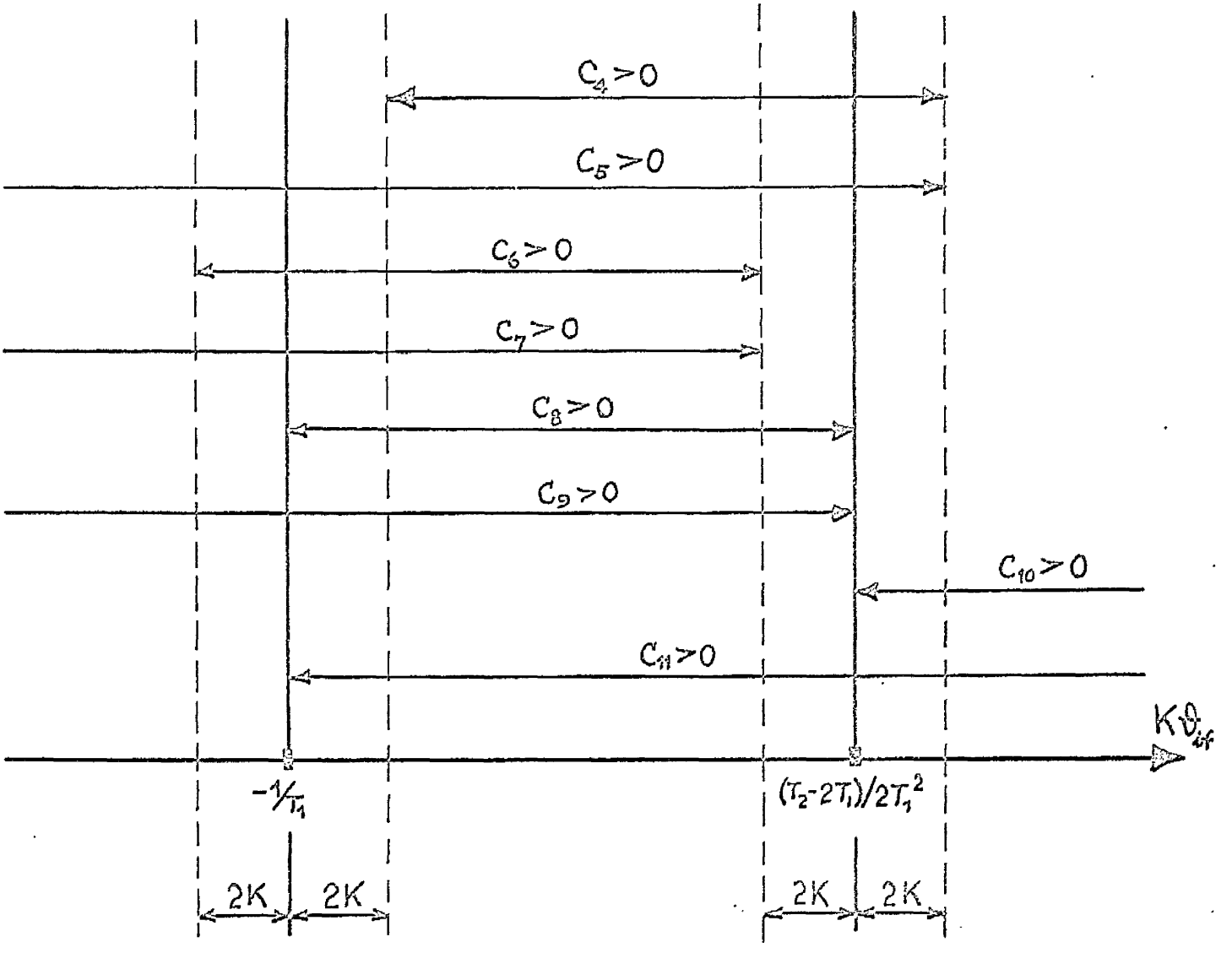

Figure 4.7 : Ranges of $K\vartheta_{if}$ for positive values of the constants C_4 to C_{11}.

so that $\frac{du}{d\tau} \gtrless 0$ as $\delta Z \gtrless 0$ if $u > -2T_1$

and $\frac{du}{d\tau} \lessgtr 0$ as $\delta Z \gtrless 0$ if $u < -2T_1$.

(v) As previously, dZ/du becomes infinite on the line

$$Z = \frac{Ku^2(u + 2T_1)}{K\theta_{if}u(u + T_1) - T_2 - u}$$

which is $\delta Z \approx \frac{4KT_1^2}{2K\theta_{if}T_1^2 - T_2 + 2T_1}\delta u = C_{10}\delta u$ if $u = -2T_1 + \delta u$

This is a straight line through $Z = 0$, $u = -2T_1$, on which

$$\frac{dZ}{d\tau} \approx \frac{8K^2T_1^3}{\left[2K\theta_{if}T_1^2 + 2T_1 - T_2\right]^2}(\delta u)^2$$

Thus, for $\delta u \gtrless 0$, $dZ/dt \gtrless 0$ in view of condition (4.2.14).

(vi) Again as before, dZ/du is zero on $Z = 0$ and on the line

$$Z = \frac{Ku(u + 2T_1)}{K\theta_{if}u + K\theta_{if}T_1 - 1}$$

which is $\delta Z \approx \frac{2KT_1}{K\theta_{if}T_1 + 1}\delta u = C_{11}\delta u$ near $u = -2T_1$.

This is another straight line through the singularity on which

$$du/d\tau = Z = C_{11}\delta u \quad .$$

A sketch of the singularity may now be made, but in this case the slopes of the trajectories on all the selected lines, as well as the slopes of the lines on which $dZ/du = 0$ and ∞, depend on the constants C_4 to C_{11}. Their values rely on the value of

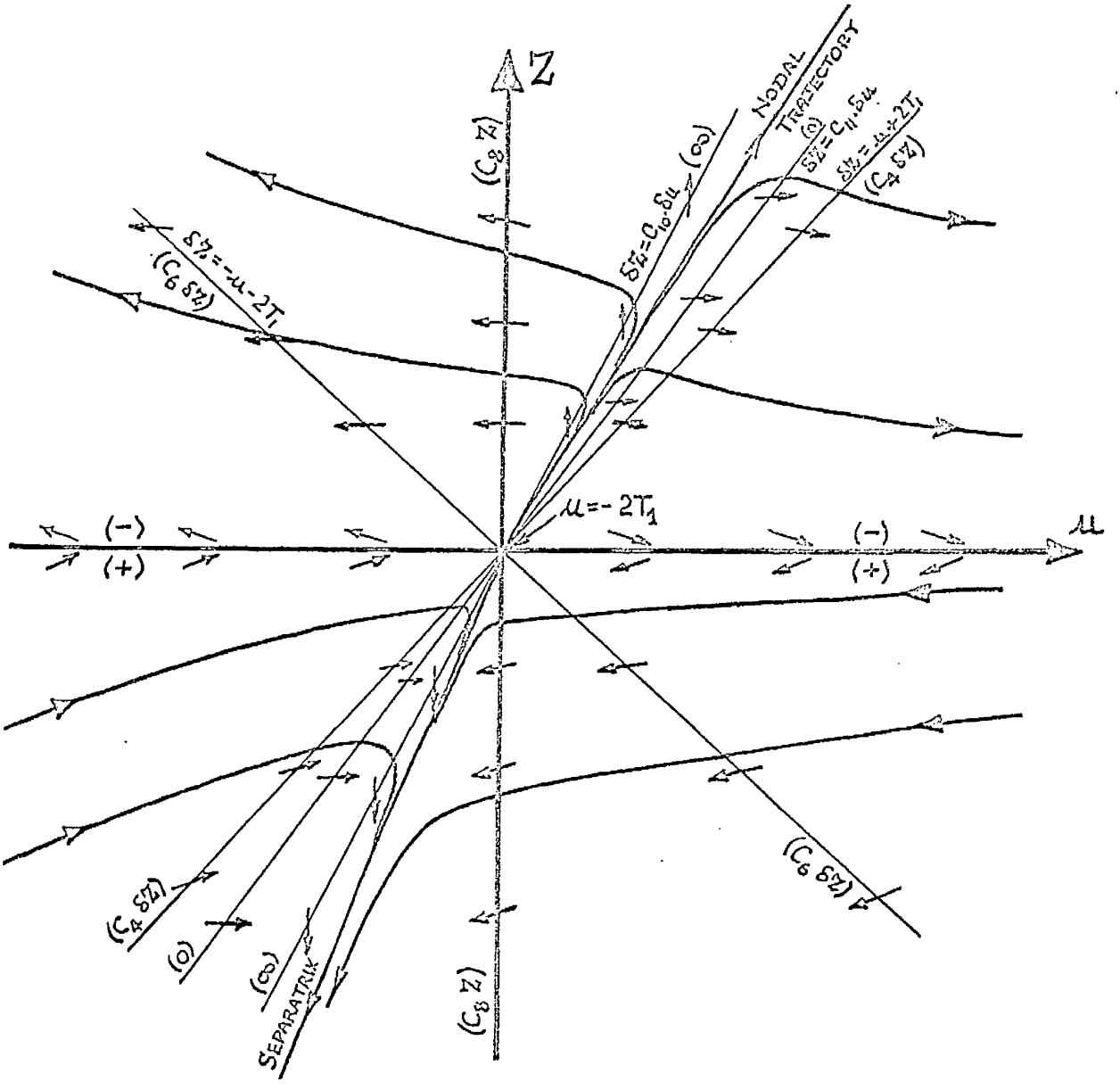

Figure 4.8 : Nature of the singularity at infinity, $Z = 0$ $u = -2T_1$, for C_5 , C_{10} and C_{11} positive, other C_n negative. (Directions of trajectories on various lines are in brackets) .

ϕ_{if} for a given set of T_1, T_2 and K, and the diagram in Figure 4.7 indicates the ranges of $K\phi_{if}$ within which each coefficient is positive.

Using the set of parameters $T_1 = 2$, $T_2 = 1$, $K = 1$ and $\phi_{if} = 1$, which are compatible with those for which Figure 4.5 is drawn, the nature of the trajectories in the neighbourhood of this singularity must be as shown in Figure 4.8. In this case, constants C_5, C_{10} and C_{11} are positive while the other five are negative. By considering the different possible sets of constants as T_1, T_2, K and ϕ_{if} vary, it may be observed that the nature of the singularity is basically unaltered from that shown: for $Z > 0$ the trajectories are like those from an unstable node, while for $Z < 0$ they are like those from a saddle point.

The separatrix for $Z < 0$ and the trajectory to which all others emanating from the singularity for $Z > 0$ are tangent may lie in the fourth and second quadrants respectively, however, rather than in the third and first as shown: the condition for this to happen is found from obtaining the direction of the separatrix and nodal trajectory at the singularity, by the method previously described. Thus, by differentiating equation (4.2.16) - in which dZ/du has been set equal to a constant S - with respect to u, by setting $Z = 0$ and $u = -2T_1$ in the resulting equation, and then by equating to S the direction dZ/du of the isocline as it appears, one obtains $S = 0$ or

$$S = \frac{4KT_1^2}{2K\vartheta_{if}T_1^2 + 2T_1 - T_2} = C_{10} \qquad (4.2.17)$$

The separatrix and nodal trajectory therefore lie in the second and fourth quadrants if $C_{10} < 0$, i.e.

$$\text{if} \quad K\vartheta_{if} < (T_2 - 2T_1)/2T_1^2 \qquad (4.2.18)$$

The second transformation to equation (4.2.1) must now be considered in case a singularity at infinity exists at the two points of the phase plane not represented in the first transformation but represented in the second. Thus,

$$\text{let} \quad \vartheta_o = 1/Z, \quad d\vartheta_o/dt = v/Z, \quad dt = Z\,d\tau$$

for which $$Z^2\,d\vartheta_o = -dZ$$

$$Z^2\,d\left(\frac{d\vartheta_o}{dt}\right) = Z\,dv - v\,dZ$$

and equation (4.2.1) is transformed to

$$\left.\begin{aligned} \frac{dZ}{d\tau} &= -vZ^2 \\ \text{and} \quad \frac{dv}{d\tau} &= Z + \frac{v}{Z}\frac{dZ}{d\tau} \\ &= \left[K(\vartheta_{if}Z - 1) - (Z - K\vartheta_{if}T_1Z + 2KT_1)\,v\right]/T_2 - v^2Z \end{aligned}\right\} \qquad (4.2.19)$$

The only singular points of this system are at $Z = 0$, $v = -1/2T_1$ and $v = 0$, $Z = 1/\vartheta_{if}$: the former is that in the first transformation at $Z = 0$, $u = -2T_1$, and the latter is the singularity at A in the finite region of the phase plane. No new singularity is therefore revealed.

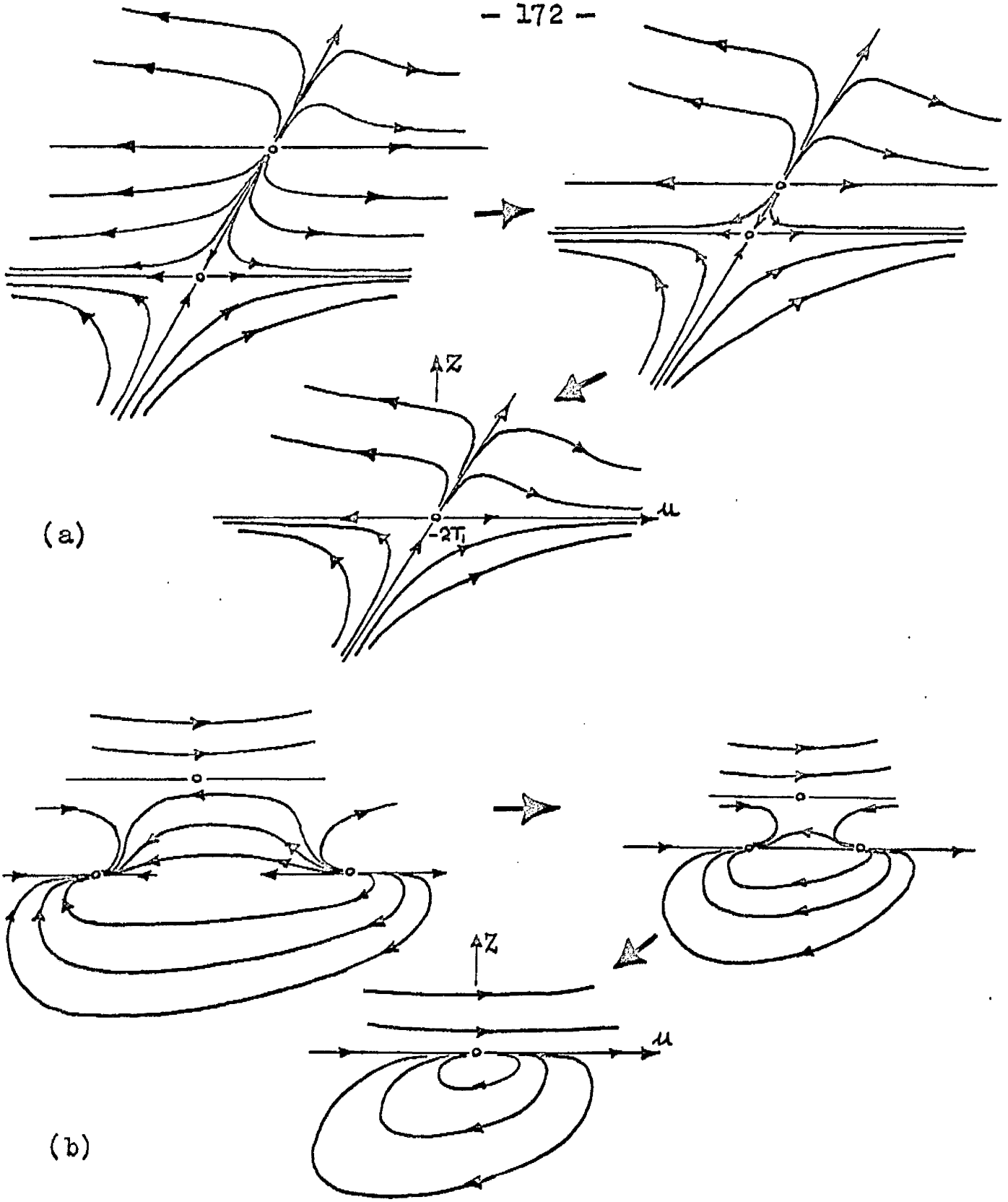

The change from t to τ reverses the indicated directions of trajectories for $Z < 0$.

Figure 4.9 : Compositions of the complex singularities at (a) $Z = 0$, $u = -2T_1$ (b) $Z = u = 0$.

To discover the constituents of the two complex singularities at infinity, the rule (3.2.15) is again invoked. In this system once more $S = 1$ and $N + F = 1$, so that the number of nodes at the two singularities at infinity exceeds the number of saddle points there by one. Thus it may be that the singularity at $u = -2T_1$ derives from the coalition of one unstable ("improper") node and one saddle point, and that the singularity at $u = 0$ derives from the coalition of one unstable (improper) node of a special type, one stable (improper) node of the same special type, and one saddle point of a special type. The feasibility of the above is justified by the diagrams of Figure 4.9, which show how this could come about. The special nature of the nodes mentioned above is that, whereas an improper node normally has two isolated trajectories with a common direction different to that of all the other trajectories, these special trajectories share the same direction (the u axis) as all others in these two nodes; the special nature of the saddle point at $u = 0$ is similar, in that the two, normally distinct, directions of the separatrices are identical (the u axis) so that two of the usual four quadrants of the saddle point do not exist.

The question of whether or not the phase plane portrait of Figure 4.5 is representative of both cases I and II in general is now given attention. The point of principal interest is the location of the whole of the separatrix approaching B from $\varphi_1 > 0$

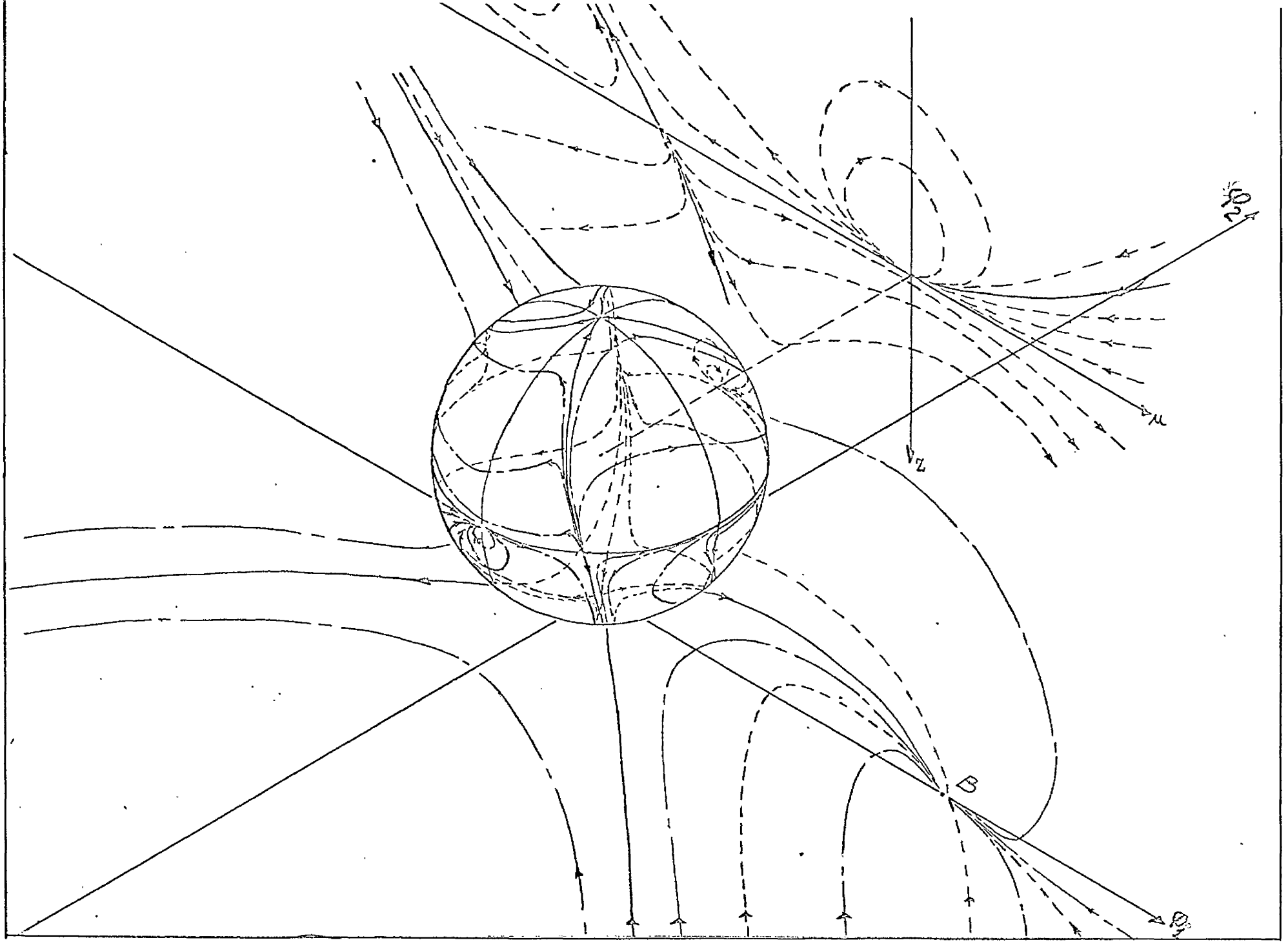

Figure 4.10 . Global representation of the entire phase plane portrait.

(when $K\vartheta_{if} > 0$), which in Figure 4.5 appears to lie completely in the fourth quadrant, or approaching A from $\varphi_1 > 0$ when $K\vartheta_{if} < 0$. By drawing the salient features on the sphere, Figure 4.10, it can readily be seen that this separatrix may stem from the singularity at $Z = u = 0$ — in which case it does lie completely in the fourth quadrant — but that it may equally well stem from the unstable node side of the singularity at $Z = 0$, $u = -2T_1$, in which case it crosses the φ_1 axis for $\varphi_1 > 1$. The matter may be settled as follows, by considering the behaviour of the departing separatrix from the saddle-point side of the singularity at $Z = 0$, $u = -2T_1$:

equation (4.2.17) gives the direction dZ/du of this separatrix at the critical point to be C_{10}; there is a connection, however, between the two expressions for the direction of any trajectory in terms of the two different co-ordinate systems, which is obtained thus from (4.2.13) :

since $\dfrac{d\vartheta_o}{dt} = \dfrac{\vartheta_o}{u}$, $\dfrac{d\varphi_2}{d\varphi_1} = \dfrac{d}{d\vartheta_o}\left(\dfrac{d\vartheta_o}{dt}\right) = \left(u - \varphi_1 \dfrac{du}{d\varphi_1}\right) / u^2$

$$= \left(1 - \frac{du}{dZ} \cdot \frac{dZ}{d\varphi_2} \cdot \frac{d\varphi_2}{d\varphi_1} / Z\right) / u$$

But $dZ/d\varphi_2 = -1/\varphi_2^2 = -Z^2$

so that finally $$\frac{d\varphi_2}{d\varphi_1} = \frac{\dfrac{dZ}{du}}{u\dfrac{dZ}{du} - Z} \qquad (4.2.20)$$

$$\text{or} \quad \frac{dZ}{du} = \frac{\dfrac{d\varphi_2}{d\varphi_1}}{\varphi_1 \dfrac{d\varphi_2}{d\varphi_1} - \varphi_2}$$

Therefore, the corresponding direction $d\varphi_2/d\varphi_1$ of the separatrix as it leaves the singularity at infinity is obtained by setting $u = -2T_1$ in (4.2.20) and letting Z tend to zero from a negative amount :

$$\left(\frac{d\varphi_2}{d\varphi_1}\right)_{\text{sep'x}} = \underset{Z=-\varepsilon \to 0}{\text{Lim}} \left(\frac{1}{-2T_1 + \varepsilon/C_{10}} \right) \qquad (4.2.21)$$

Now this singularity lies at infinity in the φ_1, φ_2 plane on the line $\varphi_2 = -\varphi_1/2T_1$, since $u = \varphi_1/\varphi_2 = -2T_1$, and this line is one of the straight-line branches of the isocline for which $S = -(K\theta_{if}T_1 + 1)/T_2$, equation (4.2.8): in the special situation of

$$S = -(K\theta_{if}T_1 + 1)/T_2 = -1/2T_1 = (d\varphi_2/d\varphi_1)_{\text{isocline}}$$

$$\text{for which} \quad K\theta_{if} = (T_2 - 2T_1)/2T_1^2 > 0 \qquad (4.2.22)$$

the separatrix from the singularity at infinity is also the separatrix into the saddle point at B, and this special double separatrix is part of the isocline $d\varphi_2/d\varphi_1 = -1/2T_1$. Equation (4.2.20) implies that $dZ/du = C_{10} = \pm\infty$ along it. However, if rather than this special situation there is

$$K\theta_{if} > (T_2 - 2T_1)/2T_1^2 > 0 \qquad (4.2.23)$$

the constant C_{10} is positive and (4.2.21) shows that the direction $d\varphi_2/d\varphi_1$ of the separatrix departing from the vicinity of $u = -2T_1$, $Z = 0$ is slightly more negative than the slope $-1/2T_1$ of the isocline branch: this separatrix cannot therefore cross this branch of the isocline anywhere and must end up at the stable singularity A, while the separatrix into B must originate from $Z = u = 0$. Lastly, if condition (4.2.18) applies, i.e. if

$$0 < K\theta_{if} < (T_2 - 2T_1)/2T_1^2 , \qquad (4.2.24)$$

C_{10} is negative, the slope of the departing separatrix is slightly less negative than $-1/2T_1$, and this separatrix must bypass B to the left and end up at $Z = u = 0$, while the separatrix into B must have crossed the positive φ_1 axis in coming from $Z = 0$, $u = -2T_1$.

To sum up, the behaviour at infinity has shown that the phase plane portrait of Figure 4.5 is representative of the system if $K\theta_{if} > 0$, so long as

$$K\theta_{if} > (T_2 - 2T_1)/2T_1^2$$

But if, instead, condition (4.2.24) applies, then a radically different portrait obtains, which is similar to that of the previous system in the possibility of responses being unstable from initially stable states. For negative values of $K\theta_{if}$, a similar argument to the above shows that Figure 4.5 (only with the roles of A and B interchanged) is representative of the

system in general so long as

$$K\vartheta_{if} < (2T_1 - T_2)/2T_1^2 < 0$$

and that the different type of portrait is only in evidence if

$$(2T_1 - T_2)/2T_1^2 < K\vartheta_{if} < 0 \qquad (4.2.25)$$

4.3 The stability of large transient responses

In case I ($T_1 > T_2$) and case II if $T_2 \leqslant 2T_1$, neither of the derived conditions (4.2.24) and (4.2.25) holds for any values of $K\vartheta_{if}$, so that Figure 4.5 is representative of the behaviour in such systems. If $\vartheta_{io} > 0$, responses from initially stable equilibrium states are therefore stable to $\vartheta_o = \vartheta_{if}$ if $\vartheta_{if} > 0$ and to $\vartheta_o = 0$ if $\vartheta_{if} \leqslant 0$; and if $\vartheta_{io} < 0$, the initially stable state is that of zero gain for $\vartheta_{oo} = 0$, and responses are stable ($\vartheta_o \equiv 0$) if $\vartheta_{if} < 0$ but unstable if $\vartheta_{if} \geqslant 0$. Reference to Section 2.4 then shows that the stability diagram for step responses from initially stable states, constructed from the above statements, is identical to that of Figure 2.15(c) which need not be repeated; an identical diagram is also obtained for the stability behaviour of such a system for step responses from initially unstable equilibrium states as belongs to the parallel first-order system of Section 2.4. Thus, consideration alone of the entire phase plane portrait has defined the stability behaviour for this system in case I and case II if $T_2 \leqslant 2T_1$. Also, since the nuclear reactor as represented by (4.1.2) belongs to case I and since ϑ_o represents

(a)

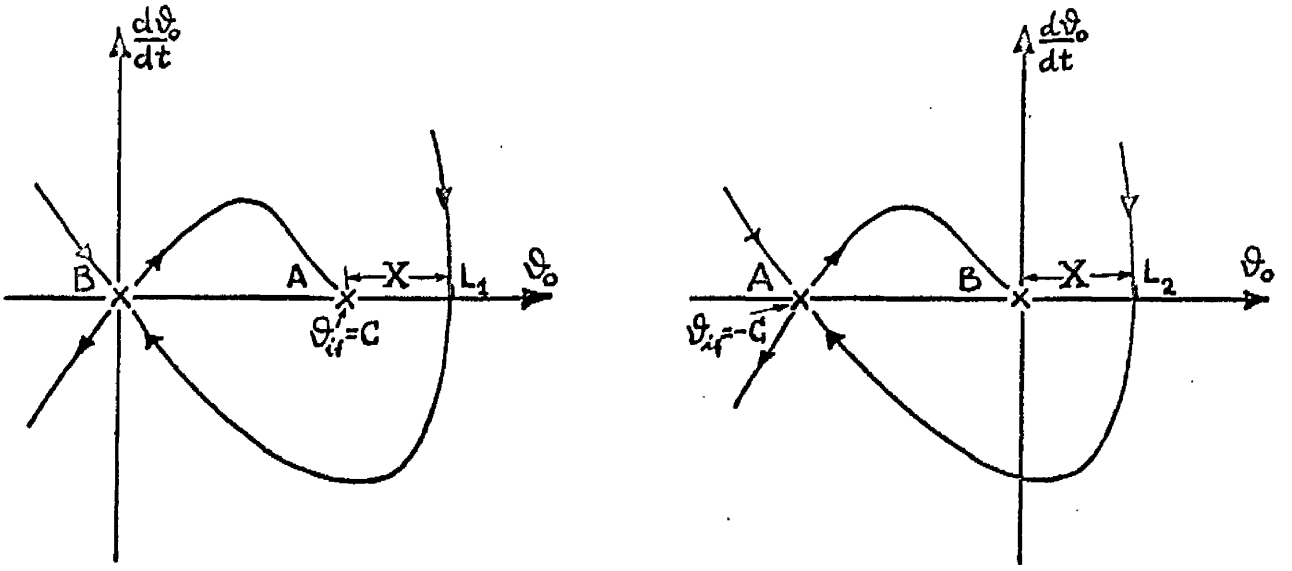

(b)

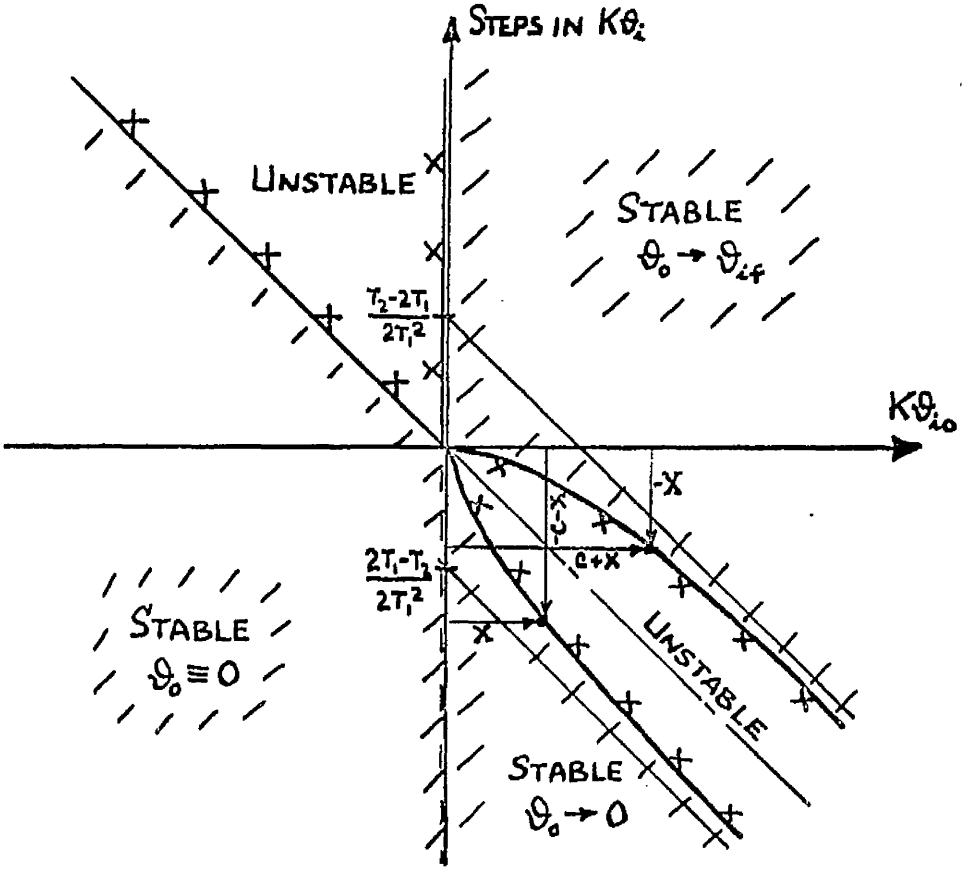

Figure 4.11: (a) Sketch phase portraits for

$$|\vartheta_{if}| < (T_2 - 2T_1)/2T_1^2K$$

(b) Stability diagram for the step response, from initially stable equilibrium states, of the second–order system with β – element, for $T_2 > 2T_1$

neutron flux which is by nature only positive, the first stability diagram of the pair indicates that step responses in power output of a proportionally controlled reactor are stable to the demanded power level for any size of step in demand in either direction.

In the excluded case II when $T_2 > 2T_1$, the diagram for initially unstable equilibrium states can clearly be dismissed from further consideration as being the same as that for the other cases, as also can the portion of the diagram for initially stable equilibrium states for $\varphi_{io} < 0$. However, as regards the completion of the latter diagram, Figure 4.5 is only representative of the behaviour if

$$|\varphi_{if}| > (T_2 - 2T_1)/2T_1^2K$$

so that the diagram, Figure 4.11(b), is the same as that for the other cases outwith the strip for $K\varphi_{io} > 0$ between the lines

$$\text{Step in } K\varphi_i = \pm \frac{T_2 - 2T_1}{2T_1^2} - K\varphi_{io}$$

To fill in the details in this strip, consider the two sketch portraits of Figure 4.11(a) which show the points L_1 and L_2 at which the separatrices of interest cross the φ_1 axis, for the cases of φ_{if} a positive value $C < (T_2 - 2T_1)/2T_1^2K$ and the corresponding value $-C$: in view of the shifting transformation (4.2.2) whereby the natures of A and B are interchanged, it is readily seen that the phase portrait in the second case is identical to that of the first shifted to the left by C, so that

the lengths AL_1 and BL_2 are equal, say X. Then, for $\vartheta_{if} = C$, at the limiting value of $\vartheta_{io} = \vartheta_{oo} = C + X$, the response is stable if the step $(= C - \vartheta_{io}) > -X$; and for $\vartheta_{if} = -C$, at the limiting value of $\vartheta_{io} = \vartheta_{oo} = X$, the response is stable if the step $(= -C - \vartheta_{io}) < -C - X$; such pairs of points, as shown in Figure 4.11(b), form a pair of lines which are symmetrically disposed about the line bisecting the fourth quadrant and lie within the strip. They must stem from the origin of the diagram, but whether they become asymptotic to the edges of the strip (as shown) or not is conjecture at this stage.

Once again, therefore, the consideration alone of the entire phase plane portrait has been sufficient to define the stability behaviour of the system, for $T_2 > 2T_1$; in particular, it has proved the existence and provided the general form of a region of instability which is additional to that of the corresponding diagram for the other cases of the system.

4.4 Applications of Lyapunov's Direct Method

In order to obtain an analytical expression for one symmetric half of the boundary of the additional region of instability of Figure 4.11(b), the Direct Method of Lyapunov is again used. Proceeding from equation (4.2.3), since the stable singularity A is suitably at $\vartheta_o' = 0$, and B is at $\vartheta_o' = -\vartheta_{if}$, it is preferable to describe the system in terms of $\varphi_1 = \vartheta_o'/\vartheta_{if}$ and a first way of

decomposing this into a pair of first-order differential equations produces

$$\frac{d\varphi_1}{dt} = \varphi_2$$

$$\frac{d\varphi_2}{dt} = -\left[K\theta_{if}(1+\varphi_1)\varphi_1 + (1 + K\theta_{if}T_1 + 2K\theta_{if}T_1\varphi_1)\varphi_2\right]/T_2 \qquad (4.4.1)$$

with A at $\varphi_1 = \varphi_2 = 0$, B at $\varphi_1 = -1$, $\varphi_2 = 0$.

On a comparison with equations (3.3.11) it is noticed that (4.4.1) are of rather similar form, except for the additional term in $\varphi_1\varphi_2$ in the second equation: the coefficients of the terms in φ_1 and φ_1^2 are again equal. This partial similarity, along with that of the shapes of the actual regions of stability for the two systems, led to the initial trial of the following as a Lyapunov function:

$$V_1 = 3\varphi_1^2 + 3T_2\varphi_2^2/K\theta_{if} + 2\varphi_1^3 \qquad (4.4.2)$$

which is almost identical to function (3.3.12). Working only with $K\theta_{if} > 0$, which will give the upper half of the required boundary, it is then found that

$$\frac{dV_1}{dt} = -6\varphi_2^2(T_1 + 1/K\theta_{if} + 2T_1\varphi_1) \qquad (4.4.3)$$

which differs from the time derivative of function (3.3.12) through the presence of the term in $\varphi_1\varphi_2^2$: however, as φ_2^2 stands out as a factor, there is an infinite half-plane of negative

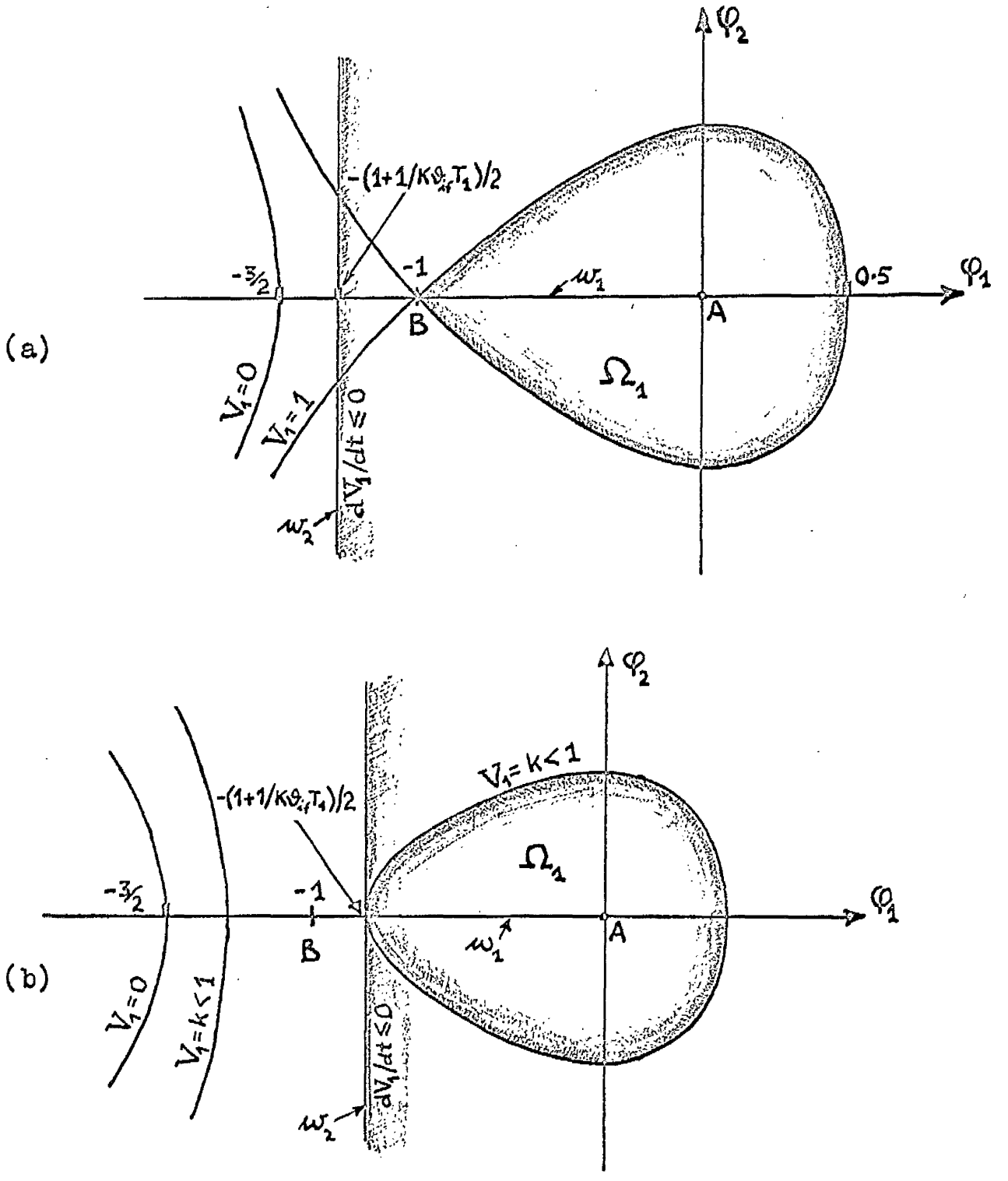

Figure 4.12 : Sketches of the regions Ω_1 of asymptotic stability for

(a) $K\vartheta_{if} \leqslant 1/T_1$

(b) $K\vartheta_{if} > 1/T_1$

semidefinite dV_1/dt on the positive side of the line

$$\varphi_1 = -(1+1/K\vartheta_{if}T_1)/2$$

which is w_2, while the φ_1 axis is w_1.

From the nature of the function V_1, which has already been recorded as Figure 3.11, it is clear that a region of positive definite V_1 contained by one of its contours and lying within the area of negative semidefinite dV_1/dt may form Ω_1. Thus, if $-1 \geqslant -(1+1/K\vartheta_{if}T_1)/2$ i.e. $K\vartheta_{if} \leqslant 1/T_1$ (since $K\vartheta_{if} > 0$), the contour $V_1 = 1$ with the saddle point at B encloses the largest region which satisfies all the requirements of the Theorem quoted and which is therefore Ω_1 : see Figure 4.12. But if $K\vartheta_{if} > 1/T_1$, the contour must be used which corresponds to a closed curve through the point $\varphi_1 = -(1+1/K\vartheta_{if}T_1)/2$, $\varphi_2 = 0$. In the first instance, the value L_1 of the intersection of Ω_1 with the positive φ_1 axis is 0·5 ; in the second, the resulting cubic equation for the three intersections is

$$\left[2\varphi_1 + 1 + \frac{1}{K\vartheta_{if}T_1}\right]\left[\varphi_1^2 + \left(1 - \frac{1}{2K\vartheta_{if}T_1}\right)\varphi_1 + \frac{(1+K\vartheta_{if}T_1)(1-2K\vartheta_{if}T_1)}{(2K\vartheta_{if}T_1)^2}\right] = 0$$

so that $$L_1 = \left[1 - 2K\vartheta_{if}T_1 + \sqrt{3}\sqrt{(2K\vartheta_{if}T_1)^2 - 1}\right]/4K\vartheta_{if}T_1 \qquad (4.4.4)$$

which is less than 0·5 .

To construct now the required boundary of the strip on Figure 4.11, if $K\vartheta_{if} = (T_2 - 2T_1)/2T_1^2 \leqslant 1/T_1$, i.e. $4T_1 \geqslant T_2 \; (> 2T_1)$

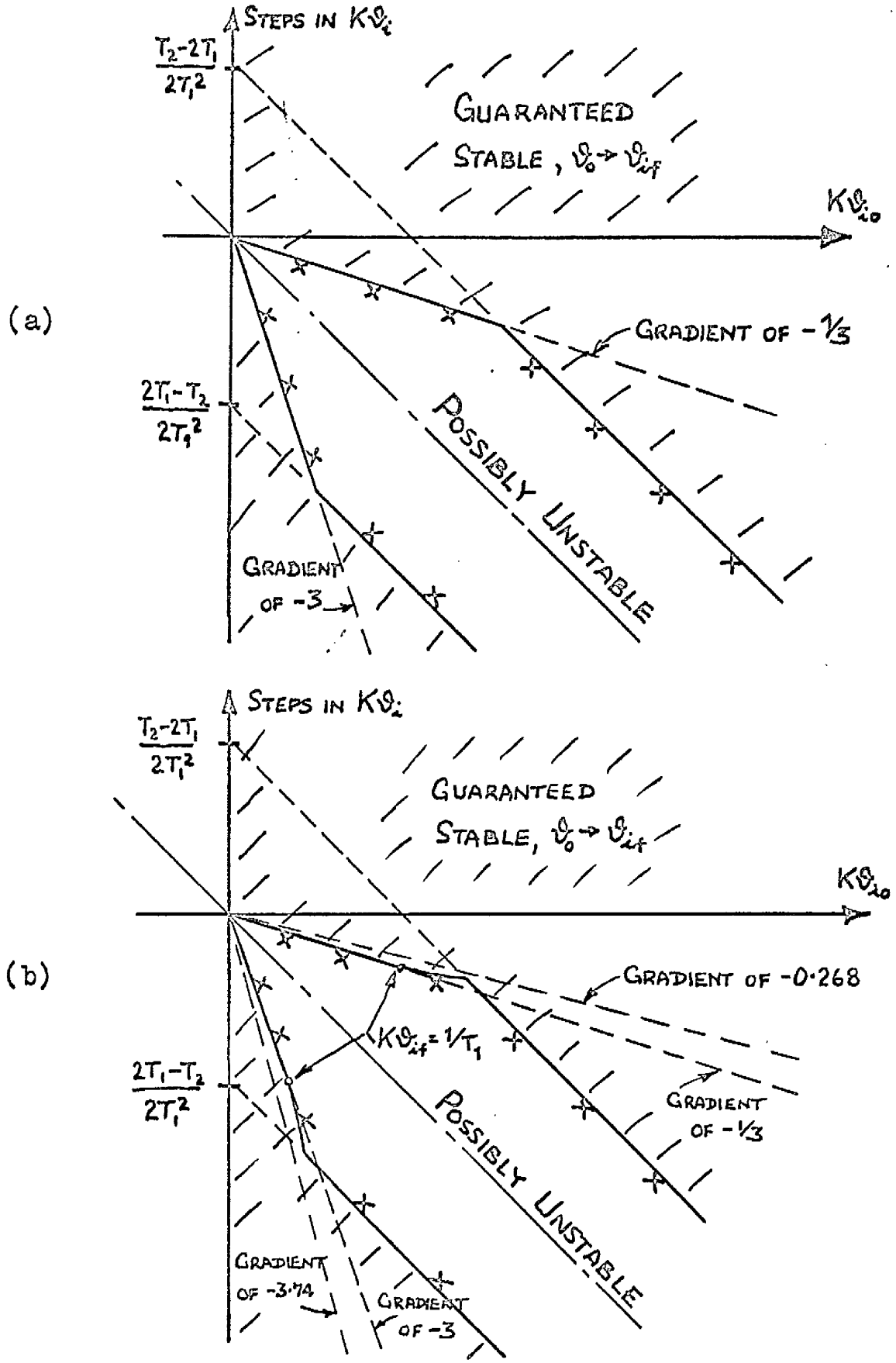

Figure 4.13: Definition from Ω_1 of the boundary of the strip region of possible instability for (a) $4T_1 \geqslant T_2$ (b) $T_2 > 4T_1$

then $L_1 = 0{\cdot}5$ applies throughout the strip: this means that $C + X = 1{\cdot}5\,\phi_{if}$ for $X = 0{\cdot}5\,\phi_{if}$, so that the upper boundary is a straight line of gradient $-1/3$ and the guaranteed region of stability locally is as shown in Figure 4.13. But if $T_2 > 4T_1$, then $L_1 = 0{\cdot}5$ only applies up to $K\phi_{if} = 1/T_1$ and expression (4.4.4) must be used thereafter up to $K\phi_{if} = (T_2 - 2T_1)/2T_1^2$: this expression decreases to a value of 0·366 as $T_1 \to 0$, so that the upper boundary tends towards a straight line of gradient $-0{\cdot}366/1{\cdot}366$, i.e. $-0{\cdot}268$.

Following on the above definition of the boundaries, use of the method of Zubov has been explored in the chance of an enlargement of the regions of guaranteed stability. Working with the φ_1, φ_2 system (4.4.1), however, attempts with the three possible quadratic forms of $\varphi(x,y)$ lead either to sets w_2 which include the origin or to forms dV_2/dt which are too high in order to be useful. As in the previous system, therefore, it may prove valuable to consider different representations of the system (4.2.3); two such alternatives are

$$\frac{d\varphi_1}{dt} = \left[T_2\varphi'_2 - (1 + K\phi_{if}T_1)\varphi_1 - K\phi_{if}T_1\varphi_1^2\right]/T_2$$
$$\frac{d\varphi'_2}{dt} = -K\phi_{if}\varphi_1(1 + \varphi_1)/T_2 \qquad (4.4.5)$$

and

$$\frac{d\varphi_1}{dt} = \left[T_2\varphi'_2 - (1 + K\mathfrak{Q}_{if}T_1)\varphi_1 \right]/T_2$$

$$\frac{d\varphi'_2}{dt} = -\left[K\mathfrak{Q}_{if}T_2\varphi_1(1 + 2T_1\varphi'_2) + \left\{ K\mathfrak{Q}_{if}T_2 - 2K\mathfrak{Q}_{if}T_1(1 + K\mathfrak{Q}_{if}T_1) \right\}\varphi_1^2 \right]/T_2^2 \qquad (4.4.6)$$

Using (4.4.5) in which $\varphi_1 \equiv x$ and $\varphi'_2 \equiv y$ for convenience, A is at the origin while B is at $x = -1$, $y = -1/T_2$. For $\varphi(x,y) = 2x^2$, solution of the partial differential equation for v_2 gives

$$v_2 = T_2 (K\mathfrak{Q}_{if}x^2 + T_2y^2)/K\mathfrak{Q}_{if}(1 + K\mathfrak{Q}_{if}T_1) \qquad \text{(positive definite)}$$

for which $$\frac{dv_2}{dt} = -2x^2\left[T_2y + K\mathfrak{Q}_{if}T_1x + 1 + K\mathfrak{Q}_{if}T_1 \right]/(1 + K\mathfrak{Q}_{if}T_1) \qquad (4.4.7)$$

so that, since the y axis is w_1 and the straight line

$$T_2 y = -(1 + K\mathfrak{Q}_{if}T_1) - K\mathfrak{Q}_{if}T_1 x$$

is w_2, there is a useful half-plane of negative semidefinite dv_2/dt "above and to the right of" this line. The minimum value (c_1) of v_2 on w_2 is readily found as

$$c_1 = \frac{T_2 (1 + K\mathfrak{Q}_{if} T_1)}{K\mathfrak{Q}_{if} T_2 + (K\mathfrak{Q}_{if} T_1)^2}$$

establishing that the region bounded by the ellipse Ω_2, for which

$$K\mathfrak{Q}_{if}x^2 + T_2 y^2 = \frac{(1 + K\mathfrak{Q}_{if}T_1)^2}{T_2 + K\mathfrak{Q}_{if}T_1^2} \qquad (4.4.8)$$

is one of asymptotic stability, since w_1 is not a trajectory within it.

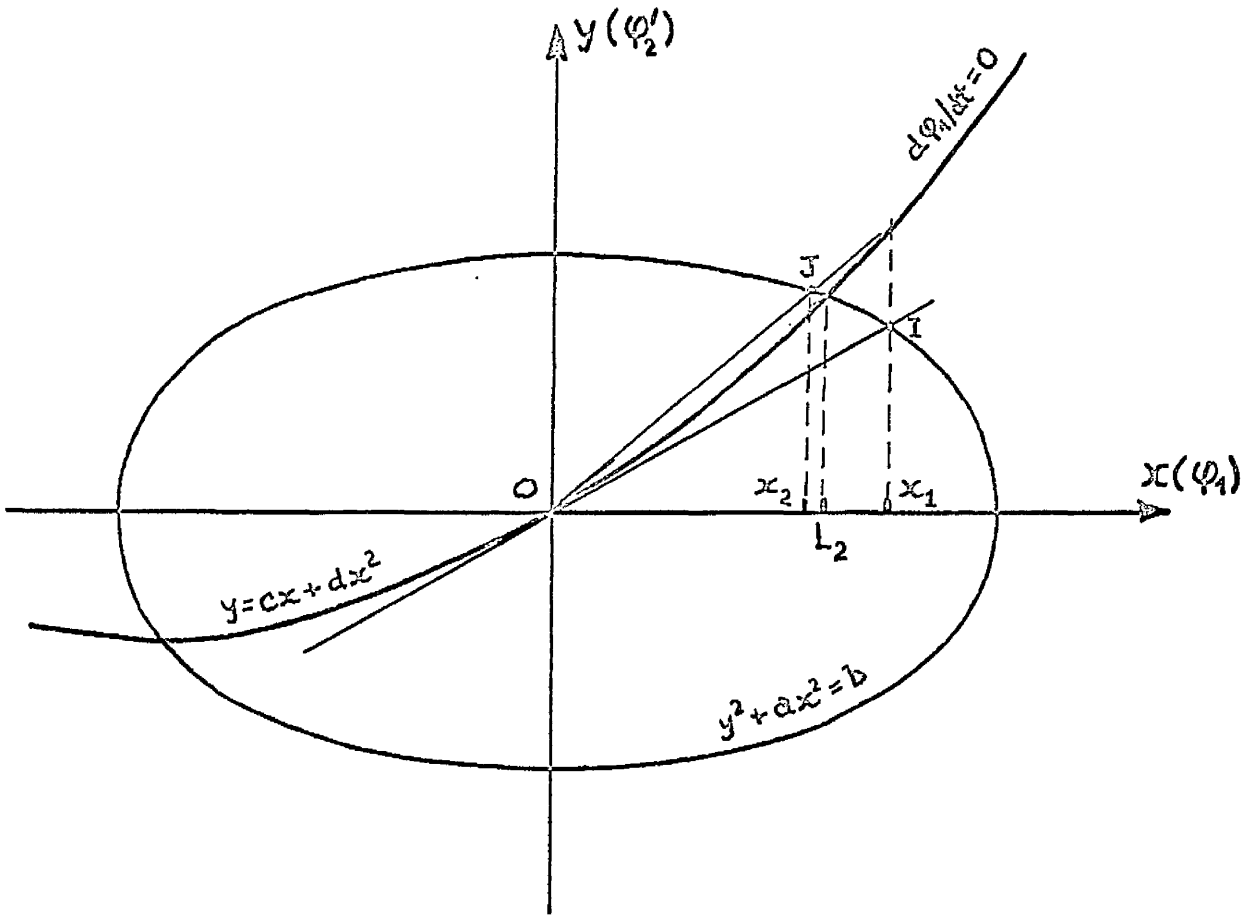

Figure 4.14 : Approximate simultaneous solution of the equations of an ellipse and a parabola to determine L_2 .

To discover the expression for L_2 in the original φ_1, φ_2 system, one must now find the intersection for $\varphi_1 > 0$ of Ω_2 and of the curve $d\varphi_1/dt = 0$, i.e. $T_2 y = (1 + K\Theta_{if} T_1)x + K\Theta_{if} T_1 x^2$. Since this involves a quartic equation, the explicit solution is extremely complicated and is not quoted; however, a useful approximation to L_2 follows. Referring to Figure 4.14, since the curve $d\varphi_1/dt = 0$ is a parabola concave upwards, it is clear that an overestimate for the point $x = L_2$ is obtained by using the value x_1 of the intersection (I) of Ω_2 with the tangent to the parabola at the origin; however, if the straight line from the origin to the point on the parabola corresponding to x_1 is considered, it is equally clear that the intersection J of Ω_2 with this line provides a value x_2 which is an underestimate of L_2. This procedure may obviously be repeated, providing successive upper and lower bounds which converge to L_2. However, x_2 provides sufficient accuracy, and is obtained thus: if the two equations are written temporarily as

$$y^2 + ax^2 = b$$

$$y = cx + dx^2$$

then $$x_1^2 = b/(a + c^2)$$

The straight line OJ is therefore

$$y = \left(c + d\sqrt{b/(a + c^2)}\right)x$$

and so $$x_2^2 = b\Big/\left[a + c^2 + \frac{bd^2}{a + c^2} + 2cd\sqrt{\frac{b}{a + c^2}}\right]$$

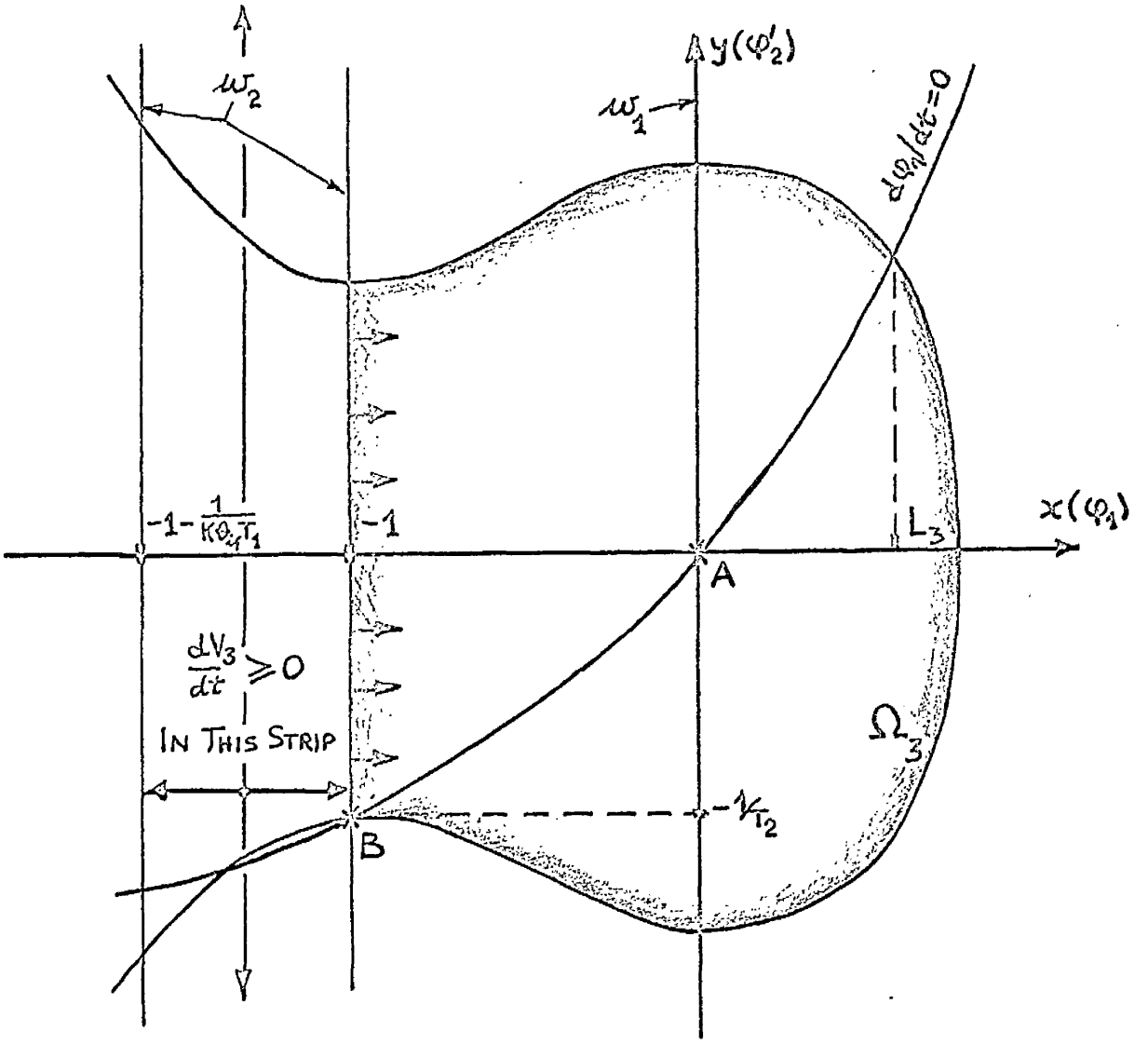

Figure 4.15 : The region Ω_3 of asymptotic stability for the second–order system with a β – element .

where $a = \dfrac{K\mathcal{Q}_{if}}{T_2}$, $b = \dfrac{(1 + K\mathcal{Q}_{if}T_1)^2}{T_2(T_2 + K\mathcal{Q}_{if}T_1^2)}$, $c = \dfrac{1 + K\mathcal{Q}_{if}T_1}{T_2}$ and $d = \dfrac{K\mathcal{Q}_{if}T_1}{T_2}$.

From this lower bound on L_2 an alternative boundary to that of Figure 4.13 may be constructed for the strip of possible instability. However, by comparing the results from Ω_1 and Ω_2 for representative sets of T_1, T_2 and $K\mathcal{Q}_{if}$, it is seen that L_2 produces little or no improvement over the values of L_1, whose form is much simpler than that for x_2. For this reason, this application of the Zubov method is not carried through to the stage of a stability diagram like Figure 4.13.

Brief mention is lastly made of one further attempt to obtain better boundaries. Continuing with the description (4.4.5) of the system, if one investigates the now-familiar form

$$V_3 = 3x^2 + 3T_2 y^2/K\mathcal{Q}_{if} + 2x^3$$

it is found that

$$\frac{dV_3}{dt} = -6x^2(1 + x)(1 + K\mathcal{Q}_{if}T_1 + K\mathcal{Q}_{if}T_1 x)/T_2$$

Thus, the y axis is w_1 while both lines $x = -1$ and $x = -1 - 1/K\mathcal{Q}_{if}T_1$ are sets w_2: see Figure 4.15. dV_3/dt is therefore negative semidefinite everywhere, except in the strip between these lines where it is positive semidefinite. Using the V_3 contour which passes through B, and the fact that all trajectories cross $x = -1$ in the positive x direction, since on it

$$\frac{dx}{dt} \geqslant -\frac{1}{T_2} + \frac{1 + K\vartheta_{if}T_1}{T_2} - \frac{K\vartheta_{if}T_1}{T_2} \geqslant 0$$

it is proved that another region Ω_3 so formed is one of asymptotic stability. However, once again when an attempt is finally made to obtain L_3, one is confronted with a fourth-order equation; although in this case it has been arranged that one root, namely -1, is known, since the curves involved intersect at B, one is still left with a cubic equation. Numerical examples have indicated no significant improvement in L due to Ω_3, so that no attempt is recorded to find an expression for L_3 from this cubic.

4.5 Correlation with the roots-surface

Applications of the techniques of Section 3.5 to the second-order system with a β-element have shown them to be of no more value than in their first application. One other approach has been investigated for this system in order to correlate the time behaviour of stable transient responses with the features of the roots-surface (-loci), which alone is reported.

This approach, largely empirical in nature, consisted in defining values for the two equivalent time constants, or the equivalent natural frequency and damping factor, from some form of averaging process on the values of the small-perturbation singularities within the range of transient variation. It is

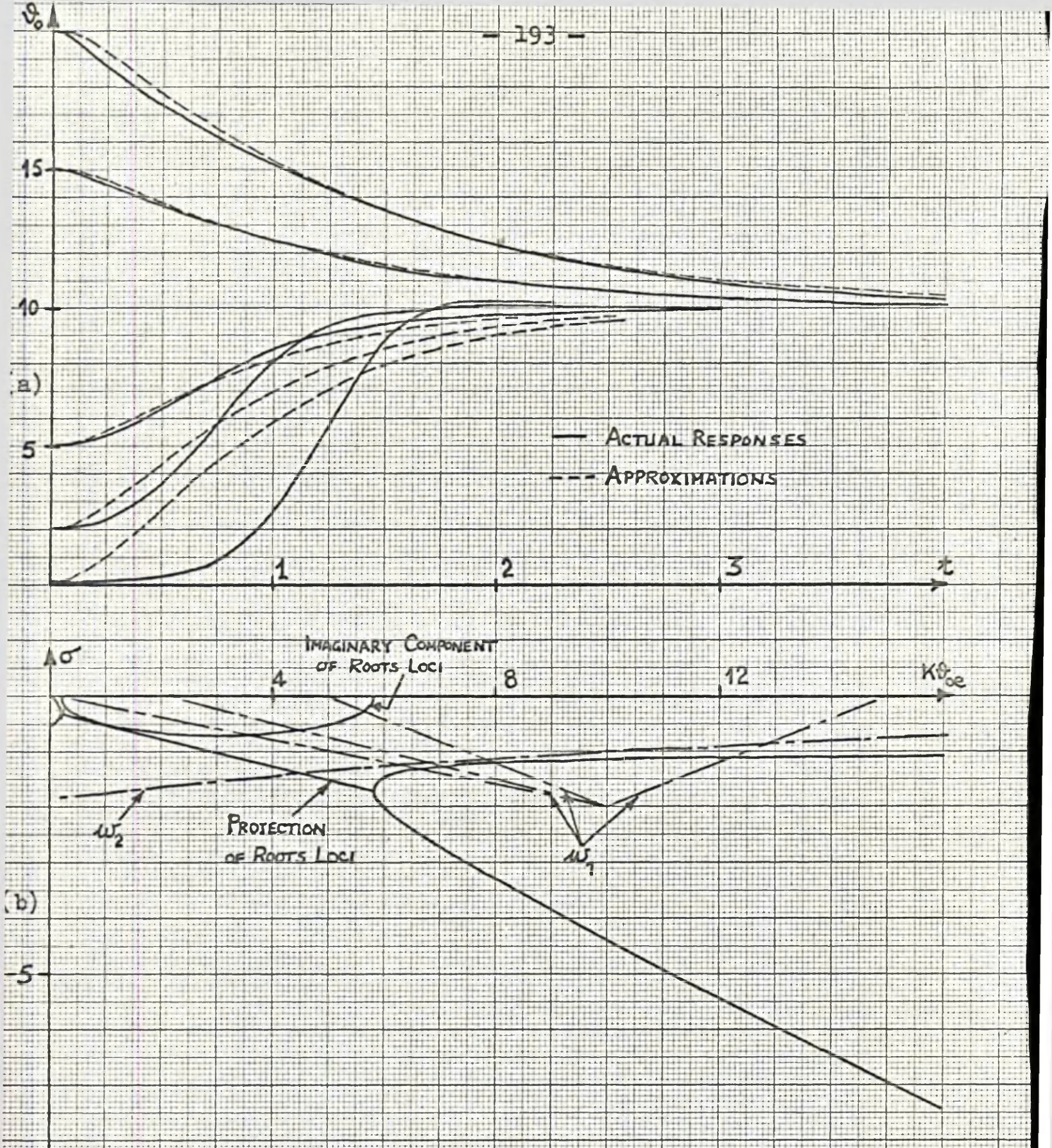

Figure 4.16: (a) Responses for the case II system with $T_1 = 1$, $T_2 = 2$, $K = 1$ and $\vartheta_{if} = 10$

(b) Roots-surface corresponding to (a), with various weighting functions.

described with reference to a typical set of time solutions, Figure 4.16(a), obtained from an analogue computer, which are for the case II system with $T_1 = 1$, $T_2 = 2$, $K = 1$ and $\vartheta_{if} = 10$, $d\vartheta_o/dt = 0$ initially, $\vartheta_o = 0{\cdot}1$, 2, 5, 15, 20 initially. The roots-loci are shown in Figure 4.16(b), where the imaginary part is rabatted into the plane of σ, $K\vartheta_{oe}$.

The value was first investigated of using a straight average of the root values over the range ϑ_{oo} to ϑ_{of}, making appropriate allowance for the imaginary component when included. Since the results were not encouraging, it appeared that a weighted average might be more suitable, where the weighting function was

$$w_1 = 2(\vartheta_o - \vartheta_{oo})/(\vartheta_{of} - \vartheta_{oo})$$

This represented an improvement, but in order to have one weighting function common to all responses from different ϑ_{oo} to a particular value of ϑ_{of}, the exponential weighting function

$$w_2 = e^{-0.06(K\vartheta_{oe} - 10)}$$

was tried, which gave best results for the response from $\vartheta_{oo} = 20$. The five equivalent second-order responses calculated using w_2 are shown on Figure 4.16(a), from which it is seen that representation is fair for the responses from $\vartheta_{oo} = 20$, 15 and 5, but poor for those from 2 and 0·1. The quality of representation may be judged by the values given to the "rise time" (to 61 per cent. of final value) and to the time of maximum velocity, or inflexion, as shown in Figure 4.17: the actual rise time for any

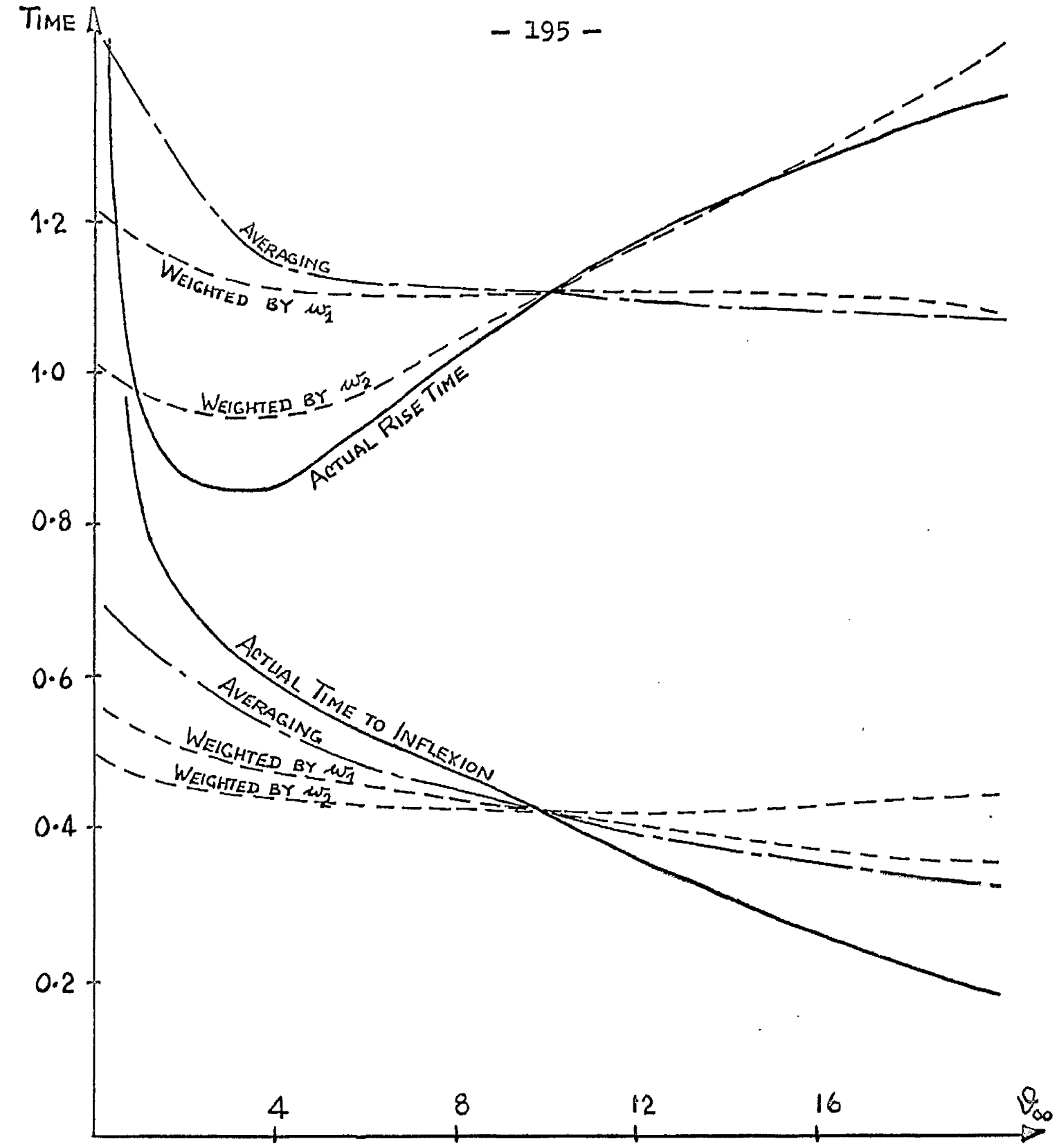

Figure 4.17 : Actual and equivalent times of rise and to maximum velocity, for the responses of Figure 4.16(a) .

response from ϑ_{oo} is best approximated by the form employing w_2, whereas the time to the point of inflexion is best approximated by the straight averaging. In either connection, the averaging approach fails at low values of ϑ_{oo} since finite times are produced, whereas the actual time behaviour becomes slower and slower as ϑ_{oo} tends to zero.

Similar conclusions are drawn about correlation in this system with its roots-surface as have been made in Section 3.5 for the earlier system. No effective means has been discovered for predicting the time behaviour from the roots-surface: though some measure of correlation has been attained with the responses of Figure 4.16, attempts to apply the same weighting procedure to responses to other values of ϑ_{of} have shown that different values of the negative exponent in w_2 are required for each value of ϑ_{of}, and that representation is rather poor even then. As regards the ability of the roots-surface to predict the forms of the stability diagrams, once again it fails to establish the regions within which negative steps falling in a certain range cause the system to go unstable from initially stable conditions.

CHAPTER 5

Conclusions

CHAPTER 5

Conclusions

The first set of conclusions relates principally to the output-dependent systems studied and reported, whereas the second and third sets embody recommendations of a more general nature and wider application.

1. It must be concluded that the roots-surface has been proved incapable of yielding useful and accurate information about large-scale behaviour. The stability of large step responses in particular has been shown not to be predictable by the appearance of a roots-surface, while no method has been discovered to correlate satisfactorily the time behaviour of the transients with the movements of the small-perturbation singularities, and these facts emerge from consideration of systems of orders as low as first and second. Even if more satisfactory correlations had been achieved in particular cases, it would have been unreliable to apply the same techniques to further roots-surfaces, especially considering the aspect of non-uniqueness of the roots-surface which has been revealed.

This study, certainly, has been restricted to consideration of transient responses of output-dependent systems where the input variable has a constant value; it may be that,

for other input functions whose time variations are slow in comparison to system time constants, the transient behaviour is capable of being predicted more dependably from the movements of the singularities, as suggested by M'Pherson[1, 2]. However, this study has provided a demonstration of the difficulties and pitfalls involved in attempts to examine such strongly nonlinear systems in a linearised way.

2. Notwithstanding the remarks in 3 below, the transformations of Poincaré for the behaviour at infinity in the phase plane have been found most useful in determining the stability of large transient responses: in this connection, the remarks of Davies[22] are interesting. It would appear to be a useful preliminary in investigating the stability of a system, which may be continued by Lyapunov's direct method or other means. An extension of the transformations to third-order systems has been outlined by Kammüller[23], and it might be useful to have further, purely analytical, extensions to higher-order systems, despite the lack of a geometrical interpretation.

3. Lyapunov's Direct Method has been used successfully throughout the study but, as has been often emphasised by other authors, many developments of the method are still possible and desirable. In this project it has been found that, working literally, a maximum amount of use must be extracted from the low-order algebraic forms for which explicit solutions are

possible, and that the existing techniques of Zubov et al. are not particularly valuable, being best suited to particular numerical systems. Various devices have produced good results from low-order forms: the method of undetermined coefficients proposed offers the advantages of simplicity and freedom to construct a time derivative which may be made negative semi-definite in a suitably restricted region commensurate with the region of asymptotic stability produced: the investigation of alternative ways of decomposing an n'th order differential equation into n of first-order may be rewarding, as discovered in Sections 3.4c and 3.4d and in connection with the preliminary study of a fourth-order output-dependent system, not reported; by this means, the total number of terms "on the right-hand side" of the equations may be reduced, and by distributing the singularities in a different pattern around the origin it may be possible to arrange for intersections of the boundary Ω with sets w_2 (or others) to occur at known fixed points, thus reducing the order of the ensuing equation for another intersection of interest (as L).

It would appear worthwhile to develop the method of undetermined coefficients for higher-order systems, perhaps to the stage where the logical choice of terms and evaluation of coefficients could be aided by a digital computer, having regard to the advantages of the different decompositions

referred to above. At the same time, there is a requirement for sign-definiteness criteria , similar to Sylvester's, for higher-order forms than quadratic, which would allow their free use : this point has also been made by Gibson et al.[24] . Any developments would also be most valuable which conveyed information about the time behaviour of trajectories within the region of stability from the Lyapunov function; it seems plausible that a Lyapunov function is capable of affording such information, even where its time derivative is only negative semidefinite.

BIBLIOGRAPHY

1. M'PHERSON, P.K. Applications of Complex Plane Methods to System Design. Trans. Soc. Instrum. Tech. 14(2) 1962, pp.89–90.

2. M'PHERSON, P.K. The Use of Complex Plane Methods in the Analysis of Plant Dynamics and the Design of Automatic Control Systems. U.K.A.E.A. Reactor Group Report AEEW–R120, Winfrith, Nov. 1961, pp.12–14.

3. WILLIAMS, T.J. Process Dynamics and its Applications to Industrial Process Design and Process Control. Survey Paper 11, Proc. Second Intern. Cong. of IFAC on Auto. Control, Basle, 1963 : to be published, Butterworths.

4. CLYNES, M.E. Circulatory System : Respiratory heart rate reflex (RHR) in Man : Mathematical Law. Medical Physics, ed. Otto Glasser, 3, p.184. The Year Book Publishers Inc.

5. GRODINS, F.S. et al. Respiratory Responses to CO_2 Inhalation : a Theoretical Study of a Nonlinear Biological Regulator. Journal of Applied Physiology, 7, 1954–55, 283–308.

6. ANDRONOW, A.A. and CHAIKIN, C.E. Theory of Oscillations, 1949, Princeton, Princeton University Press, p.32 and p.145.

7. NECHLEBA, F. Extension of the Concept of Time Constant. Electrotech. Z. 74 (1953), 98.

8. MORGAN, P.G. Definition of an Equivalent Time Constant. Control Data Sheet No.24, Oct. 1961.

9. SMETS, H.B. and GYFTOPOULOS, E.P. The Application of Topological Methods to the Kinetics of Homogeneous Reactors. Nuclear Science and Engineering, 6 (1959) , p.347.

10. POINCARÉ, H. Journal de Mathematiques (3) 7, 1881 : also Œuvres, T.I, Gauthier—Villars, Paris, 1928, p.5 et seq.

11. MINORSKY, N. Nonlinear Oscillations, 1962, New York, Van Nostrand, pp.91—96.

12. LYAPUNOV, A.M. The General Problem of the Stability of Motion. Doctoral thesis, published by Kharkov Mathematical Society; available in translation as 'Problème Général de la Stabilité du Mouvement', Annales de la Faculte des Sciences de Toulouse, 9, 1907, pp.203—474, reprinted as Annals of Mathematical Studies No.17, Princeton University Press, 1949.

13. KALMAN, R.E. and BERTRAM, J.E. Control System Analysis and Design via the "Second Method" of Lyapunov. Trans. A.S.M.E., 82 Series D, 1960, pp.371—393 and pp.394—400.

14. LASALLE, J.P. and LEFSCHETZ, S. Stability by Lyapunov's Direct Method with Applications. 1961, New York, Academic Press, p.58.

15. KRASOVSKII, N.N. Global Stability of the Solutions of a System of Nonlinear Differential Equations. Prikladnaja Matematika i Mekanika (P.M.M.), Vol.18, 1954, pp.735–737. English Translation by Rekasius, Z.V., as Appendix B of report AFMDC–TR–61–6, July 1961, of the Aeronautical Research Council.

16. SCHULTZ, D.G. and GIBSON, J.E. The Variable Gradient Method for Generating Lyapunov Functions. Paper No.62–81, 1962, Trans. AIEE.

17. ZUBOV, V.I. Mathematical Methods of Investigating Automatic Regulating Systems. (Leningrad 1959). USAEC translation AEC–tr–4494, September 1961.

18. MARGOLIS, S.G. and VOGT, W.G. Control Engineering Applications of V.I.Zubov's Construction Procedure for Lyapunov Functions. IEEE Trans. on Automatic Control, Vol.AC–8, pp.104–113, April 1963.

19. KERR, C.N. Control Engineering Applications of V.I.Zubov's Construction Procedure for Lyapunov Functions. IEEE Trans. on Automatic Control, Vol.AC–9, April 1964.

20. MURPHY, G.M. Ordinary Differential Equations and their Solutions. Van Nostrand, New York, 1960, p.168.

21. GRENSTED, P.E.W. The Frequency Response Analysis of Nonlinear Systems. Instn. Elec. Engrs., Monograph No.126 (1955).

22. DAVIES, T.V. Summing—up in a Discussion on Stability of Systems, arranged by the Automatic Control Group of the I. Mech. E., London, May 1964. Proceedings to be published by the I. Mech. E.

23. KAMMÜLLER, R. Zur Analyse der Phasenraumes. Regelungstechnik, Heft 7, 10 Jahrgang, July 1962.

24. GIBSON, J.E. et al. Stability of Nonlinear Control Systems by the Second Method of Lyapunov. Report AFMDC—TR—61—6, July 1961, of the Aeronautical Research Council, p.91.